CESSNA/ONR STUDENT DESIGN/BUILD/FLY COMPETITION

An AIAA Student Activity

The 2002 Cessna/ONR Student Design/Build/Fly competition was held at the Cessna flight test center in Wichita Kansas over the weekend of 26-28 April. Twenty eight teams from the United States and three foreign countries; Canada, Italy and Turkey, competed under sometimes challenging weather conditions to see whose aircraft would complete all three sorties over the prescribed course in the minimum time. Of the 28 teams attending the fly-off competition, 27 made at least one scoring flight attempt, with many teams making multiple flights during the two days of competition. Only one team, La Sapienza from Italy, made 5 successful scoring flights (the maximum allowed)

The competition spanned two days of flying, with the flight queue filled with aircraft waiting for their turn to make a competition flight. During the second day of the competition a total of 69 multiple sortie flights were flown.

The total score for each team was comprised of their flight performance on their best three flights, their score on a written report documenting their aircraft design and selection, and a "Rated Aircraft Cost" representing the complexity and manufacturing costs of their design.

The final results showed a close battle between teams from the University of California at San Diego, University of Southern California, and West Virginia University. In the end, the University of Southern California team was not able to match the top team from their neighbor to the south the University of California at San Diego. The highest score obtained on the written report portion of the competition was from Oklahoma State University, Team Orange with 94 of a possible 100 points awarded.

The final positions and scores for all of the competing teams are listed in the table below.

More details on the 2002 competition objectives and rules can be found at the contest web site at http://amber.aae.uiuc.edu/~aiaadbf

School	Team	Paper	RAC	Flight	Score	Position
Univ. of Calif at San Diego #2	TLAR 3	79.0	9.81	16.45	132.52	1
USC	SCrewball	92.5	13.11	16.32	115.17	2
West Virgina Univ. #2	Phastball	86.5	12.49	15.22	105.43	3
Univ. of Illinois, Champain	Illiniwek 1	88.0	13.31	12.99	85.87	4
La Sapienza, Italy	Flying Centurions	65.8	13.52	15.06	73.27	5
San Diego State University	Monty's Revenge	81.0	13.95	8.82	51.22	6
VA Polytechnic and State Univ.	Marooned	82.8	13.07	7.80	49.37	7
Calif. Polytechnic, San Luis Obispo	Third Base	86.3	8.41	4.18	42.84	8
USA Naval Academy #2	USNA Gold	82.3	13.57	4.87	29.54	9
Mississippi State Univ. #1	Fast Pitch	88.5	16.76	4.25	22.46	10

USA Naval Academy #1	USNA Blue (Tango)	79.4	15.49	2.97	15.20	11
Istanbul Technical University	ATA4	69.5	14.52	1.54	7.38	12
University of Arizona #2	AirCat2002	39.3	13.18	2.19	6.52	13
Case Western Reserve Univ.	Learning Curve	41.3	17.09	1.81	4.38	14
West Virgina Univ. #1	Daedalus	18.7	15.65	2.50	2.99	15
Oklahoma State Univ. #1	OSU Black	91.9	9.49	0.25	2.45	16
Oklahoma State Univ. #2	OSU Orange	94.0	10.09	0.11	1.07	17
University of Maryland	Terp Flyer	75.2	12.97	0.18	1.02	18
Georgia Institute of Technology	Buzz Light	87.3	13.33	0.14	0.91	19
Queen's University, Canada	Negative Margin	85.2	13.47	0.12	0.79	20
USA Military Academy #1	Team 1	83.4	16.26	0.11	0.57	21
Univ. of Calif at San Diego #1	TLAR 3.5	77.5	9.32	0.01	0.08	22
Wichita State Univ.	Swallow	92.6	11.31	0.01	0.08	23
University of Arizona #1	Evolution	66.0	12.71	0.01	0.05	24
Clarkson University	Knight Hawk	73.0	14.15	0.01	0.05	25
City College of NY #1	Falcon I	70.7	14.03	0.01	0.05	26
Syracuse University	~(Tilda)	70.3	16.24	0.01	0.04	27
Univ. of Texas at Arlington	Black Magic	70.6	17.15	0.01	0.04	28
Univ. of Texas at Austin	Better is the Enemy of Good	89.1	100.00	0.01	0.01	29
Middle East Technical University	Ruzgar Sultan	86.3	100.00	0.01	0.01	30
Mississippi State Univ. #2	Milk Run	85.9	100.00	0.01	0.01	31
Cleveland State University	The Flying Viking	76.3	100.00	0.01	0.01	32
Turkish Air Force Academy	Conqueror	69.8	100.00	0.01	0.01	33
Miami University, Ohio	It's Close Enough	69.3	100.00	0.01	0.01	34
University of Central Florida	Butter Duck	66.2	100.00	0.01	0.01	35

The success of the competition required the efforts of many individuals. A special thanks goes to the judges who assisted in the operation, technical inspections and scoring of the flight competition; and to the many judges who evaluated and scored the teams written proposal reports. Thanks also go to the Applied Aerodynamics, Aircraft Design, Design Engineering, and Flight Test Technical committees of the AIAA who organized and manage the competition, and the AIAA Foundation for their administrative support. Special thanks is due to the competitions corporate supporters, the Cessna Aircraft Company and the Office of Naval Research. And the final and biggest thank you must go to our hosts for the weekend, Cessna Aircraft.

Overall the 2002 Cessna/ONR Student Design/Build/Fly competition marked another very successful event, allowing the participating students to mix a highly enlightening educational experience with a good dose of fun. Congratulations to all the teams who participated for your great enthusiasm and achievement.

See you next year - Greg Page: Contest Director

Highest Report Score

Oklahoma State University
Orange Team

2002 Cessna/ONR
Design Build Fly Competition
Design Report

Table of Contents

Table of Figures

Table of Tables

1.0 Executive Summary

This report outlines the approach taken by the OSU Orange Team to design and construct an aircraft that best meets the goals set forth in the AIAA 2001/2002 Design/Build/Fly (DBF) Competition. The goal of the competition is to design a propeller driven, unmanned aircraft that performs at the optimum balance between payload capacity, propulsive efficiency, and rated aircraft cost around a closed course of 6 laps. The maximum payload allowed is twenty-four softballs. The total score awarded to the design is a function of the report score, flight score, and Rated Aircraft Cost.

1.1 Conceptual Design

The first step of the conceptual design was to analyze the competition requirements in terms of the three technical groups: aerodynamics, propulsion, and structures. Each group performed sensitivity studies in their respective areas, scrutinizing every aspect of the competition to determine design requirements and to identify the major contributors to overall scoring potential. Then each group generated design concepts in their respective technical areas to meet the design requirements. The next step was to perform a design optimization analysis. Results from the analysis were used to create figures of merit to compare various concepts and evaluate different approaches to achieve the highest possible score. After several iterations, attention was focused upon the optimal region as described by the optimization analysis. Concepts were narrowed down to the most promising ideas, which exhibited the greatest scoring potential and took into consideration all aspects of the competition. Each group refined their respective concepts into their final selections of aircraft configurations, construction methods, materials, and propulsive schemes.

1.1.1 Conceptual Design Alternatives

The aerodynamics group divided the aircraft configuration into modular sections. Different combinations of five fuselage shapes, five wing configurations, and six tail configurations were evaluated for advantages and disadvantages. Different structural alternatives were concurrently evaluated for the components that made up the different configurations. Ease of construction, the ability to produce a lightweight structure, and Rated Aircraft Cost were used to compare alternatives structurally. Three propulsion system alternatives were generated from combinations of different battery configurations, number of engines, and propeller configurations. Propulsive schemes were evaluated in combination with aerodynamic and structural configurations to weigh into the overall aircraft configuration in terms of scoring potential

1.1.2 Conceptual Design Tools

Several tools were employed to evaluate scoring potential of each configuration. Scoring potential was judged as a combination of Rated Aircraft Cost (RAC) and flight performance. Score sensitivities were determined using an optimization code developed from modeling all aspects of the mission. The models represented the weight and drag of the airplane, aerodynamic and propulsive effects of various components, and a Rated Aircraft Cost (RAC) model. Each model effected the time and RAC and in turn adjusted the overall score of a particular configuration. The performance program adjusted six parameters using random variables and found local maximums in the performance of the plane. Weighted decision matrices were constructed using the sensitivities studies produced from these models. Finally configurations were evaluated in the weighted decision matrices for scoring potential.

1.1.3 Conceptual Results

At the conclusion of the conceptual design phase, the design with the highest scoring potential was selection from all alternatives. The aircraft was a low wing monoplane with a V-tail. The fuselage was composite sandwich, monocoque construction. Both the wing and tail sections were constructed of foam core with composite skin. The optimum propulsive scheme was determined to be a single engine tractor configuration with batteries connected in series.

1.2 Preliminary Design

With the basic configuration of the aircraft determined different approaches to aircraft and control surface sizing, structural design, and propulsion alternatives were analyzed. The aerodynamics group focused on the component and control surface sizing and static stability of the aircraft. The structures group performed stress analysis and selected the materials for the primary components. The propulsion group determined the combination of motor and batteries and propellers to be tested.

1.2.1 Preliminary Design Alternatives

The preliminary design phase consisted of evaluating component types, sizes, and quantities against scoring potential. The aerodynamic studies consisted of wing, tail and fuselage sizing combinations and affects on the overall score. Once preliminary sizes were decided, structural analysis was performed on primary components. Material selection, and construction methods for primary components were then finalized. Finally, the propulsion group evaluated different motors, propellers, and battery configurations to narrow down the propulsive system components.

1.2.2 Preliminary Design Tools

Preliminary modeling of the aircraft was initiated by constructing a two-dimensional station chart using yarn and construction paper mounted on a pegboard. The model allowed the entire team to develop a feel for initial component sizing and placement early in the design. The next step was developing a three-dimension model using CAD software to provide more detailed information for structural analysis. Finally the structural information was inserted into spreadsheets developed to perform stress analysis on primary components. The aerodynamics group used information from the developing structural model for the development of computer code to analyze the requirements and performance of each aerodynamic surface. Information from both the structural and aerodynamic models was used to set design requirements for the propulsion group. The requirements were feed into a computer code designed to predict the performance of different combinations of motors, batteries, and propellers

1.2.3 Preliminary Results

At the conclusion of the preliminary design phase, the type, sizes, and construction methods of the primary aircraft components were finalized. The aerodynamics group determined the static stability and provided dimensions and tolerances on wing, tail, fuselage, and control surfaces to the structures group, and gave a propulsion mission profile to the propulsion group. The propulsion group used the data to narrow down component alternatives to the most promising choices for further testing. The structures group completed stress analysis on primary structures using mission loads. The final dimensions and makeup of each primary structural component were available for the detail design phase.

1.3 Detail Design

The detail design was generated from components sized during the preliminary design phase. The aerodynamics groups performed dynamic stability analysis and determined handling characteristics and control system requirements. The propulsion group finalized the combination of motor, propeller, and batteries to make up the propulsion system. The structures group completed a three dimensional model and detailed drawings of the surfaces, structures, and subsystems that comprised the final design.

1.3.1 Detail Design Alternatives

Detail design alternatives in each group focused on secondary components and process used in the construction and operation of the aircraft. The system of using figures of merit was once again implemented to analyze the impact of each decision on score. Structural alternatives such as the placement of interior components, system integration methods, wire routing, and hatch design were finalized. Different methods and hardware alternatives for mating the aircraft components were considered. Manufacturing processes were examined for each component. The propulsion group tested the performance of different propellers in combination with different battery and motor types. The propulsion group also evaluated several different types of fuse holders and methods for charging batteries. The aerodynamics group determined control system alternatives in the form of servo requirements and control characteristics.

1.3.2 Detail Design Tools

The aerodynamics group used a flight dynamics code along with an airfoil performance program to determine the dynamic stability of the aircraft, control characteristics, and servo requirements. The stability code was also adapted to generate the stability derivatives. The structures group further developed the CAD model to organize the component design and to predict the weight and center of gravity of the aircraft. A scheduling program was implemented to develop a manufacturing process schedule. Structural analysis on secondary structures and component mating hardware was performed using information in the spreadsheets and weight models. The propulsion group employed a dynamometer to compare actual system performance to analytical predictions.

1.3.3 Detail Design Result

At the conclusion of the detail design phase all aircraft dimensions, system components, and materials had been selected. The aircraft performance capabilities and control characteristics had been determined. Manufacturing processes had been developed. Finally detailed production drawings were prepared.

1.4 Manufacturing and Prototype Testing

Information gained during the construction and manufacturing of the prototype aircraft was useful to improve the design for the final aircraft. Several changes were made to the final aircraft design. During the construction of the prototype, wing difficulties were encountered when trying to produce the leading edge of the airfoil shape. To correct the problem adjustments were made to the female cradles used in the process to help keep the cross section shape. Difficulties with the construction of the fuselage female mold were also encountered. Several different methods and compounds were tested to find a process that could create the desired fuselage finish. During the flight-testing phase of the prototype difficulties were encountered with roll stability and problems were identified with aircraft visibility. The problems in conjunction with gusty wind conditions led to a crash, from which the problems were identified. To correct the problem, dihedral was added to the wing and reflective tape was applied to the top of the fuselage. After the crash, the modular design of the aircraft was discovered to have assisted in the preservation of the major aircraft components, which made possible continued flight-testing three days later.

2.0 Management Summary

2.1 Team Architecture and Personnel Assignment Areas

The OSU Orange Team was divided into three technical groups: aerodynamics, propulsion, and structures. Each technical group was comprised of a lead engineer and component specialists; each lead engineer answered to the chief engineer. Figure 1 outlines the architectural structure of the team. The chief engineer was responsible for overall team direction and performance as well as ensuring that each group had the tools and information necessary to complete assigned tasks. The lead engineer of a group was responsible for coordinating the efforts of the component specialists to meet the overall goals of that technical group, as set forth by the chief engineer. Together, the chief and lead engineers assured that the design process followed a logical progression from day to day and ensured that every aspect was properly considered.

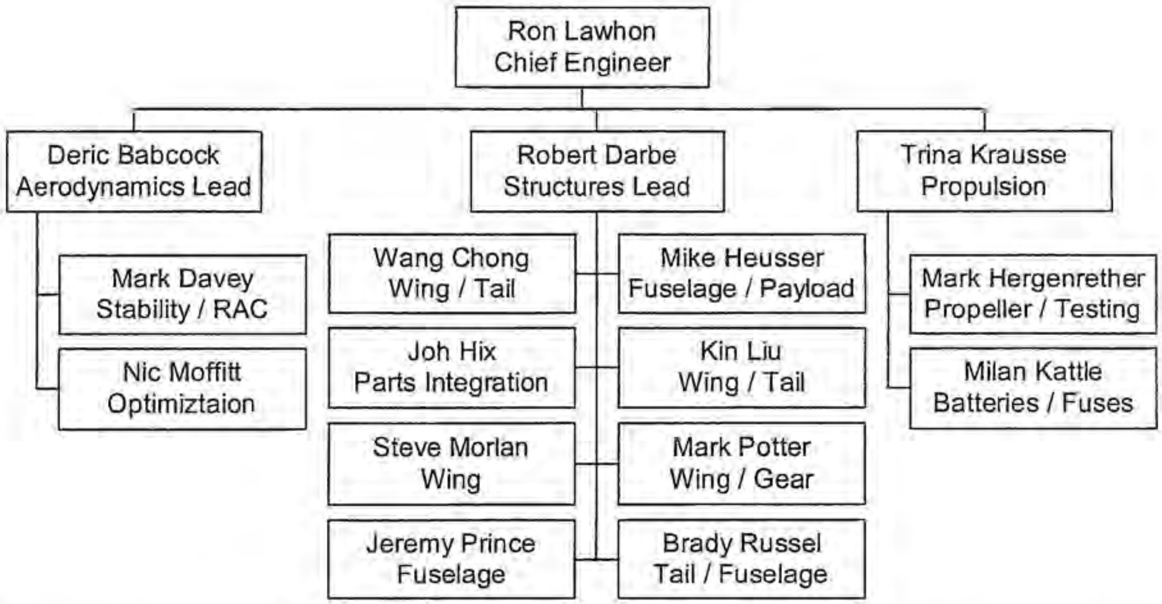

Figure 1: OSU Orange Team Architecture Chart with Design Personnel and Assignment Areas.

2.2 Responsibilities of Each Technical Group

Ultimately the configuration of the aircraft was a combination of the major components submitted by each technical group. The nature of this collaboration was such that every decision made by one group affected the constraints placed on the conceptual designs of the other groups. Each group agreed upon a single concept before further progress was made. The responsibilities of each group were divided among the members of that group. Individual contributions are displayed in Figure 1. Other team members such as the pilot, graduate students, and underclassmen were not assigned to a specific group.

2.2.1 Aerodynamics / Stability and Control Group

The first task for the aerodynamics group was to oversee the mathematical modeling process and incorporate the competition regulations. Using the resulting data, the group generated rough estimates of performance parameters for each group as a base for conceptual studies. The group then progressed to analyzing different aircraft configurations by scoring potential. Figures of merit were defined to further rate the scoring potential of each concept. The end result of the aerodynamic conceptual study was the final plane configuration. The aerodynamics group continued to develop the mathematical model during the preliminary design phase. The model was refined in areas to better represent the conceptual configuration. The results of the mathematical model were focused on the general aerodynamic sizes of the wing, tail, and fuselage. During the preliminary design phase, the aerodynamics group focused on the stability and control of the aircraft. The tail and control sizing resulted from the preliminary phase, along with the servo sizes required to create control movement.

2.2.2 Propulsion Group

The propulsion group was responsible for the design and evaluation of different motor, propeller, and battery combinations. The concepts were judged on the effective use of available power, ability to produce the desired thrust, and effect on Rated Aircraft Cost. During the conceptual phase, the propulsion group decided how many motor and propellers would be required to produce the thrusts calculated by the mathematical models. The group also decided whether a pusher or tractor configuration would be implemented. The propulsion group developed analytical and experimental means by which the wide selection of motors and propellers was narrowed to a few combinations to be prototype tested. The group continued analysis of the components during the detail design phase by checking the validity of preliminary and historical data. Prototype analysis allowed the group to further refine the combination of propulsion components to best met the mission requirements and help minimize the Rated Aircraft Cost.

2.2.3 Structures Group

The structures group was responsible for the structural design and integration of components. Considerations ranged from payload handling methods and structural analysis to material selection and manufacturing processes. During the conceptual phase, the structures group examined several different methods of building the general structures required by all aircraft. The group examined all construction materials available and considered the figures of merit of each. Further brainstorming developed component buildups for secondary structures. During the preliminary design phase, the structures group used loading parameters given by the aerodynamics and propulsion groups to decide on the quantity and size of primary structural components in the wing, fuselage, and tail. Landing gear configurations and loading were also considered so that the gear could be completely designed. During the detail design phase, the landing gear and primary structures were tested for compliance to preliminary parameters. Further analysis resulted in the sizing of the secondary structures. The structures group also considered all tooling and construction methods to be used during the manufacturing phase. Final drawings and implementation of the manufacturing process were the responsibility of the structures group.

2.3 Scheduling, Document, and Configuration Control

To meet the competition deadline, the design process had to progress at a rapid pace. During the course of the design several milestones were identified and implemented as deadlines for different phases of the process. The design process was divided into the conceptual design, preliminary design, detail design, and manufacturing phases. Dates were set for the completion of the ingredients for each of these phases. The design report was developed concurrently with the design process and marked an important milestone that had to be accomplished. Report sections were due along with respective design phase completion. Figure 2 is a milestone chart developed for the design process.

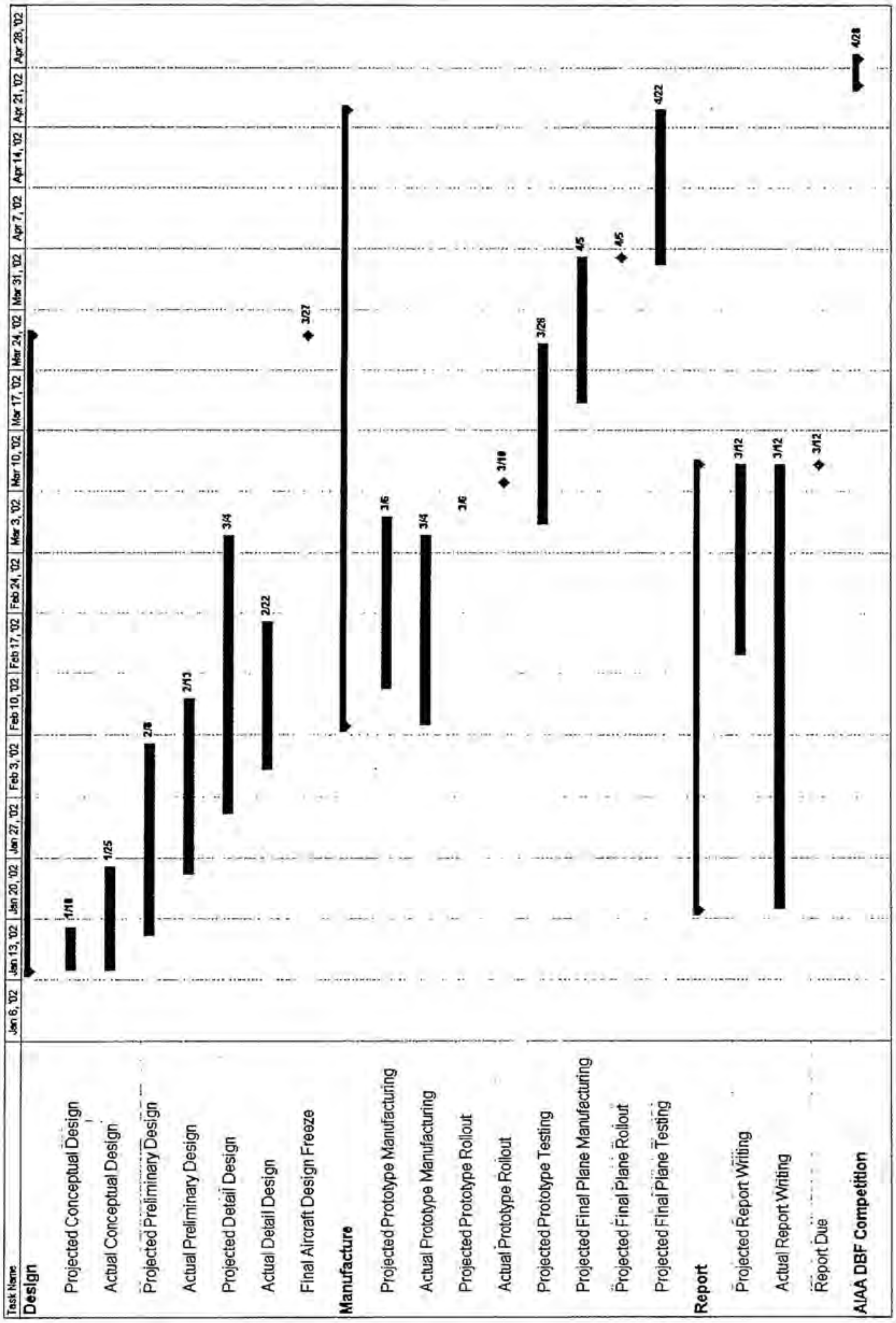

Figure 2: OSU Orange Team Milestone Chart. Red lines represent projected dates; green lines represent actual dates. **Black diamonds represent beginning and completion milestones.**

Configuration control involved the processing of new information into the current state of the design. Continued updating of the design was important in order to insure that the design iterations were not performed on outdated data. In order to implement the system, control files were created where the latest information was made available. The control files evolved from hanging folders, at the beginning of the design process, to computer files and finally to CAD drawing packages.

3.0 Conceptual Design

The first step in the concept selection process was to perform sensitivity studies on the competition in the areas of aerodynamics, propulsion, and structures. Next, ideas for accomplishing all aspects of the competition were generated. After generating ideas, each concept was discussed to determine the benefits and penalties of implementation. Ideas were combined and evolved until a final concept was reached. The final configuration chosen was best suited for the contest rules and mission, allowing for the most scoring potential.

3.1 Design Parameters

A performance program was written to investigate the design parameters of the plane over the entire mission. The program was used to perform sensitivity analysis on the design parameters. Once the sensitivity to each design parameter was known, an overall strategy was developed and implemented during the three design phases.

3.1.1 Primary Design Parameters

The performance program considered all phases of competition flight and Rated Aircraft Cost. Six primary parameters were chosen as major contributing factors in the development of the plane: weight of batteries, weight of balls, power used in cruise, power used in takeoff, planform area of the wing, and span of the wing.

The six factors were used to maximize the scoring potential of the design. The program found that the highest scoring plane configurations carried the limit of 24 softballs. Takeoff distance was limited to two hundred feet. The full 200 feet was also used by every high scoring plane configuration. Another limiting factor was the number of batteries. Each high scoring configuration used 99% to 100% of the energy capacity of the batteries. These tendencies showed the plane needed to fly efficiently in cruise, while still taking off under the limit with a payload of 24 balls. Figure 3 summarizes the sensitivity analysis results.

The power and wing parameters established areas in which optimal performance occurs; battery and ball weight tended in the largest number of balls with the fewest batteries that could be carried. Takeoff power was found to be between 850 and 1000 watts, while cruise power was between 600 and 700 watts. The wing planform ranged from 5 and 7 square feet with a span of 7 to 9 feet. The above parameters were given to the propulsion and structures group so that refined analysis could be made during the conceptual design phase.

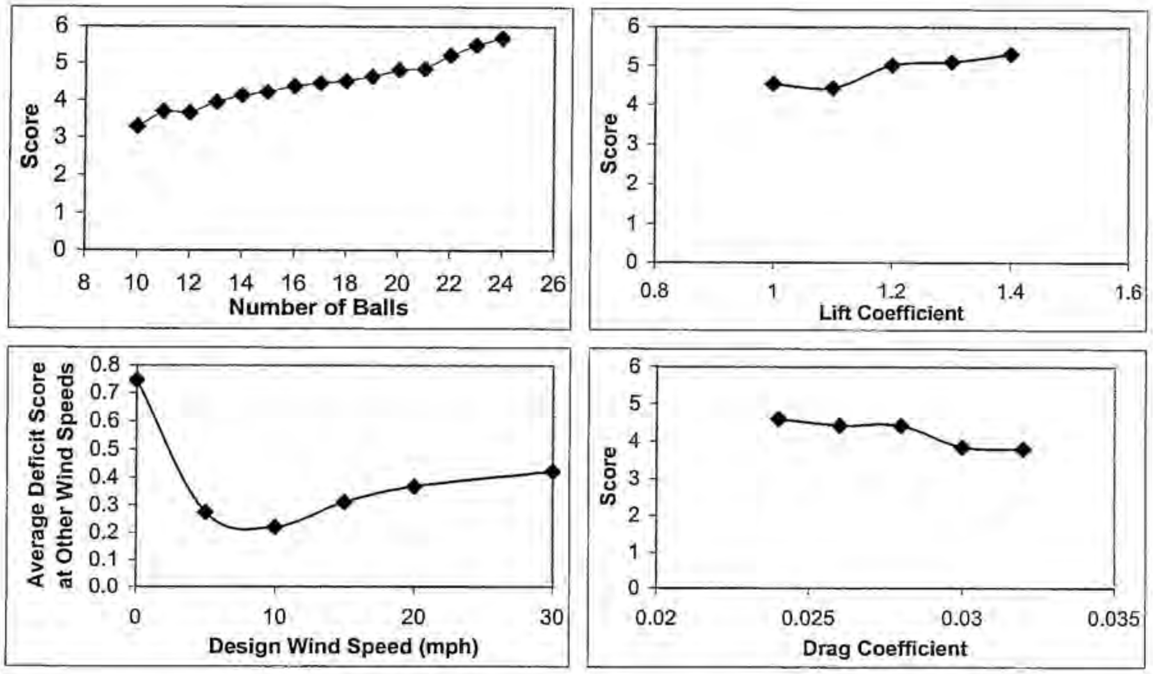

Figure 3: Sensitivity Analysis Graphics. From top left clockwise: Sensitivity to number of balls, lift coefficient sensitivity, drag coefficient sensitivity, and wind sensitivity.

3.1.2 Design Parameter Sensitivity Analysis

Sensitivity checks were made regarding other major parameters. The parameters consisted of the following: weight model of plane, lift and drag coefficients, ball configuration width, fuselage length, time of the ground, and wind sensitivity. The parameters were not flexible within the program and therefore could drastically affect the outcome if used improperly. The sensitive of the seven major parameters helped to optimize the plane and determine the desired values of the parameters within the program.

- Weight Model of Plane: Weight models for the plane were developed from historical data. These models included foam and graphite composite, foam and fiberglass composite, and wood. The weight models, when analyzed through the optimization, showed that the performance of the plane was very sensitive to the overall structural weight. Although, material could not be chosen from this modeling system, the weight model sensitivity did show that construction material selection would be very important to the final design.
- Ball Configuration Width: Ball width was modeled so that the ball configurations could be narrowed down into families of 2, 3, and 4 balls wide. One and five balls wide were discretely eliminated by the rules. Sensitivity to ball configuration proved to have little effect on scoring ability, but the three ball family had a slight advantage and was used in the rest of the analysis.
- Fuselage Length: Fuselage length was investigated for sensitivity by dividing the length into spaces needed to carry the payload and additional length for the nose and tail structures. A basic

drag model was developed to analyze the skin friction on the fuselage and an appropriately sized horizontal tail. The results concluded that the fuselage needed to be as short as possible, even if the result was a huge tail. The limiting factors were the forward and aft rake angles. The total length, taking into consideration the rake angles and three ball family, was analyzed using a combined aerodynamic and structures model.

- Wind Sensitivity: Wind sensitivity was investigated so that the performance could be optimized in preliminary design. To accomplish this goal, the six major parameters were optimized at various wind speeds and compared to other winds. Figure 3 shows an average score deficit for wind speeds from 0 to 30 mph. While each plane performed better in higher winds, softballs had to be dropped to get planes off the ground at lower wind speeds. The plane optimized at 10 mph was found to have the smallest average deficit. Preliminary optimization occurred at this speed.
- Lift and Drag Coefficients: Lift and drag coefficients were also analyzed. Analysis was accomplished by comparing the three optimal scoring capabilities of several lift and drag coefficients. Fewer batteries were required for higher coefficients of lift. The better performance prompted an airfoil study for higher lift coefficients, ranging from 1.2 to 1.4. The number of balls was limited by higher drag coefficients. Drag polars for several airfoils were found to match the lift range and lowest drag possible. Figure 3 also shows the sensitivity of score to lift and drag.
- Time on Ground: The final sensitivity analysis was the ground time. Results showed that ground time was a major factor, and that decreasing ground time would drastically boost the score.

3.1.3 Rated Aircraft Cost Analysis

Another concern was the impact that Rated Aircraft Cost (RAC) had on the design. To evaluate the RAC, a computer program was written to calculate the effects of the RAC parameters. The program was designed to calculate the RAC from a few configuration inputs. The major factor limiting configurations through the RAC was the total battery weight. The battery weight was counted in both the Rated Engine Power and in the Manufactures Empty Weight. Additionally, the Rated Engine Power Multiplier was the largest of the multiplier values. All three factors combined to give the weight of the batteries the greatest influence over the design. Other important factors were the wingspan, empty weight of the aircraft, and body length. To give an idea of the relative importance of these three components, the battery weight had a greater impact on RAC than all three of the other factors combined. Other factors, while not directly having a large effect on the RAC, greatly increased the importance of certain components. For example, the number of engines did not significantly increase the Manufacturing Man-Hours; however, when the power for the extra motors and the Rated Engine Power were considered, the impact of adding an additional motor became large. Using the RAC program, the rating of each configuration could be immediately evaluated.

3.2 Aircraft Configuration

Once the primary design parameters were identified and investigated, the various aircraft component alternatives were evaluated. For each major component, the Figures of Merit (FOM) were outlined and used to judge the various alternatives through a weighted decision matrix. The matrices determined the alternative that best meet the Figures of Merit.

3.2.1 Alternative Fuselage and Tail Configuration

Figures of Merit (FOM) in the analysis of the fuselage and tail configurations included:

- Rated Aircraft Cost: Since RAC strongly affects the overall score of the aircraft, RAC was heavily weighted.
- Take off and landing: From the design parameter studies, the takeoff lift coefficient and takeoff roll were key to producing a high scoring airplane. In the landing phase, ground effects would cause the plane to drift instead of landing quickly.
- Handling Qualities: Handling qualities were important due to the competition location. To fly an efficient circuit, the plane must be able to withstand gusty conditions and be moderately stable.
- Drag Performance: With battery weight counting twice in the RAC, a successful design must make efficient use of the available power and complete the mission quickly.

Once the design parameters and figures of merit for the fuselage and tail were defined, numerous configurations and combinations of configurations were considered. After the concept generation phase, the most promising alternatives were evaluated further. For further analysis, several assumptions were made including: The fuselage could be sized to hold the ball configuration; the propulsive efficiencies were approximately equivalent; and the difference in structural weight was negligible. The parameters could be considered constant during conceptual design because changes in the value of the parameters did not effect the conceptual configuration. Given the assumptions and the figures of merit above, the alternatives were evaluated as follows:

- Canard: The canard configuration had excellent stall characteristics; however, by preventing the main wing from stalling, this design limits the maximum lift at takeoff. The canard configuration had the added benefit of flexible motor setups, both tractor and pusher.
- Flying Wing: The flying wing had an obvious advantage in the RAC by removing the tail and tail control surfaces. The flying wing had some problems, namely extended takeoff roll and poor handling qualities in gusty winds due to a lower wing loading.
- Conventional: The conventional fuselage with a standard tail was set as a standard for comparing the various configurations. The conventional design was relatively straightforward with well-documented performance characteristics.
- Bi-wing: The biplane configuration was able to produce large amounts of lift with a smaller span.

However, the RAC counted the span of each wing and the chord penalty twice.

- Bi-wing, V-tail: A biplane configuration with a V-tail was also considered. The only significant difference would be the RAC advantage of the V-tail over the conventional tail, which resulted from few surfaces.
- Conventional, V-tail: A conventional fuselage with a V- tail had the same performance as the conventional tail alternative, but had the RAC advantage previously mentioned.
- Twin-boom: The twin-boom inverted V-tail had the same RAC benefit as the V-tail and could use either a tractor or pusher propulsion systems. The design would reduce the rigidity of the tail section and allow the booms to twist under loading reducing the handling qualities of the design.

In order to evaluate the Rated Aircraft Cost figure of merit for the various configurations, the RAC of each alternative was calculated. The results of the analysis are listed below with configuration, RAC value, and then the RAC benefits of that configuration:

- Flying Wing - RAC of 8.47 - does not have a horizontal tail surface or elevator servos
- Conventional Fuselage with V-tail - RAC of 8.77 - has passive vertical surface instead of active
- Twin Boom with invert V-tail - RAC of 8.77 - has passive vertical surface instead of active
- Conventional Fuselage with Standard tail - RAC of 8.87 - none, used as standard of comparison
- Canard - RAC of 8.87 - does not have an RAC benefit, equal to standard case
- Bi-wing with V-tail - RAC of 8.88 - has passive vertical surface instead of active, two wing penalty
- Bi-wing with conventional tail - RAC of 8.98 - no RAC benefit, two wing penalty

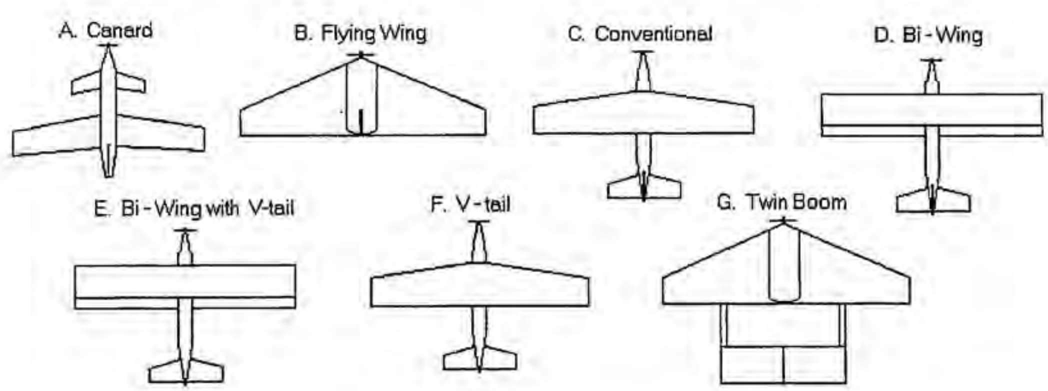

		Configurations						
Figures of Merit	Weighting Factor	A	B	C	D	E	F	G
Rated Aircraft Cost	0.4	0	1	0	-1	-0.66	0.66	0.66
Take Off and Landing	0.25	-1	-1	0	0	0	0	0
Handling Qualities	0.2	0	-1	0	0	0	0	-1
Drag	0.15	-1	1	0	-1	-1	0	0
Score	-	-0.40	0.10	0.00	-0.55	-0.41	0.26	0.06

Figure 4: Fuselage and Tail Configuration Weighted Decision Matrix

A weighted decision matrix was used to evaluate the alternatives according to the figures of merit to determine the configuration with the highest scoring potential. Weighting factors were assigned with different magnitudes according to the defined mission sensitivities. While RAC is the dominating factor, it is not the only consideration. For instance, while the flying wing has the lowest RAC, the poor performance of the design with regard to the other figures of merit limited its overall scoring potential. The results of the decision matrix can be seen in Figure 4. The highest-ranking fuselage and tail configuration is the conventional fuselage with a V-tail. This arrangement best met the figures of merit because of an improved RAC advantage and average performance qualities.

3.2.2 Alternative Wing Configuration

Figures of merit in the analysis of the wing configurations included:

- Payload Interference: In order to carry the maximum number of balls as the design studies indicated, while still minimizing internal volume and drag, the wing carry through structure should not consume a large portion of space allotted for the payload.
- Loading Payload: From analysis of the flight performance score, a minimum of time should be spent loading and unloading the payload. Therefore, wing locations that reduced the time of or interference with the loading process were awarded a higher magnitude in the decision matrix.
- Construction: The alternative selected must be within the team's construction abilities or the wing cannot be manufactured. The relative time and effort involved were estimated and compared.
- Landing Gear Interface: The gear interface was mainly a structural and construction issue. Low mounted wings provided a broader base for attaching the gear.
- Stability: The stability contributions of the wing location were estimated from historical data. High mounted wings typically provide roll stability, while low mounted wings can produce instability.

The three basic alternatives for wing location were considered: low, middle, and high wing attachment. For analysis the following assumptions were made: the taper ratio was one for better stall characteristics and ease of construction; the sweep angle was zero for ease of construction, low Reynolds number effect, and more efficient lift production; and the wing was sized to produce the necessary lift efficiently and proper wing loading for gust stability.

- High Wing: The high wing did not significantly interfere with payload volume but decreased the symmetric loading of the payload unless multiple hatches were built. The high wing produced roll stability without adding dihedral into the wings.
- Mid Wing: The mid-wing design would prove to be difficult to construct. Blending the body and wing was easier with the mid-wing design than the others considered, but the wing carry through structure would cause much more interference with the payload.
- Low Wing: The low wing alternative has less roll stability, which might require dihedral. The main advantages of the low wing were the light structural requirements and the minimal interference of

the wing with the payload configuration and handling.

Figures of Merit	Weighting Factor	High	Mid	Low
Stability	0.05	1	0	-1
Payloading	0.30	-1	0	1
Construction	0.20	0	-1	0
Payload Interference	0.30	1	-1	1
Gear Interface	0.15	0	0	1
Score	-	0.05	-0.5	0.7

Table 1: Wing Configuration Weighted Decision Matrix

The weighting factors of the wing decision matrix in Table 1 shows the relative importance of each figure of merit in the wing selection. While the payload and construction played a large part in the decision matrix, the stability and landing gear issues were secondary effects. Since the low mounted wing better addressed more of the important figures of merit than the other alternatives, the low wing rated the highest and was selected as the wing configuration for the aircraft.

3.3 Structural Configuration

3.3.1 Figures of Merit

A crucial area of the structural conceptual design was the development of figures of merit to represent mission objectives for each component to perform. The mission objectives chosen were designed to represent crucial areas within the competition that were affected by different structural components. The figures of merit which were developed for the conceptual structural design were:

- Scoring Potential: Each aircraft component had a direct effect on the ability the design to achieve a high score. Since the size, shape, and capability of each component can affect both aircraft performance and Rated Aircraft Cost, the design of each component is important to perform the mission in the most efficient way in order to maximize scoring potential this figure of merit is the overall result of all figures of merit analyzed.
- Strength and Weight: The weight of each component influences both Rated Aircraft Cost and aircraft performance in every phase of flight. Therefore the proper balance between the strength of a component and the weight of the component was necessary to determine.
- Formability: The ability to produce the desired component shape with the least amount of man-hours and components has an affect on the quality of the component, the overall weight of the structure, and the Rated Aircraft Cost
- Ease of construction: Certain construction techniques required more time and skill to produce complex shapes such as high camber airfoils and streamlined bodies. The ability to produce such shapes directly affected the capabilities of the aircraft in all phases of flight
- Repairability: During the flight-testing phase and the competition, minor to moderate damage was expected. On site repair of the damage was desired to reduce amount of time.

- Cost: While a score efficient structure was desired, the cost of certain construction methods and materials have a drastic affect on the validity of some concepts.
- Durability: During flight operations, the aircraft was expected to experience sharp winds gusts and hard landings. In order to be competitive, the aircraft had to withstand the conditions and operations of the competition through many cycles.

While the figures of merit were valid for all structures, several specialized figures of merit were developed for individual components. These figures included:

- Ground Tracking: The landing gear must be capable of precise aircraft maneuvering while the aircraft is on the ground. The mission advantage was to provide quick turnaround times between different phases of the mission sortie.
- Landing Performance: Also contributing to the aircraft score was time spent in the landing phase of the sortie. The ability for the landing gear to both endure hard landings and damp out the landing force with out springing the aircraft back into the air was important to achieving a time efficient landing maneuver.
- Chalked Fuselage Attitude: The attitude of the aircraft while static on the ground has the ability to facilitate or hinder payload-handling operations, which has a direct affect on ground time and thereby overall score.
- Braking: During the landing phase a quick, precise braking action reduced the time spent on the ground drastically. Importance was placed on using the braking power in the most efficient way.

3.3.2 Assumptions Made and Design Parameters Investigated

During the conceptual design phase assumptions were made to allow an unbiased look at different alternatives. For the four primary components analyzed, loading conditions were assumed based on simple models and historical data from previous competitions. Simple weight models were produced from available material samples. Previous experience with different materials and simple analysis validated strength estimates for conceptual studies.

During the conceptual design, parameters that had the most influence on score were identified for each primary component. The parameters influenced not only the structural design but also the conceptual studies of the aerodynamics and propulsion groups. The design parameters investigated for each structural component included scoring potential, efficient use of structural weight, strength, dimensional alternatives of the component, different material and construction alternatives, and effects on Rated Aircraft Cost.

3.3.3 Alternative Wing Structures

The figures of merit used to investigate wing alternatives were strength to weight ratio, formability, ease of construction, durability, repairability, and cost. Additional constraints were imposed on the wing design as a result of the functions of the wing: to generate lift and transfer that lifting force to the rest of the aircraft. To create lift, the wing had to be capable of holding an airfoil shape. For the high aspect ratio indicated by the mathematical model, the wing was required to be rigid enough to prevent a decrease in the angle of attack at the wing tips due to the aerodynamic loads. Due to initial estimates, the wing design was expected have an area of approximately 6 feet square and to experience a 3.4 g-load during a turn at maximum gross weight. Both the functions of the wing must be met on a weight budget for the wing to be efficient. Material alternatives and construction methods were considered. The three types were conventional buildup of lightweight wood skeleton and monocote skin, conventional buildup of carbon fiber skeleton and skin, and composite skin with foam core. Using the OSU historical database, a weight comparison was performed on the three concepts, seen in Figure 5.

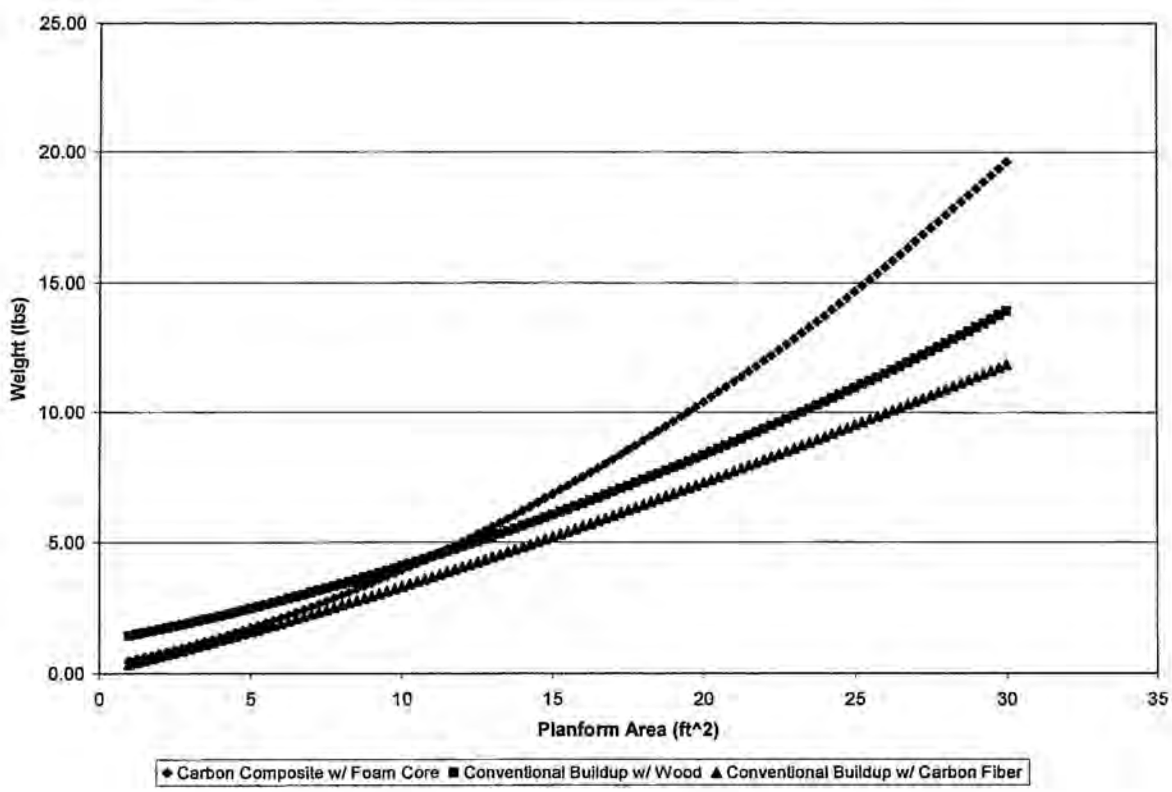

Figure 5: Wing and Tail Structural Material Comparison

Based on the models, the data concluded that composite construction with foam core had the greatest potential to produce the estimated wing area at the lightest weight possible. Composite construction using a foam core was advantageous because the foam allows for accurate construction and holds the shape through out the life of the wing. Table 2 is the weighted decision matrix used to evaluate the different construction methods. Based on the decision matrix the wing would be of composite skin with foam core construction.

Figures of Merit	Weighting Factor	Conventional Buildup with Wood	Conventional Buildup with Carbon Fiber	Composite Buildup with Foam Core
Strength to Weight Ratio	0.3	-1	1	0
Formability	0.25	-1	0	1
Ease of Construction	0.15	0	0	1
Durability	0.15	0	1	1
Repairability	0.1	-1	0	0
Cost	0.05	1	-1	-1
Score	-	-0.6	0.4	0.5

Table 2: Wing and Tail Structural Decision Matrix

In addition to the structural build up of the wing, conceptual alternatives for internal system components of the wing were generated. These included servos, wire routing, and how the wing will mate and transfer loads to the rest of the fuselage. A final conceptual sketch of the wing structure can be seen in Figure 6.

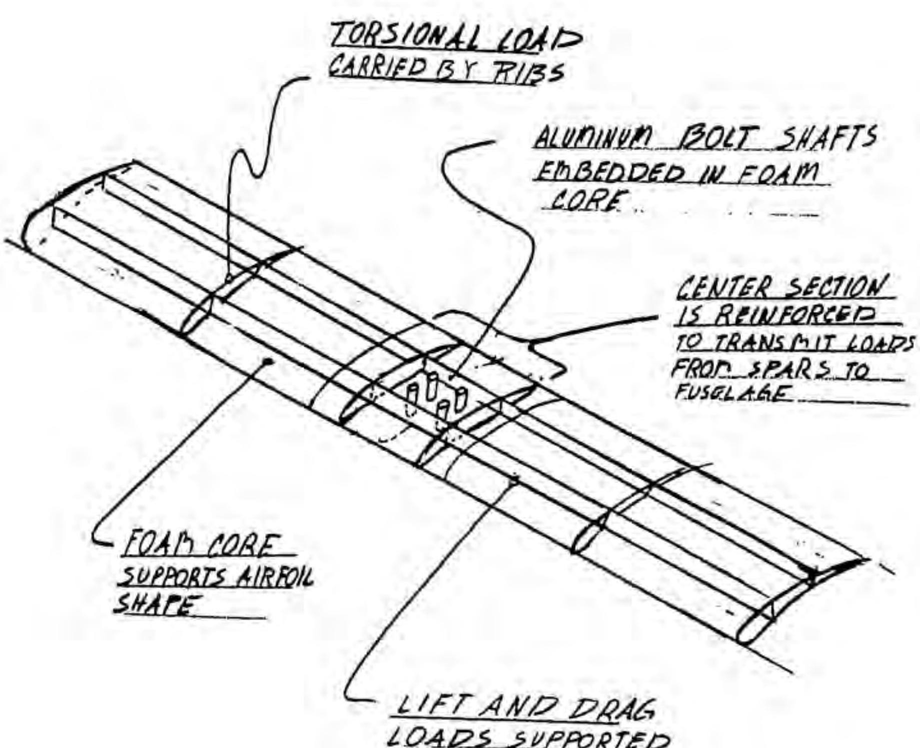

Figure 6: Final Conceptual Sketch of Wing Structure

3.3.4 Alternative Tail Structures

Similar considerations as those used on the wing were made for the tail. The figures of merit used to investigate wing alternatives were strength to weight ratio, formability, ease of construction, durability, reparability, and cost. The three types of tail construction alternatives were conventional build up of lightweight wood skeleton and monocote skin, conventional build up of carbon fiber skeleton and skin, and composite skin with foam core.

The function of the tail was to apply longitudinal and laterally stabilizing moments in order to provide control in aircraft pitch and yaw. The tail unit needed to be lightweight, durable, and able to adjust the incidence angle. Referring to Figure 5, composite construction with foam core showed to have the greatest potential to construct a rigid lightweight tail. Table 2 is the weight decision matrix used to evaluate the different construction methods. (The wing and tail decision matrices were created independently, but reached the same conclusions.) Based on the decision matrix composite buildup with foam core construction will be used to construct the tail. A final conceptual sketch of the tail structure can be seen in Figure 7.

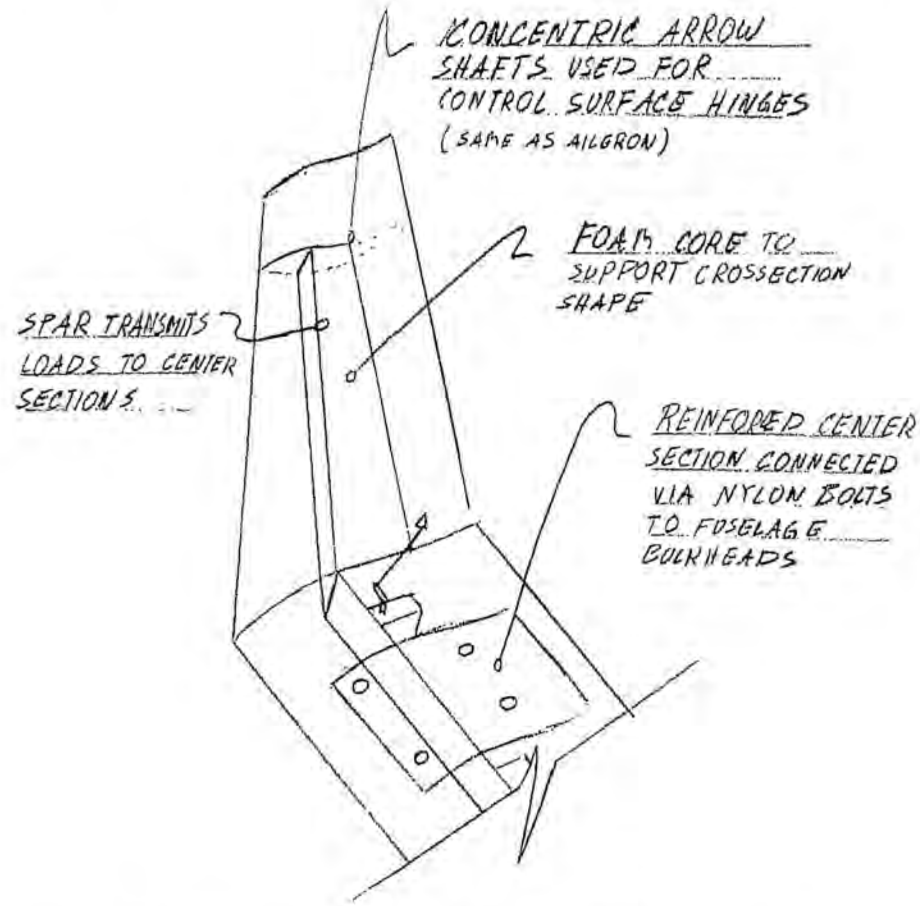

Figure 7: Final Conceptual Sketch of the Tail Structure

3.3.5 Alternative Fuselage Structures

The fuselage concept was developed as a combination of requirements. The figures of merit involved in the fuselage concept were: strength, formability, ease of construction, durability, reparability, and cost. The fuselage must be capable of handling the optimum amount of payload with the lowest drag possible while carrying all radio equipment, batteries, and the propulsion system. The fuselage also serves as the convergence point of all other aircraft components supporting the weight of the entire plane and transferring moments and loads between components. Several different construction techniques were evaluated, including convention buildup with wood, conventional build up with carbon fiber, solid foam construction, and monocoque.

- Conventional buildup with wood consisted of frames and stringer to carry loads and maintain shapes. The framework was covered with a slick monocote that has no load bearing capability. The method featured very lightweight construction but had the potential to lose the advantage if the structure was required to be very rigid. The method suffered from limited usable interior volume capacity due to the framework necessary to maintain a rigid shape. Complex contours were also difficult to achieve with the conventional buildup with wood and monocote method.
- Conventional buildup with carbon fiber was built up of the same frame work as conventional build up with wood however the use of carbon fiber skin allows loads to be transferred throughout the skin thereby eliminating the need for stringers. Frames were also replaced with bulkheads to support the payload deck as well as to stiffen the structure where needed. Complex contours were achieved with relative ease. The conventional buildup with carbon fiber method allowed a lightweight, sleek, and rigid body
- Solid foam construction consisted of a solid fuselage of foam coated with epoxy hollowed out for payload and equipment. The solid foam method afforded a very lightweight and shapeable fuselage. Drawbacks included component mating issues, reparability, and structural deficiencies.
- Monocoque fuselage consisted of a fully load bearing outer shell made of composite material built up on foam molds. Monocoque provided a very lightweight rigid structure that can be formed into almost any shape. Hatch lines were made very smooth and contours can be easily created to blend the fuselage into the different aircraft components. Bulkheads were still necessary to support internal structures but fewer were needed than with conventional buildup methods. Speed of construction as well as repeatability and reparability were all features of monocoque construction.

In order to evaluate the different fuselage construction methods, a decision matrix was formed based on the figures of merit: strength, durability, reparability, formability, ease of construction, and cost.

Table 3 illustrates the comparison of the four methods against the figures of merit.

Figures of Merit	Weighting Factor	Conventional Buildup with Wood	Conventional Buildup with Carbon Fiber	Solid Foam Buildup	Monocoque
Strength to Weight Ratio	0.35	-1	0	-1	0
Formability	0.25	0	1	-1	0
Ease of Construction	0.15	-1	-1	1	1
Durability	0.15	-1	-1	1	1
Repairability	0.1	-1	0	-1	1
Cost	0.05	1	-1	-1	0
Score	-	-0.65	-0.1	-0.4	0.4

Table 3: Fuselage Structural Concept Decision Matrix

Based on the figures of merit, monocoque construction showed the most potential for a lightweight, sleek, fuselage capable of carrying the required loads. The decision to use monocoque limited the fuselage material to carbon fiber and fiberglass. Preliminary design work was required to determine the material that provided the best balance between strength and weight.

3.3.6 Alternative Landing Gear Configurations

The aircraft landing gear system served several purposes and played an important role in payload handling and aircraft performance. The figures of merit used to evaluate different landing gear configurations were: ground tracking, landing performance, chalked fuselage attitude, braking, weight, ease of construction, aerodynamic drag, component mating, and cost. The different approaches to landing gear were first evaluated by overall configuration. Four landing gear configurations were considered: bicycle, tricycle, quad, and tail wheel (or tail dragger). The figures of merit considered for landing gear configuration included ground tracking, landing performance, rotated fuselage attitude, weight, ease of construction, drag, component mating, braking, component mating and cost. The decision matrix shown in Table 4 was used to evaluate the different landing gear configurations. Based on the decision matrix tricycle configuration was chosen as the best balance of all the figures of merit considered.

Figures of Merit	Weighting Factor	Tricycle	Quad	Bicycle	Tail Wheel
Ground Tracking	0.20	1	-1	-1	-1
Landing Performance	0.15	0	1	0	-1
Chaulked Fuselage Attitude	0.15	1	1	-1	-1
Braking	0.15	0	1	1	-1
Weight	0.10	0	-1	1	0
Ease of Construction	0.07	0	-1	-1	0
Drag	0.06	0	-1	1	0
Component Mating	0.06	1	-1	-1	1
Cost	0.06	0	0	0	0
Score	-	**0.41**	-0.04	-0.17	-0.59

Table 4: Landing Gear Concept Decision Matrix

Once the landing gear configuration was determined, three types of main gear were considered. The function of the main gear was to absorb energy during landing, to provide ground tracking, and to provide proper propeller clearance. The main gear needed to be lightweight, durable, and have low drag. Figures of merit used to evaluate the main gear included landing performance, weight, ease of construction, drag, component mating, and damping effects. Table 5 is the decision matrix used to evaluate the different types of main gear. Based on the decision matrix bow gear and leaf spring scored equally. These two designs were further tested in the preliminary design phase.

Figures of Merit	Weighting Factor	Bow	OLEO Strut	Leaf Spring
Landing Performance	0.25	0	-1	0
Weight	0.25	0	1	0
Component Mating	0.25	0	-1	0
Damping	0.15	0	0	1
Ease of Construction	0.07	1	-1	0
Drag	0.03	0	1	0
Score	-	0.07	-0.29	0.15

Table 5: Main Landing Gear Conceptual Decision Matrix

The nose gear of an aircraft was the primary steering mechanism on the ground. The nose gear also provided support for approximately ten percent of the total aircraft weight. Although ground weight loads were low, the loads placed upon the nose gear can be high during the landing phase. The nose gear provided accurate steering while under simultaneous axial and bending loads. Three types of nose gear were considered: Mouse trap (common dual strut nose gear), spring strut, and OLEO strut. The figures of merit considered for the nose gear included ground tracking, weight, ease of construction, cost, and lateral damping. Table 6 is the decision matrix used to evaluate the different types of nose gear. Based on the decision matrix the "mouse trap" style nose gear provided the best performance during the critical takeoff and landing phase when the highest loads are applied and steering was the most crucial.

Figures of Merit	Weighting Factor	Mouse Trap	Spring Strut	OLEO Strut
Ground Tracking	0.30	0	0	0
Longitudinal Damping	0.25	1	-1	-1
Ease of Construction	0.20	1	0	-1
Weight	0.15	1	0	-1
Cost	0.10	1	-1	-1
Score	-	0.7	-0.35	-0.7

Table 6: Nose Gear Conceptual Decision Matrix

3.4 Alternative Power Plant Configurations

The propulsion system had three main components: batteries, motor, and propeller. The rules limited the variety of components. Three major configuration ideas were considered: single stack, double stack, and shared electrical. Figures of merit (FOM) were developed to evaluate the three configurations. These included:

- Score Effects: The propulsion system had influence in every variable of the score function.
- Rated Aircraft Cost (RAC): The propulsion system is very influential in the RAC function.
- Power Produced: The power produced by the motor has direct effect on aircraft performance. Power also requires battery performance, which affects the weight of the aircraft and RAC.
- Weight: The battery weight was determined to consume the majority of the overall RAC
- Price: Although the highest performance possible was important, the cost of components limited the level of components used.
- Efficiency: The ability to produce the required performance with the lowest number of batteries was important in both aircraft flight performance and Rated Aircraft Cost.

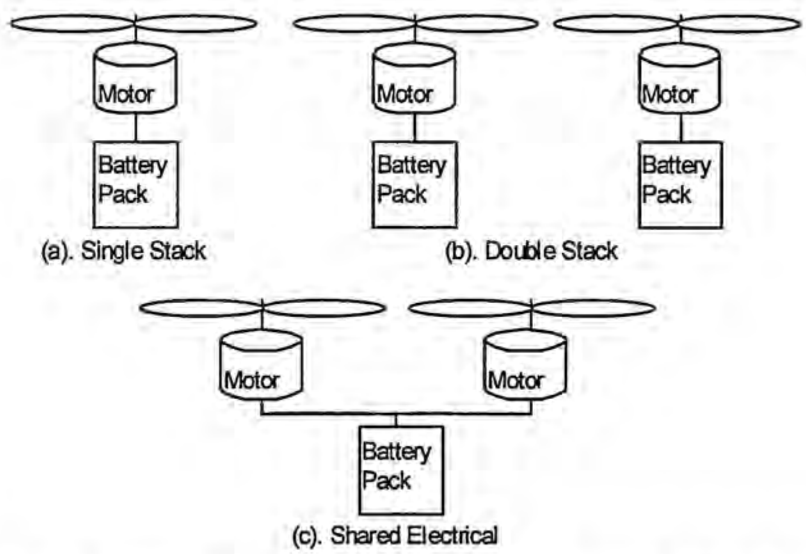

Figures of Merit	Weighting Factor	Single Stack	Double Stack	Shared Electric
RAC	0.35	1	-1	-1
Power Produced	0.25	-1	1	1
Weight	0.2	1	-1	0
Efficiency	0.15	1	-1	0
Total Number of Fuses	0.05	1	-1	1
Score	-	0.5	-0.5	-0.05

Figure 8: Battery-Motor-Propeller Alternatives and Propulsion Weighted Decision Matrix

Figure 8 shows the propulsion alternatives and decision matrix used to evaluate the different propulsion alternatives. From the decision matrix, the single stack was found to be the best option. The single stack had the lowest RAC and while meeting the required thrusts and speeds to achieve takeoff and climb. The single stack could provided enough power, thus eliminating the need for two motors. Another draw back to using two motors was the loss in efficiency. In the RAC equation, the battery weight was the most detrimental. Anything that can be done to make the system more efficient was desirable. In order to increase the efficiency of the engine, several cooling concepts were considered. The concepts investigated included air-cooled, water-cooled, and ice-cooled systems. An air-cooled system was chosen as the best concept based on cost, weight, and complexity. The battery packs were to moveable to adjust the center of gravity.

3.5 Analytical Tools

3.5.1 Optimization Program Architecture

The performance program was written to help analyze each phase of the mission individually as a contribution to the overall score. The program contained mathematical models for the structural weight, propulsive efficiency, and aerodynamic characteristics. The models were written into the program so that refinement and expansion could be done quickly and simply. The structural weight and propulsive models were constructed from OSU historical data, as calculated from component buildup. The aerodynamic model was constructed using a simple drag buildup method suggested by Jensen (1990) and the coefficient of lift corrected for aspect ratio of the wing. Characteristics, such as wind speed, takeoff lift coefficient, taper ratio, and sweep angle, were held constant and studied for sensitivity.

After the flight characteristics of the plane were calculated from the four models, the performance characteristics for each phase were calculated:

- The time and energy consumption required to takeoff under the 200-foot limit.
- Time, energy consumption, and power required to climb at a vertical speed of 3 fps.
- Time, distance and g-loading during turning were calculated from weight and stall characteristics.
- Time and distance to slow down from cruise velocity to stopping (without the use of brakes).
- Time in cruise given the selected power settings.

Finally, the times, distances, and energy consumption were summed and compared. The overall values of the three parameters were used to calculate total flight time, flight path distance, and total battery usage. Rated Aircraft Cost was further calculated, and the Flight Score was calculated using both flight time and RAC.

Score = Total Flight Score x Report Score / Rated Aircraft Cost

Further, limitations were placed upon several characteristics so to restrict the possibilities. The span was limited to 12 feet to keep the wing within reasonable structural parameters. Takeoff distance was limited to 200 feet, and battery usage to 100% of available. The limitations kept the performance characteristics within reason during conceptual calculations.

3.5.2 Other Methods Used

During the conceptual design phase, the various groups used weighted decision matrices to decide upon important decisions. Decision matrices were used so that the opinions of group members did not bias the decision, but rather the best configuration was chosen in a more numerical form. The graph of weight and volume effects along with RAC calculator were used to access parts of the factors input into the decision matrices. Strength to weight ratios found in historical data sheets were also used by the structures group to optimize the materials used.

3.6 Final Aircraft Configurations

When the final ranking phase was completed the design that stood out on top was the conventional fuselage with a low wing and V-tail, shown in Figure 9. The configuration had good handling qualities in heavy winds and a reasonable take-off distance. With the low mounted wing, access to the cargo bay from above allowed for fast handling of softballs. The V-tail produces a lower RAC value than a standard tail while still providing adequate control of the plane. The propulsion system was composed of a single propeller tractor setup. The wing and tail were to be constructed of a composite fiber and foam buildup. The fuselage was decided to be a monocoque design, and mousetrap and bow gear were found to be the best gear. The final configuration was the best compromise between all of the ranking factors.

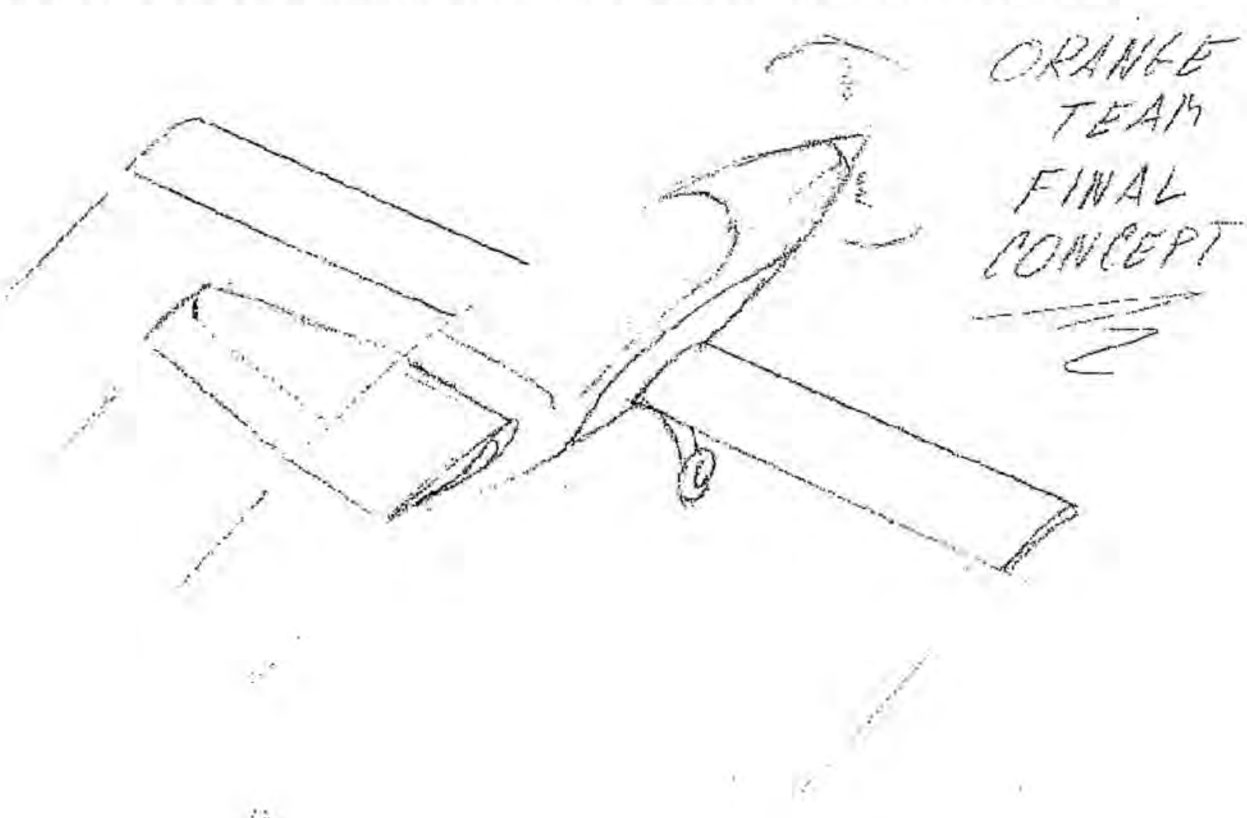

Figure 9: Final Plane Configuration

4.0 Preliminary Design

The preliminary design phase began as soon as the conceptual configuration was determined. The optimization program was refined with preliminary models and used to find parameters to begin the preliminary phase. The parameters were used as a guide to size the aerodynamic and propulsive systems. The wing and fuselage were sized using these parameters; then both were used to size the tail. The dimensions and tolerances for the components were passed on to the structures group so that the trade studies and structural analysis could be performed on primary structures. Finally, the propulsion group narrowed down the possible combinations for testing in the detail design phase.

4.1 Initial Trade Study Results

After the conceptual phase was completed, the weight, drag, propulsive, and Rated Aircraft Cost models in the optimization were updated. The previous models were considered conceptual simulations because the previous versions were developed from the OSU historical database, and the drag model was developed from a basic buildup method. The new performance program was enhanced so that the scoring potential could be maximized. The new program optimized features of the plane and helped develop trade studies for each parameter in relationship to final score. The optimization program was only able to output the local maximums for plane performance; the global maximum was solved by graphical means.

4.1.1 Study of Number of Batteries Required

The number of batteries was explored by considering the effects of battery weight on the aerodynamic performance and propulsive efficiency. Figure 10 shows the relationship of the number of batteries to the optimized score. The graph resembles an umbrella, as does the relationship of other parameters to score. The umbrella relationship shows a definite maximum value. The parameters near the top of the umbrella range from 15 to 20 batteries. The optimal number of batteries was found to be 18 cells with a weight of 2.43 pounds. The five-battery range gave the propulsive group a cushion of two or three batteries in either direction during analysis. Battery selection within the range did not affect the overall plane configuration or scoring potential.

4.1.2 Study of Take Off Battery Power Requirements

The power required from the batteries was not the propulsive throttle position or propulsive power, but the raw power that could be produced by the batteries given the base voltage and a maximum current of 40 amps. The graph of score versus takeoff power showed a similar umbrella trend that was seen in number of batteries. A band of the best values ranged from 625 to 880 Watts with an optimal value of 792 Watts.

Since both the number of batteries and the power required from the batteries during take off showed an umbrella trend, the relationship of takeoff power and batteries was investigated. Figure 10 illustrates the trend found during this investigation. The trend shows that score increased as the take off power reached the maximum power available in the batteries.

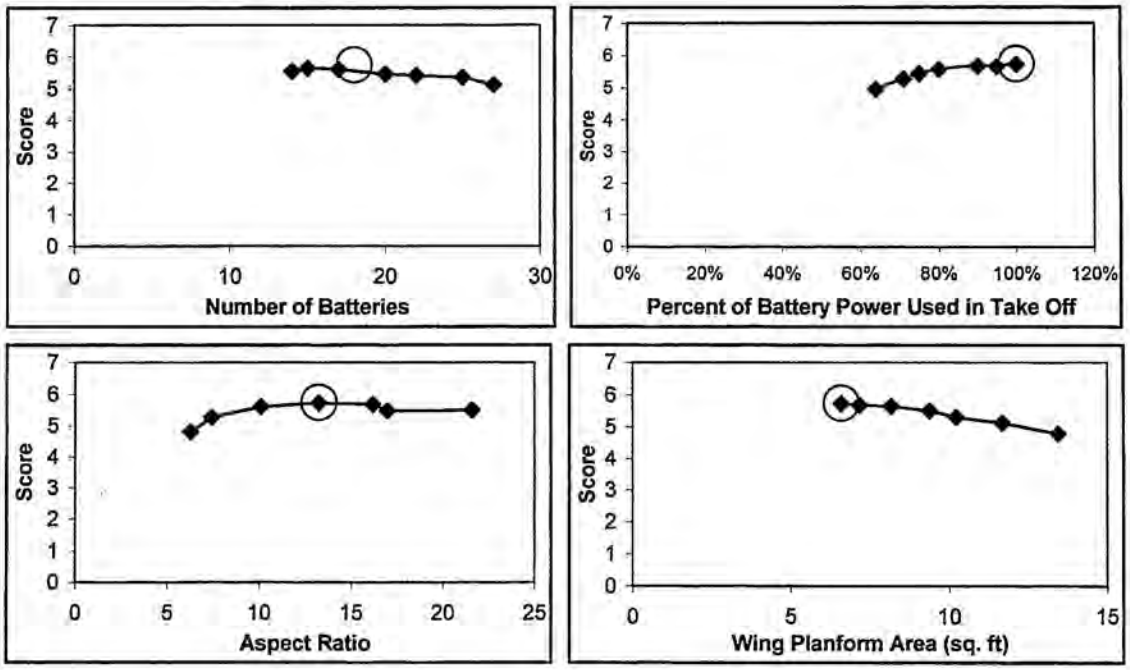

Figure 10: Tradeoff Analysis Results. From top left clockwise: Number of batteries required, takeoff power required as a percent of available power, wing planform area requirement, and aspect ratio requirement. Red circle represents the optimal value found by the program.

4.1.3 Study of Cruise Battery Power Requirements

Similar to takeoff power, the battery power required during cruise was also examined. The score comparison has maximums ranging from 355 to 580 Watts and an optimal value of 494 Watts. Again, the broad range gives a margin of safety for the propulsion group to work within.

4.1.4 Study of Wing Planform Area Requirements

The wing planform area was shown to have a linear relationship to score. The relationship existed on one side of the optimal value and dropped off sharply on the other side. The sharp drop was probably due to the added propulsive requirements to get the plane to takeoff under the limit of 200 feet. Adding battery weight added to the RAC and decreased ability to perform at cruise. Up to the optimal, the linear relationship seemed to represent the plane well because increasing the planform decreases cruise efficiency. All of the above features of the linear trend can be seen in Figure 10. The top 20 values were found to range from 6.25 to 8.2 square feet; the optimal was found to be 6.6 square feet.

4.1.5 Study of Wingspan Requirements

Wingspan was shown to have a rectangular relationship with optimal score. The rectangular scatter illustrated that many different spans can be considered optimal, but given other characteristic combinations. An optimal range of 8.5 to 10.75 feet was found with an optimal peaking at 9.5 feet. The values gave a good range to oversize or undersize the wing, which would be better explored through prototype experiments.

4.1.6 Study of Aspect Ratio Requirements

Since the optimization tended toward an efficient propulsive system, the optimal scores were graphed versus corresponding aspect ratios to illustrate the aerodynamic trends toward efficient planes. To some extents, aerodynamic efficiency was shown to be the trend. The optimal range of aspect ratios was found to lie at the top of another umbrella shape. The range of these values was from 10 to 17. The optimal configuration was found to have an aspect ratio of 13.25. The trend and optimal value can be seen in Figure 10.

4.1.7 Study of Plane Structural Weight Effects

Plane structural weight was found to be a large factor in the overall performance of the plane during the conceptual phase. The structural weight was again found to have a linear relationship with score. The relationship peaks within a range of 12.25 to 12.85 pounds; optimal being 12.73 pounds. Given the linear trend, any decrease in the overall structural weight of the plane increased the overall performance and score of the plane.

4.1.8 Study of Rated Aircraft Cost Effects

A final study of the effects of Rated Aircraft Cost on performance and score was completed during the preliminary phase. The study found that RAC was considered to be more of a factor than performance, to a point, when optimizing scoring potential. The optimization found a balance that minimized RAC while still keeping the plane within good performance parameters. The optimal plane had a RAC value of 8.91, within a range of 8.50 to 9.25 for the top 20 configurations.

4.2 Aerodynamic Considerations

Using the design parameters determined during the preliminary phase, further analysis of the aircraft was performed to refine the design. The areas examined included: wing area, tail sizing, fuselage lofts and stability and control. The concepts for each aspect were evaluated and then filtered.

4.2.1 Wing Figures of Merit, Assumptions, and Analysis

The figures of merit for the wing analysis included:

- Total Flight Score: Since the score is used to rank the aircraft for the competition, total flight score was set as the primary figure of merit. The wing sizes that produced the greatest scoring potential ranked highest. The flight score included the RAC effects of the configuration.
- Performance: Performance quantifies the effects not considered in the optimization; namely, tip strike, strength, and deflection. The performance merits tended to shorten the wing to ensure

that the wing could realistically achieve the characteristic calculated in the optimization. The wing was modeled in the optimization program to provide estimates of the flight score based on the wing area and span required for the mission profile. On the highest scoring configurations, the chord varied from 7.5 to 9.5 inches, and the wingspan ranged between 9 and 12 feet. The optimization also included other factors involved in the analysis of the wing dimensions, such as the takeoff power and cruise power. The power necessary for takeoff and cruise was related to the wing area through calculations of lift and thrust. Therefore, a study of the motor performance was necessary in the analysis of the wing dimensions. Another aspect of sizing the wing was deciding whether a greater chord length or a longer wingspan best achieved an increase in planform area. The wing span length was penalized heavily in the RAC calculations, while the chord was only a minor factor. Increasing the wing chord produced more wing area, but decreased the aspect ratio. Higher aspect ratios produced drag efficient lift production as predicted by the conceptual assumptions. The optimization program altered the constraints to find the best scoring configuration. The optimized wing was then slightly oversized to allow for both construction and aerodynamic margins of safety. The wingspan and chord were 9.5 feet and 8.625 inches, giving a wing planform of 6.83 sq. ft.

The coefficient of lift necessary for takeoff predicted by the optimization program was 1.2. Using the assumption of 80% of C_{lmax} at takeoff, the wing airfoil required a C_{lmax} around 1.5. A search on the NASG database produced several airfoils meeting the requirements. The Selig-Donovan 7062 and SG6043 were the most promising airfoils. When comparing these two airfoils, the coefficient of drag at both takeoff and cruise were examined. The SD7062 had a lower C_D at cruise, while the SG6043 had a lower C_D at takeoff. Since more time is spent at cruise, the lower C_D at cruise was better. Therefore, the SD7062 was selected as the airfoil for the wing; the lift and drag performance can be seen in Figure 11.

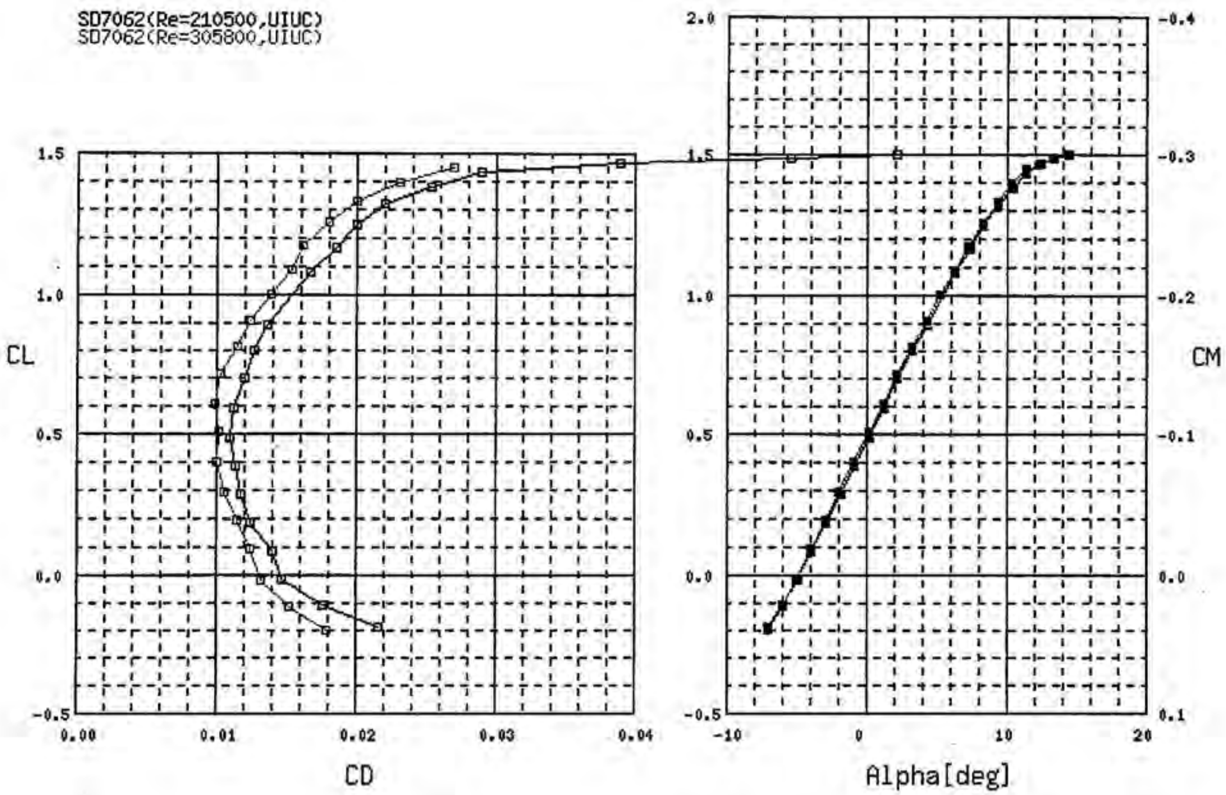

Figure 11: Drag Polar and Lift Curve for SD7062, Wing Airfoil. Cruise Reynolds number of 350,000 in red. Takeoff Reynolds number of 250,000 in black.

4.2.2 Fuselage Figures of Merit, Assumptions, and Analysis

The Figures of Merit for the fuselage analysis included:

- RAC: The main RAC affect of the fuselage was the body length. In order to reduce the RAC, the body length was minimized but still contained all components.
- Drag: The drag on the fuselage was minimized in order to reduce the thrust required ultimately decreasing the battery weight. The factors contribute to a higher score.

Further studies into the effects of the fuselage were performed to obtain better drag models and stability characteristics. During the conceptual design phase, the optimum number of softballs was found to be 24 balls. The payload configuration was determined by calculating drag effects from various fuselage cross-sections. Using the data gathered, the number and configuration of the balls governed the fuselage shape. The fuselage was broken into three sections: the propulsion compartment, cargo bay and tail section. The necessary area for each portion was evaluated independently. Propulsion equipment, such as the motor and speed controller, needed to fit within the confines of the forward compartment. The length of cargo bay was defined by the space necessary to hold the 24 softballs. In conceptual design, the length of the cargo bay and therefore the overall fuselage length were governed by the number and configuration of softballs. The governing factor in the tail section dimensioning was the rake angle for optimum performance. The propulsion equipment was arranged to fit within a 9 inch tapered nose section. The distance necessary for the cargo bay to hold the payload was 34 inches. A rake angle of 15 degrees was selected to minimize the drag due to flow separation while still considering weight and length. The angle was obtained from historical data. With a 15 degrees rake angle, the tail section is 14 inches in length. The three parts combine to form the total fuselage length of 57 inches. By designing the fuselage around the components, rather than vise versa, the length of the fuselage was minimized.

4.2.3 Tail Figures of Merit, Assumptions, and Analysis

The figures of merit for the tail analysis included:

- Performance: Two major performance factors were considered. The tail had to trim the airplane in cruise and produce the necessary pitching moment at takeoff.
- RAC: If the horizontal tail span exceeded a quarter of the wingspan, the tail was classified as a wing. The RAC effects must be investigated to determine which produced the smallest RAC.

Once the moments at cruise due to the wing and fuselage had been calculated, the moment required by the tail became a function of airfoil and root chord of the tail. The Selig 6063 and the NACA 0009 were the leading possibilities for the tail airfoil. The S6063 was selected for low drag and small lift coefficient at zero angle of attack. The S6063 airfoil required only minor adjustments of the control surfaces to trim at cruise resulting in less drag. Before the final sizing of the tail, the takeoff pitching moment was calculated and compared to the moment produced by the tail. The dimensions were then adjusted so that the tail produced the takeoff pitch moment. The parameters found for the tail can be seen in Table 8 on page 41. Note the area used in the calculations was smaller than the actual area. Some planform area was lost due to the taper of the fuselage. The conservative estimates used in the above analysis were expected to reduce the amount of deflection

Another factor influencing the tail decision included the RAC. If the projected horizontal tail span exceeded a quarter of the wingspan, the tail was classified as a wing by the RAC. Both alternatives were calculated to determine if the tail would score better if classified as a wing or V-tail. Once the tail was classified as a wing, the span and chord penalized the RAC and overall score. Therefore the RAC calculations proved that the tail span needed to stay within the quarter wing span limit. Conceptual design considerations assumed that the V-tail configuration would help to reduce RAC and boost scoring potential. Therefore the RAC calculations proved that the tail span needed to stay within the quarter wing span limit.

4.3 Structural Analysis

4.3.1 Figures of Merit

During the preliminary design phase several figures of merit were used to represent different mission features for structural design.

- Scoring Potential: Every aspect of each component had the potential to influence score through the ability to efficiently perform a task
- Weight: The weight of each component played an important role in both aircraft performance and rated aircraft cost.
- Ease of construction: The methods required to produce complex contours and shapes limited the validity of a design due to the required skill and materials
- Aerodynamic considerations: The design of the fuselage wing, tail, and landing gear influenced lift, drag, and aircraft stability. The effects that different components have on these aerodynamic considerations were examined.
- Allows easy loading and unloading of payload: In order to minimize time spent on the ground during sorties, the structural design needed not interfere with payload handling operations.
- Cost: The cost of certain materials and methods prohibited the validity of designs requiring them.

4.3.2 Design Parameters and Trade Studies Investigated

During the preliminary design phase parameters for primary components were identified for structural analysis. The design parameters investigated included:

- Material selection for the primary components
- Weights for primary components
- The number of spars required for the tail and wing
- The skin thickness of the wing and tail
- Spar shape and lay-up for both the wing and the tail
- Landing gear dimensions and spring rate
- Fuselage skin thickness and composite lay-up

During the structural analysis, different approaches to the design of each parameter were investigated to identify tradeoffs. The trade studies compared structural alternatives in the areas of material selection for each component, strength vs. weight tradeoffs, composite lay-up orientations, and component deformation and aerodynamic tradeoffs. Using information from the studies assisted in the design of each parameter to achieve each components highest scoring potential.

4.3.3 Wing Assumptions and Structural Analysis

While the wing was to be a single component that bolted directly to the fuselage, the analysis model of the wing was a cantilever beam that extended from the edge of the fuselage to the wing tip. For simplicity of the analysis, the lift and drag loads were assumed evenly distributed along the lengths of the wing portion. Since the bending stresses in the wing caused by the lift will be the dominant factors contributing to failure, an evenly distributed load assumption will provide a more conservative analysis. When the distributed load was resolved into a resultant point load, the load was applied further out on the wing compared to a resolved elliptically distribution. Therefore the calculated bending moment will be larger.

The same reasoning was used for justification for the drag load analysis. For buckling analysis the wing skins met the criteria necessary to be modeled as an Euler Column with one fixed and one free end.

A trade study on three spar cross-sections, a solid rectangular, a sandwich rectangular, and a solid C-channel was analyzed to determine which shape would provide the needed structural integrity with the least amount of material and weight. The analysis helped to decide whether one or two spars were necessary to carry and transmit the expected loads. The investigation included calculating the bending, shear, and axially tensile and compressive stresses that the spar would encounter under conditions of a fully loaded aircraft at a 3.4 g-load. At gross weight, the conditions resulted in a vertical wing loading of 0.08 pounds per square inch. The results of the spar analysis showed that one main spar located at the quarter chord of the airfoil would be sufficient to support the expected loads. The sandwich rectangular spar was the lightest spar configuration to carry the loads. The bending and shear stresses of the sandwich spar were significantly lower than the other two spars due to the larger moment of inertia obtained from the sandwich design. The axial stress was larger because the stress was calculated using only the cross sectional area of the outer shell of the sandwich, which was significantly lower than the areas of the other two spars.

The shear stress on the rib was calculated from the aerodynamic moment on the wing. The shear stress showed to be extremely low compared to the material properties of the carbon fiber. Only a two-ply rib was required to carry the load, and the weight of the ribs was almost negligible, at 0.08 ounces per rib. The maximum shear expected in the rib was calculated at 1391 psi.

The outer skin was modeled as a cantilever beam. The bending, shear, and axial tension and compression stresses were calculated using computer generated section properties for both the skin as a shell and the skin with a foam core. The results showed that due to the material properties of the carbon fiber, the wing skin withstood all of the expected loads without any internal structure, with the exception of the torsional stresses. The structural analysis was performed with the assumption that the carbon fiber lay-up was balanced and symmetrical, using a balanced weave prepreg material with no plies oriented in the 45 degree direction. The maximum bending and torsion stresses expected for the wing assembly were calculated to be 2283 psi and 1265 psi respectively. The critical load for skin buckling was estimated at 3693 lb.

For a carbon fiber lay-up of 4 plies on the spar and one ply for the skins, the wing failed in bending at the root. The factor of safety in bending was calculated at 5. The wing assembly structural weight was estimated at 1.9 pounds. In reference to the weight material comparison shown in conceptual design, the wing weight was found to be within 18% of the conceptual estimate.

4.3.4 Tail Assumptions and Structural Analysis

The moments created by the tail for longitudinal stability were a function of both the airfoil used for the cross section and the control surface deflection angle. The loading cases assumed for the structural design of the tail was the loads of a 20-degree ruddervator deflection at a flight speed of 85 fps. The loading case corresponded to an emergency control reaction at our highest cruise speed. Loads were also modeled from the aerodynamic moments and forces created by the airfoil. The stress analysis was performed in a similar manner to the wing analysis. All loads were assumed to be carried from the tail to the fuselage via a single carry through spar of rectangular cross section. The analysis was conservative because the moment of inertia provided by the carbon fiber skins of the tail was not accounted for.

For structural analysis the spar was modeled as a simple beam. The highest stress encountered was located at the root of the tail fin. The maximum bending and shear stresses were calculated to be 19000psi and 360 psi respectively. The deflection at the tip of the tail fin was calculated to be -0.43 inches. The angle of twist caused by the aerodynamic moment was calculated to be 0.086 degrees. The factor of safety was determined to be 4.2 under these loading conditions. The preliminary weight estimate for the tail was 0.98 pounds, 30% difference from conceptual design.

Estimates of the carbon fiber tail skins were sufficient to handle the loads with a reasonable factor of safety. Although the spar added weight, a tail spar was deemed necessary in order to provide a suitable load path into the fuselage. Figure 12 shows a transparency of the tail section to illustrate the spar design. The same flight scenario was used to determine the maximum static load applied to the graphite arrow shaft used for the hinges on the ailerons and the ruddervator. Analysis determined that a single graphite arrow shaft would deflect 0.15 inches. Testing proved that deflection still allowed smooth movement of the control surface.

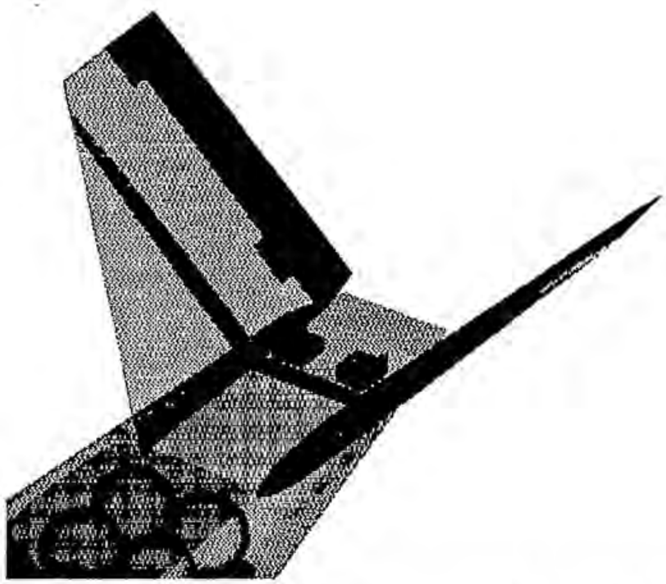

Figure 12: Transparent V-Tail Cut Away from the Rest of the Plane

4.3.5 Fuselage Assumptions and Structural Analysis

In modeling the fuselage some basic assumptions were made: Static analysis could be used when the fuselage of the aircraft was modeled as two cantilevered beams fixed at the center of gravity. The beams were modeled to represent the bottom half of the fuselage because the top half of the fuselage will be a non-load carrying payload access hatch. The center of gravity was fixed such that no rotation or translation was allowed. Dynamic tail forces were not included in the fuselage strength analysis because the aircraft was assumed to be in level flight. When applying loads to the fuselage, the following assumptions were made. All loads where modeled as point loads with a factor of safety of 1.25. The loads were developed as if the aircraft was fully loaded with 24 softballs and 20 batteries and experiencing a 3.4 g loading. Engine torque was also analyzed at maximum power settings. These assumptions were based on information from the preliminary design aerodynamic and propulsive studies and historical data.

The fuselage was broken into two sections in order to determine different inertia values at the relative location of the loads. Using singularity functions, the maximum bending stress was calculated to be 54,000 psi. Classical laminated plate theory with two plies of prepreg carbon fiber orientated at an angle of 45° relative to the axial direction of the fuselage resulted in a margin of safety of 72%.

4.3.6 Main Gear Assumptions and Structural Analysis

The analysis for the solid spring bow gear was modeled as a cantilever beam attached at the center of the fuselage. The general loading cases for the landing gear were developed based on information obtained from Raymer (1999).

The analysis began by establishing a wing tip scrape angle and a maximum gear height. The wing tip scrape angle was specified to be 13°, and the maximum gear height was set at 8 inches. The wing tip scrape angle was determined by a combination of historical data and research performed on aircraft with similar aspect ratios. Based on the above constraints and the length of the wing, the overall gear track width was calculated to be 38.70 inches with a fully extended angle of 28.3 degrees. The gear stroke length was calculated for a number of empty and loaded static loading cases. Tests were performed on two-wheel touchdown empty and loaded, and a one-wheel touchdown empty and loaded. Using the gear loading information, a gear load factor of 3 was assumed for normal two wheel landings. The value was found in Raymer (1999). The gear load factor caused the landing weight to increase by a multiple of 1.5 per wheel in two-wheel landing conditions. The landing weight was doubled for the one wheel landing analysis.

The stresses calculated included vertical bending stress and direct shear stress due to landing. The braking forces included horizontal bending stress and torsional shear stress due to wheel spin-up or braking. A horizontal acceleration of 10 ft/s^2 was used in the calculations. Because the gear was assumed to be made of a heterogeneous material and had a complex three-dimensional loading condition, advanced beam theory was used to determine the maximum stress at four key points in the main gear cross section. The upper and lower corners of the leading and trailing edge of the main gear were examined for failure. Angle of twist was calculated to finalize the spin-up and braking analysis. All calculated stresses were compared to their appropriate strengths in the form of factors of safety being calculated as well. The maximum bending and shear stress was calculated to be 17900 psi and 2000 psi respectively.

When the stress analysis equations were developed, attention turned to the design of the composite lay-up, which carries the various loads. Based on the nature of the torsional loads on spin-up or braking, 45 degree plies were needed in the lay-up. After studying several combinations of composite layers, a lay-up containing equal numbers of 90 degree and 45 degree plies proved to be the best in carrying the loads. Building the main gear entirely out of carbon fiber prepreg without sandwich construction requires 26 plies, weighing approximately 0.92 pounds. The factor of safety with this lay-up was estimated at 4.6

4.4 Propulsion Analysis

The preliminary design phase for the propulsion system involved construction of a computer program for optimizing the major components: batteries, motor, and propeller. The program simulated the complete propulsion system from the power used by the batteries to the power produced by the propeller in flight. Components were allowed to vary in such a way as to match and/or exceed the output values estimated for thrust, current, power, and efficiency for the overall propulsion system. Estimated values were provided from the optimized aerodynamic aspects of the plane.

Four propulsive components were varied in the optimization program: battery cell count, propeller dimensions, motor-size, and gearbox ratio. Battery cells were considered based on the cells that produced the best energy density (amp-hour/weight). The SR 2400 mah was determined to have the best energy density. The dimensions for the propeller were based on the relationship between diameter and pitch. A range of propellers was used to vary the performance characteristics. Six motor series were examined for the program: the Astro Cobalt 25, 40, and 60 and Astro FAI 25, 40 p/n 642, and 40 p/n 643 series. For simplicity of the design, the gearboxes were based on those available for AstroFlight motors. The gear ratios chosen for analysis were 1:1, 1.68:1 and 3.1:1. The pitch/diameter (p/d) ratio of the propeller was first varied. For higher p/d ratios, the speed and efficiency at cruise were better than the lower p/d propellers. Significant increase in the number of batteries was required to produce the desired speeds with lower p/d ratios. The gear ratios, battery cells, and propeller ranges were combined with the six motors to form a variety of configurations. Analysis was performed for the optimum configuration. The Cobalt series motors were compared to the FAI series motors. The analysis of these comparisons is shown below.

4.4.1 Figures of Merit

Figures of merit were developed to evaluate the design parameters. The figures of merit represented the relation between efficient propulsion system and the competition goals and regulations. The figures of merit used were:

- Score: In all aspects of the design, score was the ultimate figure of merit. All aspects of every design decision had the potential to influence the overall scoring potential of the aircraft
- Efficiency: The propulsion system affected score in both flight performance and Rated Aircraft Cost. Efficiency of each part was optimized to offer good performance in both areas
- Weight: The weight of the propulsion system was determined to be a large player in the Rated Aircraft Cost because battery weight was heavily penalized. Therefore reducing the weight of the batteries as well as other propulsion system components can provide a dramatic score improvement
- Current: The current draw on the batteries was a limiting factor set forth by the competition regulations
- K_V Values: The K_V Value of a motor was a ratio that relates RPM to voltage. Selecting a motor with the proper K_V Value allowed thrust to be produced at acceptable current levels
- Energy Density: The energy density of the batteries was crucial to determining which batteries provided the most energy with the lowest increase in battery weight.
- Historical Data: Historical data was invaluable in predicting efficiencies and performance during the trade studies performed on the different propulsion components.

4.4.2 Design Parameters and Trade Studies Investigated

Several design parameters were involved in the design of the propulsion system. Studies on the tradeoffs between the parameters were used to evaluate different combination of batteries, motors, and propellers.

- P/D ratios: By fine-tuning the ratio of propeller pitch to propeller diameter, it was possible to increase the efficiency of the motor and thereby reduce the number of batteries required.
- Propeller Diameters: The propeller diameter has a direct affect on the amount of current required to maintain an RPM setting. Since the propulsion system is limited to 40 amps of current the propeller diameter was a limiting design parameter.
- Number and type of batteries: Overall aircraft efficiency was a crucial parameter on the competition. An efficient propulsion system would find the optimum balance between power produced and batteries required. Balance was crucial to reach the aircrafts maximum scoring potential.
- Size and type of motor: Different motors were optimized for operation in specific ranges. Motor selection was important with the most potential to operate efficiently under the predicted flight constraints

4.4.3 Weighted Decision of Motors

The results of a weighted decision matrix were analyzed for the Cobalt series motors and the FAI motors. For the Cobalt 25 and 60 series motors, the optimal configurations produced thrust for takeoff due to much current or the number of battery cells required to produce the thrust was out of range of interest. Therefore, the motors compared in Table 7 were the Cobalt 40 and the FAI series motors. From the decision matrix, the efficiency for the Cobalt was much lower than the FAI series. Furthermore, the Cobalt series motor was determined to require more battery cells than the FAI motors. Results from the decision matrix show that the FAI motor series score were all fairly close in relationship with each other. To determine which motor was best for the design, other parameters must be considered.

Figure of Merit	Weight	Cobalt 40	FAI 25	FAI 40 / 642	FAI 40 / 643
Number of Batteries	0.3	0.7	0.9	1	1
Current	0.25	1	0.8	1	1
Takeoff Thrust	0.25	1	1	1	1
Cruise Power	0.1	1	1	1	1
Efficiency	0.1	0.5	0.9	0.8	1
Score		0.86	0.91	0.98	1

Table 7: Motor Weighted Decision Matrix

4.4.4 Investigation of Astro FAI Series Motors

To determine which FAI motors would be more desirable, the following analysis was performed on the motors. Each motor was analyzed individually to find the optimal gear ratio and propeller sizes. Each motor was then graphed vs. airspeed velocity for the following parameters: current, thrust, efficiency, and power. The results were analyzed using a constant number of battery cells since the range for the FAI was determined to be similar. Figure 13 displays the current verses velocity. The FAI 642 drew the highest current load for the optimum conditions while the other two motors drew similar current loads. Similarly, analysis of the power drawn from batteries was lower for the 25 and 643 series motors since drawn current was lower, shown in Figure 13.

Thrust analysis can also be seen in Figure 13. The thrust for the 642 was higher than the 25 and the 643. All three motors had a broad efficiency band around the designed airspeed. The best efficiency around designed airspeeds was determined to be the 643, with a broad band but peaked out near the designed airspeed.

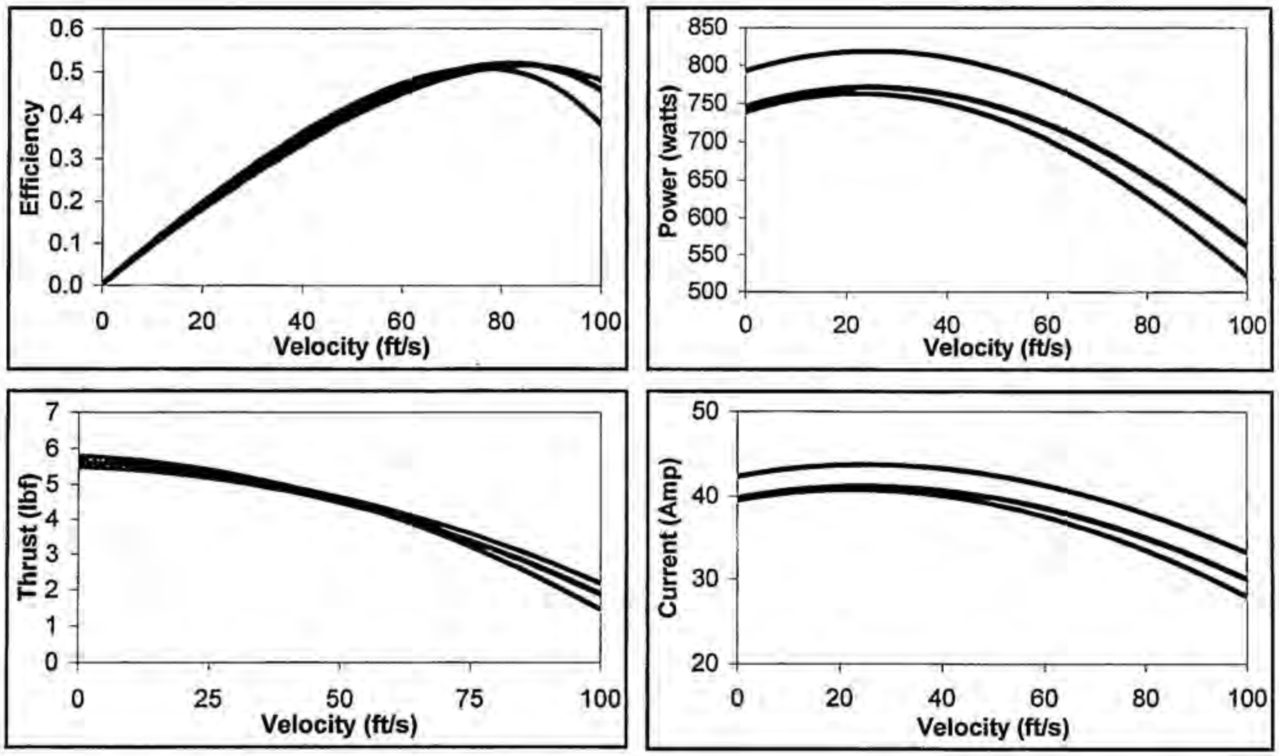

Figure 13: FAI Motor Performance Data. From top left clockwise: Efficiency, power available from the batteries, current, and takeoff thrust. Blue represents the FAI 25 motor, red represents the FAI 40 p/n 642 motor, and black represents the FAI 40 p/n 643 motor.

4.4.5 Motor Selection

The Cobalt motors had lower efficiencies for the designed airspeeds and required currents than the FAI motors. The required number of cells for the Cobalt motors was also higher then the FAI motors. Because of the trend between motors, the FAI series were chosen. All of the FAI motors had similar characteristics. The efficiencies for all three motors were fairly close. The FAI motors seemed to perform best at a p/d of 0.8. The FAI 40 p/n 642 was not chosen because the 643 had a better airspeed efficiency while keeping every thing else constant. The FAI 25 and 643 had similar efficiencies and takeoff thrusts. The FAI 642 required a current greater then 40 amps for takeoff, while the 643 required a slightly smaller current. The simulation was done for a specific head wind. For different head winds, a larger range of propellers could be used on the 643 than on the FAI 25 without drawing too much current for an extended period of time. Based on historical data, propellers with a p/d ratio of approximately 0.8 and a diameter of 13.5-15 was determined. Based on these factors, the FAI 643 motor was selected with a gear ration of 1:3.1, a battery pack size of 17 cells, and propeller size of 13.5-15.

4.5 Analytical Tools

4.5.1 Optimization Program Architecture

After the conceptual phase was completed, the weight, drag, propulsive, and Rated Aircraft Cost models in the optimization were updated. The previous models were considered conceptual simulations because the previous versions were developed from the Oklahoma State historical database, and the drag model was developed from a drag buildup method. The following models describe the updates to the program:

- Weight Model: The weight model was reconstructed according to the structural and propulsive assessments presented earlier in the conceptual design phase. The weight model was checked against the OSU historical data and the previous weight model.
- Drag Model: The drag model was reconstructed according to the drag build-up method found in Raymer (1999). The method gave a closer estimate of drag without requiring the parameters developed in the preliminary and detail design phases. The drag model also included the drag polar and lift curve for the chosen airfoil. Different values were used for both cruise and take off Reynolds numbers. Conservative margins of safety were also placed on the model (approximately 25%).
- Propulsive Model: The propulsive model was compared to the analytical model used by the propulsion group in their analysis. The model showed that the conceptual model had been too conservative. The new model was reconstructed to remain conservative yet represent the propulsive system better than the conceptual model.
- Rated Aircraft Cost Model: The RAC was also updated to meet all the RAC requirements, and better represented the features chosen in the conceptual design phase.

The drag, weight, propulsive, and RAC models were placed in the program along with the parameters that best support an optimal design. The values included a wind speed of 10 miles per hour, nine softballs, and a lift coefficient of 1.2. The program was adapted so that the scoring potential was maximized and trade studies occurred using the optimization process.

4.5.2 Other Methods Used

Other than the optimization, several other programs were used to calculate various parameters of the design. Classical stability derivative analysis was used to size the horizontal and vertical components of the V-tail. An analytical propulsion model was use to compare several combinations of motors and propellers to narrow down the wide range of options. The weight and center of gravity was also calculated using another program. Each structural analysis for each component was completed using several different spreadsheets so that as changes occurred, the updated structural data could be calculated. Initially sizes and component placements were laid out in a two-dimensional full-scale station line chart using yarn and construction paper to represent components and contour lines placed on pegboard. Then the layout was transferred to the CAD program for three-dimensional modeling.

4.6 Final Aircraft Configurations

At the end of the preliminary phase, the primary components of the configuration were all sized and placed according to the figures of merit. The wing was sized with a span of 9.5 feet and chord of 8.625 inches. The tail was sized so that the planform area of 1.3 square feet was kept within the quarter span of the wing. The fuselage length was minimized using the greatest suggested rake angles. The propulsion system was narrowed down to a few motor and propeller combinations to be tested in detail. The spars and ribs in the wing and tail were sized, along with the makeup of the fuselage monocoque design. The gear was designed so to soften landing shock while not causing the plane to bounce back into the air. A three dimensional model of the primary components was also completed.

4.6.1 Wing and Power Loading

Wing and power loading for the preliminary configuration was 3.5 lb/ft^2 and 47.4 lb/hp. The two loading values were a compromise to achieve the correct mission balance and achieve the best scoring potential. Higher wing loading allowed the plane to penetrate through the wind better, achieve higher cruise velocities, and makes the configuration less susceptible to gusting conditions because greater changes in pressure differential are required to disturb the plane. Drawbacks to high wing loading occurred at takeoff and climb. Higher wing loading was not helpful during the critical phases. To overcome the wing loading disadvantage, higher power loading was required to help the plane overcome takeoff and climb requirements. Therefore, a compromise was met between wing and power loading to result in the preliminary configuration.

5.0 Detail Design

After the primary components were sized in the preliminary phase, secondary components were sized and added. The aerodynamics group determined the dynamic stability as well as performance estimates and aircraft handling qualities. Hardware for component mating and control surface integration were selected. Manufacturing processes and tooling were developed to construct the aircraft and detail drawings for manufacturing the aircraft components were produced by the structures group. The propulsion group used the preliminary system combinations and experimental data to decide on the final propulsion configuration and number of batteries. The final configuration was then constructed and tested as a prototype to determine problems that had been previously overlooked.

5.1 Aerodynamic Performance Analysis

The optimization code was modified to provide data on the flight performance of the final configurations. The use of an airfoil analysis program allowed the characteristics of the airfoils of the wing and tail to be included in the analysis. The following sections contain results from the two computer codes, representing how the plane would perform.

5.1.1 Final Configuration Features

The final aircraft configuration is fairly conventional consisting of a low mounted wing with a large aspect ratio, approximately 13.2. The fuselage is contoured around the interior components creating a streamlined and drag efficient body. The tail is a V-tail configuration with the span of 1.75 feet, the quarter wingspan limit to avoid the RAC penalty if the tail was classified as a wing. The fins of the V-tail are approximately 40 degrees from the horizontal with a taper ratio of 0.5. The landing gear, which is 8 inches tall, provides a tail scrape angle of 25 degrees for safe pitching at takeoff. The wings can rock 13 degrees on takeoff before scraping the runway. All major components are designed to shear off under severe loading to dissipate the energy and reduce the damage sustained by the aircraft. A more complete description of the aircraft configuration features is listed in Table 8.

Fuselage	
Length	4.77 ft
Maximum width	12 in
Tail Properties	
Airfoil	S6063
Span	1.75 ft
Chord at root	14 in
Chord at tip	7 in
Projected horizontal area	1.53 ft^2
Projected vertical area	1.07 ft^2
Taper ratio	0.5
Incidence angle	0^o
Angle to horizontal	40^o
Ruddervator area	41.1 in^2

Wing	
Airfoil	SD 7062
Span	9.5 ft
Chord	8.625 in
Area	6.63 ft^2
Incidence angle	0^o
Aileron area (per wing)	57 in^2
Total aircraft	
Center of gravity location	25 in
Maximum weight	23.7 lbs
Number of softballs	24
Weight of softballs	9 lbs
Rated Aircraft Cost	8.765
Score (without Written Score)	1.75

Table 8 : Final Aircraft Configuration Features

5.1.2 Estimated Mission Performance

The estimated mission performance of the configuration was calculated from the performance code used in the optimization. Each stage of the mission was individually evaluated. The time consumed for each step was of particular interest. Table 9 shows the time spent in each portion of the mission profile. The time spent in cruise, both loaded and unloaded, was the total time at cruise velocity, including all turns and straight legs. Also included in Table 9 were the expected flight velocities and distance of each phase. The performance information was calculated assuming a wind speed of 10 mph. Accounting for all phases of the mission as well as the RAC, the aircraft was predicted to score 1.75 times the report score.

Mission Components	Time Performed	Time Spent	Distance	Velocity
Takeoff unloaded	2	2.6 sec	37.81 ft	44.25 fps
Climb unloaded	2	10.2 sec	---	46.25 fps
Cruise unloaded (all 4 laps included)	1	89.2 sec	---	85.13 fps
Slow down unloaded	2	14.4 sec	---	---
Ground time for loading	1	45 sec	---	---
Takeoff loaded	1	8.6 sec	180 ft	56.10 fps
Climb loaded	1	24.1 sec	---	59.14 fps
Cruise loaded (both laps included)	1	75.8 sec	---	79.61 fps
Slow down loaded	1	9.11 sec	---	---
Ground time for unloading	1	45 sec	---	---
Total Time	---	5.85 min	---	---

Table 9: Time Spent in Mission Phases. Value predicted by performance program.

5.1.3 Takeoff and Climb

The takeoff distance for loaded conditions was 180 feet from the optimization code. Takeoff velocity was approximately 55 fps. The plane needed to accelerate after takeoff to a velocity of 60 fps to maintain the proper climb speed. For unloaded conditions, the takeoff distance decreased significantly to 40 feet, and takeoff velocity also decreased to a speed of 45 fps. When the plane accelerated to climb velocity at unloaded conditions, the plane moved at an airspeed of 47 fps. The time for takeoff and climb scenarios can be seen above in Table 9. The power loading at takeoff was determined to be 47.4 lb/hp, when the plane was fully loaded with softballs.

5.1.4 Flight Conditions

The aircraft was designed to perform best in a 10mph wind. At this wind speed, the empty cruise speed was projected to be 85.1 fps while the loaded speed was projected at 79.6 fps. When the plane carried the 9-pound softball payload, the wing loading is 3.5 lb/ft^2.

5.1.5 Handling Qualities

Once the final dimensions were known, the handling characteristics were calculated and trimmed to satisfy stability requirements. For example, the pitching moment contributions of each component were calculated and then summed to evaluate the pitching characteristics of the entire aircraft. Figure 14 shows the effect of each component on the total pitch moment. From the graph, the aircraft trimmed at 1.25 degrees angle of attack in cruise. The static margin was also calculated and found to be 13%. While the value produces a more stable plane, the preliminary estimates ranged from 5% to 10%.

Other handling qualities of interest were the control power derivatives, which are also listed in Figure 14. The control power was found with an airfoil program by determining the change in lift on the surface due to the deflection of the control surface. After correcting for the aspect ratio, the change in lift was converted into the appropriate moment and non-dimensionalized. The equations used in the static stability and control power analysis were obtained from Raymer (1999) and Nelson (1998).

Test flights of the prototype revealed even more handling quality issues than expected. One critical factor was the visibility of the aircraft. Without visual cues to help the pilot determine the orientation of the plane, maneuvers performed at the distant ends of the circuit become very difficult. This problem was compounded by designing the plane to be only slightly roll stable. The prototype testing also demonstrated the pitch and weathercock stability of the aircraft in takeoff under windy conditions.

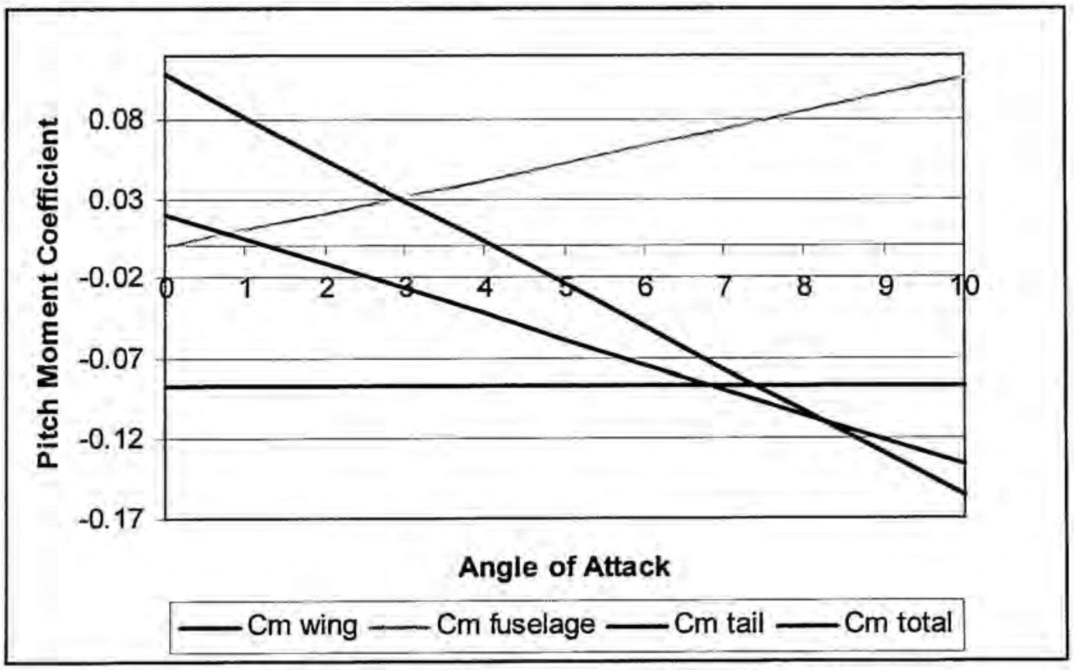

Static Margin	CLα	Cmα	Cnβ	Clβ
13%	5.05	-0.895	0.085	-0.016
Cmδe	Cnδr	Cnδa	Clδr	Clδa
-1.16	-0.0480	-0.0142	0.0147	0.194

Figure 14: Coefficient of Moment of Aircraft Components Versus Angle of Attack and Stability Derivatives

5.2 Propulsive Performance Analysis

The final propulsion system was designed in the preliminary phase using analytical methods. Using a dynamometer, the propulsion group tested several of the top motors that remained at the end of the preliminary phase. The final motor and propeller combination was decided to be the AstroFlight 643S, an FAI 40 motor with a super box, and a 14.4 inch diameter propeller with a p/d ratio of 0.8. A gearbox was not needed for this combination to produce the thrust and velocities required. Seventeen batteries were needed to produce the thrust. The batteries were decided to be 2400 milliamp hour, high rate, SR NiCad batteries. The final output from the above propulsion setup was found to be a takeoff thrust of 4.8 pounds, using approximately 760 watts from the batteries. Cruise thrust was found to be 1.9 pounds and only drew 490 watts from the batteries. The above values and setup were used in the construction of the prototype and refined the optimal results.

5.3 Structural Considerations

The focus of the detail design phase was the integration of the primary components with each other and the various systems comprising the aircraft as a whole. The details of the four major aircraft components, the fuselage, wing, tail, and gear, were designed to insure form, fit, and function of each component.

5.3.1 Fuselage Structural Details

The form of the fuselage was designed to accommodate the internal components and payload while exhibiting the lowest drag possible. Fuselage design was accomplished using CAD to shape the fuselage around internal components while minimizing wetted surface area. The contours of the fuselage were also designed to blend from one component to the next in a way that minimized interference drag between components. Functionally, the fuselage served as the junction between all aircraft systems, components, and payload. Propulsion system components were arranged in a fashion that would minimize wire length between components. The close packed configuration also allowed airflow to be routed from a chin scope in the forward bulkhead over the motor and around the battery packs. The payload deck was designed to be lightweight and removable. Lightening holes in the payload deck acted as cradles to secure the softballs during flight as well as permit precise loading and unloading. The payload deck was supported by the wing carry through section and both the forward and aft bulkheads. The payload hatch was designed to be removed in a simple quick motion allowing quick turn around times. The hatch release mechanism consisted of a four pins mounted on the fuselage, which slide into grooves cut into the payload hatch. The mechanism allows the hatch to be removed with a simple push, slide, and lift motion. Another factor in ground time was a fuse that could be easily and quickly removed. Finally, component weights and station locations were entered into a weight balance spreadsheet, Figure 16, to keep track of aircraft inertial properties and to place the aircraft center of gravity at the center of lift.

5.3.2 Wing Structural Details

The internal wing structure was comprised of four ribs, a full-length spar, and blue foam core. The foam core holds the airfoil shape while the spars and ribs provide load paths to the fuselage. Accommodations for the aileron servos were made in the two outboard spars, which can be accessed via removable plates on the lower surface of the wing skin. The plates were included in the wing lay-up during construction to ensure a snug fit and are secured by small screws. The hinge mechanism for the aileron was designed to minimize the gap between the aileron and wing surface. Graphite arrow shafts were embedded into the wing core and into the aileron before the wing skins was applied and cured. After curing a second smaller graphite shaft was inserted though the tip of the wing into the larger shafts. The shafts in the aileron pivoted around the smaller concentric shaft creating a low friction lightweight hinge. The wing was also designed to breakaway in the incident of a crash. The breakaway design was to minimize damage to wing as well as the rest of the fuselage. The wing carry through section in the fuselage was designed to allow the wing to shear off the aircraft without damaging the structure. The breakaway was accomplished through the use of nylon connector bolts that are designed to fail under the high shear loads associated with a wing tip strike. The connecting wires for the servos embedded into the wing were also designed to shear without damaging the servos. Using CAD, design goals were incorporated into the wing without distorting the airfoil shape. Figure 15 illustrates the component configurations used to efficiently use available space and the contour the shape around the interior layout.

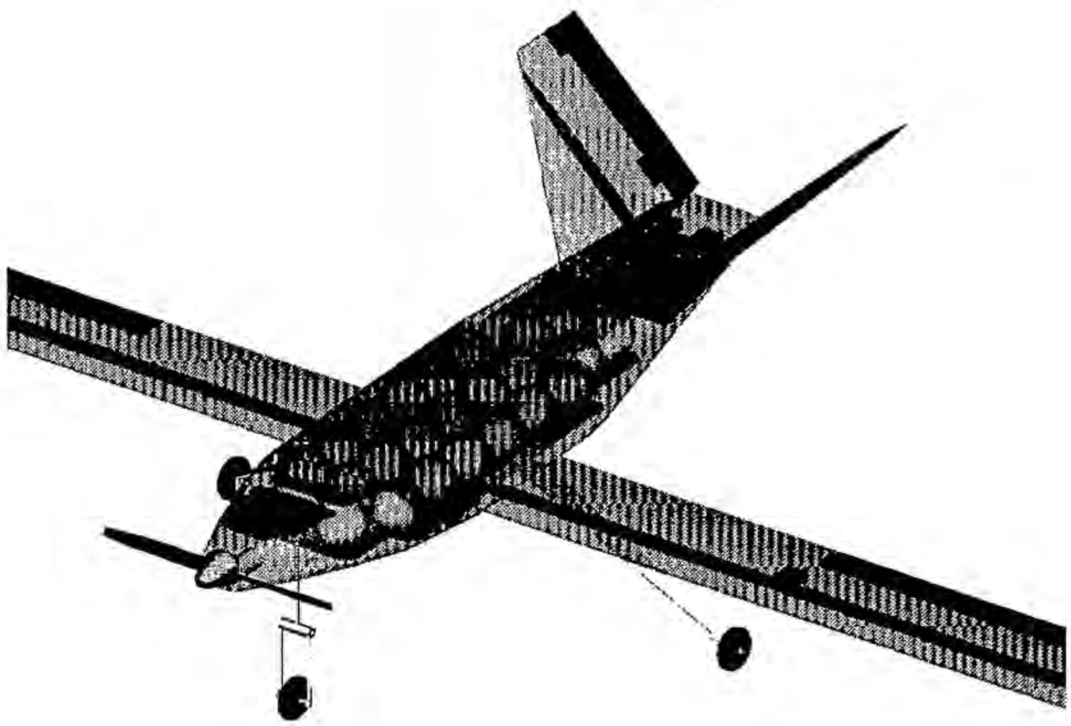

Figure 15: Transparence of Entire Plane

5.3.3 Tail Structural Details

The tail section was designed with similar goals to the wing. Once again graphite arrow shafts served as the hinge mechanism for the control surfaces. Like the wing a single carry through spar was incorporated to transfer loads to the fuselage. The tail was also built as a single module that could be easily removed and that could break away in the event of a crash with minimal damage to the aircraft structure. Servos were mounted in the tail module with breakaway wires to allow them to remain with the tail instead of damaging the control surfaces during a crash. Nylon bolts were again incorporated as the shear mechanism to allow the tail to detach before it fails structurally. Control rods were placed in an area that will minimize drag and allow the servo to push instead of pull against the higher loads associated with pitching the nose up. All of the design goals for the tail were incorporated into a compact design that could be constructed, repaired, or even replaced with minimal modification to the rest of the aircraft.

5.3.4 Structural Ground Test Results

Before ground and flight-testing commenced a series of test were performed to test the interior and exterior structures of the aircraft. The wing was subjected to a 3.4 g load through the use of weights and a test stand. Deflections estimated were within 2% of the predicted values. The fuselage was also tested to a 3.4 g load. The fuselage deflection was within 5% of predicted values however the sides of the fuselage bowed out of tolerances under load. To correct for this stiffeners and doublers were placed in the high stress areas. In order to test the landing gear system an apparatus was developed to attach the gear to. Weight were added to the test rig and the gear was sent through a series of drop and impact tests. The bow gear provided adequate spring damping and deflection and stroke were very close to predicted values.

5.4 Detail Design Assumptions and Comparisons

During detail design analytical assumptions made in preliminary design were reinforced by static structural testing, propulsion dynamometer testing, and finally prototype flight-testing. The prototype aircraft, less payload and batteries, weighed in at 10.75 lbs during flight test number one. The models used to perform the structural analysis in preliminary design estimated the weight to be 12.39 lbs. The numbers helped validate the assumptions used to perform the structural analysis. Center of gravity estimates, shown in Figure 16, proved to be valid to within one half of an inch. In flight the aircraft proved to be stable in pitch and yaw but assumptions made concerning roll stability proved to be inadequate to produce adequate control. Two degrees of dihedral were added to correct for this. Takeoff thrust and climb performance were better than expected primarily due to the difference between early weight assumptions and actual structural weight.

5.5 Drawing Package

Detail drawings are provided in the last five pages of this document.

Aircraft Component	Station (inches)	Weight (pounds)	Moment (pound-in)
Batteries			
Brake battery	36	0.0882	3.17
Propulsion batteries	19	2.4119	45.83
Servo batteries	34	0.2006	6.821
Propulsion System			
Engine	2	0.8444	1.689
Propeller	-1	0.2050	-0.205
Watt-Meter	6	0.2491	1.495
Aircraft Structures			
Brake Controller	36	0.0441	1.587
Cargo Deck	24	0.4189	10.05
Fuselage (with hatch)	25	2.6081	65.20
Main Gear	27	0.8686	23.45
Nose Gear (with servo)	8	0.6151	4.921
Tail (with servos)	51	1.3999	71.57
Wing (with servos)	25	3.3951	84.88
Payload			
Payload of 24 softballs	11	9.764	107.4

Figure 16: Weight Balance Spreadsheet. Center of gravity located at wing quarter chord.

6.0 Manufacturing Plan

6.1 Manufacturing Process Investigated and Figures of Merit

In order to produce the aircraft, several different manufacturing techniques would have to be employed for the different components. Several different methods for obtaining the desired shapes and surface finishes were investigated for each component. The figures of merit used to evaluate different manufacturing techniques included the ability to produce the desired shape and finish, cost of tooling and manufacturing, build time, required materials, skill levels, and process repeatability.

6.2 Processes Selected for Component Manufacturing

6.2.1 Fuselage Manufacturing Process and Tooling

Careful consideration was given to the exterior shape and surface of the fuselage. The fuselage was shaped in a way that minimized wetted area and interference drag, resulting in a complex shape with compound curves and radii. Careful attention was also given to the surface finish on the outer mold line. Both male and female molds were considered to create the desired fuselage.

The principle difference between the methods was the dimensional tolerances and the outer surface finish. A female mold allows the dimensional tolerance to be kept on the outer mold line while providing a smooth exterior surface of the carbon fiber resin. A male mold would keep dimensional tolerance on the inner mold line. In order to produce a smooth exterior surface with a male mold, a separate mold conforming to the outer surface would have to be prepared and included in the lay-up. Both methods had similar requirements in terms of tooling and manufacturing time. The female mold held an advantage in that the exterior finish and dimensional tolerances could be repeated easily on the final aircraft. Considering all figures of merit, the female mold was chosen.

Once the decision to use a female mold was made, the process of how to build the mold began. The first step was to create a male mold conforming to the outer mold line of the aircraft. Laminating resin was applied to the exterior of the male mold. The cured resin was sanded and polished to the desired finish. Several coats of release agents were applied to the surface and cured. A gel coat was than applied to the release material followed by several layers of fiberglass. The lay-up was vacuum bagged to the male mold and allowed to cure. The female mold, consisting of the fiberglass and the gel coat, was removed from the male mold and polished to the desired finish.

The final step in the fuselage construction was to lay-up in the female molds. The fuselage was split into top and bottom halves. Each section required a female mold. Hatches and access panels were included in the lay-up to ensure a tight fit against the fuselage. The lay-up consisted of carbon fiber and honeycomb core were vacuum bagged to the female molds in one assembly.

6.2.2 Wing and Tail Manufacturing Process and Tooling

The wing construction was a build up of foam core with a composite skin. To create the foam core, airfoil templates were created using computer software. The female sections of foam created from cutting the airfoil were finished using epoxy resin and used in the wing lay-up to give the resin in the carbon fiber prepreg a smooth surface to form against. The wing and spar was constructed in two sections and mated at the centerline of the fuselage. First, the foam airfoil for each section was cut and the spar material removed from the airfoil sections. The removed spar material was used as sandwich material for the carbon fiber spar skins. The front and aft sections of the airfoils were then re-bonded to the spar. Finally, the carbon fiber skins were applied and both sections vacuum bagged and allowed to cure separately. Bonding the spar sections and applying a wet lay-up technique to the center section of the wing mated the two sections.

The V-tail surfaces were constructed in similar fashion. The aft section of the fuselage and the V-tail constituted the tail assembly. Like the wing, the V-tails share a spar that carries through the aft section of the fuselage. The tail surfaces were foam core with carbon fiber skin and were constructed as one component; the tail assembly was then bonded to the aft fuselage section.

6.2.3 Landing Gear Manufacturing Process and Tooling

The composite lay-up for the bow gear was constructed on a male plug. The plug was cut from blue foam using templates made from CAD drawings. Layers of composite material were then laid up on top of the male plug. The nose gear was a stock Fults RF400 Dual Strut.

6.3 Analytic Methods Including Cost, scheduling and Skills matrix

6.3.1 Manufacturing Cost

With the preliminary design study complete, manufacturing and tooling costs were estimated. Projections showed sufficient carbon fiber prepreg was in stock to construct the prototype, leaving the major cost of manufacturing to be consumed by the propulsion equipment required for flight testing. Provisions for consumable materials such as breather, release, and epoxies were purchased for both the prototype and the final aircraft to cut down on lead-time. The total projected cost for the construction of the prototype aircraft and propulsion testing is $1175.

6.3.2 Skills Matrix

In order to assign tasks for the manufacturing process it was necessary to develop a matrix of the skills required for each task. Table 10 contains the skills matrix. In the matrix a component that requires a lot of skill in a certain area was rated a two, a component that required average skill in an area was score with a one, and a component that required no skill in an area received a zero. The columns of the skill matrix represent required skills in the manufacturing process; the rows represent the major assemblies and system of the aircraft. Members were assigned to components matching their expertise.

Primary Aircraft Assemblies and Systems	Foam Cutting	Composite Layup	Mold Preperation	Radio Equipment Installation	Electrical Work	CAD Modeling
Wing	2	2	1	2	1	2
Fuselage	2	2	2	2	2	2
Landing Gear	1	2	1	2	1	2
Tail	2	2	1	2	2	2
Propulsion System	0	1	0	2	2	1

Table 10: Skills Matrix for Oklahoma State Orange Team

6.3.3 Manufacturing Scheduling

The aircraft was constructed in four assemblies: the fuselage, wing, tail, and landing gear. The assemblies were constructed to allow components to be constructed simultaneously. Considerations such as material availability and coordination of oven times were of critical importance to maintaining a smooth manufacturing process. Figure 17 is the milestone chart developed for the manufacturing process. Figure 18 shows a photograph of the completed prototype after final assembly and completion of the prototype rollout milestone.

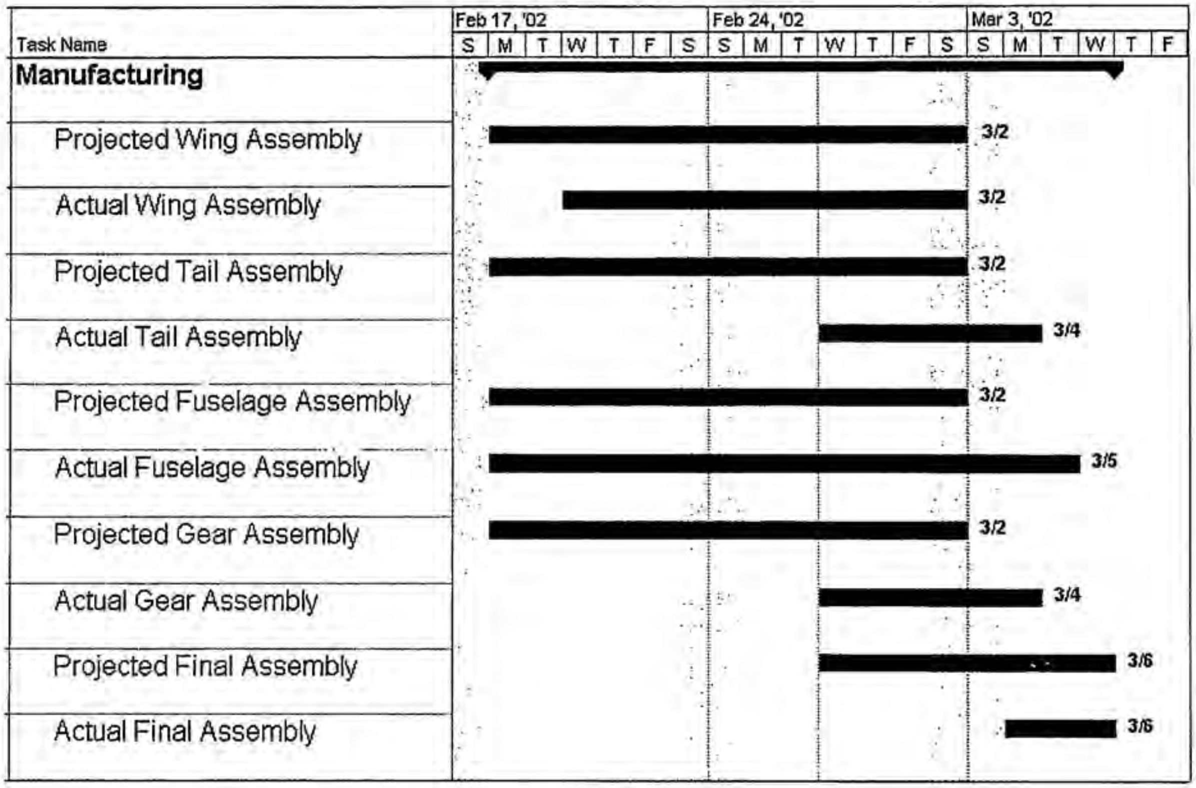

Figure 17: Manufacturing Schedule. **Red represents the projected dates; green represents the actual dates.**

Figure 18: Picture of the Orange Team Prototype

7.0 Rated Aircraft Cost

After parameters of the plane were determined, the dimensions were entered into the RAC program developed in the conceptual design phase. The RAC of the design was 8.925. The breakdown of each component's contribution to the RAC value can be seen in Figure 19.

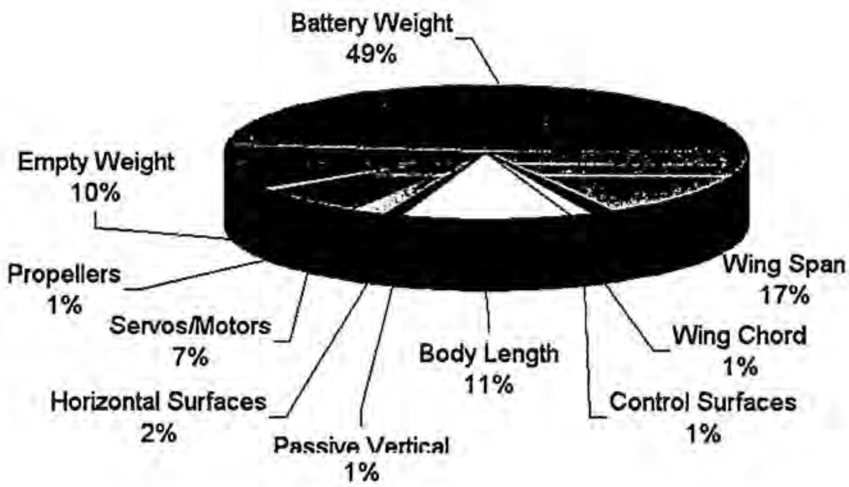

Manufacturing Man Hours: Work Breakdown Structures					
Aircraft Component		Man Hours/Unit	Aircraft Parameter	Individual Hours	Individual Contributions
Wing WBS - sum for multiple wings					
	Wing Span	8 hr/ft	9.5 feet	76	1520
	Maximum exposed chord	8 hr/ft	0.71875 feet	5.75	115
	Control Surface	3 hr/surface	2 surfaces	6	120
Fuselage WBS					
	Maximum body length	10 hr/ft	4.75 feet	47.5	950
Empenage WBS					
	Vertical surface with no active control	5 hr/surface	1 surface	5	100
	Horizontal surface	10 hr/surface	1 surface	10	200
Flight Systems WBS					
	Servo/motor controller	5 hr/servo	6 servos	30	600
Propulsion Systems WBS					
	Engines	5 hr/engine	1 engine	5	100
	Propeller/fan	5 hr/propeller	1 propeller	5	100
		Total Manufacturing Man Hours			**3805**

Description	Value Definition	Multiplier	Aircraft Parameter	Man Hours	RAC
Manufactures Empty Weight (MEW)	Actual airframe weight, lb., with all flight and propulsion batteries but without any payload.	$100	10.7 lb.	NA	**1070**
Rated Engine Power (REP)	"Total Battery Weight" defined as weight of propulsion batteries.	$1,500	1 Engine 2.7 lb. Batteries	NA	**4050**
Manufacturing Man Hours (MMH)	Sum of assembly hours defined by Work Breakdown Structure (WBS).	$20/hour	----	190.25	**3805**
		Rated Aircraft Cost			**8925**

Figure 19: Rated Aircraft Cost Worksheet and Pie Chart. Predicted Rated Aircraft Cost of 8.925

8.0 References

Allen, D. H. and W. E. Haisler, *Introduction to Aerospace Structural Analysis,* John Wiley and Sons, New York, 1985.

Bertin, J. J. and M. L. Smith, *Aerodynamics for Engineers,* 3rd Edition, Prentice Hall, Upper Saddle River, New Jersey, 1998.

Dieter, G. E, *Engineering Design,* 3rd Edition, McGraw-Hill, Boston, 2000.

Donald, D., *The Complete Encyclopedia of World Aircraft,* Barnes and Noble Books, New York, 1997.

Jensen, D. T., *A Drag Prediction Methodology for Low Reynolds Number Flight Vehicles,* Notre Dame, Indiana, 1990.

Munson, B. R., D. F. Young, and T. H. Okiishi, *Fundamentals of Fluid Mechanics,* 3rd Edition, John Wiley and Sons, New York, 1998.

Nelson, R. C., *Flight Stability and Automatic Control,* 2nd Edition, McGraw-Hill, Boston, 1998.

Raymer, D. P., *Aircraft Design: A Conceptual Approach,* 3rd Edition, AIAA, Reston, VA, 1999.

Shigley, J. E. and C. R. Mischke, *Mechanical Engineering Design,* 6th Edition, McGraw-Hill, Boston, 2001.

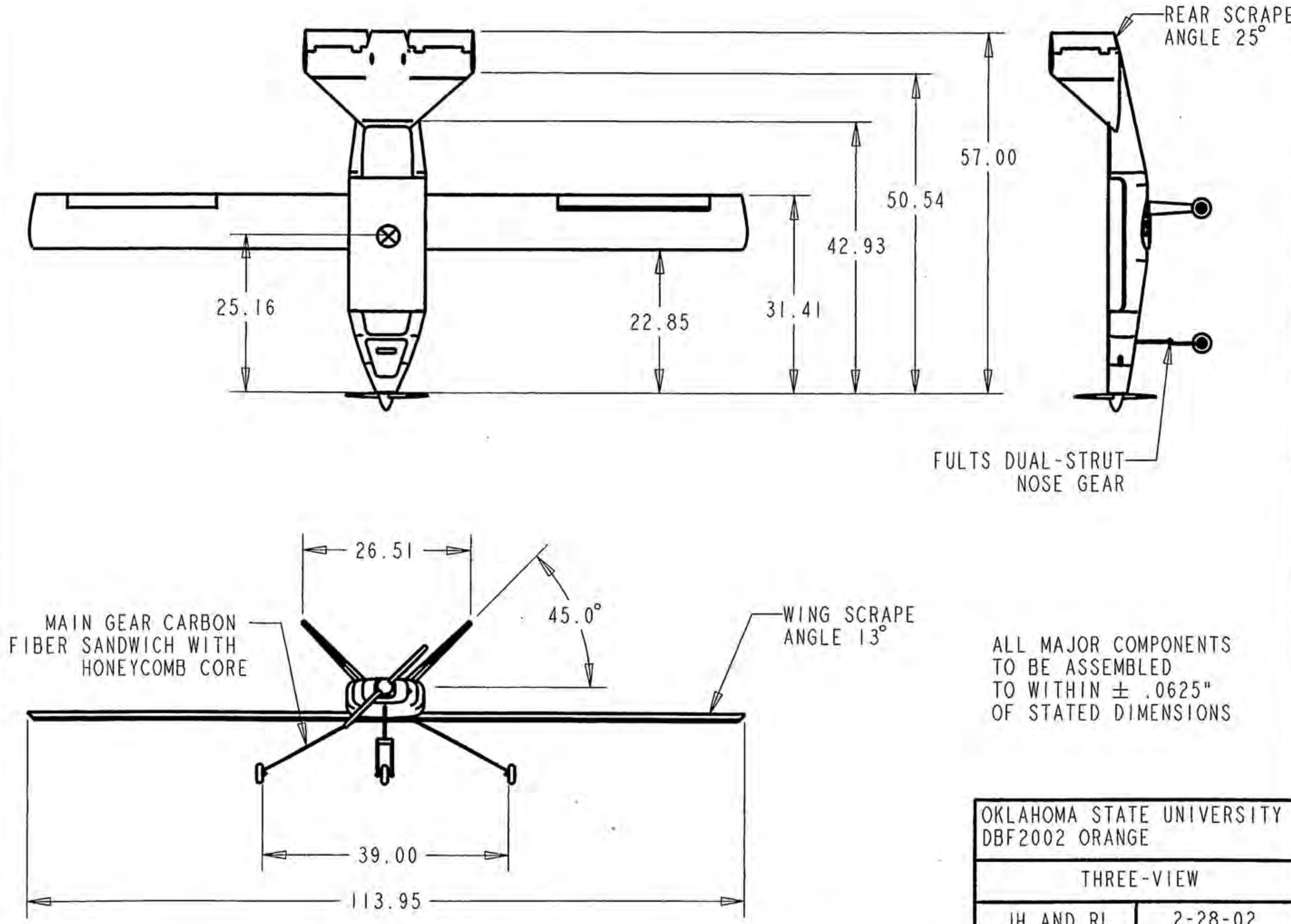

ALL MAJOR COMPONENTS
TO BE ASSEMBLED
TO WITHIN ± .0625"
OF STATED DIMENSIONS

OKLAHOMA STATE UNIVERSITY DBF2002 ORANGE	
THREE-VIEW	
JH AND RL	2-28-02

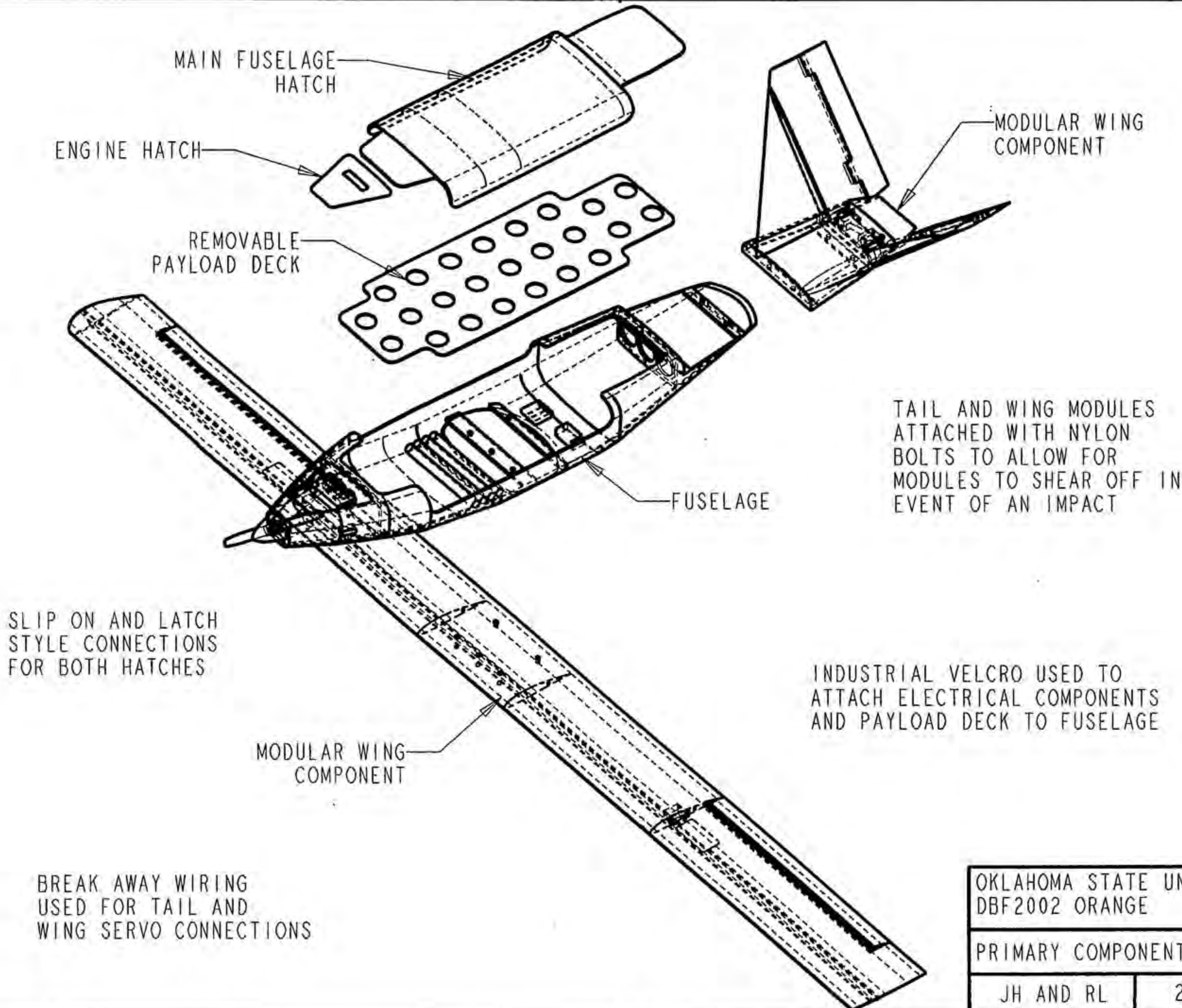

OKLAHOMA STATE UNIVERSITY DBF2002 ORANGE	
PRIMARY COMPONENT OVERVIEW	
JH AND RL	2-28-02

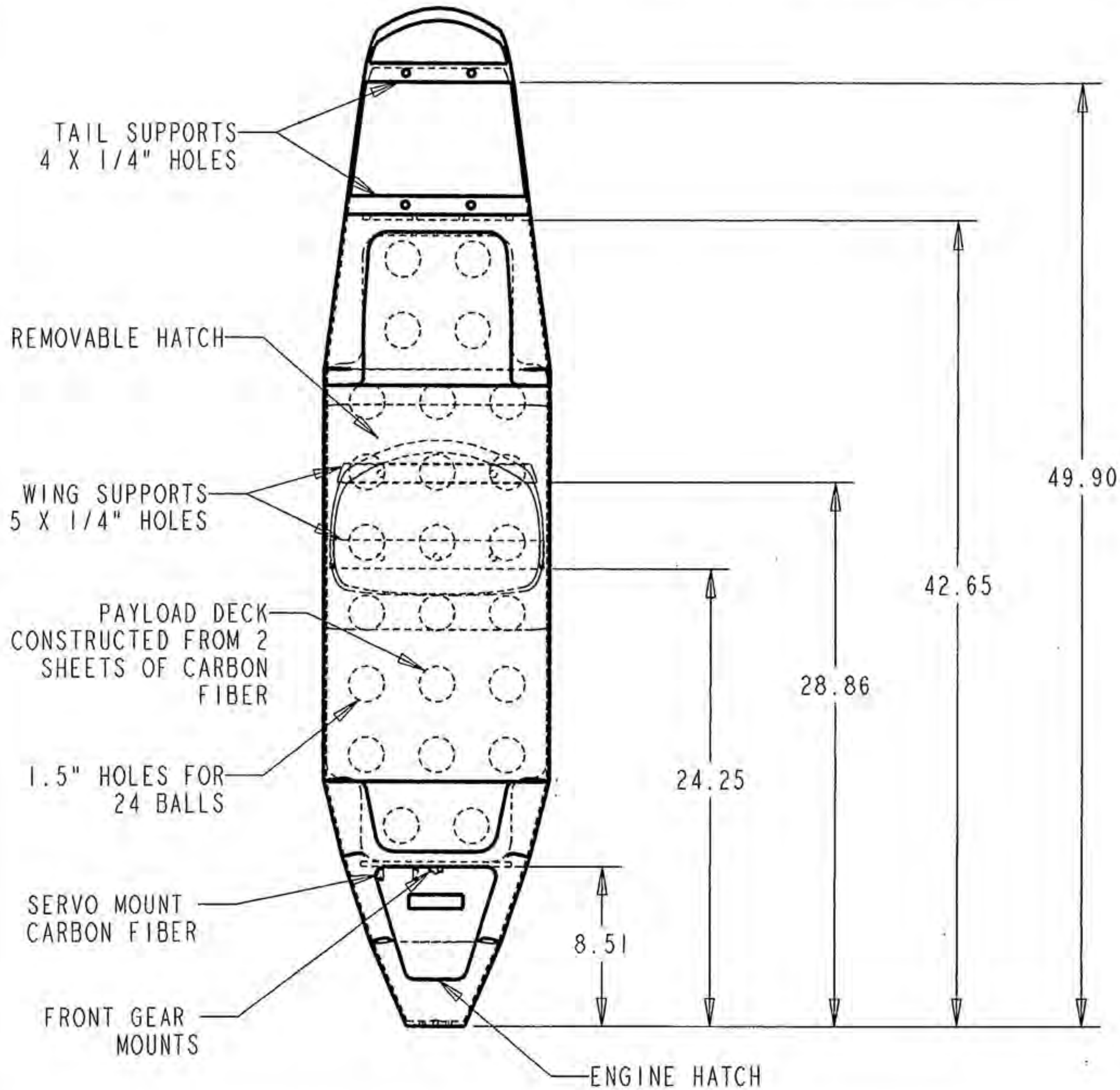

WING AND TAIL ATTACHED TO FUSELAGE WITH 2" X 1/4" 20 NYLON BOLTS

ACRYLIC WINDOW DISPLAY ON ENGINE HATCH FOR EASY VIEW OF WATT METER

ALL MAJOR COMPONENTS TO BE ASSEMBLED TO WITHIN ± .0625" OF STATED DIMENSIONS

OKLAHOMA STATE UNIVERSITY DBF2002 ORANGE	
FUSELAGE DIMENSIONS	
JH AND RL	2-28-02

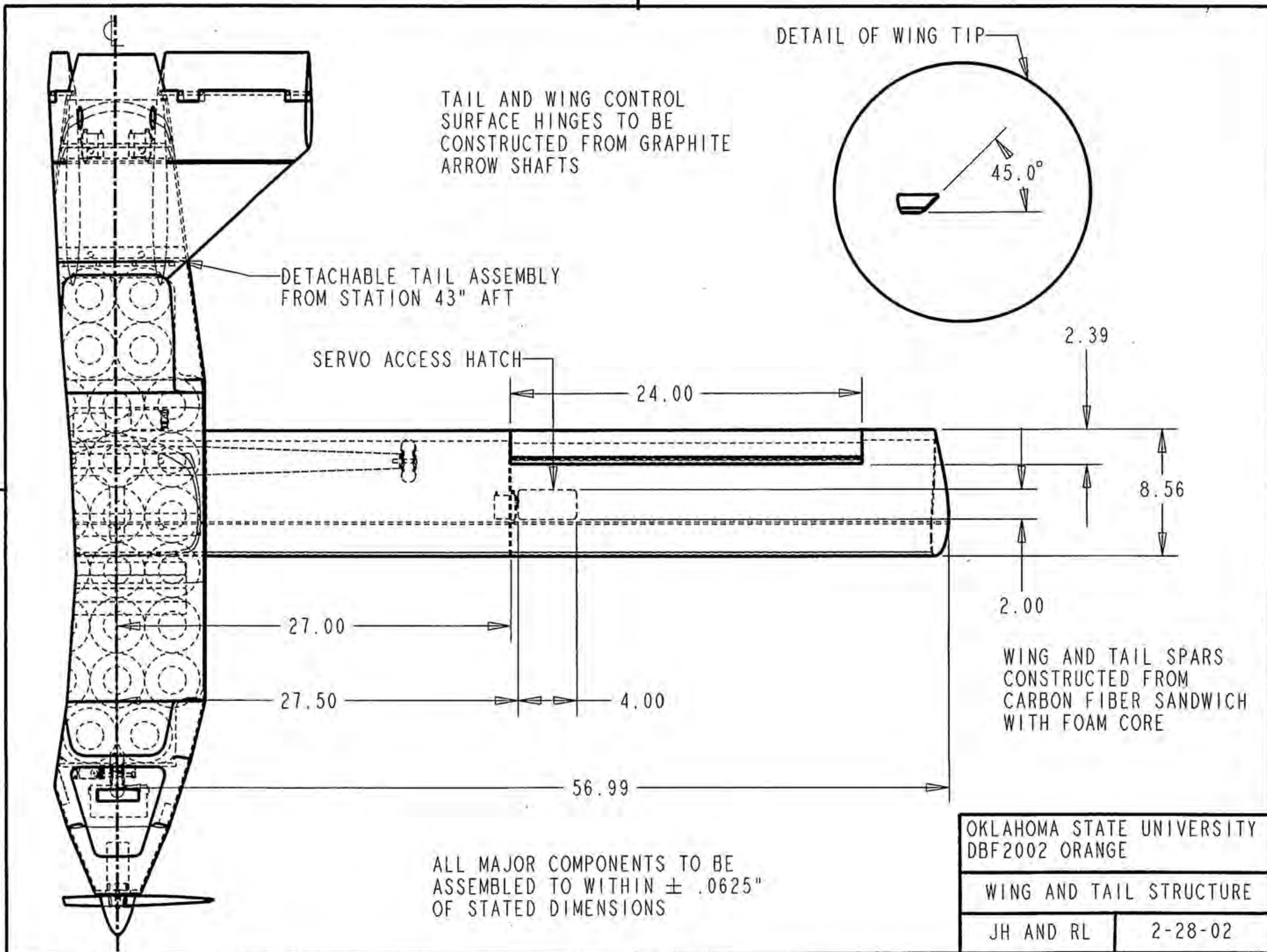
TAIL AND WING CONTROL SURFACE HINGES TO BE CONSTRUCTED FROM GRAPHITE ARROW SHAFTS
DETAIL OF WING TIP
45.0°
DETACHABLE TAIL ASSEMBLY FROM STATION 43" AFT
SERVO ACCESS HATCH
24.00
2.39
8.56
2.00
27.00
27.50
4.00
56.99
WING AND TAIL SPARS CONSTRUCTED FROM CARBON FIBER SANDWICH WITH FOAM CORE
ALL MAJOR COMPONENTS TO BE ASSEMBLED TO WITHIN ± .0625" OF STATED DIMENSIONS
OKLAHOMA STATE UNIVERSITY DBF2002 ORANGE
WING AND TAIL STRUCTURE
JH AND RL
2-28-02

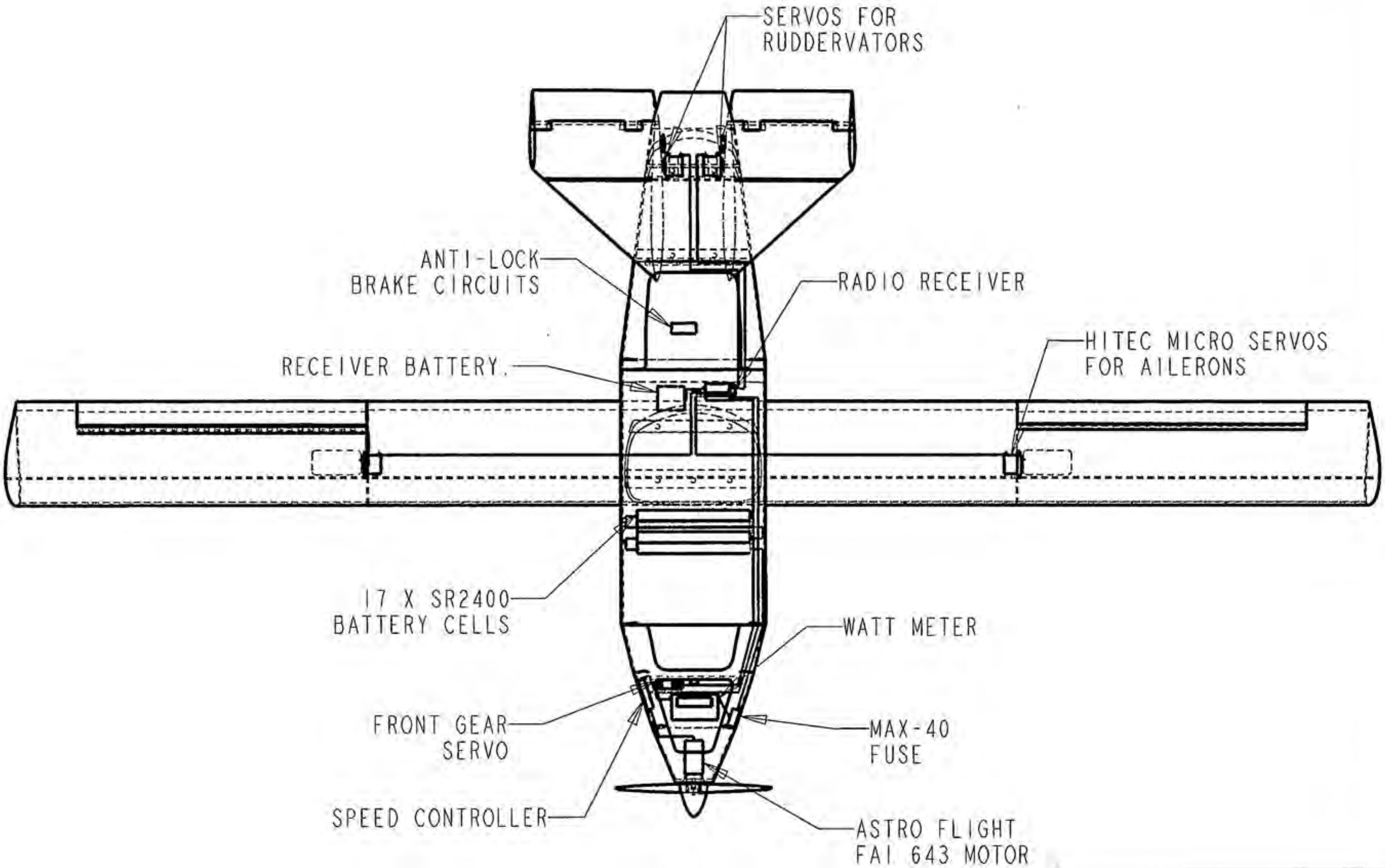

OKLAHOMA STATE UNIVERSITY DBF2002 ORANGE	
SYSTEMS LAYOUT	
JH AND RL	2-28-02

UNIVERSITY OF CALIFORNIA, SAN DIEGO

Proposal Phase Design Report

Submitted March 12, 2002

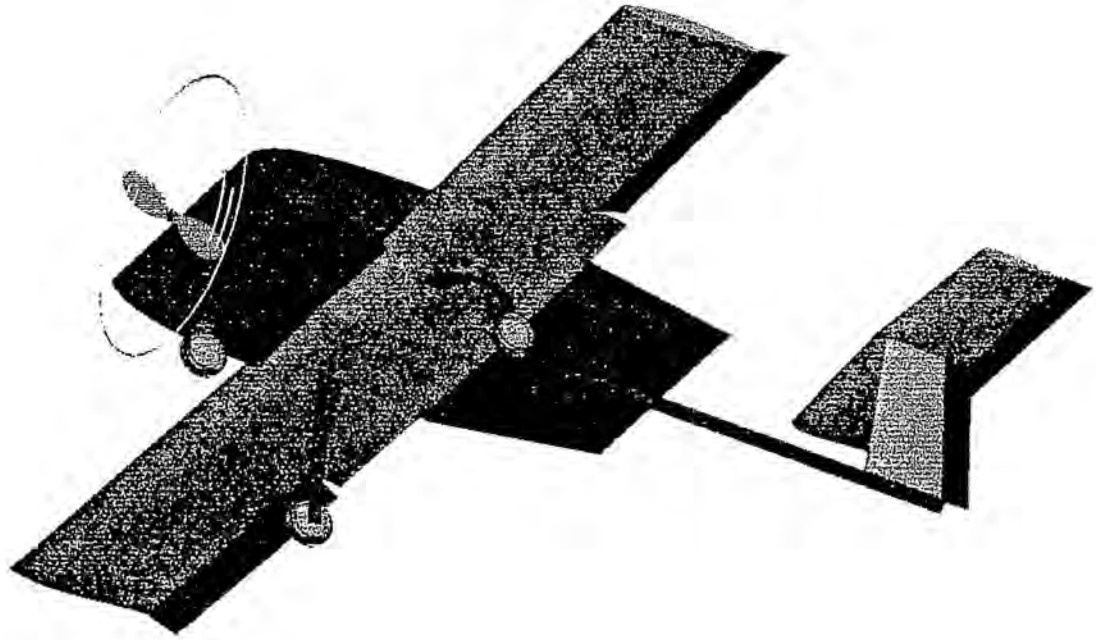

TLAR III

TLAR III

Table of Contents

List of Figures

List of Tables

1 Executive Summary

Student members of the American Institute of Aeronautics and Astronautics (AIAA) at the University of California, San Diego designed and built a remote-controlled aircraft for the 2002 AIAA Design/Build/Fly Competition to apply and broaden their knowledge of aircraft design and manufacturing.

The AIAA Design/Build/Fly Competition emphasizes the importance of design, construction, and the actual flight performance of the final plane. Based on one of the Mission Tasks requiring the aircraft to carry between 10 to 24 softballs, the team designed the aircraft to carry a high volume payload of 24 softballs each weighing approximately 180 grams with a take-off distance less than 200 ft. The wingspan is approximately 84 in. in length, and the empty weight is 14.9 lbs.

1.1 Objectives

The main objective of the team is to earn the highest score possible. The Rated Aircraft Cost (RAC) must be as low as possible; the Written Report must be as high as possible; and during the actual flight competition, the flight speed must be high while the pit stops must be quick. The lowest RAC was achieved through trial calculations for all of the design phases. To achieve the highest Written Report score, the team edited the Written Report based on the reviews of the faculty and mentor advisors during all paper preparation phase. To achieve the highest flight speed, the team selected the airfoil and propulsion system for TLAR III, and to achieve the quickest pit stop, the team ran pit stop coordination practices.

The second objective is to allow experienced members of the UCSD team to pass knowledge onto novice members. This year, most of the team members are new, being involved in the project for the first time and/or as first year students entering college. The competition is meant to convey the importance of responsible leadership and teamwork.

1.2 Analytical Tools

Several analytical tools were used throughout the entire design process. The most important was Microsoft Excel, which was used for everything from calculations of weight-and-balance, the quickest time to complete task, climb rate, take-off distance, and turn radius, to financial analysis and Rated Aircraft Cost (RAC). General aviation design principles and equations were used in determining exact dimensions and specifications. The mathematical toolbox, Matlab 6.0, was used to perform numerical analysis of flight performance of the chosen wing configuration. Finally, the programs AutoCAD 2000 and PRO/E 2000i were crucial tools used to visualize and present aircraft design ideas.

FOMs and Design Parameters were chosen to provide requirements to ensure that the design would meet the functional requirements dictated by the contest administrators, as well as the design goals as defined by the UCSD AIAA team. They were applied to each stage within the entire design process to analyze the strengths and weaknesses of each component as well as those of the overall aircraft configurations. The design process used to determine the final configuration began with the Conceptual Design Phase (CDP). Next was the Preliminary Design Phase (PDP) followed by the Detail Design Phase (DDP), from which emerged the final configuration of the aircraft.

1.3 Conceptual Design Phase Outline

The CDP consists of two stages, Stage I and Stage II. Stage I incorporates a range of ideas for each component that was considered. The FOMs of Stage I were geared towards eliminating ideas that were intuitively and/or obviously impractical. These FOMs centered on material availability, handling characteristics, RAC, ease of transportation and complexity of manufacture in relation to time and skill level required. Stage I analysis resulted in component concepts that were determined to be viable. These components were assembled into three different configurations that initially met the design parameters and FOMs. The three configurations were then progressed into Stage II.

The goals of applying Stage II FOMs were to maximize the overall flight score, minimize the RAC, and develop a preliminary aircraft design. Stage II FOMs focus on an in depth analysis of the components, with specific attention to payload access, construction feasibility, propulsion and maximizing strength to weight ratios, operator and component safety, difficulty of repairs, component and interfacing strength, and payload capacity. The analysis of Stage II resulted in a single overall design configuration, at which point, the question was raised of whether it met the functional and design goal requirements. If it was determined that the configuration met these requirements, it continued into the PDP. Otherwise, it was reiterated through Stage II of the CDP in an attempt to optimize the configuration with alternate component designs.

1.4 Preliminary Design Phase Outline

Once an overall design configuration was decided upon, the next step was to conduct a more thorough and detailed analysis of the configuration using the PDP FOMs. The main purpose of the PDP was to optimize sortie performance, RAC, and structural integrity of each component individually, and as part of the entire configuration. Specific design parameters, such as sizing, materials, connection interfaces, and exact location of each part within the assembly were also determined. These, combined with optimization of power requirements, led to a complete detailed aircraft configuration.

1.5 Detail Design Phase Outline

The DDP was less focused on actual aircraft configuration design as compared to the previous two phases. The focus in this section was on determining the flight performance of the detail configuration to discern whether or not the design met the functional requirements. To complete these calculations the team made use of performance analysis techniques suited to propeller driven general aviation and radio controlled aircraft. These techniques were validated by the previous year's design, "TLAR II" and used to determine characteristics such as takeoff distance, turn radius, stall speed and sortie times.

Though manufacturing related FOMs had been applied to eliminate ideas throughout the both the Conceptual and Preliminary Design Phases, in the Manufacturing Phase, each component underwent a rigorous investigation as to the best method of construction possible. Specific FOMs were developed to take into consideration the restrictions of skill level, availability of materials and machinery as well as time constraints and cost.

The final product of the design process was a configuration in which each component satisfied the contest functional requirements, design goals as well as the FOMs of each category. The resulting design was conventional, single engine, single fuselage, low mono-wing aircraft with a 84 in. wingspan and a 54 in. nose-to-tail length. The specific details of the aircraft are given in Table 1.1.

Table 1-1 Final Design Specifications

Design Parameter	Specification
Manufacturer's Empty Weight	14.9 lbs
Payload Capacity/Weight	24 Softballs/9.6 lbs.
Main Wing Configuration	Low Mono-Wing
Main Wing Airfoil	Eppler-212
Wing Span	84 in.
Length	54 in.
Motor	Graupner Ultra 3300/7
Rated Aircraft Cost	**9.29**
Final Flight Score	6.2

2 Management Summary

2.1 Architecture of the Design Team

The 2002 UCSD Design/Build/Fly Project team consists of seventeen undergraduate students from various engineering disciplines. At the first project meeting it was decided that the most efficient way to design and build the plane would be to group members together with assigned areas to work on. The project manager, Maziar Sefidan, assigned each group with one of the following focuses: wing, fuselage, propulsion, landing gear or the tail. All members were responsible for fundraising. The specific team member profiles and assignment areas are shown in the table below.

Table 20-1 Archtecture of Team Members

Name	Major	Year	CAD Programs			Matlab	Technical Writing	Machining	Assignment Area
			Pro-Engineer	AutoCAD	SolidWorks				
Maziar Sefidan	ME	SR	X	X		X	X	X	Wings
Josh Adams	ME	SR	X	X		X	X	X	Fuselage
Chad Valenzuela	AE	JR		X			X	X	Propulsion System
Mark Shtayerman	AE	JR	X	X		X	X	X	Landing Gear
Brooke Mosley	AE	FR		X				X	Manufacturing
Steve Wong	ME	SR	X	X	X				Drawing Package
Aaron Pebley	AE	SR			X				Systems Architecture
Hamarz Argafar	AE	SO		X				X	Manufacturing
Justin Smith	AE	SR	X	X					Power Management
Guy Watanabe	AE	SR	X	X		X	X	X	Finite Element Analysis
Matthew Napoli	AE	FR					X		Tail
Brian Berg	AE	FR		X			X		Manufacturing
Carrie Nishimura	AE	FR							Systems Architecture
Lynn Chouw	AE	FR					X		Manufacturing
Jillian Allan	BE	JR			X			X	Graphic Design
Mann Chau	ME	SR	X		X		X	X	Fundraising
Ceazar Javallana	AE	JR	X	X				X	Fundraising

Weekly meetings were set where each sub-group discussed their design ideas, chose designs that were useable, then reported it to the entire team. The end of each meeting was designated as a time to assign topics for which ideas would be needed for the next week's meeting. The product of these brainstorming meetings commenced in the conceptual design of our plane. This management structure allowed the plane to have a safe, stable, and fast design while considering the contributions and ideas of all members of the team. In addition, this format was conductive to a timely completion of the airplane's configuration.

2.1.1 Task Scheduling

In early September, the group decided upon a schedule of completion dates. Each subgroup was expected to complete tasks by a certain deadline. The chart below (Figure 2.1.2) depicts the planned and actual dates of completion (D.O.C.) of each major event. Problems that were encountered completing these tasks were quickly resolved through teamwork and subgroup collaboration. The subgroup dependencies were as follows, each task's completion vital to starting the next:

Assembly of Design Team: The returning DBF members from 2001 met two weeks before the start of school to decide how many new members the project would need to compete in this years competition. A meeting was held the first week of classes, and the team began to form. Only a month from competition, the team has solidified with 17 members.

Notice of Intent to Compete: This notice was sent by the project manager, Maziar Sefidan, on October 19, 2001, binding our participation in the work ahead of us.

Obtain Funding: While our search for project funding has been continuous over the past 11 months, our saving grace has come in the form of grants from General Atomics (Aeronautical Systems), Jacobs School of Engineering (UCSD), Hitec RCD, Corland Co., San Diego Silent Fliers, and Diversity Model Aircraft .

Concepts and Preliminary Design FOMs: The figures of merit were applied to all conceptual and preliminary designs in order to either eliminate or accept designs based on the structural, weight, safety, or financial needs of the plane.

Conceptual Design: Having found designs that met all of our necessities, a final conceptual design could be assembled and taken to be critiqued by our mentors.

Preliminary Design: The conceptual design having been finalized, a preliminary design could be made and analyzed.

Data Design: Taking our preliminary design to the computers, we digitally took apart our design analyzing each piece to ensure the best flight characteristics possible under design parameters.

Acquire Materials and Parts: The ongoing task of replacing materials that have been used in the manufacture of the plane, and acquiring needed manufactured parts as the project calls for them.

Proposal Phase: Having a large part of the manufacturing complete and all of the data collected, the design proposal phase report was able to be written for submission to competition judges.

Aircraft Construction: The longest and most important process of the entire project, having started in December, will commence with the test flights of our plane in late March.

Test Flight(s): Having completed construction, test flights are vital to ensure flyability, structural integrity under true loads, and good component interaction, as well as serving as practice for the pilot.

Pit Crew Selection and Coordination Drills: Since the competition will be timed, having a good "Pit Crew" that is coordinated in thoughts and procedures in different scenarios to unload our cargo will be imperative to scoring well and winning the contest.

2.1.2 M stone Chart

Figure 2.1.2 Mi one Chart

ID	Task Name	Start	Finish
1	Assembly of Design	21-Sep	17-Oct
	Team	21-Sep	17-Oct
2	Notice of Intent to	19-Oct	19-Oct
	Complete	19-Oct	19-Oct
3		22-Oct	4-Mar
	Obtain Funding	22-Oct	10-Feb
4	Concepts and Preliminary Design	20-Oct	2-Nov
	FOMS	20-Oct	28-Oct
5		2-Nov	14-Nov
	Conceptual Design	2-Nov	14-Nov
6		15-Nov	29-Nov
	Preliminary Design	15-Nov	29-Nov
7		30-Nov	19-Dec
	Data Design	30-Nov	23-Dec
8	Aquire Materials and	22-Oct	14-Jan
	Parts	22-Oct	20-Jan
9		19-Jan	9-Mar
	Proposal Phase	19-Jan	3-Mar
10		16-Dec	30-Mar
	Aircraft Construction	3-Dec	30-Mar
11	First Test Flight	31-Mar	31-Mar
12	Pit Crew Selection/ Coordination Drills/ Test Flights	31-Mar	21-Apr

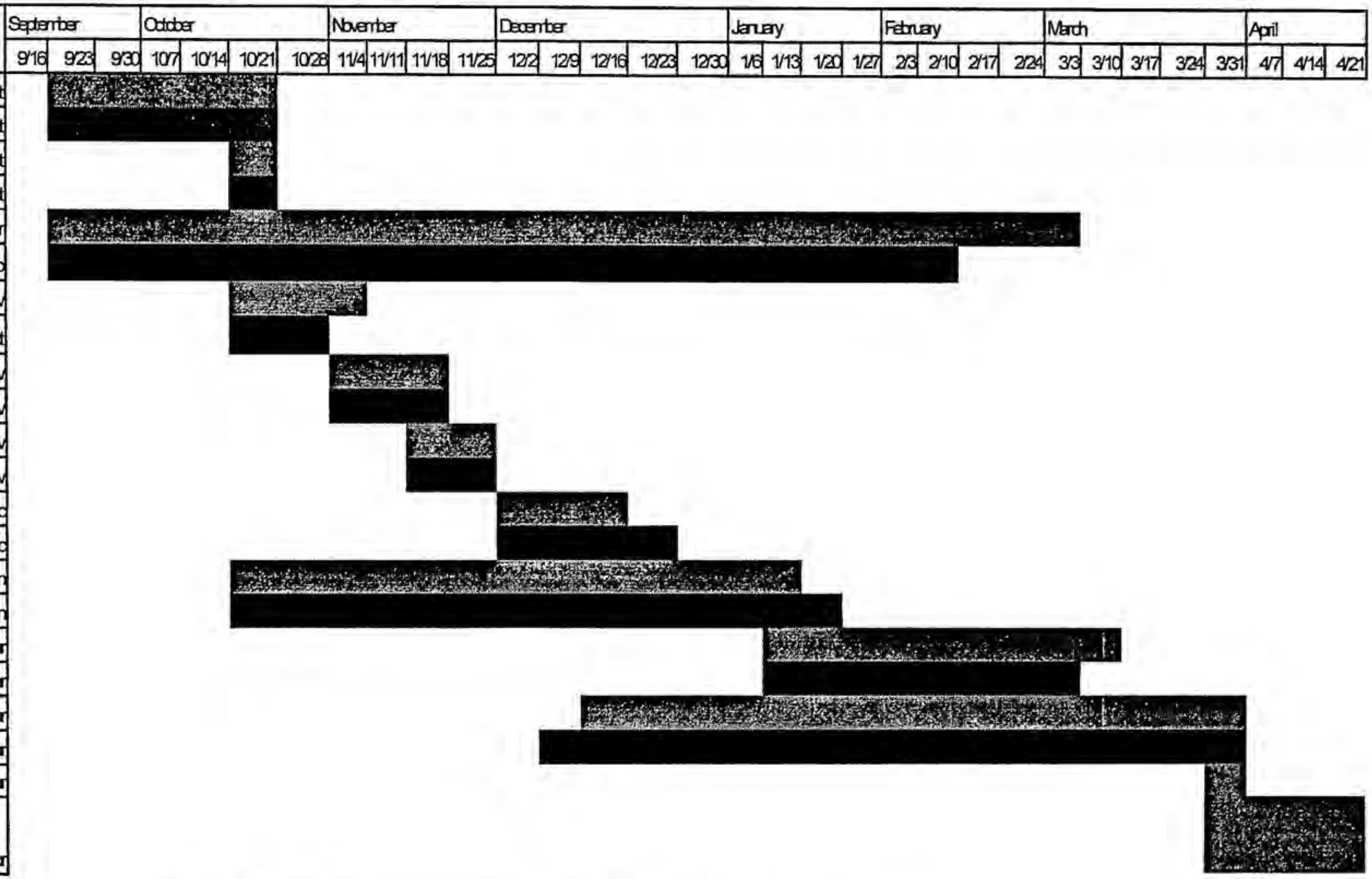

Key: Grey = **Proposed duration of task,** Blue = **Actual duration of task**

3 Conceptual Phase

3.1 Stage I – Feasibility Analysis

Table 3-1 Design Parameter FOM analysis – Stage I

(-) - Not Applicable
(r) - Rejected
(K) - Kept

Design Parameters – Stage I		Ease of Manufacture (x2)	Material Availability (x1)	Strength to Weight Ratio (x2)	Handling Characteristics (x1)	Rated Aircraft Cost (x1)	Cost (x1)	Motor Power Limitations (x1)	Thrust Ratings (x2)	Motor Installation Flexibility (x1)	Sum of Ratings	Decision
		Figures of Merit – Stage I (x weighting)										
Wing Configuration	Low	1	-	-	0	0	0	-	-	-	2	K
	Mid	-1	-	-	0	0	0	-	-	-	-2	r
	High	1	-	-	0	0	0	-	-	-	2	K
	Bi-plane	0	-	-	0	-1	0	-	-	-	-1	r
Wing Planform	Delta	-1	0	-1	-1	-1	0	-	-	-	-6	r
	Elliptical	-1	0	1	1	1	0	-	-	-	2	r
	Tapered	1	0	1	1	0	0	-	-	-	5	K
	Rectangular	1	0	1	1	0	0	-	-	-	5	K
Airfoil	E214	0	0	-	-1	0	0	-	-	-	-1	r
	E211	0	0	-	-1	0	0	-	-	-	-1	r
	E212	0	0	-	1	0	0	-	-	-	1	K
Structural System	One Piece	-1	-	0	-	-	-	-	-	-	-2	r
	Two Piece	0	-	0	-	-	-	-	-	-	0	K
	Three Piece	0	-	0	-	-	-	-	-	-	0	K
	Strut Braced	-1	-	0	-	-	-	-	-	-	-2	r
	Bending Beam	0	-	1	-	-	-	-	-	-	2	K
	Ring Frame	-1	-	1	-	-	-	-	-	-	0	K
Tail Structure	Conventional	1	-	-	1	0	-1	-	-	-	2	r
	Canard	-1	-	-	0	-1	-1	-	-	-	-4	r
	T-tail	1	-	-	1	0	0	-	-	-	3	K
	Cruciform	0	-	-	0	0	0	-	-	-	0	r
	V-tail	1	-	-	-1	0	0	-	-	-	1	r
	Inverted V-tail	1	-	-	1	0	0	-	-	-	3	K
	H-tail	-1	-	-	1	-1	-1	-	-	-	-3	K
Fuselage Structure	Trusses	-1	-	0	1	-	1	-	-	-	0	r
	Monocoque	1	-	-1	-1	-	0	-	-	-	0	r
	Semi-monocoque	0	-	1	1	-	0	-	-	-	3	K
Landing Gear	Tail-Dragger	1	-	-	1	-	-	-	-	-	3	K
	Tricycle	0	-	-	1	-	-	-	-	-	1	K
	Bicycle	-1	-	-	0	-	-	-	-	-	-2	r
	Quadracycle	0	-	-	-1	-	-	-	-	-	-1	K
Power Plant	1 motor 19 cells	-	-	-	-	-	-	1	-1	1	0	r
	1 motor 22 cells	-	-	-	-	-	-	0	1	1	3	K
	2 motors/20 cells	-	-	-	-	-	-	1	0	0	1	K
	2 motors/22 cells	-	-	-	-	-	-	0	0	0	0	r

The purpose of Stage I was to apply FOMs to eliminate and analyze concepts for aircraft components that were proposed during brainstorming sessions at the beginning of the design process. The goal was to produce a set of desirable components to incorporate into three conceptual aircraft designs. The Stage I FOMs consisted of five primary areas. First, material availability required that any material not commercially available or unreasonably expensive be ruled out. Second, handling characteristics were used to eliminate concepts that were initially thought to have poor ground or flight performance. Third, designs that did not promote ease of transportation and/or manufacture were dismissed from consideration. The fourth consideration for Stage I was simplicity and tooling. Simple structures are easier to analyze and build without necessarily losing functionality or performance characteristics. These guidelines established a solid set of conceptual components to consider for the aircraft.

3.1.1 Airfoil

When choosing an airfoil, the lift to drag ratio was the most important feature to be considered. For the final design, an aircraft constrained by take-off distance, an airfoil that maximized lift while minimizing drag was necessary. Three airfoils (Eppler 211, 212, and 214) were analyzed in order to obtain their respective coefficients of lift and drag. We chose the airfoil Eppler 212 over the two others due to its desirable lift and drag coefficients. When calculating the C_L and C_D coefficients, a Reynolds number of 200,000-300,000 was considered, which was determined by an average cruise velocity of 65 MPH.

The maximum lift and drag coefficients calculated for airfoil Eppler 212 were 0.79 and 0.0142, respectively. The maximum lift and drag coefficients calculated were 0.78 and 0.012, respectively, for airfoil Eppler 214. For the E212, the maximum lift and drag coefficients were found to be 1.544 and 0.023104, respectively. While the other Eppler airfoils are low drag sections that would be better than the E212 for cruise performance, they are predicted to generate insufficient lift to achieve takeoff in 200 ft given power limitations imposed by contest rules. The lift generated by E212 section was determined to be sufficient for takeoff within 200 feet distance limit and was chosen as the plane's airfoil.

3.1.2 Wings

The wings are a primary defining characteristic of an aircraft. In this year's design, they were optimized to the role of the aircraft's flight objectives. Other primary, secondary and tertiary structures were designed around the general wing structure. In this design process, there were limitations imposed by contest rules, flight conditions, and structural feasibility. The initial design parameters being investigated were wing configuration and wing planform. The available wing configurations included a high and low placement mono-wing and a bi-plane configuration. The considered wing types were delta, elliptical, tapered, and rectangular. The intent of the Stage I wing analysis was to eliminate design parameters based on FOMs to determine their applicability to the design goals. FOMs that were used consisted of handling characteristics, RAC, ease of transportation, and complexity of manufacture.

3.1.2.1 Wing Configuration

The wing configurations presented as options (low and high mono-wing and bi-plane) represented the traditional configurations that were well documented for planes of our size. One of the basic limitations was that the payload was to be carried within the fuselage. Bi-plane configuration would have caused an array of problems with payload access and would have increased the planes RAC thus was ruled out of consideration. The high and low wing configurations would not pose a payload problem and were therefore left for further analysis.

3.1.2.2 Wing Planform

Delta: A delta wing was eliminated immediately as a design possibility due to the fact that it is optimized for transonic and supersonic flight.

Elliptical: Elliptical wings, which feature a constantly varying chord length, were eliminated due to their difficulty of manufacture and increase of the RAC.

Rectangular: The rectangular wing satisfied the initial set of FOMs and was selected for further analysis in Stage II.

Tapered: The tapered wing also satisfied Stage 1 FOMs and will be further analyzed in Stage II.

3.1.3 Empennage

The tail surfaces of TLAR III will be referred to as empennage, and are an essential part of an aircraft's control and stability.

Existing empennage configurations were selected from documented styles (stage 1 – feasibility analysis). Each was analyzed based on the experience of the team members gained in past year's competitions and through application of basic FOMs. The goal of the first stage of the CDP was to complete the analysis of proven empennage configurations so as to select three designs to investigate further in the second stage.

The purpose of empennage is to provide stability and pitch/yaw control. The three main FOMs were handling characteristics, RAC, and ease of manufacture. Other FOMs, such as material availability, ease of transportation, and reparability were not considered explicitly in this section, as the materials of all designs were understood to be the same, and the types of tails were assumed to be equally transportable and repairable.

3.1.3.1 Tail Configuration

Canard: A canard configuration would reduce the required control surfaces at the rear of the aircraft to a single vertical stabilizer. The benefit of a reduction in control surfaces at the rear, however, would be negated by the complexity of both pitch and roll capabilities integrated into the aileron control. While this configuration had benefits that included main wing stall prevention and less control surface actuators, the design, analysis and fabrication was complex and was eliminated for these reasons.

Conventional: Major benefits of a conventional design were ease of construction and lightweight design. However, the low placement of the horizontal stabilizer usually puts it in the wake of the main wing "washing out" the airflow over the horizontal stabilizer and rendering elevator control ineffective. This configuration was eliminated due to its poor efficiency, susceptibility to damage and loss of control.

"T": The most important benefit of the "T"-Tail design is that the horizontal stabilizer is above the turbulence from the body and main wing, thus allowing the horizontal control area to be reduced. It also acts as an endplate for any control deflections caused by the vertical fin, which increases the vertical fin's efficiency and allows a reduction in the fin's area. This allowed a large reduction in weight and the "T" style tail was deemed the first design to be considered in Stage II.

Cruciform: The fourth concept examined was the cruciform design, a hybrid of the Conventional and the "T"-Tail. It was determined that this style shared several benefits of both, but was difficult to construct and the end plate effect from the "T" was lost. For those reasons, this design was eliminated.

"V": The next configuration investigated was the "V"-Tail design, which was efficient because it eliminates one wing tip vortex, decreasing induced drag. The design was discarded due to its many disadvantages, including high control surface complexity, and an induced opposite roll when given rudder input.

Inverted "V": The inverted "V", by contrast, produces favorable yaw-roll coupling. Elevator control was less affected by turbulent wake from the fuselage and main wing, and the use of only two control surfaces reduced the number of servos needed for both rudder and elevator control. This design had bad ground clearance and complex control surface design. However, it was kept for further analysis because of the good turning characteristics and the reduced drag of one less wing tip vortex.

"H": This was deemed a good design, as turbulence from the fuselage does not flow around the vertical fins. The vertical fins also prevent spillover of the elevator with an end plate effect, therefore eliminating drag from tip vortices induced by elevator input. Although this design is complex, it was kept for further analysis as it worked well with a twin-body design.

3.1.4 Fuselage

The fuselage serves as a primary structure of the aircraft and acts as a critical load path for the aircraft to transmit forces between the tail and wings, in addition to housing flight equipment and payload. Design of the fuselage is somewhat dependent on the design of the wing and tail because it links the components. The FOMs that were used to optimize the design parameter of structural reinforcement were ease of manufacture, strength to weight ratio, handling characteristics, and cost. The four types of fuselage structural reinforcement investigated were trusses, monocoque, semi-monocoque, and box-beam.

3.1.4.1 Structural Reinforcement

Truss: While a truss structure in the fuselage would have a relatively good strength to weight ratio, it may interfere with the payload volume. Trusses are very difficult to manufacture, so it was quickly dismissed as a means of reinforcement in the fuselage.

Monocoque: A monocoque design has good torsional strength, but it is weak in bending, which is the type of load transferred by the tail to the fuselage. The required skin thickness needed to support these bending loads would increase the weight significantly and therefore it was eliminated as a design parameter.

Semi-Monocoque: A semi-monocoque structure combines the torsional strength of the skin with bending strength that can be customized for the aircraft by means of stringers and ribs. This type of configuration allows the strength to be customized for specific loads. However, due to the positioning of the cargo, a semi-monocoque structure would be too large and not feasible.

Box Beam: A box-beam structure utilizes the fuselage's skeletal frame for structural strength. This frame would be made of a carbon/foam/carbon sandwiched material. This material would act much like steel "I" beams of buildings act. This box structure could sufficiently accommodate the torsional forces induced during flight thus was chosen for further analysis.

3.1.5 Landing Gear

The functional requirement of the main landing gear is to absorb and dissipate landing loads effectively. The design parameters considered included: tail dragger, quadracycle, bicycle and tricycle. During Stage I of the CDP various landing gear configurations were screened according to the established FOMs, such as ease of manufacture and ground handling characteristics.

3.1.5.1 Landing Gear Configurations

Bicycle: The bicycle landing gear configuration consisted of two in-line wheels straddling the CG of the fuselage and another wheel on each wing for balance. Due to complexity of manufacture and poor ground handling characteristics, the bicycle design was immediately eliminated.

Tricycle: The tricycle landing gear has two main wheels aft of the CG and an auxiliary wheel forward of the CG. The advantage of this arrangement is that it is stable and the aircraft can be landed at a large "crab" angle. Also, the tricycle landing gear allows for a level fuselage which is helpful when loading the softballs. The tricycle will be kept for further analysis.

Tail dragger: This design would place two main wheels forward of the CG, and a small auxiliary wheel attached to the boom directly below the empennage. This configuration would be sufficiently stable on the ground while giving the propeller extra ground clearance. The tail dragger will be kept for further analysis.

Quadracycle: This configuration would be used in the event that we choose the dual fuselage body structure. It would be very stable on the ground due to it's two wheels forward the CG along with one wheel placed under each of vertical stabilizers on the "H" style empennage. The quadracycle will also be kept for further analysis.

3.1.6 Propulsion and Power System

The propulsion design began with little knowledge about the overall configuration of the aircraft, so the initial decisions related to propulsion choices were based on experience gained from last year's project.

The amount of power available to propel the aircraft is dependent upon the total power of the system and the efficiency of the entire propulsion system. To maximize this number, given that the battery power was limited by weight restrictions, a maximally efficient engine/propeller combination was chosen. Optimizing the efficiency of the motor as well as motor configurations while lowering the REP was the goal of the propulsion design portion of the conceptual phase.

The battery weight restriction of 5 lbs. limited the number of battery cells to 38, which amounted to approximately 40 volts. For standard radio controlled propulsion systems, 40 volts exceeded the rated power of many motor possibilities. While a motor's power is related to the input voltage, they can normally withstand higher voltages. Problems experienced in the competition two years ago showed that this was not a desirable arrangement, yet it was determined that a single motor design was still a valid concept.

Single-Motor: Initially, due to concerns with overpowering the single motor, the single motor configuration was developed with a maximum of 19 cells connected to the motor. However, due to the lower thrust of this configuration, the single motor connected to 22 cells was considered instead. This design was left for analysis in Stage II.

3.1.7 Structural System

The structural system was required to provide efficient "load paths" which resolve forces experienced during landing and flight sequences. The spar structure, which reinforces the wings, transmits the bending loads through the fuselage, is the major component of the structural system. When considering viable structural configurations it was noted that several options placed constraints on other component design solutions. These affected components included the wing platform (swept and tapered), wing configuration (biplane, delta and monoplane) and fuselage parameters. Several of these concepts were analyzed during Stage I of the CDP to effectively meet the various requirements of the structural system. Various spar cross-sectional geometric shapes were also considered for each of the competing component designs. These included the box beam, hollow cylindrical, solid rectangular and I-beam cross-sections.

The primary objective of the Stage I screening process was to eliminate design concepts that were complex, raised the RAC, and/or were difficult to repair or replace. The one structural system design idea that remained following the application of the Stage I FOMs follows:

Spar Structure: Initial concepts that were considered were the one and two piece spars. The one-piece spar was chosen.

3.1.8 Conceptual Design Phase – Stage I Summary

The CDP Stage I was focused on the development of initial aircraft designs that feature various component concepts that were determined to have merits applicable to the mission goal. By the end of the first stage, concepts that were immediately discernable as inadequate had been eliminated. Any remaining concepts were combined into several comparable configurations. These configurations would be evaluated further in the second stage of the CDP as to their individual component interactions and total system performance.

The decisions made when combining the components into complete configurations were somewhat arbitrary. However, each component that survived the first stage was examined to determine its ability to interact with other components. For each component, this process was done to piece compatible components together and develop three aircraft configurations.

First configuration, featured a single fuselage mounted over a low mono-wing. The tail dragger concept was considered for this model with an advantage of propeller clearance. However, the unstable nature of the tail dragger design made the team skeptical of this configuration.

Second configuration employed a single fuselage with a high mono-wing concept. The high wing necessitated the use of the tricycle landing gear concept and allowed, due to the height of the fuselage, an inverted "V" tail mounted to a tail boom. The single motor mounted to the front of the fuselage also required that the payload access be from the rear of the fuselage.

Other designs consisting of "hybrids" of the above mentioned configurations will most likely yield more and better designs that will incorporate the best aspects of each into the most efficient, lowest cost, best performing design desired. These concepts will be taken as the configurations examined in the second stage of the CDP. There, they are to be analyzed with regards to component interaction and initial flight characteristics while further determination of RAC and ease of manufacture will be made.

3.2 Stage II – Generalized Analysis

Table 3-2 Design Parameter FOM Analysis – Stage II

(-) - Not Applicable
(r) - Rejected
(K) - Kept

Design Parameters – Stage II		Figures of Merit – Stage II (x weighting)											
		Ease of Construction (x2)	Component Safety (x1)	Component Safety (x1)	Component Interactions (x2)	Sortie Performance (x2)	Difficulty of Repairs (x1)	Rated Aircraft Cost (x1)	Cost (x1)	Motor Aerodynamic Flow (x2)	Motor Access/Mounting Ease (x1)	Sum of Ratings	Decision
Wing Types	Low Mono-wing	1	-	-	1	0	0	0	0	-	-	4	K
	Bi-plane	-1	-	-	-1	0	0	0	0	-	-	-4	R
	High Mono-wing	1	-	-	0	0	0	0	0	-	-	2	R
Wing Structure and Materials	Rib Structure	-1	0	-1	-1	0	-1	-	1	-	-	-5	R
	Foam Core	1	0	0	0	0	-1	-	0	-	-	1	K
Structural System	One Piece	1	-	1	1	-	0	0	-	-	-	5	K
	Three Piece	0	-	0	-1	-	0	0	-	-	-	-2	R
	Bending Beam	1	-	-	1	-	0	0	-	-	-	4	K
	Ring Frame	-1	-	-	-1	-	0	0	-	-	-	-4	R
Tail Structure	Twin Body H	-1	0	0	-1	0	-1	0	0	-	-	-5	R
	Inverted V-tail	0	0	-1	0	0	0	0	-1	-	-	-2	R
	T-tail	1	0	0	1	1	0	0	0	-	-	6	K
Fuselage Configuration	Flying Wing	-1	-	-	-1	0	-1	1	0	-	-	-4	R
	Lifting-Body	0	-	-	1	1	1	-1	0	-	-	4	K
Fuselage Materials	Fiberglass	0	-	-1	0	1	1	0	0	-	-	2	R
	Aircraft Grade Plywood	-1	-	-1	0	1	0	0	1	-	-	0	R
	Kevlar	0	-	1	0	-1	1	0	-1	-	-	-1	R
	Carbon Fiber Reinforced Kevlar	-1	-	1	1	1	1	0	-1	-	-	3	K
Landing Gear	Tail-Dragger	0	-	1	0	0	0	0	0	-	-	1	R
	Tricycle	0	-	1	1	0	0	0	0	-	-	3	K
	Quadracycle	-1	-	-1	1	0	-1	-1	-1	-	-	-4	R
Power Plant	1 motor 22 cells	-	-	-	1	-	-	1	1	0	1	6	K
	2 motors 11 cells each	-	-	-	0	-	-	-1	-1	0	-1	-2	R

Stage II of the CDP was necessary to obtain our final aircraft characteristics. This stage rendered the designs that promoted a finished product, which in turn satisfied all of the design parameters. FOMs for Stage II included ease of construction, payload access and capacity, strength to weight ratio, difficulty of repair, component and interfacing strength, and component/flight safety. The application of these FOMs to specific design parameters resulted in a final set of components that, when assembled, produced an aircraft design with all of the desired characteristics.

3.2.1 Wings

Wing FOMs in Stage II focused mainly on structural complexity and construction. The FOMs were applied to the determination of the best wing type.

3.2.1.1 Wing Type

Bi-wing: The bi-wing implemented failed to satisfy the ease of manufacture FOM as it required the fuselage to be reinforced in multiple places and had the possible necessity of external bracers. The increased difficulty of manufacturing, increased cost, and additional induced drag thus eliminated it as a design concept.

High Mono-wing: High mono-wing design carried the benefit of large ground clearances for propellers (for wing mounted motors). It was however a major challenge in terms of designing fuselage mounted landing gear, which would not interfere with the payload. This was therefore eliminated due to the structural stipulations.

Low Mono-Wing: Low mono-wing configuration demonstrated to be effective in both TLAR I and TLAR II. Landing gear length is minimized, allowing for lighter and/or stronger struts. Torsion load transfer can be accomplished with limited interference with fuselage layout. The possibility of low propeller clearance was shown to be inconsequential due to the nose mounted motor which yielded several extra inches of clearance. This configuration was chosen for further analysis and development.

3.2.2 Empennage

The goal for the second stage of the CDP of empennage was to analyze the interaction of the surviving Stage I conceptual designs as combined with the rest of the aircraft. The primary focus areas were the structural and aerodynamic dependencies and interactions with other components in the design under the application of further FOMs. The sorties that TLAR III will fly consist of steep climbs, tight turns and short take-off and landings.

"Twin Body H": In the conceptual design "Twin Body H" configuration was implemented. While the construction was viewed as reasonably simple and sturdy, several disadvantages were immediately apparent. This design required having two fuselages and an additional servo, both of which significantly increase the RAC and add to the aircraft weight. While the structural and aerodynamic properties of this design were favorable, the added cost to the overall weight and RAC of the aircraft was too much to consider it further for the final design.

Inverted "V": A tricycle landing gear and high tail boom, provided the opportunity to apply the "Inverted V" configuration due to the fact that it would have enough ground clearance. Aerodynamically, the concept was free of major concerns related to interaction with the fuselage and main wing. While the aerodynamic and structural constraints were satisfied by this configuration, there were distinct drawbacks related to the complexity of the control design and the ease of manufacture. This increased complexity eliminated the possibility of an Inverted "V" configuration.

"T" Tail: T-tail configuration prevents tail surface washout and related loss of stability, the high placement of the horizontal stabilizer was essential. The fact that this configuration has been proven effective in the flight competition in past years while still being simple and efficient, led to the decision that it would again be the tail configuration of choice for TLAR III.

3.2.3 Fuselage

Stage II fuselage design involved the evaluation of the fuselage design possibilities within the various configurations. The FOMs used to ensure that the design goals were met included ease of construction, payload access, RAC and component and interfacing strength. The two aircraft configurations considered Blended Wing and Lifting Body. An analysis of the characteristics of these three styles was necessary to decide which will best satisfy the FOMs.

Blended Wing: first design featured a fuselage blended into a wing thus providing a good drag characteristics. Also there is no empenage thus provides a better RAC because of time saved in not making those components. One major concern arose in this design that lack of tail empenage provides a poor stability thus can lead to increased risk of crashing the plane.

Lifting Body: second design style featured a single fuselage that would house the payload and flight equipment. This configuration was considered because it provides good airflow around the fuselage, maintains interfacing strength and would not affect the RAC drastically. In addition, efficient access to the payload is granted via a hatch located at the end of the fuselage. This design meets all the FOMs and was thus considered a viable design option.

3.2.4 Landing Gear

In Stage II of the CDP, advantages and disadvantages of each remaining landing gear configuration were explored as they related to specific design choices made for other components of the aircraft. The three major considerations focused on were; ground handling, plausibility of adding brakes, and minimization of weight and drag during flight.

3.2.4.1 Landing Gear Configuration

Tricycle: Tricycle arrangement was implemented because of the additional stability due to the center of gravity is ahead of the main (rear) wheels, the aircraft would be inherently more stable on the ground and can be landed at a fairly large "crab" angle. While this configuration required one extra gear block and steering servo for the nose landing gear, which added more weight to the design and increased the RAC, the increased ground stability and ability to add brakes to the rear wheels was a desirable perk. Having brakes would enable shorter landing roll time thus bettering the flight scores. This concept therefore satisfied the Stage II FOMs and was chosen as the landing gear configuration for TLAR III.

Quadra-cycle: This configuration has good ground handling stability and an improved strength to weight ratio due to the lack of struts. However, two wheels require two servos for steering ability, thereby increasing the RAC greatly. Due to these unnecessary RAC increases, the Quadracycle was eliminated as a viable configuration.

Tail Dragger: The tail dragger landing gear configuration provided ample propeller clearance by angling the nose off the ground. In addition, its simple configuration of connecting the tail wheel to the same servo that controls the rudder would make the aircraft more easily controlled on the ground. While this dual use for a servo provided an excellent reduction in RAC, the design had structural strength concerns due to the thin rear wheel strut being under increased plane and payload weight. Therefore the tail dragger design was eliminated as being a configuration for further analysis.

3.2.5 Propulsion and Power System

The three configurations developed in Stage I of the CDP provide a basis for the propulsion requirements that needed to be met. At this stage however, thrust or specific efficiency requirements were not determined. Instead, FOMs such as power limitations of the motor and a low REP were applied to the design parameters such as number of motors and number of batteries per motor. This was similar to the FOM/design parameter process applied during Stage I of the conceptual phase, except that here it was applied in parallel, with analysis of the interaction with the other components in the design. This was accomplished by applying FOMs relating to aerodynamic flow of the thrusting air, ease of construction and motor/controller cooling to determining the final rating of each design.

Single Motor: The single engine configuration was the only configuration seriously considered for the design of the aircraft. Even though multiple motors result in better trust and power, the penalty incurred for this option is extremely high. This penalty would also factor into the total number of batteries being used to power the aircraft motors. For this reason the total weight of the battery pack must be kept to the bare minimum.

Summary: In order to minimize the RAC of the aircraft the only acceptable form of power system would have to be a single motor configuration. This configuration would also have to be powered via a single battery pack with minimum weight. The propellors, will have to be optimized for cruise speed, as this will be crucial in reducing the mission completion time. Further analysis of all these configurations will be required to conclude if a gearbox will be necessary.

3.2.6 Structural System

The purpose of Stage II for the structural system was to evaluate the individual strength as well as the interface strength within the various configurations. The Stage II FOMs that were pertinent to the structural system were RAC, component interaction and ease of construction. Through the application of these FOMs the individual structural components remaining from Stage I are evaluated. The structural system components were evaluated as follows:

3.2.6.1 Spar Structure

The shear and bending stress increases approaching the fuselage interface, therefore in the interest of weight conservation, the size of the spar structure could be made to vary. In all CDP aircraft configurations, it was also determined that torsional loads were a major concern, needing to be addressed by the design of the spar structure.

Two piece: The two piece spar model consisted of two separate spar lengths, one from the wing tip to half of the wing span, and the other continuing to the wing's root. The exact size would be determined by the existing stresses due to the shear and moment. However, the required torsional strength was not sufficient enough to consider this design further.

One piece: The one piece model is a solid, single-piece spar running the length of the wing. The size, and therefore weight, of the spar could be further reduced in respect to multiple piece spars. An additional benefit of the One Piece was its ability to accurately maintain the wing angle of attack. This model satisfied the Stage II FOMs and thus was considered a feasible spar design.

3.2.7 Conceptual Design Phase – Stage II Summary

The combined Conceptual Stage I and Stage II had the goal of determining a final configuration for the aircraft design. For each possible component of the configuration: airfoil; wing; tail; fuselage; landing gear and power supply, design parameters were defined and then eliminated through the application of FOM to determine the best final choices for the preliminary aircraft design.

The result of this process was the aircraft designated as "TLAR 2.9", a design very close to the final design, "TLAR III", though lacking final sizing and optimization of the components. "TLAR 2.9" features a single aerodynamically faired cylindrical fuselage riding over a low mono-wing. The payload access, through the nose of the fuselage, was facilitated by the symmetric mounting of two motors to the leading edges of the wings. Similar to last year's design was the implementation of a "T" tail configuration on a tail boom extending from the center of rear of the fuselage. This lengthened design allowed the use of the tail dragger landing gear to increase the lateral stability of the aircraft on the ground. Overall the preliminary design was simple and efficient and reflects the great effort put forth in the conceptual design to determine the best choice for each concept.

4 Preliminary Design Phase

As the design of the aircraft progresses, estimates for actual design specifications need to be made. The PDP of the design focuses on completing the initial calculation and estimation of general sizing, performance, and configuration with regards to the final aircraft design created in the second stage CDP.

During this process, techniques developed for the design of propeller driven general aviation aircraft were used to a large extent. Standard aerodynamic theories, such as Prandtl's lifting line method, were also implemented in computer algorithms to analyze the aerodynamic properties of the wing. While these techniques are not expected to be exact, they were implemented with confidence as TLAR II validated their accuracy in last year's competition. Overall, these proven methods provided excellent analysis results while directly exposing the design team to the fundamental principles of aircraft design.

As the CDP was highly focused on determining design parameters and FOMs to apply to the design process, so was the PDP. Here, however, the considerations that need to be made are more related to the optimization of flight performance and aircraft component interaction, than with the broader concerns examined in the previous sections. For each area of the preliminary phase, design parameters and FOMs will be applied as suit that particular area, and will be described specifically. Overall, we are still concerned with component and personnel safety, structurally and aerodynamically favorable component interaction, ease of manufacture and construction, and a low RAC.

4.1 Wings

The wings PDP deals with the general sizing of the wing and associated components as well as materials selection. Wing geometry was chiefly governed by necessary flight characteristics and optimized by RAC concerns.

Materials: Strength to weight ratio was a primary FOM in this stage, as was cost. The goal was to maximize the strength to weight ratio, while also considering the implications to construction. Aircraft grade plywood is relatively cheap and lightweight. Manufacturing a wing with this material, however, is a complicated task. The wing would have to be made out of a series of ribs, each of which had to be individually assembled and shaped. The difficulty of this fails to satisfy the ease of construction FOM. A composite wing holds several advantages over the plywood wing. It was easier to construct and was considerably stronger while being comparable in weight. The structure and procedure were established by TLAR II in the 2001 competition. Composite wings are somewhat more expensive than plywood, but the increased ease of construction resulted in their selection for the final wing structure.

Wing Geometry: The rectangular wing planform selected out of the CDP required optimization to reduce unnecessary drag and maximize lift and stability. Many geometric characteristics either had an adverse impact on performance or simply were not applicable to a model aircraft. Adaptations such as sweep and wing twist were not considered due to complexity of design and manufacture.

The wing sizing was begun with a desired aspect ratio of at least 8. Since there is no wingspan limitations, it was necessary to design the wing to not just perform well, but also reduce RAC as much as possible. In short, it is easy to over-design a wing that will produce lots of lift, but it might not be fully optimized. After analysis of the power system and an estimate of the fully loaded aircraft, and 84" wingspan with a 13.5" chord length was decided upon. It was also decided that no taper would be introduced in the design of the wing. Although a taper tends to reduce the wing tip angle of attack during high G maneuvers, thus unloading the wing, it also reduces the wing's area, therefore reducing the lift attained from the wing. Because of the way the RAC of the aircraft is calculated, it would be more advantages to have a wing without any taper. Finally, the wings are connected to each other. This significantly makes construction easier by eliminating the need for a wing joiner.

Stability: Documented performance characteristics of the chosen platform and low wing configuration led to some concern over roll axis stability. The low wing configuration creates a pressure buildup during a banked turn due to side-slipping (the fuselage interferes with airflow over the upwind wing). This causes a tendency for the aircraft to roll into a turn as the leading wing loses lift. To compensate for this, a dihedral angle was introduced to roll the aircraft back to its stable flight position. Due to the lack of a simple method to calculate the appropriate dihedral angle, empirical data was used to determine that, for radio controlled aircraft design, a 3° dihedral is most effective.

Control Surfaces: The type and location of control surfaces were dependent, in part, upon the rest of the primary aircraft structures. The available options included flaps, ailerons, or a hybrid control surface. Achieving the necessary level of control was the principal concern, followed by the impact to the RAC and building complexity.

Flaps were considered to increase lift during takeoff in order to minimize the takeoff distance. However, the inclusion of flaps would add significantly to the RAC. Spoilerons were chosen in place of ailerons to ensure control of the rolling/turning of the aircraft at low airspeeds. They are hybrid structures combining spoiler effects with aileron control surfaces. They help the flow stay attached to the wing during slow, high AOA flight, ensuring that the ailerons do not stall before the main part of the wing. They can also be used after touch down to reduce the lift of the main wing and ensure that the aircraft stays on the ground. In using spoilerons, the RAC penalty of the flaperons is avoided. Typical sizing of an aileron structure is approximately 25% of the span, extending to the outer edge of the wing. Thus our initial control surfaces were each 21 inches long.

4.2 Empennage

The preliminary phase of the Tail design focused on the initial determination of the sizes of the vertical and horizontal members, the size of the control surfaces, and the placement of the tail surfaces away from the aircraft's CG. Other design parameters considered at that point in the design were material choices, and manufacturing techniques. The main FOMs that were applied to these design parameters were ease of construction and stability.

General Sizing: The Tail sizing calculations used were a combination of general aviation and R/C aviation empirical data relations. Specifically to design the volume coefficient of both the horizontal and vertical members as well as the size of the elevator and rudder control surfaces.

The sizes of the tail components are functions of their distance from the CG of the aircraft and main wing size. Empirical data gives a function for tail volume coefficient, which is the standard method of approximating initial tail size, dependant on these parameters (equations shown below). Modifications to this empirical relationship for a T-tail allowed the vertical coefficient to be reduced by approximately 5%

due to end plate effect of the horizontal member. Also, with the engines mounted on the leading edge of the fuselage, the tail arm was given to be roughly 50% of the fuselage length as measured from the mean aerodynamic chord of the main wing.

Typical values used for the volume coefficients depend on the type of aircraft and, from experience for homebuilt aircraft, are approximated as 0.5 and 0.03 for the horizontal and vertical respectively. With these available parameters, and the size of the aircraft configuration at this stage giving an arm of 31 in, the initial areas of the tail sections were determined to be 237 in^2 for the horizontal and 96 in^2 for the vertical.

$$Area_{HorizontalStabilizer} = \left(Coefficient_{HorizontalVolume}\right)\left(MAC_{MainWing}\right)\left(Area_{MainWing}\right)/\left(Arm_{HorizontalStabilizer}\right)$$
$$Area_{VerticalStabilizer} = \left(Coefficient_{VerticalVolume}\right)\left(Span_{MainWing}\right)\left(Area_{MainWing}\right)/\left(Arm_{VerticalStabilizer}\right)$$

An empirical approach was utilized in the preliminary sizing of the tail control surfaces. Guidelines derived from empirical data suggest that the rudders and elevators be approximately 25% of the tail chord, while extending from the tail boom to about 80-90% of the tail span. Given these areas and control surface relationships, as well as an Aspect Ratio and Taper Ratio of 3.4 and 0.92 proven successful for TLAR II, the horizontal stabilizer was determined to need a span, root chord, tip chord and elevator chord of 26.0, 9.5, 8.75, and 2.0 inches respectively. With the Aspect Ratio and Taper Ratio of 1.59 and 0.76, again from TLAR II, the vertical stabilizer was determined to need a span, root chord, tip chord and elevator chord of 12.0 in, 8.50 in, 7.0 in, 2.5 in. respectively.

Manufacturability: Similar to the main wings, FOMs such as ease of construction and strength to weight ratio must be applied to all material choices. One technique considered was a rib/spar structure of aircraft ply, which is lightweight and strong, but again very complex and time consuming to manufacture. The materials that were finally chosen fitted well with the most simple of available manufacturing techniques which was foam core, carbon spar, and fiberglass skin structure. These materials provide excellent strength to weight ratios and the ability to manufacture the components quickly with tools already available from the construction of TLAR II.

4.3 Fuselage

Optimization of the fuselage included determining a viable support structure and the necessary dimensions for maximum payload capacity. In order to determine the necessary dimensions for the fuselage a packing structure for the softballs was needed. The FOMs that were considered pertinent during this design phase were interfacing and component strength, weight and payload access.

A satisfactory packing arrangement was found following several attempts to find an arrangement that was not too long or too wide. This arrangement consisted of a rectangular organization of 4 softballs wide and 6 softballs long giving a total of 24 softballs (See Drawing Package). With the softballs packed as tightly as possible this resulted in a cargo loading area of 16x24 inches. However this rectangular box sitting on top of the wing would create much undesirable drag. In order to mitigate this problem, a symmetric airfoil (NACA 0013) would be designed to overlay the cargo ball array.

In order to avoid payload access problems and to accommodate the batteries and flight equipment, the fuselage dimensions would have to be slightly larger. This was not a problem, as the thickest part of the symmetric airfoil allowed for ample room for these accessories. The room created also accommodates a support structure for the wing and boom interfaces. Working closely with the structural system group allowed for mutually beneficial solutions.

Box Beam Structure: This arrangement describes a box type structure designed to be able to withstand shear and torsional stresses. Since the top skin of the fuselage would be breached to access the payload, the fuselage needs to have an internal structure designed to withstand the transfer of forces and moments from the tail and wing. Similar to a drawer from a cabinet, in essence the structure of the fuselage is an open-topped box that is able to resist shear and torsional forces. This torque box consists of ball-floor, airfoil-shaped sides, lower skin, and wing. The walls of this box would have to be very strong, yet very light. This introduced the idea of "Sandwich Material" for this design. "Sandwich Material" consists of two very stiff but thin layers of carbon, which surround a slightly thicker layer of anisotropic (stronger in one dimension than the other) foam or balsa. This creates an I-beam effect, resulting in great strength-to-weight ratio.

Final Sizing: The final size of the fuselage was determined to be 39.5" in length, 16.25" in width and 5.5" in height at its thickest point. The box structure itself (entirely made of "Sandwich Material") consists of two side walls in the shape of a symmetrical airfoil. These two side walls are then connected together with a 39.5"x16.25" bottom with circular cutouts for where softballs can be placed. This structure is then reinforced with three bulkheads placed 4.25, 27.5, and 31.5 inches from the leading edge of the side walls. The wing sits directly beneath the latter 2/3 of the softballs, as there is an airfoil cutout for which the wing fits into. Hard-points on both wing and fuselage allow for the attachment of these two components to each other.

4.4 Landing Gear

Due to the previous year's bad experience with failed landing gears this portion of the aircraft was given much attention. It was necessary to optimize the landing gear configuration as well as specific components associated with the landing gear including gear struts, wheels, and gear blocks.

Landing Configuration: At this point, the preliminary calculations and design of a tricycle landing configuration could be completed. To prevent the aircraft from overturning, the main wheels should be laterally separated beyond 25 degrees angle off the center of gravity as measured from the rear in a nose-down attitude. This was evaluated to be a distance of approximately 15 in. from the aircraft centerline at the spar location. The nose landing gear should be placed as close to the front of the aircraft as possible to prevent the propellers from hitting the ground on a hard landing.

Gear Struts: A number of materials were considered for the gear strut, which was designed to interface with the wing spar, including steel, aluminum, and carbon. Carbon and steel would provide the most strength, while aluminum and carbon would be the lightest. Although light, aluminum would not provide the strength required for harsh landings. Due to the previous year's experience with a steel gear strut, the team was confronted with two options; Design a thicker strut from steel, or design a strut from Carbon. It was calculated that steel would be far heavier than a carbon strut with similar strength. The only downside would be the difficulty of manufacturing associated with the composite strut. Despite this, the team decided that composite strut would much greatly improve performance and reliability.

Wheels: Although construction of a lightweight aluminum wheel was a possibility, previous year's experience allowed the team to eliminate this option. It was difficult to attain transverse skid resistance from aluminum wheels, and gluing of rubber o-rings to the aluminum proved a poor tactic as the thin rubber quickly disintegrated upon landing impact. The alternative would be rubber wheels, which are heavier than the custom-made aluminum wheels. To remedy this problem, in-line skating wheels will be purchased and machined to reduce their weight.

4.5 Propulsion and Power System

The propulsion choices that were made in the conceptual phase of the paper were based on general power management, motor life, and RAC concerns. In the PDP, there was a lot more known about the aircraft configuration and more precise propulsion system design could be conducted.

In limiting the motor type and manufacturer, the contest organizers made the determination of motor type a fairly narrow search. Due to recommendations from a number of people with previous experience with such motors, the Astro line of motors was eliminated. We also had our Graupner Ultra 3300 7-wind series motor from the 2001 competition, which was still in great condition and will satisfy this plane's needs and the competition requirements. This motor is designed to run off of 20 volts and turn a direct drive propeller. Assuming a maximum current draw of 35 Amps, safely below the 40 Amp limit, the 7 wind series motor gave an efficiency, output wattage and RPM of 83.5%, 650 Watts, and 8300 RPM, respectively

At this point, using a setup built by the team mentor Steve Neu, a preliminary experiment was performed to qualitatively test how the motor performs under a load. The testing platform was setup precisely for this purpose, as the RPM, Output Voltage, and Input Current were measured. This test also applied a load onto the motor (using hysteresis brakes) and measured the torque applied (using a strain gage) by the motor. From this information, the motor efficiency was calculated. A plot of this experiment can be seen in the following figure. As can be seen from the following figure, the efficiency of the motor is maximized between 12,500 and 13,500 RPM. Because of this and the choice of propeller diameter and pitch, a 2:1 gear ratio will be used to ensure that the motor RPM's are kept at the optimum range.

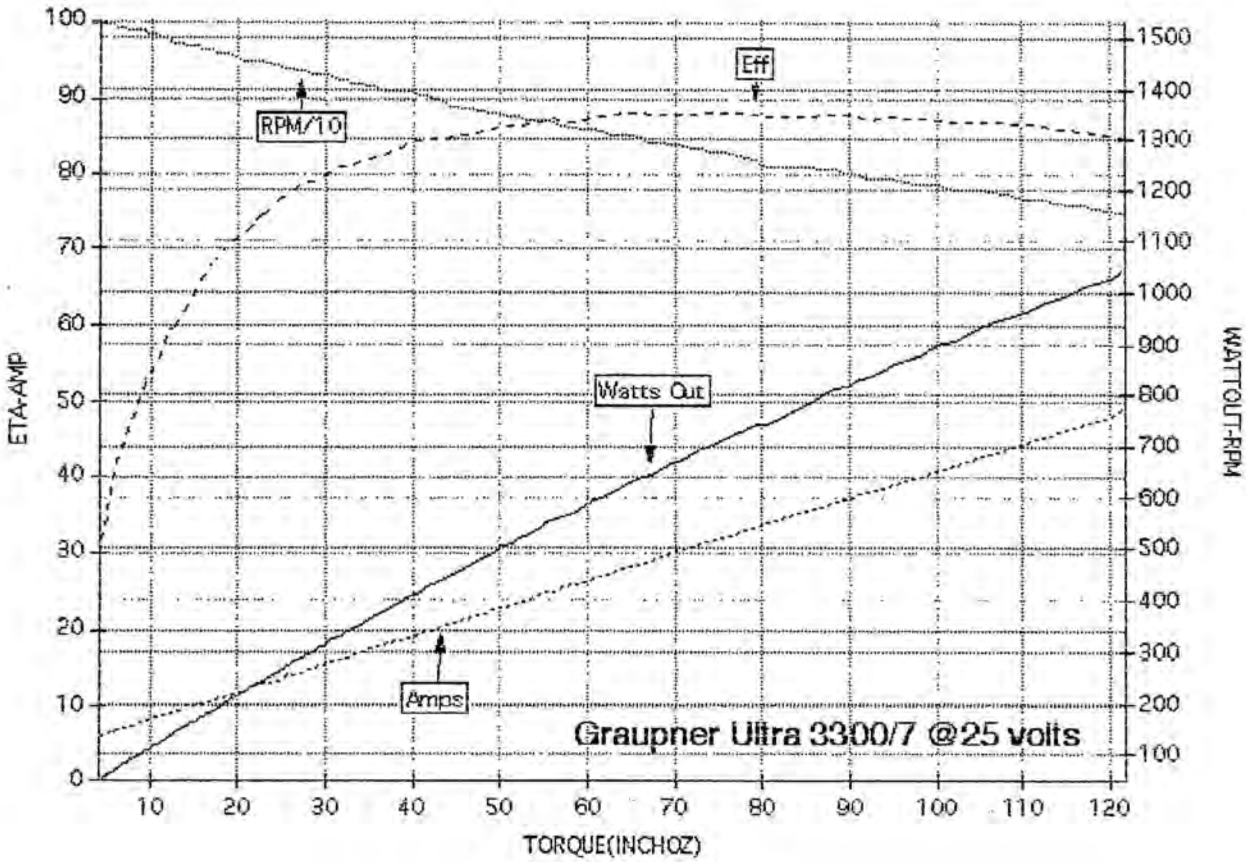

Figure 4.1

Initial testing on the Graupner Ultra 3300/7 motors showing vital statistics.

Courtesy of Steve Neu

The propeller choice was made from a decision for a cruise speed of 65 mph, at a current-draw setting below maximum. The Graupner Ultra 3300/7 motor operates most efficiently at an input voltage of between 23 and 29 volts. At this setting and RPM, a 20" diameter x 20" pitch propeller gives a speed of approximately 65 mph. This factor of safety will be verified during flight testing to determine if an alternate propeller will be needed.

The final step in determining the power system was the choice of batteries. The weight, voltage and current limit was dictated in the rules. The batteries were chosen based on durability, availability and cost. The Sanyo 2400 batteries that were used in last year's competition performed very well under raised current levels and fast discharging, so their reliability had been proven. This fact, combined with their increased availability and reduced cost this year, led to them being selected.

The final configuration for the power plant of TLAR III featured a single Graupner 3300/7 motor, powered by 22 Sanyo 2400 batteries through a 2:1 gear ratio and a commercially purchased propeller of 20" diameter and 20" pitch.

4.6 Structural System

The principal objectives of the PDP for the structural system were to maximize the strength to weight ratio without adversely affecting the payload capacity and access. Focus was placed on structural integrity, to avoid failure under flight and landing loads and component interfacing, as most systems fail at joints and interfaces.

Application of theory from solid mechanics and statics provided the basis upon which necessary design adjustments were made. These adjustments were the variation of the cross-section of the spar structure and the fuselage/wing interface method. In order to determine the best cross-section for the spar structure, stress and static analyses were conducted via the use of Microsoft Excel. Optimization of the fuselage/wing interface involved the determining the maximum stresses, for which it was necessary to determine the maximum load experienced (during banked turns). The following equations were utilized to determine the necessary values of maximum moment and bending loads:

Newton's Law: $\sum F = ma$

Moment Equation: $M = Fd$

Maximum Bending Stress: $\sigma = \frac{Mc}{I}$

Moments of Inertia: $I_x = \int_A y^2 dA$ & $I_y = \int_A x^2 dA$

4.6.1 Spar Structure Optimization:

The wing's thickest point was chosen as the location for the spar structure so as to allow the furthest distance, 'c', from the neutral axis for bending. At the wing root and tip the width of the carbon were 2.25" and 1.5", respectively. At specific points along the span, the values of 'c' and 'M' were fixed thus allowing for variation of the moment of inertia by varying the cross-sectional area. The above equations were used, along with values for a 27 lb. aircraft travelling at 65 mph, to calculate the following load values:

Maximum G Force (with safety factor): 9.7

Maximum Load (per wing panel): 2118.5 oz.

Maximum Moment: 18345.6 in.-oz.

Moments of Inertia: 0.3869 in^4 (box beam)

Maximum Bending Stress: 1,002,000 psi (box beam)

Although the maximum bending stress can be taken by both the box-beam and I-beam sections, the box-beam cross-section was chosen due to the additional strength that would result.

4.7 Preliminary Design Phase Summary

The PDP analyzed the preliminary configuration as developed in the CDP with regard to the determination of exact sizing and component interaction. Design parameters that were related to the purpose of sizing the components were defined locally. FOMs such as component safety, structurally and aerodynamically favorable component interaction, ease of construction, and a low RAC were the primary factors determining much of the component design. Most general sizing calculations that were done were based upon those used in designing a propeller-driven general aviation and radio controlled aircraft. Precise calculations on flight performance will be completed during the DDP now that the detail configuration of TLAR II has been established.

5 Detail Design

The goal of the DDP is to optimize the sizing and design parameters that were developed in the PDP with regard to flight and takeoff performance. Similar to the PDP, the primary performance analysis techniques used were those applied to propeller driven general aviation aircraft. The calculation of basic characteristics, such as lift and thrust, allowed for the computation of more specific flight characteristics such as takeoff distance, rate of climb and endurance. In each section of the PDP, individual component weights were estimated.

5.1 General Sizing

5.1.1 Weight Estimate

Estimates based on experience gained from last year's design were assembled into a preliminary weight estimate of 20 lbs. Upon completion of the DDP and construction of the aircraft, the final value for aircraft weight was estimated at 24.5 lbs. While heavier than first estimated, it was still well within the competition rules and design limitations of the aircraft.

5.1.2 Wing Performance

The detailed performance calculations of the main wing were based upon Prandtl's classic lifting line theory. Prandtl's theory was implemented numerically in Matlab code and run with the sizing parameters developed in the PDP given inputs for wing dimensions of span, root chord length, aspect ratio, $\alpha_{CL=0}$. These values were reduced from the theoretical infinite wing data by approximately 26%, which was relatively efficient despite the low aspect ratio. However, by altering the values of the taper ratio, it was possible to achieve a 20% reduction. To minimize RAC, we had to use rectangular wing because the advantages of the tapered wing were negated by the cost factor. The final values for $C_{L\alpha=0}$ and C_{Lmax} 0.562 and 1.544 respectively and for $Cd_{\alpha=0}$ and $Cd_{\alpha max}$ .007055 and .023104 respectively, were realized with a root chord of 13.5 in. This gave the final wing an aspect ratio of 6.22, taper ratio of 1.00, platform area of 1134 in^2. An important quantity resulting from these refined sizing and performance characteristics was a wing loading, W/S, of 2.74lbf/ft^2.

5.1.3 Fuselage Layout

The final configuration of 4x6 softballs in the fuselage brought a peculiar problem of increased drag over the very wide (16.25 in) fuselage. To reduce the drag a more streamlined fuselage was suggested and implemented. NACA 0013 airfoil shape was used for this purpose. Additionally, there will be a benefit of the lift produced at angle of attack, which will decrease the take-off distance and increase the rate of climb. Consideration of the lift generated by the fuselage shall be limited to replacing the wing area displaced by the fuselage. Since a hatch will be cut into the fuselage skin for loading the payload, torsional strength of fuselage will be lost. Torsional stiffness comes from the torque box made up of the fuse sides, bulkheads, ball floor, wing and bottom skin.

5.1.4 Motor Thrust Available

While the static thrust of an engine was a necessary calculation related to the determination of performance characteristics such as takeoff distance and rate of climb. Analysis of power supplied being reduced by the inefficiency of the motor and propeller was used to indicate the amount of power available to actually propel the aircraft. Having determined the number of cells to power each motor in the preliminary phase, the total power available to the motor was calculated using the equation $P = VI$, giving an available power of 1017 Watts. With a combined efficiency of .78, the thrust developed per engine was 6.18 lbs. This gave a final thrust-to-weight ratio of 0.286.

5.2 Flight Performance Calculations

In optimizing sortie performance, it was necessary to evaluate takeoff, rate of climb and range/endurance characteristics as well as static stability. While dynamic stability was also a concern, for a fairly conventional design as TLAR III, dynamic instability has proven to be highly transient in modes that are easily controlled by a skilled pilot.

5.2.1 Takeoff Performance

The takeoff profile for TLAR III was essential, as it was a competition constraint. It was determined for takeoff that the rotate/stall speed needed was 42.1 ft/s, while the actual takeoff speed was 46.3 ft/s.

For the Reynolds's number (~200,000 to 300,000 based on M.A.C.) at which the takeoff was performed, the induced drag of the aircraft was small enough to be approximated to zero. This enables the approximation of integrating Newton's second law over the ground run of the aircraft. This integration of the acceleration can be reduced to the following equations from reference 1:

$$\left(\frac{1}{2gK_A}\right)\ln\left(\frac{K_T + K_A V_f^2}{K_T + K_A V_i^2}\right) \quad \text{with} \quad K_T = \left(\frac{T}{W}\right) - \mu, \quad \text{and} \quad \frac{\rho}{2(W/S)}\left(\mu\, C_L - C_{D_0} - KC_L^2\right)$$

A ground roll of 166 ft was calculated for a rolling resistance factor (μ) of 0.05 and a total takeoff distance of 183.5 ft. While this seems close to the distance limit, the likelihood of winds being present during the competition will shorten the actual takeoff distance. If this is not the case, and taking off within the limit proves difficult, reducing the payload may be considered.

5.2.2 Rate of Climb

The rate of climb (R/C) is the vertical component of the aircraft velocity. It can be expressed in terms of weight (W), perpendicular component of drag (W_D) and velocity (V). W_D is a function of thrust (T) and drag (D), therefore yielding:

$$\frac{R}{C} = \frac{(T - D) \times V}{W}$$

The best climb rate will occur at the velocity for maximum lift to drag ratio, L/D_{max}. Although the thrust produced by the propeller and corresponding power available changes with the airspeed, an approximation was made to show that the maximum lift to drag depends only on the values for the parasite drag coefficient, C_D and the wing's aspect ratio, AR.

$$\frac{L}{D_{\max}} = 0.886\sqrt{\frac{AR}{C_D}}$$

Using these formulas, the rate of climb for the aircraft was calculated to be 597 ft/min.

5.2.3 Turning Radius

The turning radius gives an indication of how much distance, time and power are needed to perform a turn and is necessary because it affects sortie flight time and power management.

The turn radius calculations began with the assumption that the turn will be made at the cruise speed of 65-MPH. The equation

$$n = \frac{\left(V_{cruise}\right)^2\left(C_{L_{\max}}\right)}{2\left(W_{aircraft}\right)}\left(Area_{wing}\right)$$

gave a load factor of 4.87 for the turn. From this, and geometry, a bank angle of 78.1 degrees and turn radius value of 59.3 ft was calculated.

5.2.4 Range and Endurance

Range and endurance characteristics are essential performance indicators for an aircraft designed to participate in timed, limited fuel flight profiles. The range figure of TLAR III was based on the power available and the power that the missions will require, so that the time can be estimated.

Initially, this was accomplished by examining TLAR III in steady flight. The power available is the number of cells multiplied by the power rating for each cell. This equated to 1 battery pack multiplied by 2400 milliAmp-hours for at total of 2.4 Amp-hours. This allows 6.3 minutes of flight time at the current setting of 22.8 Amps, which subsequently gave a cruise range of 6.8 miles and 3.6 minutes and maximum thrust.

While this flight time was less than the maximum flight period, an Excel spreadsheet was used to determine a flight plan. It calculated using average speed and current setting breakdown for the entire mission profiles, with gliding and powered back cruises; the flight time was under five minutes which is far less then the maximum time given.

5.2.5 Static Stability

The ability of the aircraft to return to trimmed flight, if it was somehow deflected, was an important consideration. Due to the symmetry of the aircraft about the centerline of the fuselage, it was possible to achieve some roll stability of the design, with the selection of 3° dihedral in the preliminary phase. The focus was placed on the pitch stability (the directional stability was already addressed in the sizing of the vertical tail stabilizer). A well-designed aircraft that has good static stability, historically will also behave well dynamically.

The pitch stability is related to how the main-wing and horizontal stabilizer work together to correct pitch deflection. For TLAR III, this was especially critical due to the choice of a symmetrical airfoil for the tail. To prevent excessive corrective elevator deflection during steady flight, the pitching moment of the airfoil needs to be balanced by the placement of the center of gravity relative to the center of pressure of the wing. Assuming that any pitch deflections would be small, the pitch static stability is directly dependent on the horizontal stabilizer. The calculations focused on determining the exact placement of aircraft CG for a desired Stability Margin of 0.3. This margin is the geometrical distance between the location of the CG and the location of the neutral point. The neutral point was determined with the following equation along with design parameters defined earlier in the paper.

$$x_{np} = x_{AerodynamicCenter} + V_t\left[1 - \left(\frac{4}{AR_{MainWing}}\right)\right]$$

This allowed the placement of the wing at the optimum position for stability. The main wing leading edge was located at 11.375 in from the nose of the aircraft, which places the CG almost directly on the spar location. Additional pitch stability was achieved through decalage (angle between the horizontal stabilizer and the main wing), which was initially set at 1° and will be finalized during flight-testing.

5.2.6 Systems Architecture

The Systems Architecture describes the electrical components used to fly the aircraft including the batteries, servos, receivers, and transmitter. The number, location, and type of motors and batteries were determined in the propulsion section of the PDP. Determining the types of servos remained.

Given the values obtained for the torque required by each servo, two different servos (HS-225MG and HS-545BB) manufactured by Hitec RCD Inc. were chosen for the rudder, elevator, and aileron controls. The HS-225MG, capable of 55-67 $^{oz}/_{in}$ of torque was used to control the elevator. The HS-225MG was also used for the rudder, despite the rudder having less control surface area than the elevator, because the same servo controls both the rudder and the nose wheel. The spoilerons however require more torque to control due to higher surface area, therefore a more powerful servo, HS-545BB, capable of 62-73 $^{oz}/_{in}$ of torque was used.

(Tables on Next Page)

5.2.7 Detail Design Summary

Table 5-1 General Sizing

Design Parameter	Size
Aircraft Dry Weight	12 lbs.
Manufacturers Empty Weight	14.9 lbs.
Full Capacity Weight	24.5lbs. (with 24 Softballs 9.5 lbs.)
Battery Pack Weight	2.9 lbs. (22-2.4 Amp Cells)
Main Wing Configuration	Low Mono-Wing
Main Wing Airfoil	E212
Main Wing Area	1134 in^2
Taper Ratio	1
Aspect Ratio	6.22
Number of Motors	1
Propeller Size	20" x 20"
Total Thrust	5.31 lbs.
Horizontal Stabilizer Area	226 in^2
Vertical Stabilizer Area	125 in^2
Tail Airfoil	NACA 0009
Fuselage Height	5.25 in
Fuselage Length	39.5 in
Fuselage Width	16.25 in
Fuselage Foil	Modified NACA 0013

Table 5-2 Systems Architecture

Component	Description (Amount)
Motors	Graupner Ultra 3300/7
Servos	HS-225MG (2), HS-545BB (2)
Batteries	Sanyo 2400 (22 cells)
Receiver	HPD-07RB (PCM)
Handset (Radio Transmitter)	Prism 7X (PCM)

Table 5-3 Flight Performance Data

Design Parameter	Performance
Cruise Speed	65 mph (95.3 $^{ft}/_{s}$)
Takeoff Distance	183.5 ft
Climb Rate	597 ft/min
Turning Radius	59.3 ft
Payload/Gross Weight Ratio	0.44
Cruise Endurance	6.3 minutes
Mission Completion Goal	All 3 missions in 5 minutes
Rated Aircraft Cost	9.29
Final Flight Score	6.2

Rated Aircraft Cost (RAC) = (A * MEW + B * REP + C * MFHR) / 1000 = **9.28**

Manufacturers Empty Weight Multiplier (MEW)					A= $	100
Total Weight w/o payload =	14.9	lbs				
					MEW =	14.9
Rated Engine Power (REP)					B= $	1500
# of engines =	1					
Battery Weight =	2.9	lbs				
					REP =	2.9
Manufacturing Man Hours (MFHR = SUM(WBS))					C= $	20 /hour
WBS 1.0 Wings						
Wing Span =	7	ft	*	8 hr/ft		
Max Chord =	1.13	ft	*	8 hr/ft		
# of Control Surfaces =	4	c.s.	*	3 hr/c.s.		
					WBS 1.0 =	77 hr
WBS 2.0 Fuselage						
Fuselage Length =	4.5	ft	*	10 hr/ft		
					WBS 2.0 =	45 hr
WBS 3.0 Empenage						
# of Vertical Surfaces =	0	v.s.	*	5 hr/v.s.		
# of Vertical Surfaces w/ =	1	v.s.	*	10 hr/v.s.		
# of Horizon Surfaces w/ =	1	h.s.	*	10 hr/h.s.		
					WBS 3.0 =	20 hr
WBS 4.0 Flight System						
# Servo or Motor Contro. =	4	ser	*	5 hr/ser		
					WBS 4.0 =	20 hr
WBS 5.0 Propulsion Systems						
# of engines =	1	eng	*	5 hr/eng		
# of props =	1	prop	*	5 hr/prop		
					WBS 5.0 =	10 hr
					MFHR =	172
					RAC =	**9.28**

5.2.8 Weights and Balances Worksheet

Total Length (in)	54				
Length of the shell	36	11.375	Distance from the nose cone to the leading edge at the root		
Boom Length (in)	18				
Item Name	Item Weight (oz.)	Arm (in)	Moment (in-oz.)		
Main Wing	40	15.875	635		
Rear Stabilizer	6	49.75	298.5		
Tail	3.5	47.75	167.125		
Boom	5.4	45	243		
Fuselage Shell	29.592	18	532.656		
Fuselage Spar Support	50	15.251	762.54925		
Main Landing Gear (x2)	10	15.875	158.75		
Nose Gear Structure	5	2	10		
Engine (x1)	21.12	4	84.48		
Battery Packs (x1)	48	10	480		
Propellor (x1)	6	3	18		
Wiring Harness	2	30	60		
Speed Controller	6	4	24		
Receiver	1.65	25	41.25		
Main Wing Servos (x2)	2	21.5	43		
Elevator Servo	1	49.75	49.75		
Rudder Servo	1	47.75	47.75		
S-Ball Payload	154.2857143	16.00	2468.571429	Number of Soft Balls	24
Heavy (S-Ball) Payload	392.5477143	24.6342	6124.381679	Total Soft Balls	24
No Payload	238.262	14.8914	3655.81025		

w/ Payload		No Payload	
MEW	11.9 lb	MEW	11.9 lb
Gross T/O Weight	24.5 lb	Gross T/O Weight	14.9 lb
CG (F.S. in)	16.60 in	CG (F.S. in)	15.94 in
Dist. To Leading edge at root	11.38 in	Dist. To Cent. Press. (1/2 c) at MAC	11.38 in
CG (%MAC)	31.3 %	CG (%MAC)	29.4 %
Distance in Front of the spar	0.35 in	Distance in front of Cp	0.09 in

Notes:

1) All distances are from the CG of the individual item to the nose of the A/C.

2) All weights include attachment hardware.

5.3.2 Flight Component Dimensions

5.3.2.1 WING:

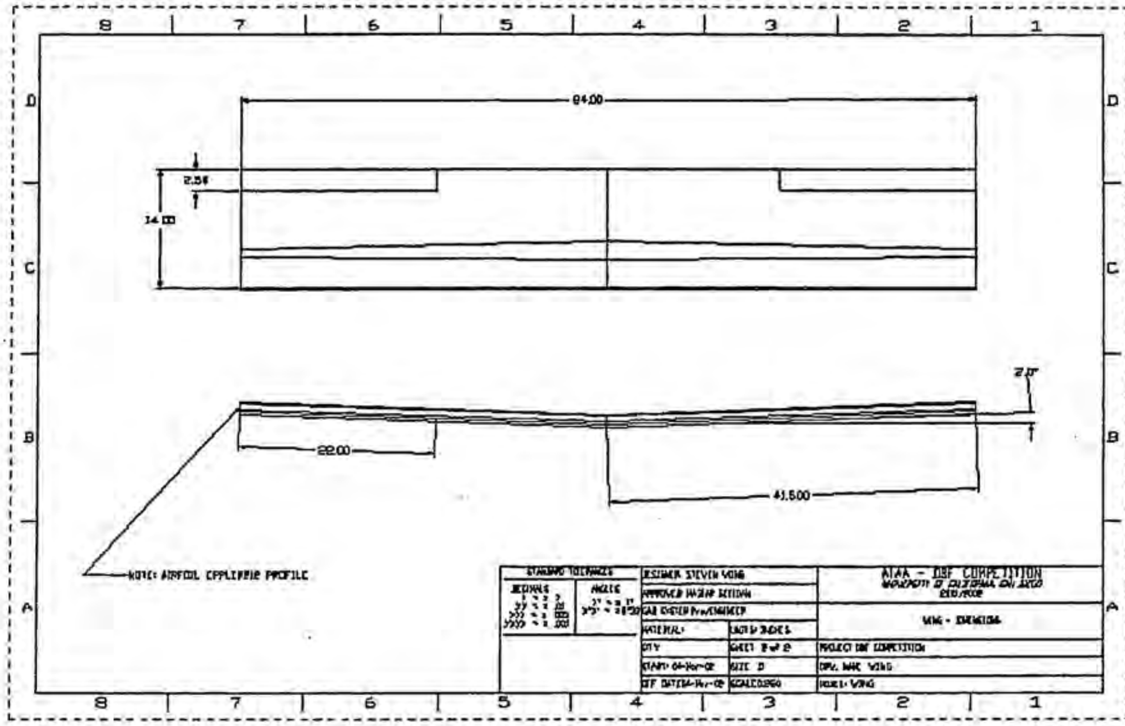

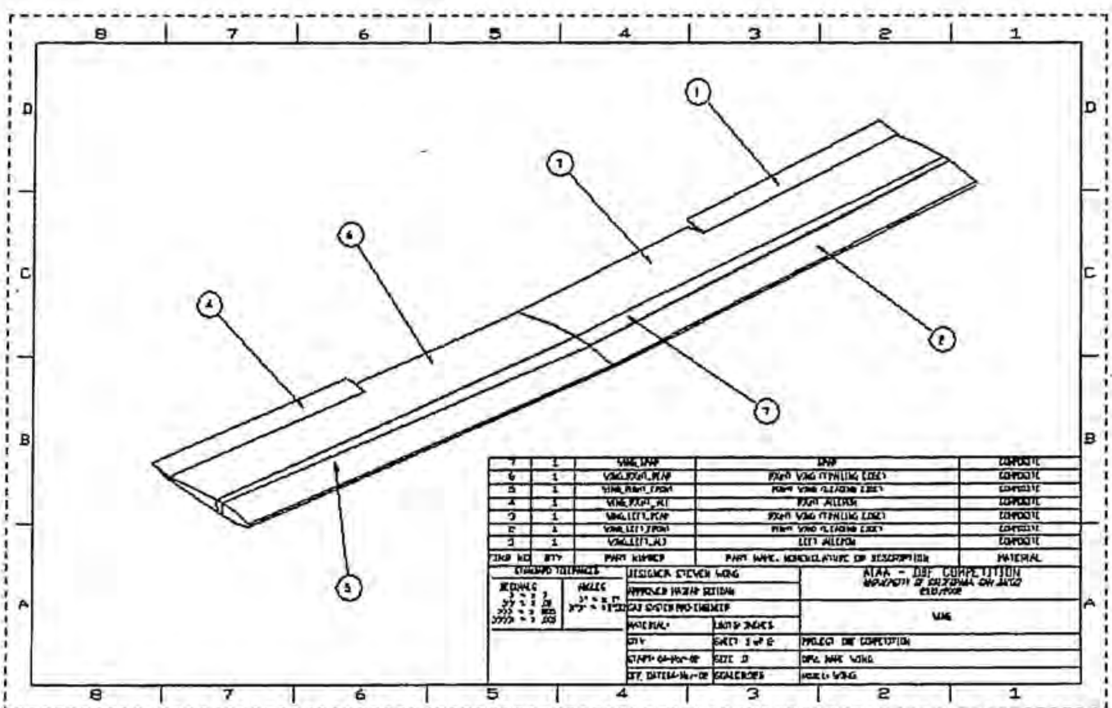

5.3 Drawing Package

5.3.1 Three View Drawing

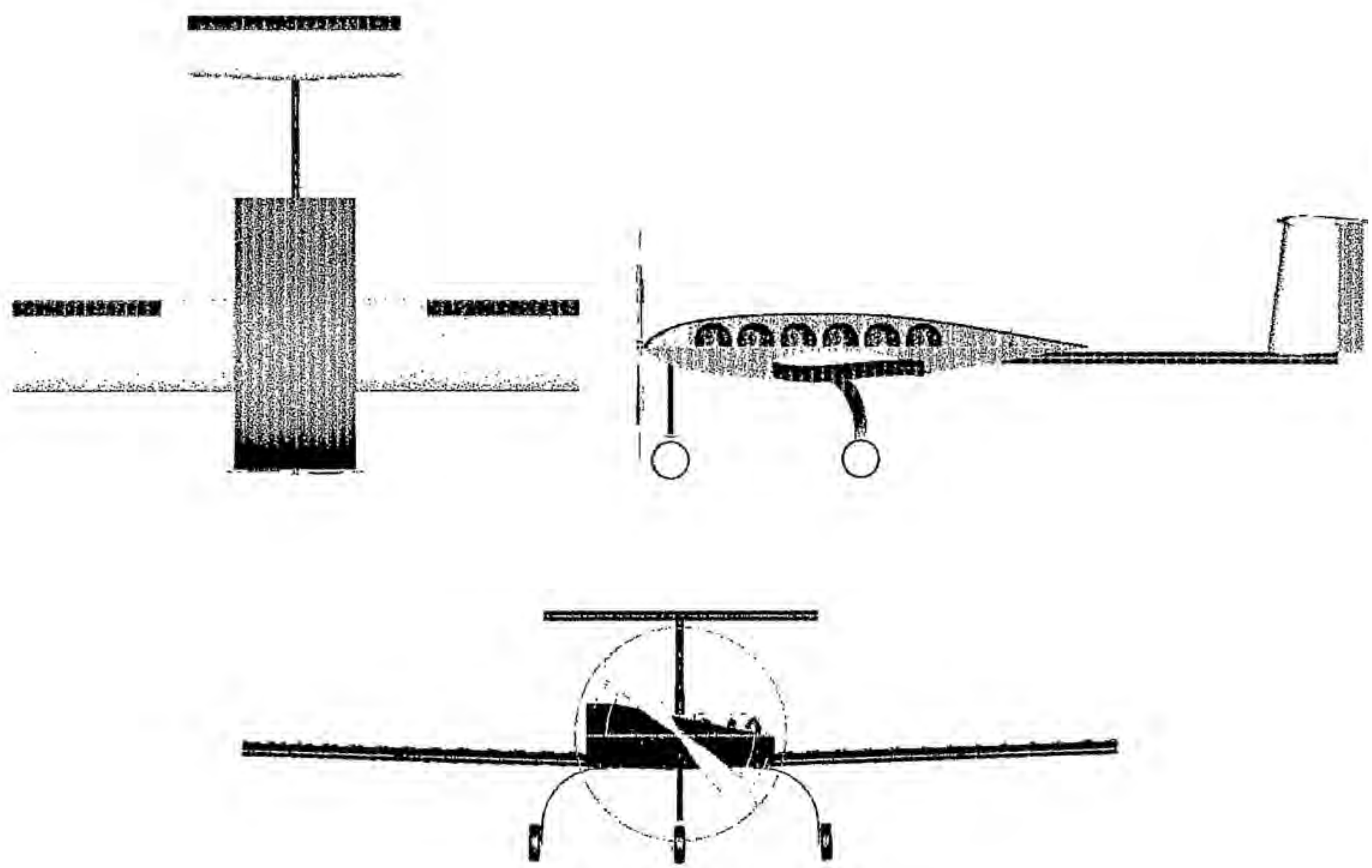

5.3.2 Flight Component Dimensions

5.3.2.1 WING:

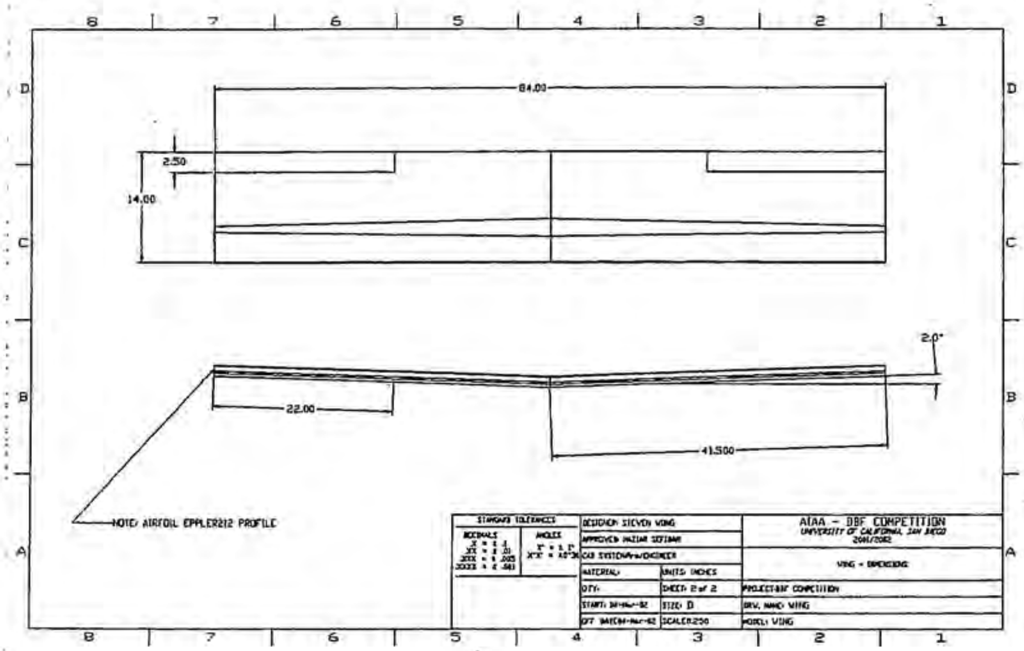

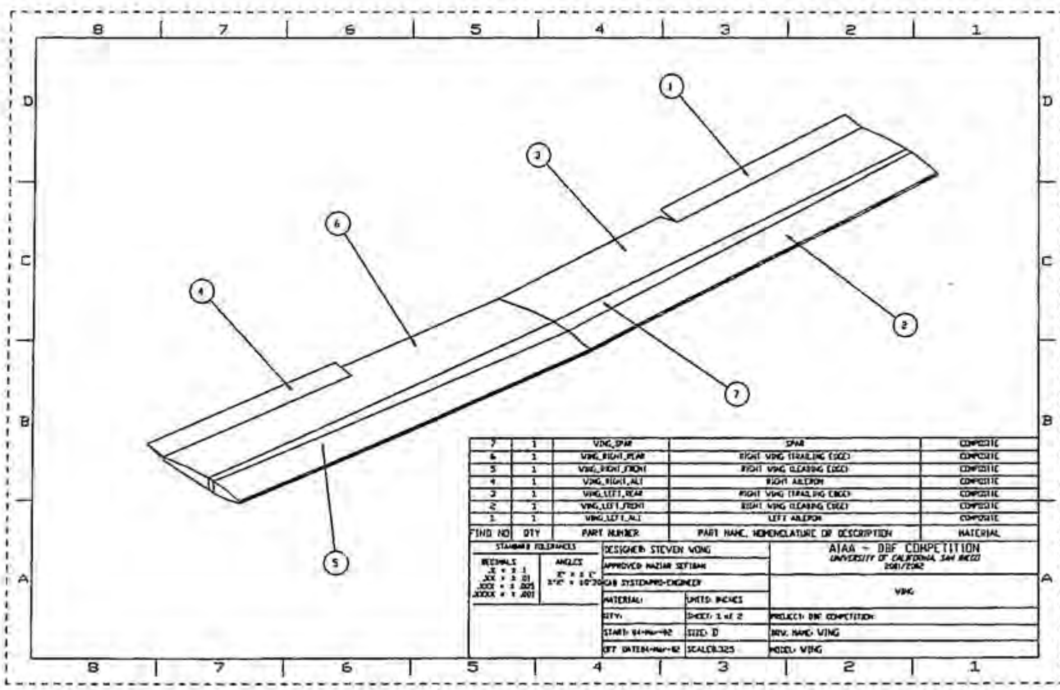

5.3.2.2 HORIZONTAL AND VERTICAL STABILIZER:

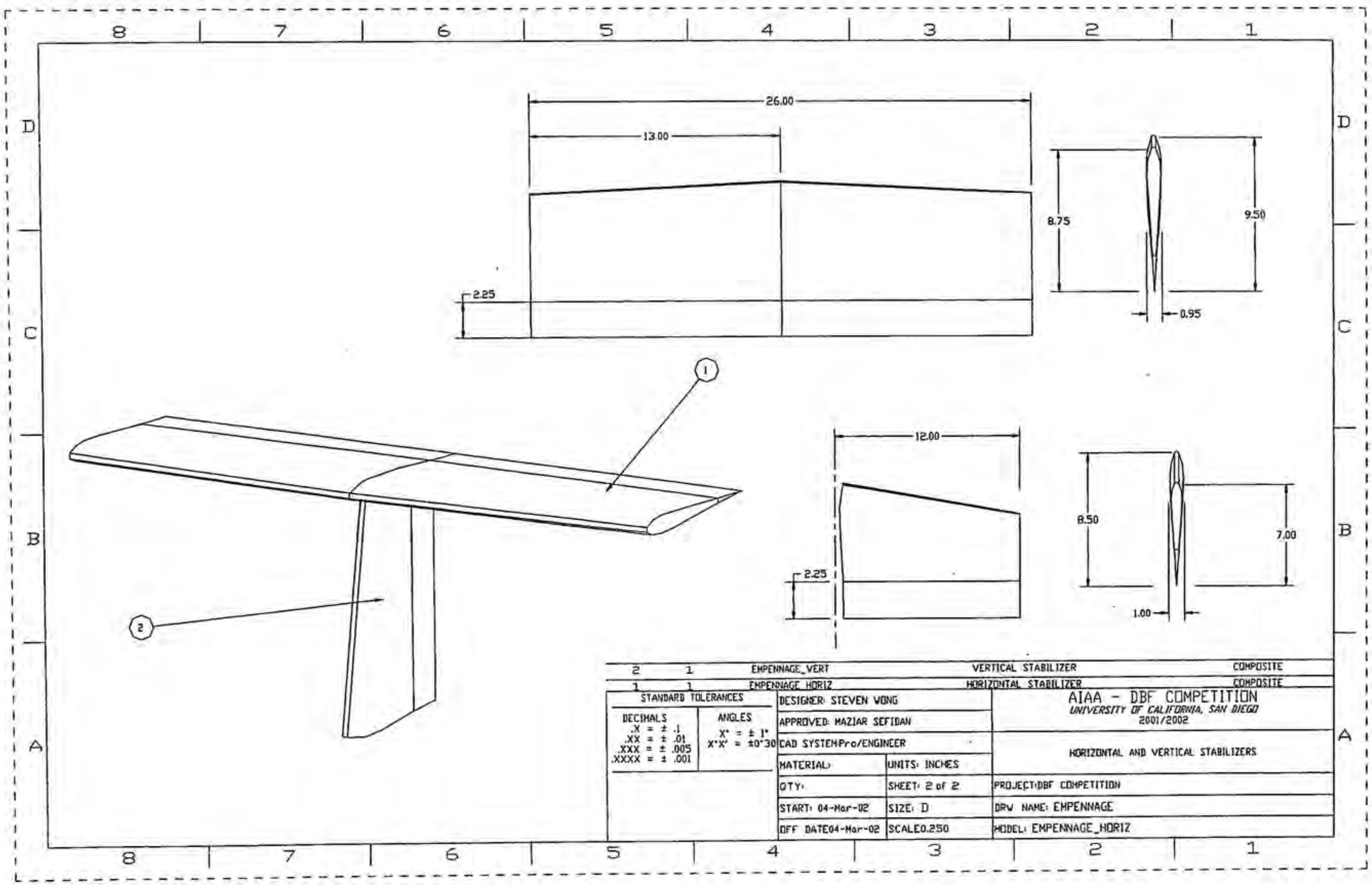

5.3.2.3 FUSELAGE:

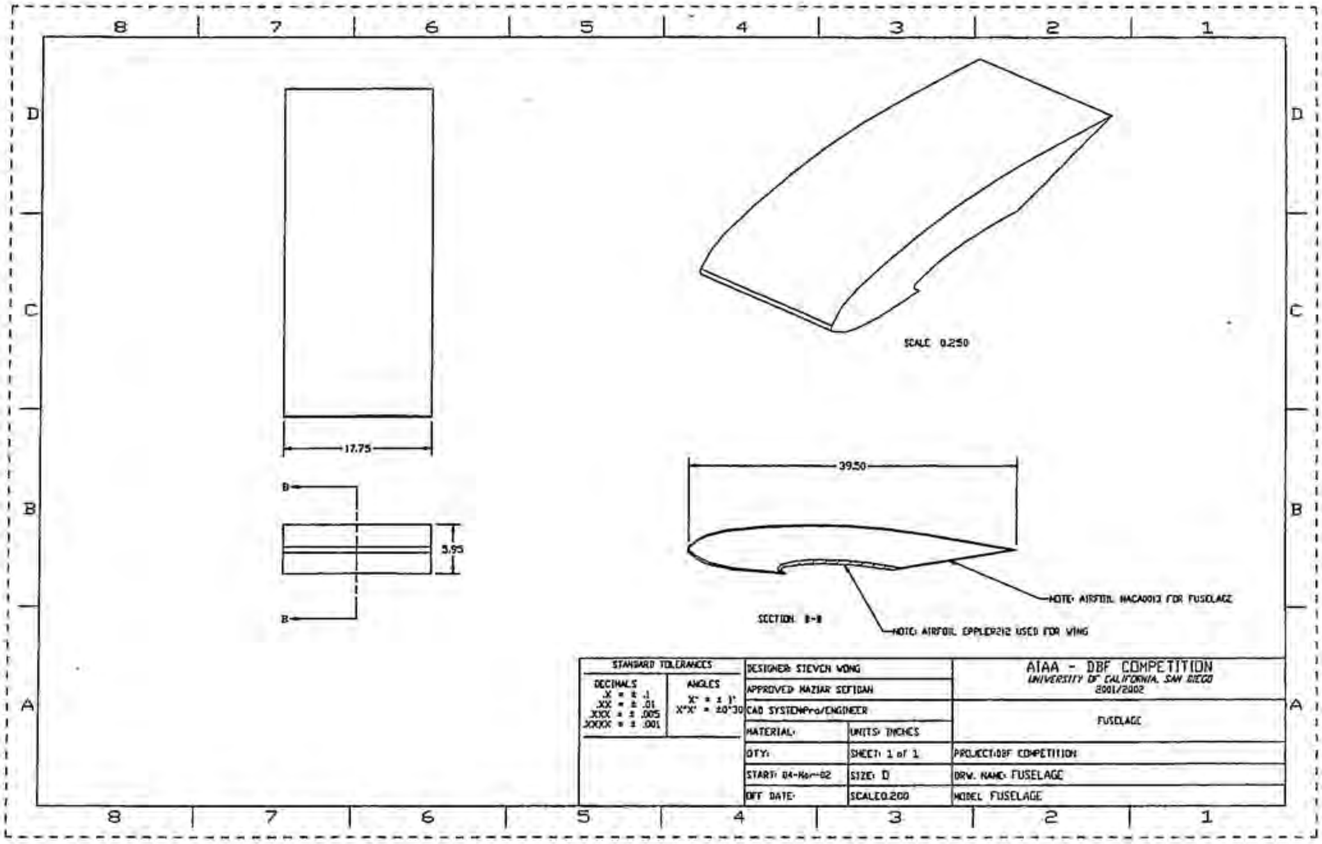

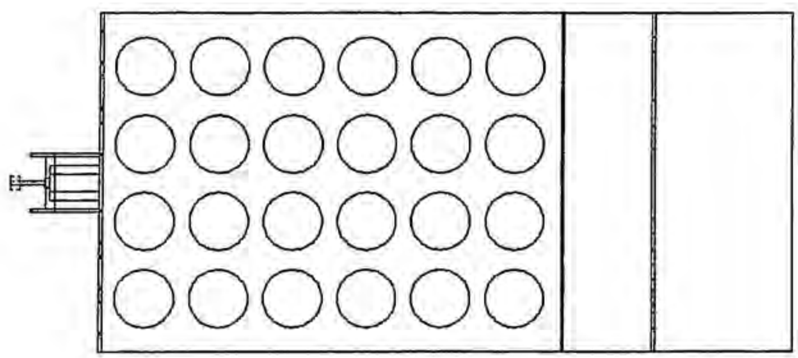

6 Manufacturing Plan

Logistics and required skill level to manufacturing component design ideas imposed constraints on design options. The manufacturing constraints were continually considered in order to avoid conflicts between a chosen design idea and the ability to construct it. The manufacturing FOMs were used to screen construction techniques and materials based on skill level, physical properties, component and interfacing strength, and logistics. The material FOMs were sometimes used to eliminate construction methods, while construction FOMs were sometimes used to eliminate materials. The order in which the various components and assemblies were completed are shown in the manufacturing timeline presented in section 6.4.

6.1 FOM Reasoning/Discussion

Materials: Materials were screened due to their strength-to-weight ratios, availability, cost and required skill level.

Construction Techniques: "Home-built" construction with limited techniques were the only methods available to the team due to limited experience with an autoclave, time restrictions, and the unavailability of a large CNC machine. Construction FOMs are composed of required skill level, machinery, tools, tooling time, robustness and ease of repair.

6.2 Component Manufacturing Description

6.2.1 Spar Structure

The spar structure assembly consists of the shear web and spar cap. Although the wing itself is constructed of low density white foam, high density blue foam is used in the section where the spar would be placed.

Spar Cap Materials: The spar cap absorbs the majority of the bending stress and is of variable thickness (it is reinforced at the center of the spar). A carbon material was best suited for this component because of its high axial load capacity.

Spar Cap Construction Techniques: Two layers of unidirectional carbon were wetted out with epoxy The strands of 12 K carbon tow were wetted-out with epoxy and laid on top of the spar foam. This was then placed inside a polyurethane bag and vacuum-sealed to roughly 12 PSI.

Shear Web Materials: The shear web is only required to give spacing between the spar caps and to absorb a nominal amount of shear stress. Material FOMs were applied to various lightweight materials in order extract the best material. The materials investigated for the shear web were carbon plate, fiberglass, balsa, and Aircraft plywood. Aircraft plywood was eliminated due to its high relative weight and balsa was eliminated due to its low strength. Fiberglass was eventually chosen over carbon due to its weight and ease of construction.

Shear Web Construction Techniques: The fiberglass was cut out at 45° bias, as this angle provides maximum shear strength. Two layers of this cut fiberglass were then wetted out with epoxy and placed on high-density spar foam between the two spar caps. This technique was applied to both sides of the foam, after which the entire spar structure was placed inside a polyurethane bag and vacuum-sealed to roughly 12 PSI.

6.2.2 Wing Airfoil

Airfoil Templates: The first step in the process of fabricating the wings was to make Eppler 212 airfoil templates.

Materials: The materials considered for the airfoil templates were 6061 aluminum, aircraft plywood and Formica. Since the hot wire method was the desired cutting process for the wing cores, it was necessary for the chosen material to be smooth for the wire path, and not melt under hot wire temperatures. Formica was the clear choice due to smooth surface finish and low thermal conductivity.

Construction Techniques: The two techniques for construction of airfoil templates considered were the "cut-and-paste" and a CNC machine cutting method. The "cut-and-paste" process was used because it was easier. Using data points obtained from the UIUC Database, printouts of the airfoil for chord length of 13.5 inches was created. Since the wing would be rectangular, the root, midpoint, and tip of the wing would have the same chord length, making construction that much less complicated. Printouts were bonded to the Formica, which were then cut into the shape of the airfoil and pegged into both edges of a rectangular piece of low-density EPS foam.

6.2.3 Wing Cores

The purposes of the wing core are to maintain the airfoil cross-sectional shape and to contribute to the composite strength.

Materials: The materials considered were aircraft ply, and blue and EPS foam. Using aircraft ply, would result in a design using a rib structure overlaid with MonoKote, while the foam design could form a solid core for composite lay up. The foam was chosen because a solid core was more structurally sound and required less construction. The stiffness and compressive strength of the blue foam and low weight of the EPS foam made both of them viable choices for the core. A combination of blue and white EPS foam was used. The dense blue foam provides stiffness so it was used in the spar structure while the less dense white EPS foam conserves weight and it used for the rest of the wing core.

Construction Techniques: The two construction techniques investigated for cutting the foam core were utilization of a large CNC machine and a hot-wire cutting process. The CNC machine was immediately eliminated due to the unavailability. The hot-wire technique satisfied the logistical issues and the skill level requirements.

The two wings were 42" in length, which was slightly shorter than the length of the hot-wire cutter. This made construction only a one-cut process. A 45"x15"x3" (slightly larger dimensions than the wing) white EPS foam rectangular block was used to cut the airfoil profile of the wing. The Formica templates were pegged onto the edges of the foam using reference pins. After the reference pins were inserted into the foam blocks, the hot wire was drawn through the foam, following the template, creating the desired E212 airfoil cross-section. The spar area was then hot-wire cut from the wing core. After the instersion of the spar, the two wings are then epoxied together.

6.2.4 Spar Assembly

Even thought the two wings are made separately, the spar is made as one piece. This is essential for load transfers involved with the spar. The strength of the spar also makes it the idea candidate for the insertion of landing gear hard-points. These hard-points are made of airplane grade plywood and are placed on top of the blue foam beneath the spar caps. The spar assembly is then epoxied to the rest of the wing.

6.2.5 Wing Skins

The functional requirement of the wing skin is to provide a smooth surface for airflow over the wings, which reduces parasitic drag. The skin is also required to provide torsional strength to dissipate stresses generated during flight.

Materials: Carbon and fiberglass cloths were the materials considered for the wing skins. Carbon cloth was eliminated due to high cost and difficulty of working with the dimensions that were required. Fiberglass cloth was chosen because it was cheap and easy to work with.

Construction Techniques: The use of foam as the core excluded the possibility of using an autoclave, therefore a wet lay up process was needed. Fiberglass was laid at a 45° bias over Mylar. Each wing core was then sandwiched between the sheets of fiberglass/Mylar. The whole assembly was then placed in a vacuum bag to compress the fiberglass/Mylar. After the epoxy had finished curing, the wings were removed from the vacuum bag, the Mylar was peeled off and the excess fiberglass was trimmed or sanded off.

6.2.6 Final Wing Assembly

The fiberglass covering the hard points was trimmed off, allowing access to the plywood below. The spoilerons were cut out and trimmed to allow enough clearance for full range of motion. The recesses to hold the servos were cut into the wings and the wing tips were cut at a 45-degree angle. Fiberglass was then adhered to the exposed core surfaces to provide strength.

6.2.7 Stabilizers

The airfoil decided on for the horizontal and vertical stabilizers was the NACA 0009. The same materials and construction techniques were chosen for the two stabilizers.

Materials: The horizontal and vertical stabilizers were made from foam and fiberglass for the cores and skins, respectively. The only difference from the wings was that only blue foam was used. To provide stiffness and strength unidirectional carbon cloth was laid along the span at half the chord length. The final material used in the tail was aircraft ply that acted as hard points at the interface with the boom.

Construction Techniques: The final lay-up of the stabilizers was exactly the same as the wings.

6.2.8 Main Landing Gear Strut

The gear struts need to withstand fatigue and to absorb the majority of the loads applied at landing.

Materials: The materials considered for the main landing gear struts were carbon, 6061 aluminum and 1095 cold rolled steel piano wire. Aluminum was eliminated due to its lack of strength, and the steel eliminated due to its weight. This left carbon as the only option. The best type of carbon for this job would be multiple layers of pre-impregnated carbon which would have to baked within an autoclave.

Construction Techniques: Carbon landing gears are not easy to manufacture. First a mold was made from a sheet of aluminum by bending it to semi-circle shape. Next, pre-impregnated carbon was cut at 60°, -60°, 90°, and 0° biases and 22 layers were placed on top of the mold. This created a layout that has high torsional and tensile strength. This whole assembly was then vacuum bagged and placed inside the autoclave. Once the epoxy cured under the intense heat and pressure, it was cut into the desired shape using the band saw.

6.2.9 Gear Blocks

Materials: The two possible materials investigated were aluminum and aircraft ply. Tooling time required caused the aluminum to be eliminated. Aircraft ply was chosen since tooling time, cost and skill level were nominal.

Construction Techniques: Prior experience with the materials and component design eliminated the need to investigate construction techniques. The aircraft ply was cut into the required dimensions and then stacked together and bonded with epoxy. A second layer of plywood consisted of two pieces, thinner than the first layer, for the landing gear strut. Epoxy was applied to T-nuts that were pressed into the wood to hold the bolts that would keep the piano wire in place.

6.2.10 Wheels

Materials: Two possible materials for the wheels were aluminum and high-density rubber. Although the aluminum wheels would be lighter, their manufacturing would be difficult and their lack of traction makes them a poor choice. Because of this, 3" diameter commercially available rubber wheels were used for the aircraft.

6.2.11 Nose Landing Gear

Materials: Due to ease of manufacturing, a 3/16" strut commercially available landing gear was used for the construction of this aircraft.

6.2.12 Fuselage

Materials: The three materials investigated for the construction of the skeleton of the fuselage was bi-directional carbon, spider-foam, and balsa wood. Since the skin would be also constructed from carbon, it was crucial that a light variety of carbon cloth be chosen. After some investigation, a 4.8 oz/yd^2 bi-directional carbon fiber cloth was chosen for this purpose. Although lighter cloth could have been purchased, the cost of this very specialized cloth would have been unaffordable. The spider-foam and balsa wood were considered for the inner layer of the sandwich material. They are both light, yet strong.

Construction Techniques: The construction of the fuselage was a very time consuming and laborious task. First, the skeleton of the fuselage was constructed from sandwich material as described in the PDP section. The spider foam was cut into a 1/8" thick piece and into an airfoil shape using a razor blade. Similarly, the bottom piece spiderfoam, was cut into a 1/8" thick piece and circular holes where softballs sit were cut out of the foam. Lastly, the same technique and material was used to make bulkheads that would fit between the two airfoil-shaped pieces. This foam was then sandwiched by two layers of bi-directional carbon essentially creating an I-Beam structure. Each piece was then vacuum-sealed overnight and trimmed to the exact necessary shape. These pieces were then bonded together using an epoxy/cavasil mixture. The fuselage skin was constructed of bi-directional carbon that was shaped using a male mold of the fuselage. The

6.2.13 Boom

The functional requirements for the boom were stiffness and bending strength to support loads from the tail and landing gear.

Materials: Two materials that were considered for the boom were carbon and aluminum. The carbon was chosen over the aluminum due to issues with weight and stiffness.

Construction Techniques: Due to prior experience with carbon tubes, no addition construction techniques were investigated. A 60" long (1" ID x .032" WT) carbon tube was cut to the necessary 22" length. Aircraft ply was bonded to the inner diameter to provide strength for the connection to the vertical stabilizer and tail gear.

6.3 Manufacturing Timeline

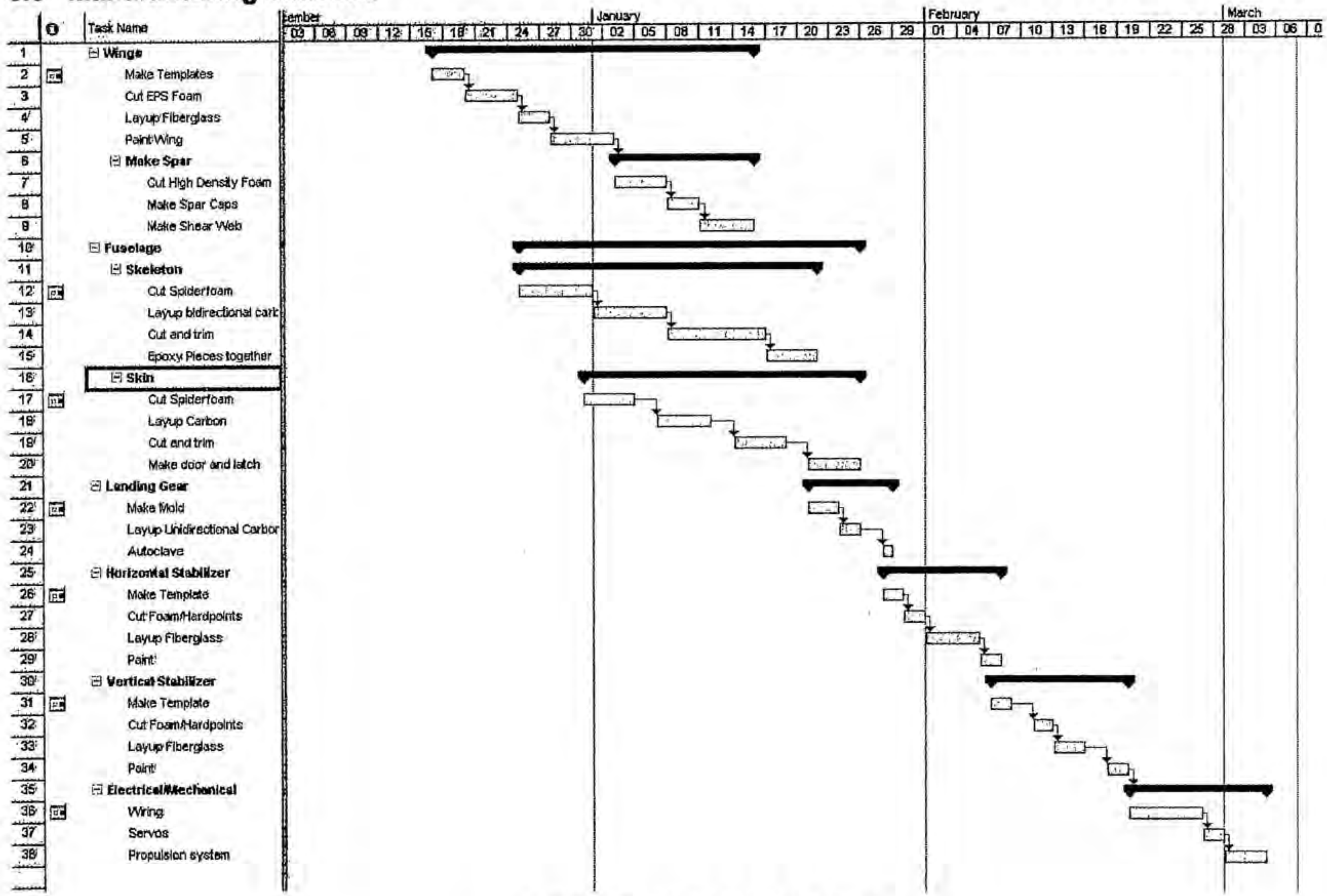

Figure 6-1 Manufacturing Timeline

6.3.1 Cost Matrix

Description	Cost/Unit	Unit	Unit Description	Total Cost
Bi-Directional Carbon Cloth (4.8oz/yard^2)	$ 15.00	5	Linear Yards	$ 75.00
Uni-Directional Carbon Strands	$ 10.00	2	Square Yards	$ 20.00
Bi-Directional Fiberglass Cloth (1.0 oz/yard^2)	$ 10.00	7	Linear Yards	$ 70.00
Epoxy Resin and Hardener	$ 30.00	1	Quart	$ 30.00
EPS Foam (1 lb/ft^3)	$ 25.00	2	3"x36"x60"	$ 50.00
High Density Blue Foam (2 lb/ft^3)	$ 50.00	1	3"x36"x60"	$ 50.00
Spider Foam (4 lb/ft^3)	$ 20.00	1	2"x12"x24"	$ 20.00
Tape/Paint/Glue/Other consumables	$ 100.00	1		$ 100.00
Graupner 3300/7 Electric Motors	$ 300.00	1	Motor	$ 300.00
HS-225MG	$ 25.00	1	Servos	$ 25.00
HS-545BB	$ 35.00	3	Servos	$ 105.00
Recievers	$ 75.00	1	Reciever	$ 75.00
Transimitter	$ 350.00	1	Transmitter	$ 350.00
Speed Controllers	$ 50.00	1	Controller	$ 50.00
Propellors (20" Diameter 20" Pitch)	$ 80.00	1	Prop	$ 80.00
Graupner Spinner	$ 32.00	1	Spinner	$ 32.00
Sanyo 2400 Batteries	$ 5.00	44	Battery	$ 220.00
Hysteris Brakes	$ 25.00	2	Brake	$ 50.00
2:1 ratio Gearbox	$ 150.00	1	Gearbox	$ 150.00
Axel/Wheels/Bearings/Nose Strut	$ 45.00	1		$ 45.00
Expendable Tools	$ 125.00	1		$ 125.00
Softballs	$ 3.00	24	ball	$ 72.00
Total				**$ 2,094.00**

7 Proposal Phase References

1. Raymer, D.P., Aircraft Design: A Conceptual Approach, AIAA Education Series, 1989.

2. Simons, M., Model Aircraft Aerodynamics, Argus Books, 3rd edition, 1994.

3. Lennon, A., The Basics of R/C Model Aircraft Design, Air Age Inc., 1996.

4. McCormick, B.W., Aerodynamics Aeronautics and Flight Mechanics, John Wiley and Sons, 2nd edition, 1995.

5. Nelson, R., Flight Stability and Automatic Control, McGraw Hill, 1989.

6. Stinton, D., The Design of the Airplane, Van Nostrand Reinhold, 1983.

8 Lessons Learned

8.1 Introduction

Throughout the design process, many important lessons were learned and valuable experience was gained. The success of this project relied on the diverse backgrounds and skills contributed by each team member. This included experience with composite materials, structural and aerodynamic analysis, machining techniques, electronics, power systems, computer programs, team/time management, and fundraising.

8.2 Time Management

Establishing a management structure and starting the design process as early as possible allowed room to deal with unforeseen obstacles. An early start enabled the conceptual phase of the design to be completed so that the basic aircraft layout was defined. With this layout, estimations for manufacturing timelines and expenses set a baseline for planning the rest of the project. As the manufacturing process continued, preliminary and detail design could be completed with more information of the actual aircraft characteristics, resulting in the optimum design.

It was important to set a timeline with realistic goals at the start of the project and then adhere to it throughout the design process. One example was planning the Proposal Phase paper well in advance. An outline was created and sections were divided among team members to distribute the workload.

8.3 Teamwork

Creating an organized team was essential in order to allocate responsibilities among the team members. One of the major lessons learned working as a team, was that productivity can decrease with too many people assigned to one element of the project. Delegating separate individual responsibilities allowed specialization. Incorporating each team member's concepts and ideas about their specialized areas into the final design was a process that a great deal was learned from. Dealing with trade off issues between the various component configurations was important to realize the optimum design.

8.4 Design Process

While many of the senior team members had taken advanced design courses, a lesson that was learned early was that the classroom is an ideal. With a short term project, it was found that less complex designs which enabled more simple analysis and took less time to manufacture were desirable. Experience gained from the design classes, combined with practical experience gained by last year's team members provided knowledge that was shared by the newer team members to learn from and apply to their efforts for this year. By providing this knowledge openly, the full talent of every team member could be used most effectively.

8.5 Theoretical vs. Actual

A lesson that was learned last year and re-affirmed with this year's design was that the actual characteristics of TLAR III differed from the designed theoretical characteristics. With even the most careful manufacturing techniques, the components will inevitably change. For example, as the propeller diameter changes, so will the required landing gear length, as the weight increases or decreases so will the required engine thrust. These types of trade-offs were needed throughout the construction even with the extensive factors of safety used during the proposal phase of the design. This is a very important point to realize for any design process.

8.6 Finance

Working within a set budget emulated a real-world design setting. Due to the limited budget, the team was required to rely heavily on analysis to ensure that fabrication went smoothly and to avoid errors that could potentially increase the amount of materials needed. One of the main fundraising techniques learned last year was how to create a well-written proposal package. In addition, establishing and maintaining good relationships with sponsors and keeping them up-to-date on the project was important.

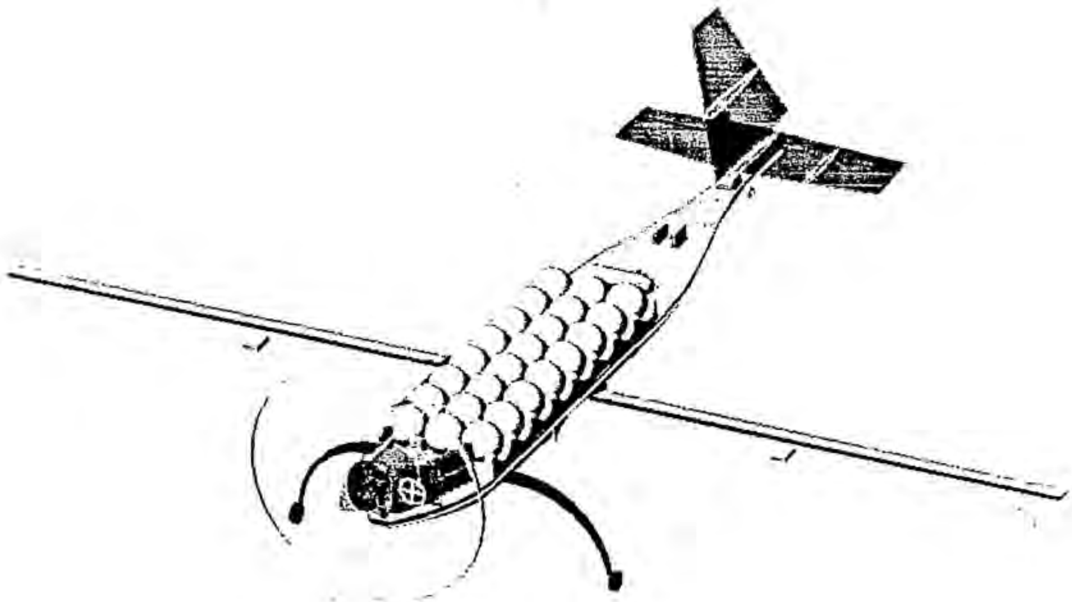

UNIVERSITY OF SOUTHERN CALIFORNIA

SCrewball

Cessna AIAA DBF Entry 2001-2002

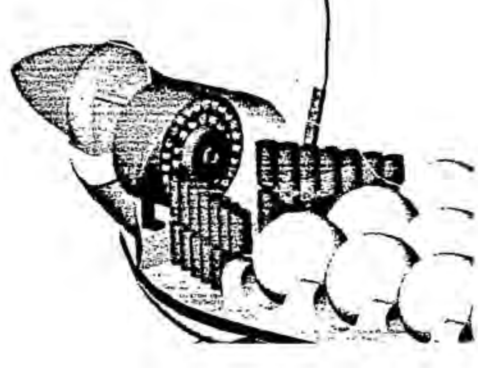

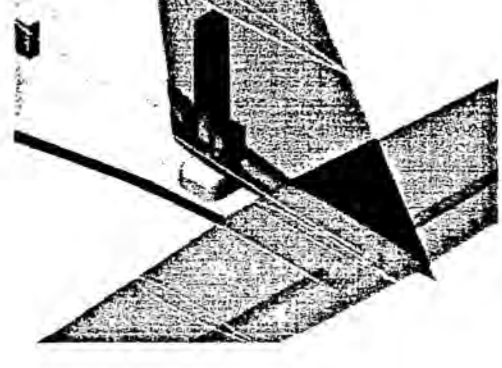

Table of Contents

Page

1. EXECUTIVE SUMMARY

1.1. Introduction

The University of Southern California's Student Aero Design Team will participate in the 2001-2002 AIAA/Cessna/ONR Student Design/Build/Fly Competition. The competition calls for designing and building a propeller driven, remotely piloted aircraft using an electric motor. Each year, the competition presents new rules and regulations, which prevents teams from using the same exact design from a previous year for the contest mission. The goal of the Aero Design Team was to design and build a plane that will achieve the highest possible score in the contest. The final score is determined by three other factors: the mission score, the rated aircraft cost and the written report score. The schedule was broken down into five phases: Conceptual, Preliminary, and Detailed Design followed by construction and flight testing.

1.2. Overview of Design Tools Used

The mission simulator, called "Mission" was an Excel spreadsheet originally written to support the 1997/1998 AIAA DBF efforts. It consists of an Excel workbook with several spreadsheets that model various components of the aircraft during a scoring flight. It models all legs of the flight including: takeoff, cruise, turning flight, descent, landing, and ground handling. Some of the different modeling spreadsheets include: electrical, propulsion, weights, cost and aerodynamics. All these pages take geometry inputs from the user and rapidly evaluate different aircraft configurations and score the design based on payload carried and the cost of the craft. Some of these inputs are: airfoil type, wing area, propeller diameter and advance ratio, motor and gearbox type and count, battery type and count, and amount of payload carried. "Mission" derives its primary parameters from these inputs plus throttle setting, airspeed, initial altitude, aircraft weight, and load factor of each leg. This data from each sheet is used to calculate the energy consumption, time required, and altitude change for each leg. The output consists of the sum of the total energy and time consumed and predicts how many sorties will be completed given the initial parameters and constraints. The overall score is determined by multiplying the total number of sorties completed by the amount of payload carried then dividing by the calculated cost of the airplane.

Over the years, "Mission" has been optimized and modified to accurately predict performance based on previous years data. In addition, new abilities are added each year to "Mission". This year, one of the more important additions was the "Shotgun" feature. This feature would freeze several design parameters of the plane, and allow the user to then compare components such as number of motors or propeller selection with an identical plane in all cases. This feature helped the team to conduct trade studies with relative ease.

The following are all the models present in "Mission".

1. *Electrical model*: The electrical model is designed to analyze electrical motors used for small aircraft. The equations programmed into "Mission" follow the analysis presented by R.J. Boucher (1995). Inputs into this page include: throttle setting for each leg, propeller diameter and pitch, number of battery cells, volts per cell etc. taken from the input page of "Mission". Using the selected motor, battery, and gearbox type, it calculated the values of torque, voltage, current loaded and unloaded, and resistance. The electrical model sets an initial value of current, and the propeller page provides efficiencies and coefficients of thrust and power. It then feeds this data into a set of formulae to calculate thrust, motor RPM, and power. A feature in Excel called "goal seek" then adjusts current draw until it matches the current needed to spin the propeller at the desired RPM. This current is then used to find the energy consumption, thrust produced, and total system efficiency to export to the front page of "Mission". A correction factor of 0.65 is applied to the theoretical battery energy to improve correlation with flight test.
2. *Propeller model*: This model takes the propeller diameter and pitch and generates a map of thrust and power coefficients, C_T and C_p respectively. A plot of these coefficients and efficiencies (Figure 4.4) was generated from this data and brought to the test flights for comparisons with actual measured thrust. During test flights, differences between the predicted and measured thrust resulted in 1.1 power coefficient multiplier added to the propeller model.
3. *Weights model*: The weight of the plane is calculated by summing the weights of the individual components. For the constructed materials, a weight estimate was calculated from the volume of material used in the design multiplied by the density of the specific material. The weights of the pre-manufactured parts, i.e. motor, propeller, batteries etc., were stored in their respective models. The weight page looks up the component weights from each of the component pages and adds them to find the total weight of the aircraft. The center-of-gravity is also calculated.
4. *Stability and Control*: Handling characteristics were displayed in the stability and control worksheet. The worksheet takes inputs from the main page and displays flight conditions at cruise and at minimum airspeed, ground handling, and stability characteristics of the plane. In addition, the worksheet displays a two dimensional drawing of the current plane and shows data such as the airplane's C.G., heavy and light lap C.G. configurations, and the static margin. The aircraft had to pass all requirements set in the S&C page, such as yaw frequency, pitch stability, and the max allowable crosswind for takeoff and landing. Cruise wing incidence, required wing washout, and gear rigging are also addressed in the stability & control worksheet.

1.3. Conceptual Design

During this design phase, all possible configurations of the aircraft were discussed. The primary design tool used during the conceptual design phase was "Mission".

Design Alternatives Investigated

Initially, the team considered five different planes configurations at the start of this design phase: conventional plane with tricycle gear, flying wing, conventional with tail dragger, and biplane. For figures of merit, the team used sortie time, structural robustness, and rated cost to evaluate each design. Design parameters within these FOM's were also used to further break down and evaluate all five configurations.

Results

After careful review of each concept, the team decided on one design to be further studied in the preliminary design phase. The conventional plane with tail dragger was the design chosen to be further studied and configured during the preliminary design phase.

1.4 Preliminary Design

Many different components for the aircraft where discussed and analyzed during this phase. The primary design tool used was "MISSION".

Design Alternatives Investigated

Further trade studies were conducted on the monoplane configuration that resulted from the Conceptual Design Phase. Specific items such as payload to be carried, construction materials needed, number of motors, landing gear configuration, airfoils, gearbox, prop diameter & pitch, and number of battery cells were addressed during the Preliminary Design Phase. The figures of merit generated in the Conceptual Design Phase were used during the Preliminary Design Phase to evaluate all designs.

Results

At the end of the design phase, a conventional low-wing aft tail monoplane was selected. The plane will carry 24 softballs (for maximum flight score),, use only one Cobalt 60 motor with a 2.7:1 gearbox (major cost benefit), driving a 24-24 prop (big diameter for high static thrust, low pitch for high straight speeds & efficiency), have a design takeoff field length of 150ft, and a wing area of 6.61ft^2, with a wingspan of 9ft and carry 30 Ni-Cad cells for power. A tail wheel configuration was also decided upon for weight and drag savings.

1.5 Detailed Design

The finalized sizing for every component was done using the "Mission" design tool.

Design Alternatives Investigated

The team studied several alternatives in this design stage such as a full flying vertical vs conventional rudder, number of batteries to be used, and alternatives to the cooling system which used combinations of heat sinks, different cooling areas, and exhaust areas. The final plane has a full flying vertical tail for better crosswind at takeoff capabilities and 30 Ni-Cad batteries and a cooling system which includes an aluminum honeycomb heat sink around the motor, an air intake at the front of the aircraft, exhaust vents on the sides of the forward fuselage, and battery placement along the sidewalls of the forward fuselage.

2. Management Summary

2.1 The Aero Design Team

USC's Aero Design Team consisted of five faculty and industry advisors, a core group of experienced upperclassmen, and a number of new members. Dr. Ron Blackwelder and Mark Page served as the faculty advisors. Wyatt Sadler and Stuart Sechrist, both from Aerovironment Inc., and Nathaniel Palmer from Raytheon were the team's industry advisors. The student leaders included David Lazzara, George Cano, Jacob Evert, Cheng-Yuan(Jerry) Chen, Phillippe Kassouf, Charles Heintz, George Sechrist, Tim Bentley, Michael Mace, Jonathan Hartley, Tai Merzel, and Stephane Gallet. The team was roughly divided into Design/Report and Construction sections and had a semiformal command structure. Positions were assigned according to experience and interest; the responsibilities were flexible, with team members helping out when and where needed.

David Lazzara served as the overall student leader for the team. His responsibilities included setting the agenda for the weekly meetings, generating a schedule with input from each captain, and to oversee all of the design phases. Dr. Ron Blackwelder also served as our liaison with the university and the contest. Mark Page, an adjunct professor at the university who is also chief aerodynamicist at Swift Racing, advised the team on aerodynamics and helped develop the analysis spreadsheet. Stuart Sechrist, Wyatt Sadler, and Nathaniel Palmer, all participants of past DBF competitions, helped provide assistance in constructing the plane. Wyatt Sadler coached the build teams and served as the primary pilot, with Jerry Chen as the back-up pilot. Nathan Palmer coached the students involved in software development.

The team was organized into groups each having two to four students. Group captains were upperclassmen and each group contained some underclassmen. One of the more experienced members was chosen as group captain and had the responsibility to organize the group and insure that the group's deadlines and goals were achieved. Weekly team meetings were held for everyone to discuss overall problems, discuss common issues, and inform everyone of the team's progress. Initially these meetings concentrated on developing the aircraft design and setting a schedule. As the design matured, topics changed to construction issues and later to test flying. The group leaders and the team captain met separately one additional time during the week to discuss management and personnel issues. The main groups and their responsibilities follow.

2.2 Group and Personnel Assignments

Conceptual, Preliminary, and Detailed Design

The Conceptual, Preliminary, and Detailed Design sections were lead by David Lazzara. The areas of responsibility under this task were coordination of Information Technology, Propulsion Testing, Design Spreadsheet Development, Weights and Balance, Structural Sizing, and Configuration and Structural Design. In addition, further responsibilities involved managing the entire design and construction schedules as well as designating dates of important events throughout each phase.

Critical Design Review

A Critical Design Review was held on November 19th, 2001. Reviewers from Boeing Phantom Works were invited who had considerable AIAA DBF experience. All team Captains presented a problem statement, design criteria, alternatives considered analysis process, and design selection for their area. This proved to be quite helpful. Critique from the reviewers led the team to revise the wing position from above the fuselage plank to below, and encouraged the development of a no-spar wing design.

Report Captain

The report captain was responsible for taking minutes at every meeting, as well as preparing the report at an early stage. This included submitting rough drafts of each design phase a week after the phase was completed. In addition, editing the final report was the responsibility of the report captain. George Cano was chosen to carry out this task, with additional editing assistance from Dr. Ron Blackwelder, Mark Page, and David Lazzara.

Information Technology and Design Spreadsheet Development

The Informational Technology group, led by Phillippe Kassouf, created the computer graphics in the report, and generated isometric views of the aircraft during each design phase. The Design Spreadsheet Development group updated, refined and integrated the various analysis spreadsheets used to design the plane. Jake Evert, Nathaniel Palmer, and Andres Figueroa were responsible for these tasks, with considerable aid from Mark Page.

Configuration and Structural Design/Sizing

The Configuration and Structural Design group was responsible for the overall design of the plane using SolidWorks CAD software. Phillippe Kassouf was the configurator of the plane throughout each stage of development, with assistance provided by Stephane Gallet for sub components of the aircraft.

Construction

The construction captain was George Sechrist with assistance provided by Wyatt Sadler. The construction captain ran the laboratory and insured that component group had their part finished by their designated deadline. The construction group was assisted by a number of underclassmen that lent their time when needed. These people include Tyler Golightly, Tim Schoen, Jonathan Hartley, Stephane Galley, Tai Merzel, Doris Pease, Andres Figueroa, Cristina Nichitean, Stephanie Hunt, Billy Kaplan, Tim Phillips, Brian Wetzel, Lester Kang, and Boris Gee. In addition, several smaller projects were assigned to this group to involve the newer members of the team. These projects included designing and constructing parts such as an aircraft tow bar and a center of gravity test apparatus.

Aero Surfaces and Fuselage

This group was responsible for constructing the aero surfaces and the fuselage including the wing, fuselage plank, fuselage shell, and all aero-farings required for the aircraft. George Sechrist was captain of this group.

Landing Gear and Lab Manager

The Landing Gear and Brakes group was responsible for constructing, testing and installing the tail and main landing gear, brakes, wheels and steering system. Charles Heintz was the group captain for these tasks.

Controls and Propulsion

The Controls group took responsibility for the radio and servo systems, as well as the servo linkages. The Propulsion group was tasked with constructing and testing the entire power plant and power supply, as well as designing and constructing the motor mount. Jerry Chen lead both of these groups with aid from Tim Bentley for propulsion and Stephane Gallet for the motor mount.

Flight Test

The Flight Test group was in charge of organizing the test flight, as well as collecting and processing data. The group devised a flight test procedure used during the flight test that included the necessary setup required for the aircraft, preflight check on subsystems, and post-flight feedback from the pilot. Michael Mace was the captain for this group, with assistance from David Lazzara and Wyatt Sadler.

2.3 Configuration and Schedule Control

To visualize the deadlines for every phase of design and construction, a schedule was set for the team to follow (Figure 2.1). Sufficient time was allowed for schedule delays so that paths critical paths for completion could be maintained. For example, much of the construction was planned to be completed in December but did not need to be finished until late January in time for flight testing.The team leader updated and maintained the schedule every week, and informed the group on approaching deadlines.

The team held meetings every Monday to discuss the progression of the aircraft design and construction phases. In addition, weekly Friday meetings for the group leaders were held during the design phases to discuss changes made to the current aircraft configuration. These changes were incorporated into new configuration drawings to be shown at the team meeting the following week. The team created a web page that provided information such as a team member contact information list, a copy of the latest schedule for download, and weekly meeting agendas for members who were unable to attend.

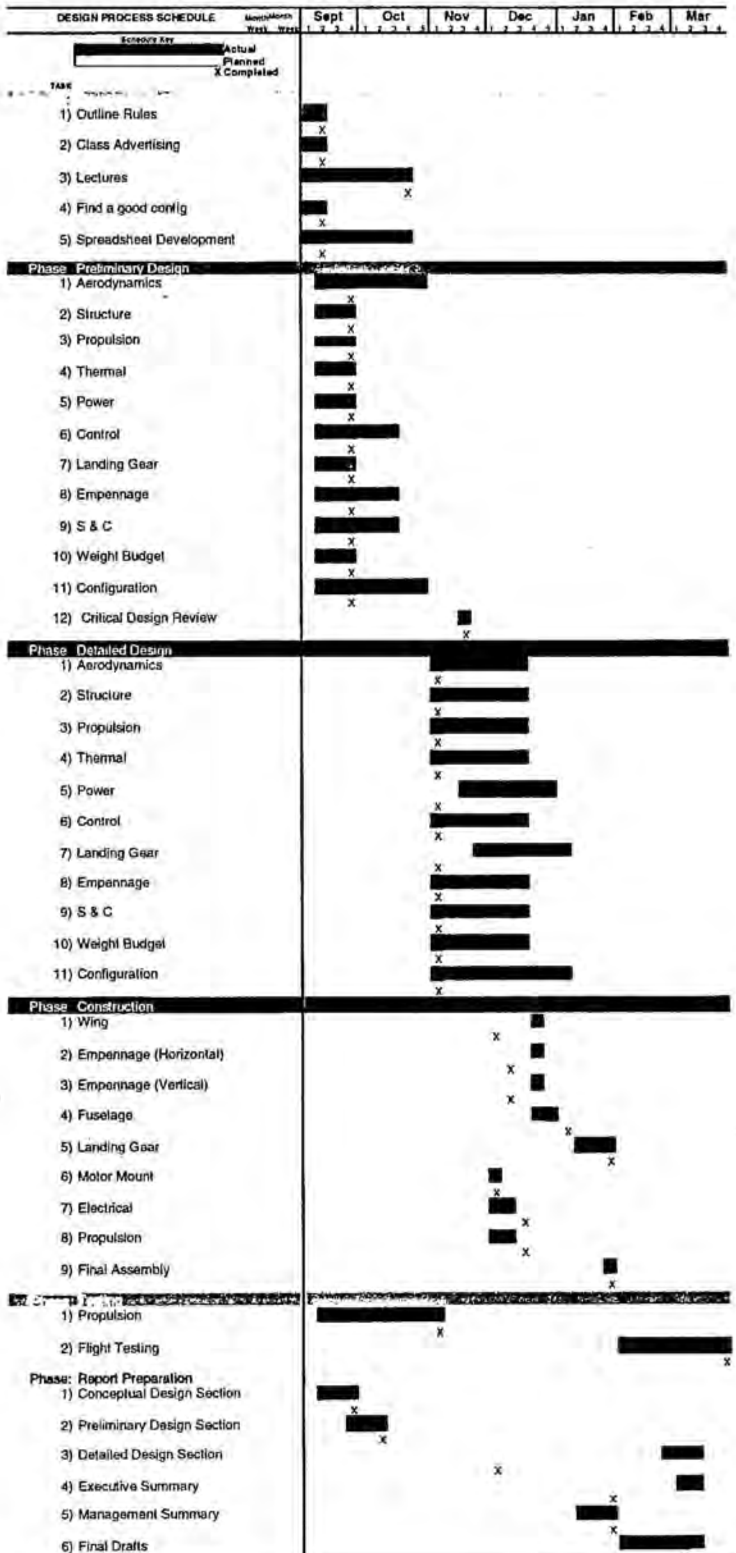

Figure 2.1. Management Schedule and Milestone Chart

3. Conceptual Design Phase

Five aircraft were defined to address the 2001/2002 Design/Build/Fly rules; conventional with tricycle gear, flying wing, conventional tail-dragger, biplane tricycle, and a biplane tail dragger. Three *Figures of Merit* (FOM) were selected; Sortie Time, Structural Robustness, and Rated Aircraft Cost. In addition, eight key assumptions (listed below) were made that applied to all five designs. These conceptual designs were all drawn with the following assumptions so that wetted area and complexity assessments could be made. Each subjective FOM was awarded a 1 to 5 rating. The rated aircraft cost was added to the subjective FOM's for the final ranking.

3.1 Assumptions Made and Justifications for their Validity

The following ground rules were applied to all five candidates for a fair comparison.

1. *10-24 Softball Payload Capacity*: The contest rules mandated this payload requirement. Each conceptual configuration required sufficient volume for this payload range.
2. *Aircraft Center of Gravity (CG) coincident with Payload CG at the Wing c/4*: The wing center of lift was taken to be at the root quarter-chord location. The payload centroid was located to be coincident with the quarter chord. This minimizes C.G. variation with and without payload.
3. *Composite Materials for Construction*: The high strength-to-weight ratios of composite materials, such as carbon-fiber and honeycomb core material, minimized weight while protecting the aircraft against any design load scenario.
4. *1 to 3 Motors Required:* To meet the 200' TOFL requirement, each conceptual configuration needed the ability to house 1 to 3 motors.
5. *10 ft^2 Wing Area if Empennage Used; 20 ft^2 Wing Area if No Empennage Used*: The wing area was similar to that used by the 2000-2001 USC *DBF* team due to comparable payload mass requirements. Configurations that lacked an empennage were required twice the wing area. This accounts for halving the trimmed $C_{l,max}$ due to the negative flap angles for trim. Otherwise, a conventional elevator with a large lever arm to the CG was assumed.
6. *Spacing between Payload, Fuselage Bulkheads, Batteries, and Motors are Constant*: These components were equally spaced fore and aft of the CG to negate any differences in longitudinal moments among the five conceptual aircraft because they dominated the weight and balance considerations. Fuselage designs that enclosed these components were variable.
7. *150' TOFL*: The 2000-2001 USC *DBF* Team experimentally determined an uncertainty of ±50' in TOFL for an aircraft designed with payload mass requirements similar to the 2001-2002 *DBF* payload rules. This maximum TOFL minimized the possibility of overshooting the maximum allowed 200' TOFL set by the 2001-2002 contest rules.

8. *5 lb. Battery Weight Capacity*: In addition to meeting the maximum allowable battery weight condition in the 2001-2002 contest rules, this limit ensured that each conceptual configuration could carry the maximum specific energy when needed.

3.2 Alternate Configurations Investigated

Five configurations were considered for the Conceptual Design Phase.

1. *Monoplane with Empennage & Tricycle Landing Gear*: This aircraft configuration resembled the USC 2000-2001 *DBF* contest aircraft due to similarities in the payload mass requirements and the mission profile with the 2001-2002 contest rules. This general configuration supported various fuselage designs, payload restraint and egress techniques, and wing locations above or below the payload compartment.
2. *Monoplane with Tricycle Landing Gear & without Empennage*: The flying wing configuration offered a potential cost advantage that could be exploited. A fuselage was replaced by locating the payload inside the wing center section, thereby reducing wing-body aerodynamic affects. Fewer control surfaces and servos reduced the aircraft weight as well. The use of a canard surface for pitch control was also considered.
3. *Monoplane with Empennage & Tail-Dragger Landing Gear*: This aircraft only varied from the first conventional Monoplane configuration above by replacing a nose gear with a tail wheel capable of steering. The biggest benefit of the tail wheel is removing the heavy nose gear and its dedicated servo. In the past, the USC team reasoned a nose gear would offer protection to the prop, gear, box and motor shaft in the case of a runway departure. In practice, the nose gear could fail and break the prop as well.
4. *Biplane with Empennage and Tricycle Landing Gear*: A conventional Biplane configuration varied from the conventional Monoplane by the addition of an extra wing. Vertical struts between the high and low wings would serve as structural members and reduce vortex drag by acting as winglets. Furthermore, with the total wing area and span held constant, the Biplane could achieve lower vortex drag than the conventional Monoplane configuration if its wings were separated substantially.
5. *Biplane with Empennage and Tail-Dragger Landing Gear*: This Biplane configuration varied from the previous biplane concept by replacing the nose gear with a tail wheel. The advantages/disadvantages are the same as given in the third conceptual design above. In addition, the wings achieved higher C_L at lower takeoff velocity due to the large angle of attack resulting from the lowered aft section of the fuselage.

3.3 Figures of Merit

To discriminate configurations with good performance and high reliability, the following FOM's were selected.

1. *Sortie Time*: The 2001-2002 contest rules specified a formula for determining a flight score that contained sortie time as a normalizing term. The inverse proportionality between flight score and sortie time provides maximum flight score with minimal sortie time for a given payload carried and sorties flown. A conceptual configuration could accomplish this by minimizing total aircraft C_D for higher flight velocity and decreasing the ground handling time.
2. *Structural Robustness*: Structural restrictions were set in order for the conceptual aircraft to survive a host of scenarios where aircraft damage was most likely to occur. The extent of damage was a function of the aircraft structural integrity. Structural integrity was deemed excellent for configurations with minimal number of joints or other geometric discontinuity. Such features are vulnerable to crash loads even if they are adequate for flight loads. The number of structural discontinuities was used to indicate poor robustness.
3. *Rated Aircraft Cost*: The 2001-2002 contest rules define a total score formula with a normalizing term that penalized complex designs., This parameter is a function of the number and size of components on the aircraft used to accomplish the mission profile. In summary, lower costs are achieved by using the fewest motors for propulsion with the lowest battery specific energy, the smallest wing area for lift, the minimal number of actuators for aircraft control, and the leanest MTOGW. The inverse proportionality of the *Rated Aircraft Cost* to total score indicated that the lowest possible cost parameter would maximize the total score, for a given flight score and report score.

Further quantification of these FOM's was necessary to fairly compare configurations. The following discussion shows how the 3 FOM's were broken down into finer discriminators.

3.4 Design Parameters Quantifying the *Sortie Time* Figure of Merit

The *Sortie Time* FOM was specifically defined with design parameters that had the greatest influence on the overall time required to complete a mission. These parameters were explained as follows:

1. *Minimum Total Aircraft C_D*: This parameter is a linear combination of the aircraft parasite drag and vortex drag. Reducing the total aircraft C_D increases max cruise speed for a fixed available thrust.
2. *Minimum Taxi and Payload Swap Time*: Taxi time was determined by the ability of a conceptual design to maneuver under high crosswind conditions. Unacceptable ground handling in such conditions could cause the aircraft to roll off the runway or increase the necessary time to correct for overshoot on a landing approach. The affect of using brakes

was deferred for study in a later design phase. Payload swap time was a function of how easily the payload insertion and egress was possible with a given configuration. Mitigating the interference of wings, propellers, and empennage with respect to the payload hatch access was an important consideration. Minimal mechanisms and restraint devices were necessary for installing and removing payload efficiently.

3.5 Design Parameters Quantifying the *Structural Robustness* Figure of Merit

1. *Minimal Structural Discontinuities*: The conceptual aircraft needed to withstand all design loads with the fewest structural members to satisfy this requirement. Fewer junctions between load bearing components minimized the need for reinforcing such attachment locations. The assumption of composite material construction enabled unique structural designs that did not rely on trusses or various load bearing members for the distribution of load paths. Instead, a limited number of load paths among fewer load-bearing members reduced the need for complex construction in the conceptual designs.
2. *Efficient Distribution of Load Paths*: Long load paths between a load source and the structural components of the conceptual designs were deemed inefficient due to the exaggerated stresses caused by large moment arms. These large stresses required larger area moments of inertia among the load bearing members to provide ample reaction loads up to the ultimate design load limits. Load distribution throughout skins and shells provided torsional rigidity that structural beam components would lack, in general. The use of efficient load paths through skins and specific structural components in areas of concentrated loads, such as attachment point regions, increased the strength to weight ratio of the structural design by minimizing structural weight.

3.6 Design Parameters Quantifying the *Rated Aircraft Cost* Figure of Merit

Optimizing the *Rated Aircraft Cost* FOM required minimizing the use of aircraft components that received the greatest penalty due to their geometry or quantity. This was also reflected in an improvement in the overall performance of the aircraft in accomplishing the mission profile. The geometry and quantity of the following four aircraft components were considered the most important design parameters for the *Rated Aircraft Cost* FOM:

1. *Propulsion System*: The number of motors and the total battery weight influenced a large percentage of the *Rated Aircraft Cost* because its weighted value was one order of magnitude larger than any other parameter in the cost formula. The balance between cost penalties and performance was critical; sufficient thrust was needed to meet TOFL limits mandated by the contest rules and ample specific energy was necessary to complete the three sorties in the mission profile.

2. *Primary Lifting Mechanism*: The number of wings used, increased wing area and the number of control surfaces used to generate lift were penalized. These issues required intelligent compromise with performance criteria such as TOFL requirements, C_L, $C_{L,\alpha}$, and both longitudinal and lateral stability. In addition, the number of control surfaces was related to the number of required actuators, which added a small percentage to the *Rated Aircraft Cost* in comparison.
3. *Empennage*: The means for providing pitch and yaw authority were the function of the horizontal and vertical stabilizer, respectively. The number of elevators and rudders used on these control surfaces also contributed to the total score reduction. Although not directly accounted for in the cost formula, the contest rules also defined an upper span limit for the horizontal stabilizer that was $0.25b_w$.
4. *Mean Takeoff Gross Weight*: The penalties associated by the *Primary Lift Mechanisms* and *Empennage* were of the same order of magnitude as the penalty for average takeoff gross weight of the aircraft without payload. This penalty was only minimized through the use of high strength to weight ratio materials, efficient structural design, and high specific energy from the propulsion system. Improving the affect of this parameter also assisted in reducing the aircraft wing loading and TOFL, which increased turning rates and reduced the power required for liftoff.

The five conceptual configurations were analyzed to judge their technical merit before converging on a single conceptual design and initiating the Preliminary Design Phase.

3.7 Configuration Downselect

Derivative Trade Study Results: Trade studies were conducted on derivative designs of the five conceptual configurations. These studies varied the number of motors used, the use of winglets (or interplanar struts, the payload quantity, and the affect of non-empennage and canard utilizing configurations. These studies used the USC developed "MISSION" simulation package. "MISSION" sizes wing area and cruise speed to satisfy takeoff field length and cruise altitude constraints. "Mission" results include: cost, sortie time, gross weight, percentage of excess energy, and both L/D_{crz} and L/D_{turn}. This full simulation allowed the fixed $S_w = 10$ ft^2 assumption to be waived. Thus, in terms of S_w, a trend was illustrated throughout the trade studies of 4 ft$^2 < S_w <$ 8 ft^2. Such results were initial clues for converging subsystem sizing in the Preliminary and Detailed Design Phases. Other trends and conclusions derived from the trade studies were summarized below.

Variable Number of Motors Used: Each conceptual design and their derivatives provided the same conclusive information about the optimal number of motors. Figure 3.1 depicted a continual decrease of 25% for each additional motor. Thus the optimal total score was possible with the use of only one motor. The additional thrust requirements for TOFL are addressed in the preliminary design section.

Variable Winglet Height: Winglet height was varied for various $S_{winglet}$ values, such as 1 ft^2 and greater. Figure 3.2 illustrates a minimal change in total score for various winglet heights at $S_{winglet} = 1$ ft^2. This was attributed to the L/D_{turn} increase with winglet height. However, the reduction in vortex drag was countered by the increase in parasite drag and weight due to the presence of the winglet. The trade studies that utilized winglets consistently provided a total score that was approximately 20% lower than the total scores obtained without the use of winglets. Thus an increase in b_w was the only primary option that was variable for reducing vortex drag at the conclusion of this trade study.

Variable Payload Quantity: This trade study was conducted to determine the payload within the 10 to 24 softball capacity range appropriate for the highest total score. Each configuration simulated in the MISSION software concluded that only 24 softballs provided the highest total score. Figure 3.3 showed the monotonically increasing total score, where only 50% of the maximum score was obtained at the lowest payload capacity. The possibility of obtaining a higher total score with a payload capacity of 10 softballs and much faster sortie time was considered as well. Trends indicated that a large reduction in aircraft size was necessary to sufficiently decrease the sortie time and reduce the overall cost. In order to match the score of a 24 softball payload the following two alternatives were studied.

1. Case 1: Rated Aircraft Cost must be reduced by at least 1% per unused softball *and* flight velocity increased for a faster sortie time.
2. Case 2: Sortie time must be reduced by almost 50% at a rated cost similar to the 24 ball case. The second case required flight velocities near 100 mph. Optimizing the propulsion system to accomplish this required an exotic gearbox and propeller. Thus, a 24 softball payload capacity was selected.

Flying Wing and Canard Alternatives: The affect of having no empennage on the conceptual design aircraft posed critical performance considerations. To maintain $\partial C_{m,cg}/\partial\alpha < 0$, the condition for longitudinal stability, negative flap angles were necessary to trim at higher lift coefficients. This reduces trim $C_{L,max}$ at any given α by approximately 50% of the trim $C_{L,max}$ on a configuration with an empennage. This trade study also incorporated a canard control surface ahead of the wing. The canard contained two major flaws that inhibited maximum performance of the conceptual aircraft, namely downwash from the canard would reduce the effective angle of attack on the center section of the wing, where the majority of lift was generated, and both the wing flaps and canard contained approximately equal moment arms about the CG. The weight of the canard and its supporting structure moved the aircraft CG forward, thereby requiring the wing to substantially reduce lift with negative flap angles or airfoil reflex for a pitch-down moment. This design derivative was inherently unstable longitudinally, and required a large aft wing shift to recover acceptable stability. At the conclusion of this trade study the efficient pitch and yaw control available from

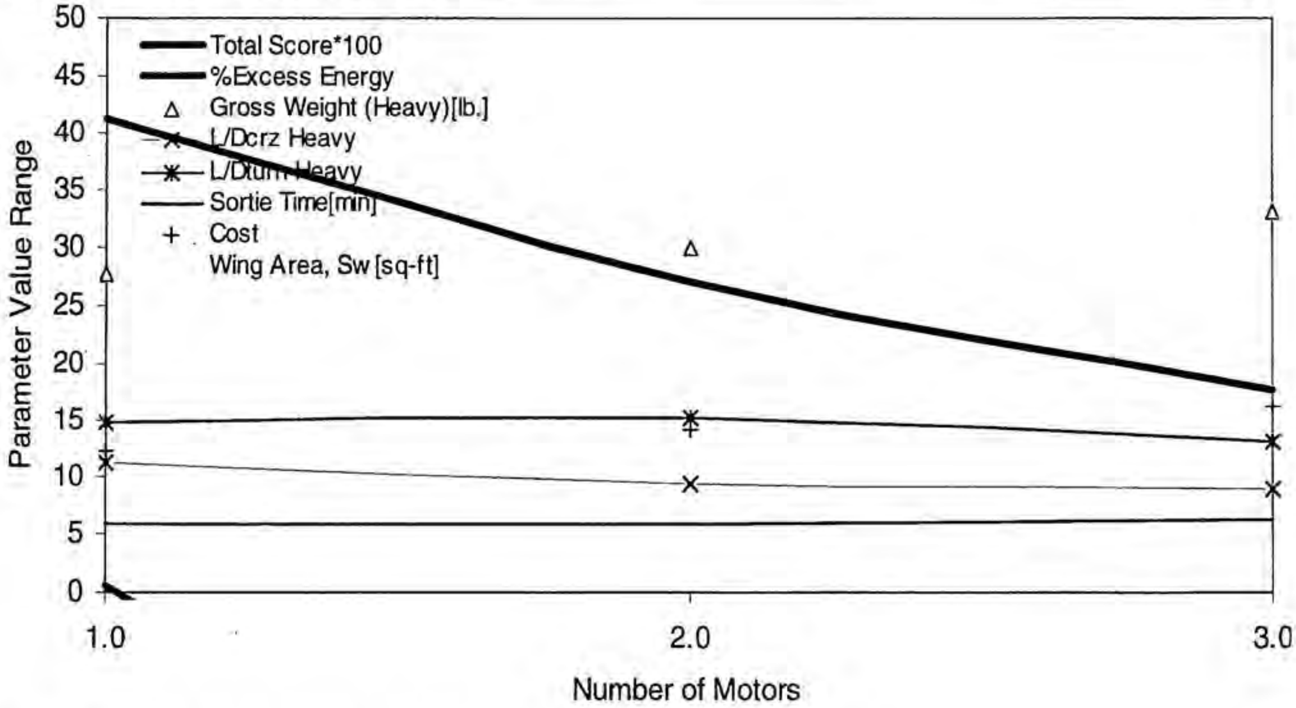

Figure 3.1. Trade study result for variable motor number.

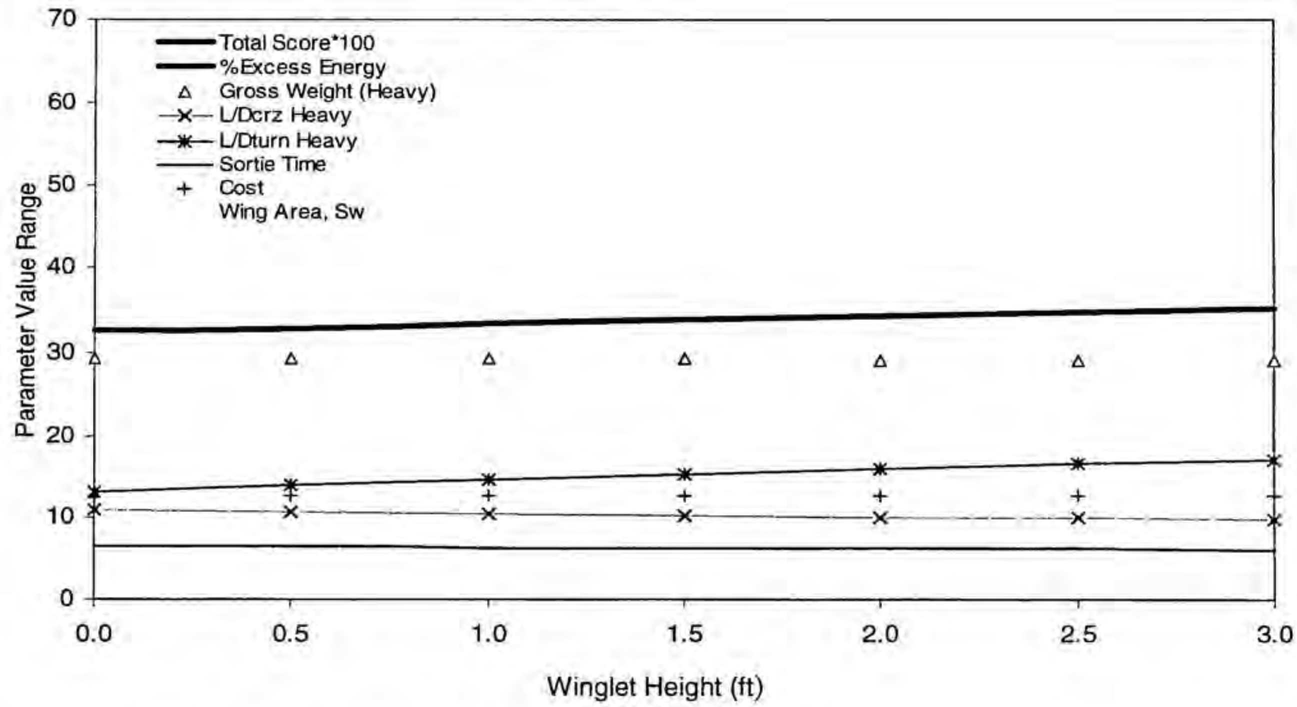

Figure 3.2. Trade study results for variable winglet height at S_w=1 ft^2.

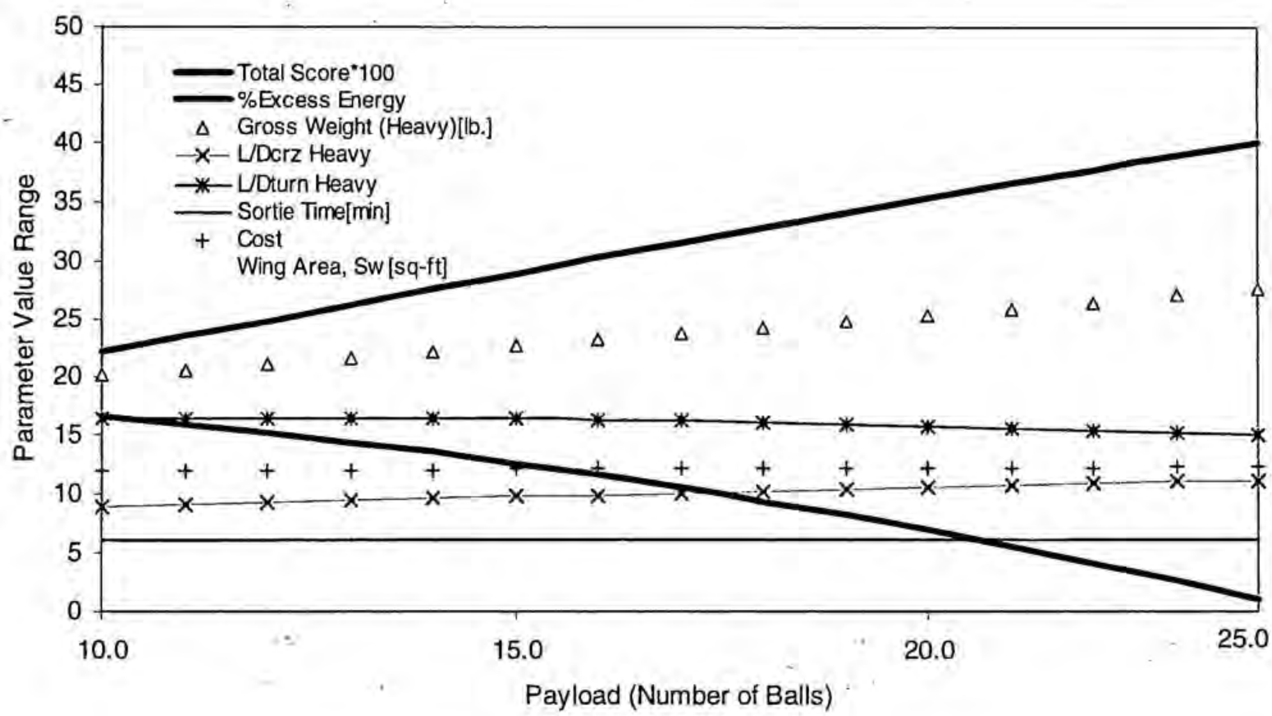

Figure 3.3. Payload capacity trade study results.

empennage was deemed most beneficial due to the longer moment arms about the CG and inherent longitudinal stability.

Monoplane and Biplane Comparison: A trade study initially indicated that the total score possible for a biplane was equivalent to that of a monoplane. Compared to the monoplane, the sortie time was improved and flight velocity was greater. In reality, though, ample vertical spacing between the wings was necessary to reduce the downwash interference and vertical struts at the wingtips were also needed to reduce vortex drag. These changes required a tall fuselage configuration, an extra junction for mounting the second wing, and structure at the wingtips for the wing strut attachments. These additions added structural discontinuities and complicated the load path correlation throughout the wings and fuselage. Furthermore, payload restraint and egress became inefficient with the interference posed by a second wing. Tests were conducted to validate the payload restraint and egress time with different hatch configurations on a fuselage. The test results demonstrated that the most influential parameter for efficient payload handling was a single-hinged hatch located on the fuselage topside; however, such a payload hatch was inaccessible with the presence of a high wing on a biplane.

The possibility of the biplane achieving the same maximum score as a monoplane was unlikely also because of the added structural discontinuities. Inefficient load paths would require reinforcements that were not modeled in the "MISSION" simulation, thereby increasing the true MTOGW of the aircraft and the cost parameter. Furthermore, two identical wings were required to accomplish the same mission that a single wing was capable of completing. Considering the time frame, the optimization of a single wing was more practical than the construction and validation of two wings. The total aircraft C_D was expected to improve with the biplane; yet any vortex drag savings earned with sufficient vertical wing spacing was negated by the added frictional drag on the fuselage due to the substantial fuselage length required to recover the pressure losses from a blunt fuselage forward section. Designs with more than one fuselage to divide the payload were also unacceptable due to the increase in the aircraft parasite drag with greater surface area. Furthermore, using wing struts also added to the aircraft parasite drag and weight. These issues eliminated the biplane configurations from any further design considerations.

Landing Gear Configuration Comparison: For all conceptual designs, the tail wheel landing gear reduced the cost parameter in comparison to designs that incorporated a nose gear. The tail wheel configuration was less massive than a nose gear because under taxing conditions it typically bore only 4%-7% of the aircraft weight, compared to the 10%-15% for a nose gear system. A nose gear also required extraneous structure to provide sufficient propeller ground clearance; in contrast, the tail wheel offered improved propeller ground clearance by lowering the aft end of the fuselage. Propeller strike was also limited in a tail wheel configuration by locating the main landing gear forward of the CG until the moment arm between the main landing gear and the aircraft center of gravity mitigated a downward pitching moment during deceleration. The tail wheel configuration also contained a larger moment arm from the main landing gear than a nose gear system. This superior steering authority allowed the aircraft to direct itself windward during crosswind perturbations. These findings led to the selection of a tail wheel.

3.8 *Rated Aircraft Cost* Comparison with Conceptual Design Rankings and Final Design Features

The foregoing trade studies led to the selection of a single motor and a full 24 ball payload, Table 3.1 summarized the five refined conceptual configurations with their respective FOM rankings. The *Sortie Time* and *Structural Robustness* FOM were each subdivided into two sub-FOM and assigned values of 1-5 where 5 is the superior design. The total score for both FOM's was the sum of its two sub components. Each FOM was given a 1-10 rating, where 10 was the best design. The *Rated Aircraft Cost* FOM value in Table 3.1 was obtained from the "Mission" spreadsheet for each of the configurations; e.g. the classical empennage with nose wheel had a RAC of 12.28. The breakdown showed the percentage of the total cost contributed by each cost design parameter. These percentages did not sum to 100% because other lower percentage cost design parameters were not listed. The Total Score in Table 3.1 was the sum of the Sortie Time and Structural FOMs divided by the RAC. This provided an analytical measure of the design rankings.

Rated Aircraft Cost Comparison: The flying wing configuration had insufficient energy to complete the mission due to the increased vortex drag of the reflexed airfoil and parasite drag of the massive wing needed for TOFL. However, the final cost for this configuration was the lowest of all because it did not have an empennage. The monoplane with empennage and a tail wheel had the second lowest total cost, followed by the monoplane with empennage and nose wheel. The tail wheel landing gear configuration decreased MTOGW and reduced overall cost. The biplane configurations

Table 3.1 Final Conceptual Design Rankings and Rated Aircraft Cost Summary

	Monoplane			Biplane	
	Classical Empennage & Nose Wheel	*Flying Wing with Nose Wheel*	*Classical Empennage & Tail Wheel*	*Classical Empennage & Nose Wheel*	*Classical Empennage & Tail Wheel*
***Sortie Time* FOM**	**7**	**6**	**10**	**5**	**6**
• Minimum Aircraft C_D	*3*	*2*	*5*	*3*	*4*
• Minimum Taxi & Payload Exchange Time	*4*	*4*	*5*	*2*	*2*
***Structural Robustness* FOM**	**7**	**9**	**9**	**5**	**5**
• Minimal Structural Discontinuities	*3*	*5*	*4*	*2*	*2*
• Efficient Load Path Distribution	*4*	*4*	*5*	*3*	*3*
***Rated Aircraft Cost* FOM**	**12.28**	**11.68**	**12.26**	**12.41**	**12.39**
• Propulsion System	*50.8%*	*53.4%*	*50.8%*	*50.2%*	*50.3%*
• Primary Lifting Mechanism	*13.7%*	*14.4%*	*13.8%*	*13.6%*	*13.6%*
• Empennage	*3.3%*	*0.0%*	*3.3%*	*4.8%*	*4.8%*
• MTOGW	*14.6%*	*15.3%*	*14.4%*	*14.2%*	*14.0%*
TOTAL SCORE	**1.14**	**1.28**	**1.55**	**0.81**	**0.89**

contained the highest total cost due to the use of vertical wing struts. Without the vertical wing struts, a 0.2 reduction in cost was achieved by lowering the Empennage design parameter percentage, causing the biplane to surpass the monoplane with empennage cost rating.

Conceptual Design Rankings: Despite the *Rated Aircraft Cost* results, the *Sortie Time* and *Structural Robustness* FOM were the decisive FOM in the final configuration selection. The *Total Score* depicted in Table 3.1 reflected the ratio between the summation of *Sortie Time* and *Structural Robustness* FOM values to the *Rated Aircraft Cost.* The minimal aircraft C_D was heavily influenced by the vortex drag in a configuration, the parasite drag of a nose gear system and skin friction drag from excessive surface area. The taxi and payload exchange design parameter was generally a function of payload access and the superior steering capabilities of a tail wheel system rather than a nose gear system. Structural discontinuities and efficient load paths were characterized by the number of attachment locations in a configuration, the possibility of concentrated loads with large moment arms, and the inefficient use of skins or load bearing members for load path transmission.

The biplane configurations contained the most structural discontinuities and inefficient load paths due to redundant wing structure, whereas the flying wing configuration was deemed the most efficient design for structural efficiency due to less attachment locations.

Final Configuration Features: The monoplane with empennage and a tail wheel configuration received the highest final score in the Conceptual Design Phase. This design achieved the best *Sortie Time* FOM rating due to the lower parasite drag of a tail wheel system, minimal wing parasite drag by virtue of the high trimmed C_{Lmax}, and minimal vortex drag since no outboard airfoil reflex was needed for trim. The ability to install and remove payload from the fuselage topside with minimal interference also provided a reduction in payload exchange time. The *Structural Robustness* FOM was satisfied by the final configuration as well. Even though an empennage was used for the final configuration, there was only one wing with no struts or winglets, and no nose gear.

The *Rated Aircraft Cost* FOM was optimized using the final configuration and conclusions derived from the derivative subsystem trade studies. A minimal cost parameter was obtained by using a single motor for propulsion, no winglets or nose gear, and efficient structural design for lower MTOGW.

The maximum total score was achieved by containing the maximum payload capacity within a single fuselage. The monoplane with a classical empennage and tail wheel was selected for further development in the Preliminary Design Phase.

4. Preliminary Design Phase

This second phase in the design process was organized to conduct further trade studies for each subsystem on the monoplane configuration derived in the Conceptual Design Phase. These trade studies incorporated a different set of assumptions and design parameters; however, the Conceptual Design Phase FOM's were not changed. Wing and Power loading requirements were established during the trade studies to optimize each FOM.

4.1 Revised Assumptions

Assumptions used in the Conceptual Design Phase were valid for the Preliminary Design Phase in terms of defining a general aircraft configuration. The overall justification for these assumptions was explained in the Conceptual Design Phase as well. Modifications to these assumptions allowed a specific design focus on certain subsystems studied in the preliminary design. These reasons are summarized below:

1. *24 Softball Payload Capacity*: This payload capacity was a direct result of the Conceptual Design Phase trade studies which yielded the highest possible flight score for any given configuration and flight time.
2. *Aircraft Center of Gravity (CG) coincident with Payload CG at the Wing c/4*: Variable CG locations were studied in the stability analysis in the Detailed Design Phase. The coincidence of the CG with and without payload eases the stability and control issues as stated in the Conceptual Design section.
3. *Composite Materials for Construction*: This assumption was not changed because a materials trade study was necessary to select which composites were adequate to tolerate given design load conditions.
4. *Only 1 Motor Used:* Motor count was fixed because the Conceptual Design Phase associated a severe cost penalty for using more than one motor.
5. *Monoplane with $4\ ft^2 < S_w < 8\ ft^2$*: Previously, $S_w = 10\ ft^2$ was assumed for the configuration downselect. Trade studies conducted in MISSION simulations during the Conceptual Design Phase converged on solutions with wing area to this specific range instead.
6. *Variable Spacing between Payload, Fuselage Bulkheads, Batteries, and Motors*: These internal components were no longer fixed in order to explore various subsystem locations within the fuselage.
7. *150' TOFL*: Until the aircraft was completed and true TOFL measurements were taken, the reasons stated in the Conceptual Design Phase sufficed for assuming this maximum TOFL.
8. *4-5 lb. Battery Pack Weight*: The battery pack weight assumption was relaxed to allow for various battery pack configurations that matched the specific energy needed to the power loading requirements.

9. *Tail-Wheel Landing Gear Configuration*: The Conceptual Design Phase trade studies provided sufficient evidence that this landing gear configuration was superior to a nose gear system.

A consideration of the FOM's in the Preliminary Design Phase was possible using this new set of assumptions.

4.2 Figures of Merit Summary

The same FOM's used in the Conceptual Design Phase were implemented in the Preliminary Design Phase. These FOM's were repeated below with an emphasis on the different trade studies that were developed for this design phase:

1. *Sortie Time*: New trade studies in aerodynamic efficiency quantified the aircraft C_D. Propulsion efficiency studies established the available and required aircraft power.
2. *Structural Robustness*: The wing, fuselage, and landing gear structure were considered the main structural components of the aircraft. Their structures were analyzed to optimize the distribution of load paths.
3. *Rated Aircraft Cost*: Cost was accounted for during iterations on fuselage design and necessary battery pack weight. A cost analysis was also done for the general sizing of the wing and MTOGW in addition to the performance analysis. This analysis changed the rated aircraft cost of the monoplane configuration rather insignificantly. A small percentage of the cost was eliminated due to the lower wing area assumption and lower battery pack weight. Small deviations from the cost parameter during subsequent analysis of structure, aerodynamic efficiency, and propulsive efficiency were not discussed.

These FOM's were refined for specific technical studies that involved the individual subsystems on the aircraft rather than the overall aircraft configuration.

4.3 Design Parameters & Sizing Trade Studies for Wing & Power Loading Requirements

The "Mission" simulation software was used to conduct the following trade studies for minimizing sortie time:

Aerodynamic Efficiency: Aircraft efficiency was defined by its L/D ratio both in cruise and in turning flight. An aerodynamics subroutine in the "Mission" simulation calculated the parasite drag for the landing gear, fuselage, wing-body junction, controls gaps, cooling, empennage-body junction, and wing at $C_L = 0.5$. Each non-wing component parasite drag was a weighted percentage of the airfoil parasite drag at the given C_L.

Airfoil selection was achieved by studying the relative C_D induced at a given C_L for different airfoils. Considerations included high lift capability to meet TOFL requirements, minimal C_D at high velocity, and gradual C_D increase when approaching $C_{L,max}$ at lower velocity. An airfoil database was compiled using a Selig web-based solver employing a panel-method calculation of the pressure distribution, C_L vs. α, and C_{MO} vs. α for a given airfoil coordinate matrix. Six airfoils were studied, ranging from high speed airfoils to high lift airfoils: S1210, SD 6060, S1223, MH 45, FX74CL5140, SD 7032, and LA 203a. By integrating the pressure distribution around each airfoil at Re = 1,000,000, a collection of drag polars was compiled in Figure 4.1, including full flap deflection at approximately 22°. Both the SD 7032 and LA 203a airfoils had the lowest C_D for the largest range of C_L. However, the LA 203a was a high lift airfoil that lowered the necessary wing area to achieve TOFL. Predicted cruise and turn C_L were generally at lower C_D for the LA 203a than the SD 7032 as well. By selecting the LA 203a airfoil the wing parasite drag was minimized.

Wingspan was varied to study its effects on the aerodynamic parameters. Figure 4.2 indicates that a 9 ft. wingspan was optimal for an overall score. As expected from aerodynamic theory, higher AR wings reduced the vortex drag in cruise. This did not imply a small taper ratio, though, because the shedding vortex system could strengthen inboard from the wingtips and create a large upwash felt by the horizontal stabilizer. A negative pitching moment could ensue that could destabilized the aircraft. In addition, at $C_{L,max}$ the empennage could be in the stalled wing wake and lose control authority. A substantial taper ratio, on the order of 0.7, ensured a downwash in the vicinity of the horizontal stabilizer that created a positive pitching moment and kept the vortex system near the wingtips at $C_{L,max}$.

Furthermore, aerodynamic theory also predicted that an elliptical lift distribution was ideal for minimal induced drag. However, an elliptical wing planform was disregarded because the root chord increased substantially in order to maintain the above wingspan. Each trade study solution converged on a wing area that satisfied TOFL and reduced wing loading for lower turning radius and higher turning rate. These trends indicated that $S_w = 6.61$ ft^2 was sufficient. The aerodynamic performance curves were deferred for studies in the Detailed Design Phase.

Propulsive Efficiency: Available energy in the batteries needed efficient conversion to kinetic energy of the aircraft via thrust. Reductions in the available stored energy were accounted for by taking into account the temperature-dependent internal resistance of each battery cell, speed controller, motor, and wiring, as well as I^2R losses and back emf. This resulted in only 60% of the listed storage capacity of each battery cell being used when sizing the battery pack.

Proper motor, gear box, and propeller matching was a critical trade study because the appropriate propeller advance ratio and activity factor was required to match its best efficiency with the predicted flight velocities. Propeller RPM was directly related to the gear ratios in the gear box and the load it induced on the motor was limited by the 40 A maximum current draw. Various Astroflight motors were considered, each containing unique torque and speed constants. Higher torque and speed constants were important for conservation of battery energy because more torque was achieved per amp and higher RPMs were available for a given voltage. Low motor internal resistance was essential as well. Large pitch propellers required more current draw, whereas larger diameter propellers permitted faster tip speed for a given RPM, where much of the propeller load was concentrated due to the propeller twist. Current draw was also reduced with an appropriate gear box ratio, which increased the propeller RPMs for a given motor RPM. Surface plots for various gear box, propeller, and motor configurations were generated using the "Mission" simulation software to find which combination provided the highest possible score for a given aircraft. Figure 4.3 represented the best scoring configuration consisting of an Astroflight Cobalt 60 motor, a 24-24 propeller, and a 2.7:1 gear box ratio. This configuration also scored the highest propulsive efficiency. The "Mission" simulation was unable to converge for solutions that used a smaller diameter propeller or advance ratio because TOFL requirements were unsatisfied despite a compromise with increasing wing area.

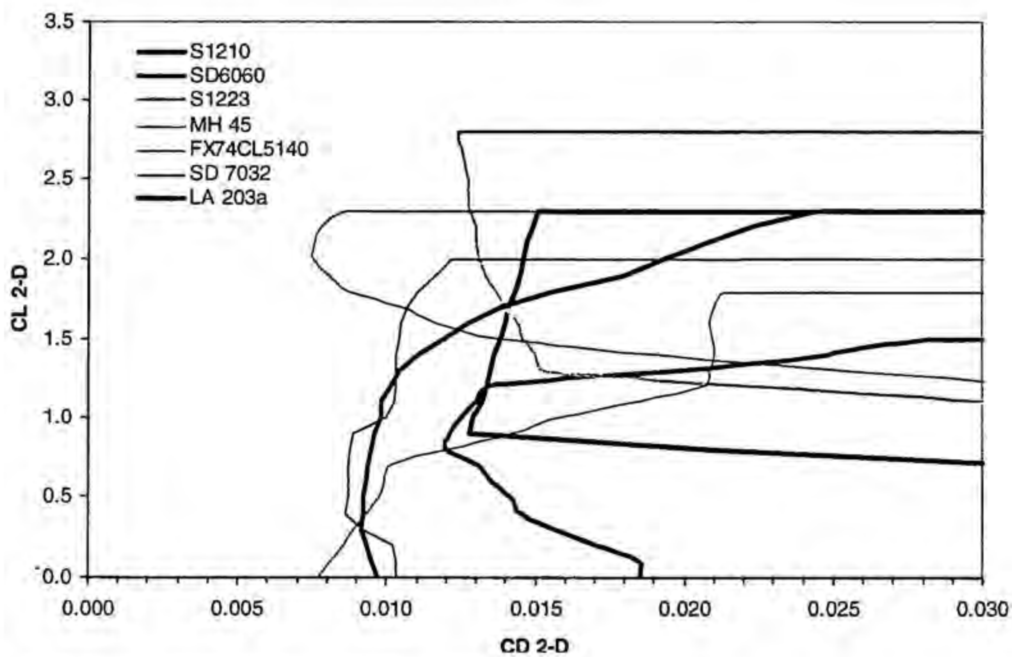

Figure 4.1 Airfoil drag polars, including geared flap effects.

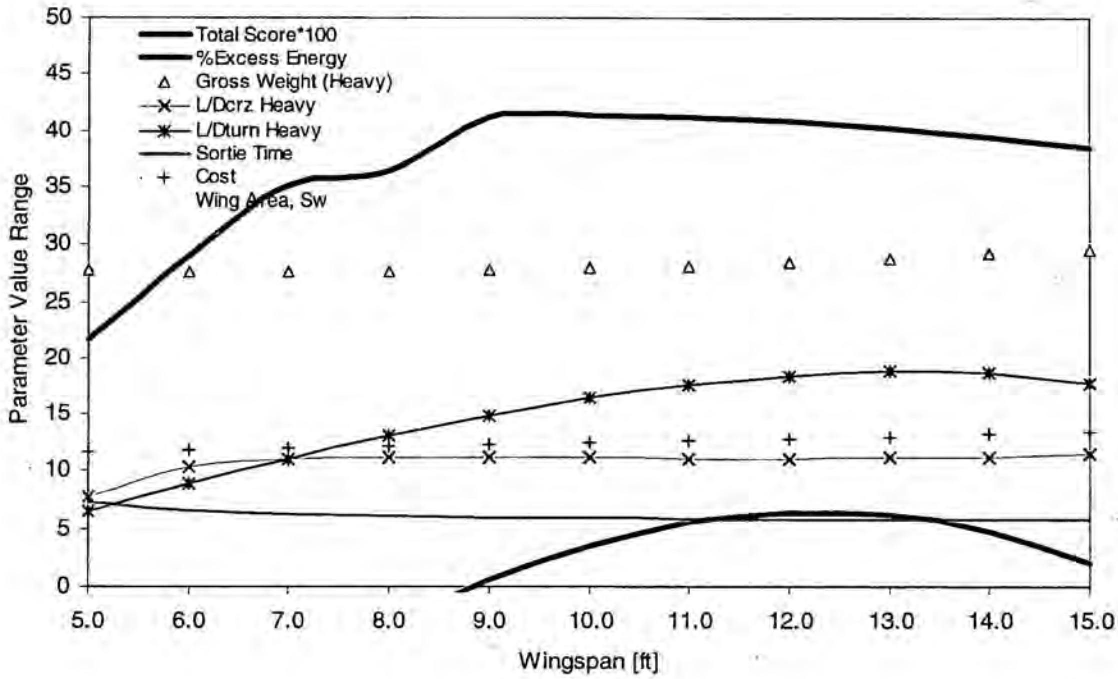

Figure 4.2 Wingspan trade study showing optimum $b_w = 9$ ft.

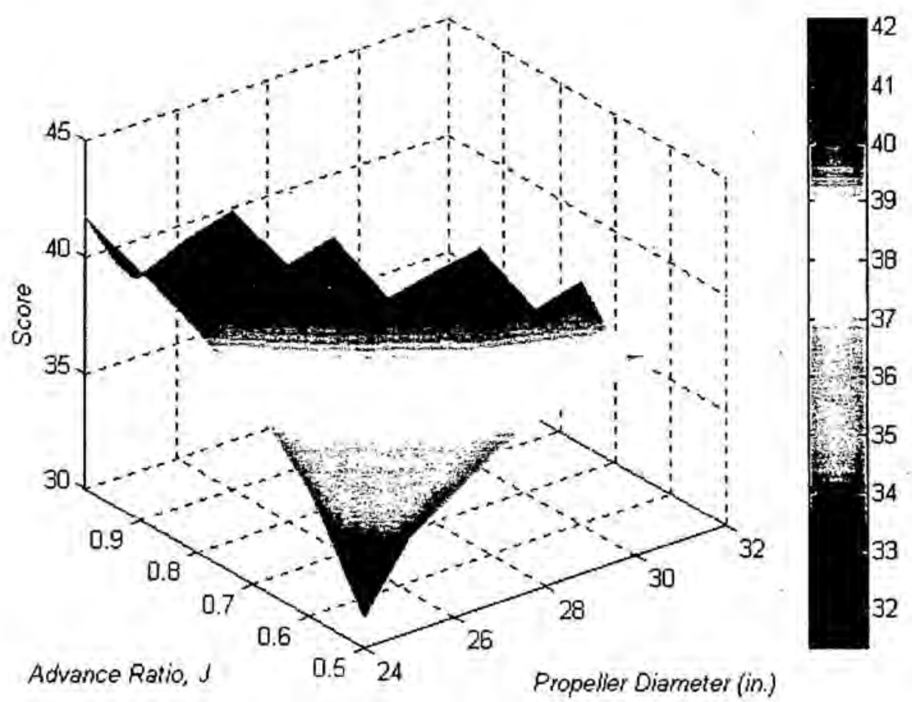

Figure 4.3 Surface plot depicting a maximum score possible with a 24" diameter propeller at $J = 1$, 2.7:1 gear box ratio, and Cobalt 60 motor.

Thrust curves were generated after the results from the motor, propeller, and gear box matching trade studies were presented. These trade studies provided insight concerning the affect of velocity and variable throttle settings on thrust (Figure 4.4), total propulsive efficiency (Figure 4.5), and energy consumption (Figure 4.6). Thrust declined at higher velocities because the ratio between propeller RPM and incident freestream velocity increased, meaning that the propeller imparted less momentum into the incoming flow at a given RPM. The total propulsive efficiency curves (Figure 4.5) demonstrated that at 100% throttle the highest efficiency was permitted at speeds near 60 mph. Matching cruise velocity to this value would ensure optimum usage of battery energy and lower the sortie time. Plots of energy consumption versus velocity further indicated lower energy consumption for these higher velocities.

In addition to the trade studies discussed above, a heat transfer model in "Mission" was implemented to see how the propulsion system dissipated energy at cruise velocities near 60 mph. The internal resistance of the motor, batteries, and speed controller were a function of temperature. Figure 4.7 shows that by the end of a mission, the motor remained under its recommended temperature limit. Similar results were obtained for the batteries and controller. To accomplish this, the heat transfer model required a heat sink and forced convection by a flow ducting mechanism within the fuselage. This study was deferred for the Detailed Design Phase.

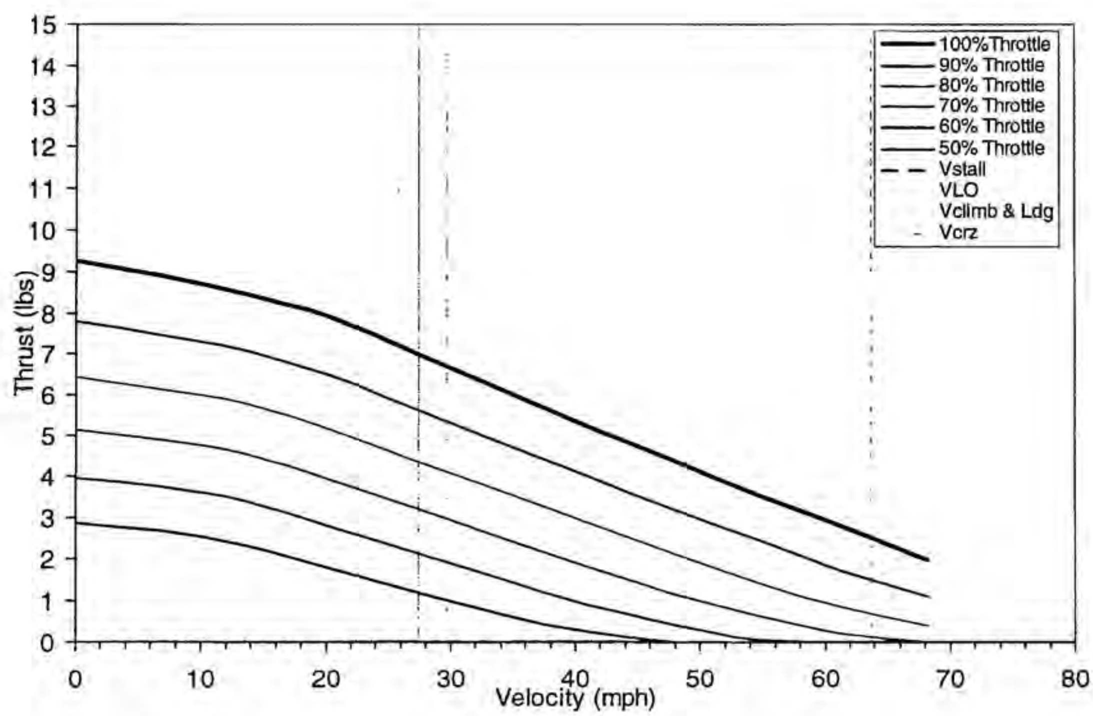

Figure 4.4 Affect of variable throttle and cruise velocity on thrust.

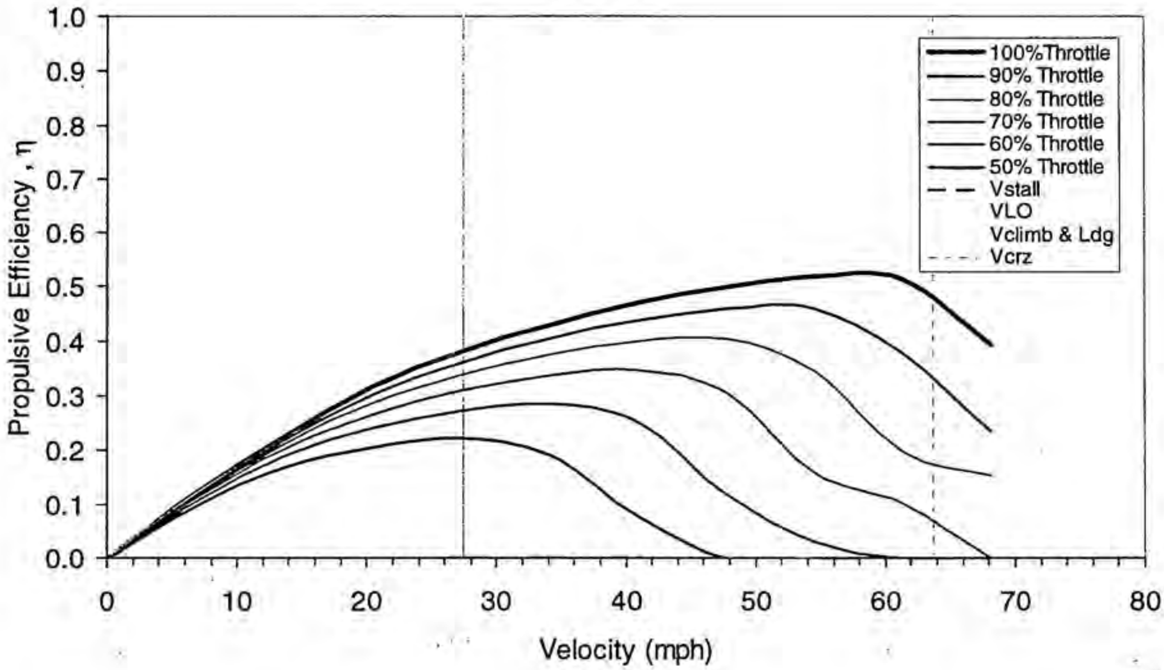

Figure 4.5 Propulsive efficiency plotted as a function of cruise velocity and variable throttle settings.

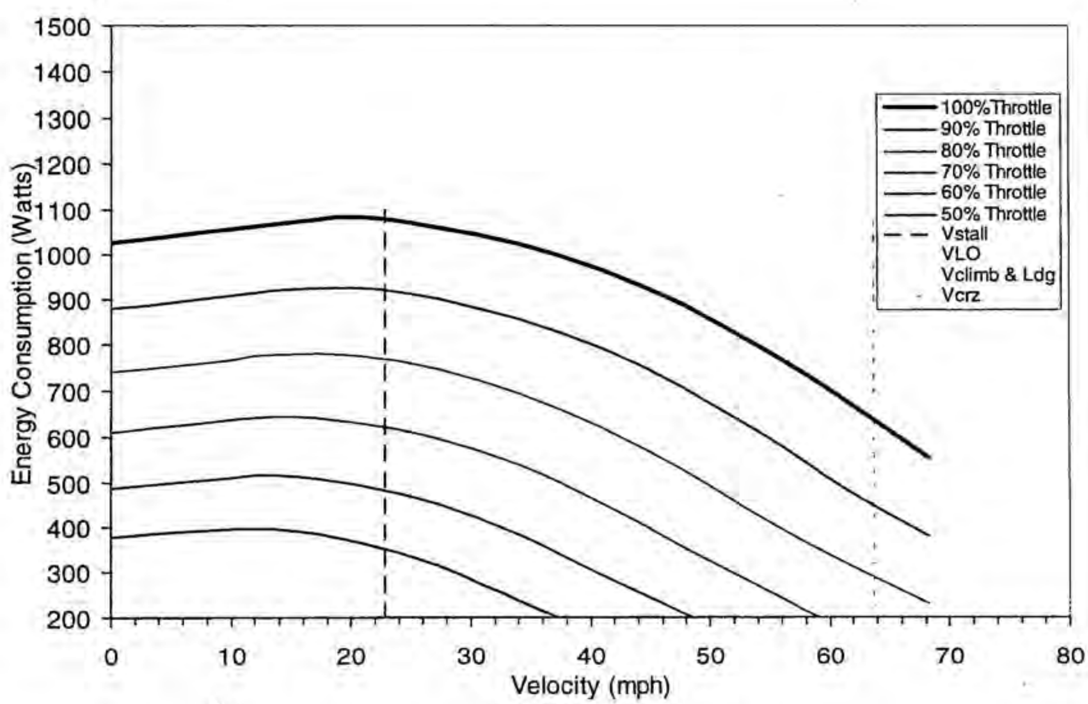

Figure 4.6 Energy consumption at various throttle settings and cruise velocities.

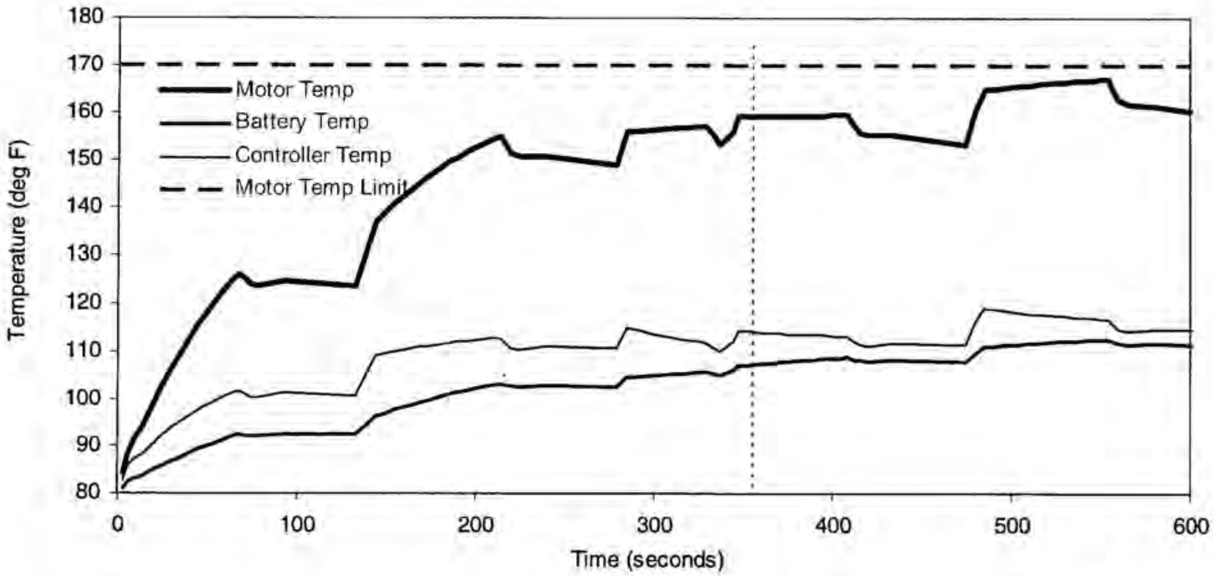

Figure 4.7. Propulsion system component predicted temperatures during mission operation.

Design Parameters & Sizing Trade Studies Focused on *Structural Robustness*

Wing Structure: A spar was the main element that distributed the load from the fuselage throughout the wing. Different spar designs were considered, such as a tube spar, I-beam spar, and spar caps with a shear resisting D-section on the forward section of the airfoil rather than a solid I-beam web. A subroutine in the "Mission" simulation incorporated a cantilevered beam model for a wing. Different materials for the spar stucture and wing core were studied for each spar configuration. An elliptical lift distribution was modeled and the center of pressure felt by discrete lengths along the wing was used to generate shear and moment diagrams versus wing span.

Maximum assumed loading for the spars were 5.25g, with an added safety factor of 1.5. Under this condition, no skin rupture, shear failure, core crushing, or skin buckling was allowed. Calculations for ultimate stresses, shear stresses, core crushing, wing bending radius, and face wrinkling were conducted in the structure model to size appropriate spar cap width and thickness, as well as the spar webbing width.

The tube spar posed several disadvantages, particularly a lack of shear web that caused a predicted failure in shear and possible core crushing. Torsional stiffness was excellent in this design; however integration with a foam core was difficult due to alignment. Airfoil shape preservation and the required area moment of inertia was difficult to achieve without a thick tube. An I-beam spar was possible for satisfying every design criteria mentioned above. Load concentrations occurred, though, at the cap and web junction. To make use of the vast wing area and wing skins, a derivative of the I-beam was analyzed that did not have the concentrated loads at the cap and web junction. This design used spar caps mated with the wing skin section that was forward of 25% MAC, thus creating a D-section. The wing skin in this region needed greater thickness than the aft wing section to act as the shear web. In addition, the D-section was filled with foam core for rigidity and provided torsional stiffness.

Carbon fiber spar caps and fiberglass wing skins were the optimal solution for the wing structure. Each material provided high strength-to-weight ratios in comparison to materials such as balsa wood, spruce, and aluminum. The carbon-fiber caps were tapered in thickness and width from the root chord to the wingtips, where loading conditions were negligible. Figures 4.8 and 4.9 displayed the distribution of stresses and shear loads in the spar caps and fiber-glass D-section, respectively. The material's ultimate stress limits are well above the design loading conditions; face wrinkling was not a problem as well because the material would fail before experiencing any face wrinkling. Discontinuities in spar cap stress occur due to the changing spar cap width at different distances along the wing semispan. The shear discontinuity at the side of body was due to the attachment load concentration in that area, which was offset from the wing centerline.

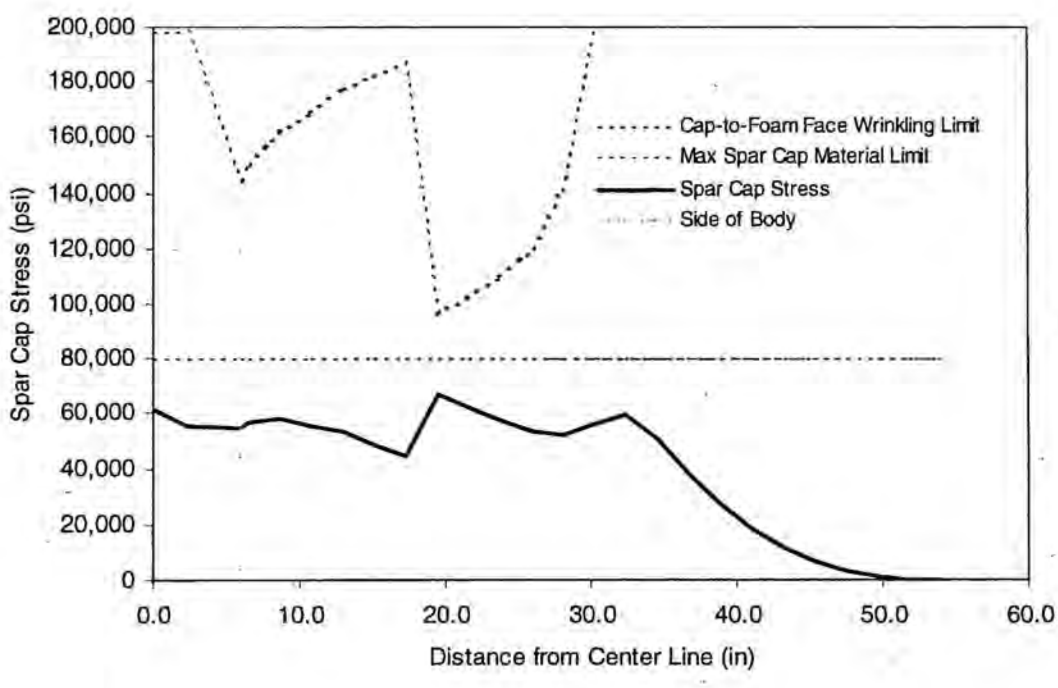

Figure 4.8. Spar cap stress and face wrinkling trade study results.

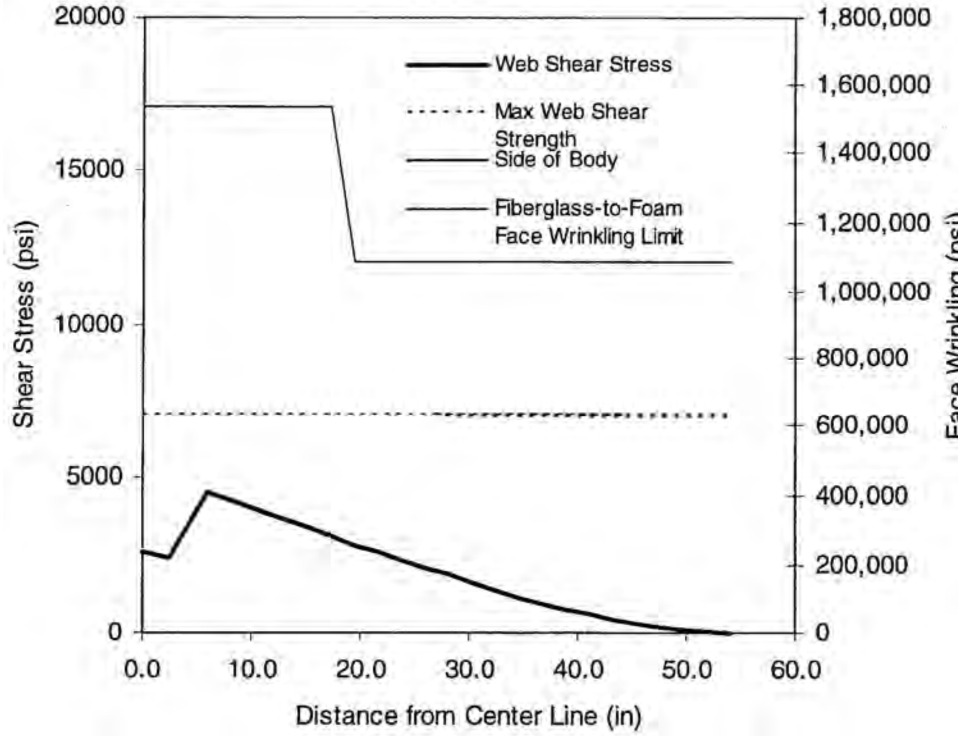

Figure 4.9. D-section shear and face wrinkling behavior.

Fuselage Structure: A monocoque fuselage was compared with a fuselage containing various bulkheads joined together by a structural skin. The monocoque structure eliminated the need for bulkheads and provided torsional stiffness; the bulkhead structure fuselage was advantageous because only the necessary structure was located near regions of concentrated loads. A derivative of both of these ideas was a fuselage that contained a single longitudinal structural member and a non-structural aerodynamic shell. This concept reduced the weight of the skin and minimized the necessary skin-bulkhead junctions. A light weight board to be used as the fuselage floor was considered for this case and trade studies were conducted to verify the location of hard point structure and appropriate thickness.

In addition to sizing the fuselage board, the attachment points for large structural members, including the wing, landing gear, empennage, and motor mounts, were sized to fail under certain loading conditions prior to the failure of each component. The landing gear attachment bolts were sized for a 10 g-load in the drag direction; wing bolts were sized for a 10 g-load in drag, as well as a 3 g-load from a wingtip strike. The empennage and tail-wheel assembly was designed for a 4 g-load in the vertical direction, and a 3 g-load in side force.

The stress analysis trade study indicated that the fuselage board could consist of a honeycomb core covered by carbon-fiber skins. The skins would provide ample shear and bending stress rigidity, whereas the honeycomb core provided strength against core crushing. The attachment hardpoints for the wing, landing gear, empennage, and motor mount contained balsa wood inserts in the honeycomb core.

Landing Gear: The main gear was sized for a 4 g-load vertical load case. This scenario reflected a hard landing where sufficient energy dissipation was required by structural flexing. A carbon-fiber landing gear provided stiffness against bending stress and face wrinkling. The required dissipation energy was calculated by incorporating a 4 ft/s rate of sink at a 5 deg. descent angle. Propeller clearance was also an issue; therefore, the landing gear height was designed to provide 1.5" of clearance at full deflection. Furthermore, the landing gear width (wheel to wheel) was established with a 12° angle of roll clearance for protecting against wingtip strike.

5. Detailed Design Phase

The final design phase incorporated the engineering parameters obtained in trade studies during the Preliminary Design Phase. New assumptions were implemented that focused on particular components in various subsystems, rather than the overall configuration. The component selection process and system integration were evaluated to allow uniform functionality among the various aircraft subsystems without interference. This permitted final mission performance estimates using the "MISSION" simulation software. True performance data was also obtained through various flight tests, structural tests, and propulsion tests that provided feedback in "MISSION" for optimizing the final aircraft once it was built.

5.1 New Assumptions for Specific Subsystems

The following new assumptions were necessary to simulate the contest mission with realistic flight conditions:

1. *25 fps Winds*: The contest location in Wichita, Kansas may subject the aircraft to winds with this velocity magnitude due to climate conditions in that region during the spring.
2. *1320 ft Altitude at 60 °F*: Air density and temperature at this altitude were obtained from Standard Atmosphere Tables and average weather conditions in Wichita, Kansas.
3. *0.65 Battery Energy Factor*: Ample discharge studies with battery packs determined that only 65% of their rated capacity was available due to rapid discharge rates.
4. *40 sec. Average Payload Swap Time*: Payload exchange time was estimated based on average payload swap times recorded by USC teams in previous DBF competitions.
5. *100% Throttle Setting*: Full throttle setting was enabled to obtain the highest cruise velocity and operate at the highest propulsive efficiency.
6. *No Energy Penalty in Turns*: The cosine losses from incident airflow on the propeller cause the motor to continue with constant torque while moving fewer slugs of air, thereby increase current draw and decreasing the available energy.

5.2 Component Selection & Systems Architecture

The propulsion, control, cooling, brake, and payload restraint systems were arranged in the aircraft to maintain the CG at the desired location and still provide easy access. Each subsystem was mounted to the fuselage board. The components were summarized as follows:

Propulsion System: The Astroflight Cobalt 60 and PC-2400 NiCd batteries were chosen for propulsion and power. This battery type was rated at the lowest internal resistance and highest specific energy out of the extensive battery database in the "MISSION" simulation. The battery pack was designed for 30 cells to provide sufficient energy to complete a single mission sortie. The total battery pack weight was well under the 5 lb. limit required by the contest rules, thereby allowing for extra cells to be used if the mission sortie cannot be completed.

Control: Flaperons were incorporated on the wings instead of separate flaps and ailerons. This reduced the servo count and enabled a full span increase in C_L when deflected. Slower landing speed was possible in this configuration. The elevator and flaperons were geared inversely to have a net elliptical lift distribution during cruise for low trim drag. The vertical stabilizer was sized as a full-flying rudder to allow ample control authority for the 25 fps winds in Wichita, Kansas. Otherwise only 12 fps crosswinds were manageable. In order to avoid flutter, the vertical tail's center of pressure was located forward of the rotation point so that the control servo could provide yaw stability. In this configuration, divergence was possible; yet sufficiently large servos were selected based on hinge moment calculations for the predicted flight velocity. The divergence limit was not considered an issue because the average dynamic pressure in the mission flight envelope was substantially lower than that needed for divergence. A single servo was utilized to control both the vertical tail and the tail wheel to reduce the servo count. In crosswind scenarios during takeoff and landing, the coupled steering ability with rudder deflection would provide the pilot with sufficient yaw control.

All control surfaces were designed using a skin-hinge; i.e. the fiberglass skin on the wing and empennage served as the hinge and provided the point of rotation. This ensured that the airfoil skin was continuous at the control surface rotation point. The discontinuity on the opposite side of the hinged surface was covered with thin mylar to provide a smooth surface.

The "MISSION" simulation software was used for stability and control exercises. By iterating the wing position and tail sizes, the design stability parameters specified in Table 5.1 were obtained.

Table 5.1 Stability Parameters calculated for cruise conditions.

Stability Characteristics		
Pitch Stability, Static Margin	%mac	34.8%
Pitch Frequency (@ Cruise)	Hz	3.28
Pitch Damping Ratio (@ Cruise)	n.d.	88%
Directional Stability, CnBeta	1/deg	0.00216
Yaw Frequency (@ Cruise)	Hz	1.63
Recommended Aileron-Rudder-Interconnect Gain	n.d.	0.32
Instantaneous Roll/Yaw in a side gust	n.d.	0.39
Unrecoverable Spin Factor (%fin blanking by Htail)	%	11%
Adverse Yaw due to 15deg aileron (@climb CL)	deg	6.4
$C_{M,Cl,c\alpha}$	n.d.	-0.3482
$C_{M,\alpha}$	n.d.	-0.0324
Lateral Stability	1/deg	0.0004

The static margin was substantial for any variation in CG and pitch stability was guaranteed with a negative moment coefficient for all variations of C_L and α. This was necessary to accommodate different CG locations for sorties with and without payload. In addition pilot trim inputs were required for both flight conditions. Pitch frequency was sufficient to avoid sluggish handling and the 88% pitch damping ratio ensured a lower overshoot and faster settling time after the pilot provide elevator inputs.

Lateral stability was indicated by a positive directional stability term. Yaw frequency was sufficient to avoid sluggish handling as well. Due to the possibility of strong cross-winds in Wichita, Kansas, a 39% gain in aileron deflection per degree of rudder deflection was necessary to negate any adverse yaw, especially since approximately 6° of adverse yaw was possible with any flaperon deflections. This lateral stability behavior was important when initiating turns towards landing approach, since strong cross winds could exacerbate the adverse yaw condition and cause unwanted sideslip or roll due to corrective pilot inputs.

Cooling System: The "MISSION" heat transfer simulation indicated that 40 in.^{2} aluminum heat sink would conduct sufficient heat away from the motor casing to maintain its temperature within specifications. The steady-state model also looked at the effects of forced convection and converged on a solution for inlet and exhaust duct areas. A 9 in.^{2} inlet duct was placed in the fuselage nose and exposed the motor heat sink to incoming freestream air. An internal foam flow diverter did not allow the flow to diffuse, but rather accelerated it around the battery packs and towards exhausts placed laterally on both sides of the fuselage. A third exhaust on the topside of the fuselage allowed the air heated by the motor heat sink to exit without heating the battery packs. The total exhaust area required was 16 in.^{2}.

Payload Restraint & Brake System: The 24 softball payload needed a simple restraining solution. A foam cradle was designed to carry the softballs in a 3x8 configuration. This configuration resulted from a compromise between reducing the hidden wing area and minimizing the overall fuselage length.

The pneumatic braking system contained an air bottle and a proportional release valve that was servo controlled. The amount of pressure released to the brakes was determined by conducting rolling ground tests. Since the main landing gear was placed forward of the CG, the CG moment arm was calculated to avoid tipover and propeller strike when brakes were applied. However, only 80% of the brake valve was opened in order to avoid a sudden negative pitching moment during taxi.

Estimated Mission Performance

Using "Mission", the team was able to estimate the mission performance for the aircraft. The takeoff field length was estimated to be 55 feet for the first empty lap, 150 feet for the heavy lap, and 58 feet for the second empty lap. "Mission" predicted that the plane will be able to complete all six laps, and have an estimated mission time of 5.93 minutes, which includes 40 seconds for payload swap and 15 seconds for taxiing..

Table 5.2 shows the different velocities, propulsion, and aero data at certain periods during the mission, for both light and heavy laps. The program predicted an average cruise velocity of 63mph throughout the entire mission. The table also the estimated values for the aircraft's propulsion system. Aero data, at the bottom of the table, shows different C_L during parts of the flight, as well as lift to drag ratios.

Table 5.2. Estimated Mission Performance Table

Velocity Breakdown	**Light**	**Heavy**	
V_{Climb}	30	37	mph
V_{LO}	27	34	mph
V_{Crz}	64	61	mph
V_{Ldg}	30	37	mph
V_{stall}	23	28	mph
Propulsion			
Available Energy	143,382	ft-lbs	
Max Current	35.15	amps	
Motor Temp at end of mission	160	deg F	
Battery	108	deg F	
Speed Controller	114	deg F	
Aero	**Lap 1 (Light)**	**Lap 2 (Heavy)**	**Lap 3 (Light)**
Unpowered C_{Lmax}	1.93	1.93	1.93
Powered C_{Lmax}	2.12	2.12	2.12
$C_{LStraight}$	0.27	0.47	0.26
$C_{L\,Turn}$	1.35	1.35	1.35
L/D Straight	7.29	11.22	7.11
L/D Turn	14.9	14.9	14.9
Turn Bank Angle	78.4	69.9	78.8

The rate of climb and sink for both light laps and heavy laps are shown in Figures 5.3 and 5.4 respectively. For light flights, the rate of climb was estimated to be just above 950 fpm, with a rate of sink slightly above -150 fpm. For heavy flights, the predicted rate of climb was about 580 fpm, while the rate of sink was estimated to be around -200 fpm. "Mission" estimated a flight score of 4.90. The spreadsheet also predicted that the plane would only be able to complete one sortie, due to limitations in energy. The excess energy "Mission" predicted was 1%.

5.4 Performance Data

Takeoff Performance: More energy is needed for our plane. Observed from our test flights, we need additional excess energy to supply enough power to complete its mission. From take off, our plane without payload travels approximately 70 feet before lifting off the ground. With payload, the distance required is about 190 feet. Additional excess energy to our power system is needed to be able to complete additional laps in the mission.

Bolt Testing: Structural tests were conducted on the bolts to determine their performance and load capacity. The bolts selected for use were nylon bolts ranging from 1/4" to 3/8" in diameter. The test on the nylon bolts determined its ultimate shear and ultimate tensile strength. The ultimate shear load of the bolts was found to be approximately 600 pounds, while the ultimate tensile load was about 1000 pounds. Our design intent was to break the bolts at 10 g loadings in the drag direction to prevent major damage to the plane body. From observations in test flights, the bolts must have ¼" diameter to rupture at the desired loading. The ideal bolt diameter selected for the landing gear was 5/16" and 1/4" for the wing to achieve the design condition.

Flight Test Performance Summary: For a successful flight performance, one of the key components for the plane is cooling the motor. Based upon the temperatures recorded after a series of flight tests, the cooling performance was excellent. The motor temperature measured 110° F; the battery pack ranged from 90° -100° F; and the controller reached 80° F. The observed temperatures were all lower than the listed manufacturer limits.

Battery conditioning proved to be a key component of the plane's endurance. The batteries performed best when charged slowly. Based upon the test flights, all the available energy within the batteries is necessary to perform the entire mission. After testing, it was observed that the optimum performance could only be obtained with a slow charging rate. Efforts to increase the battery energy further are presently being looked at.

The observed cruise speed average was measured to be within 10% of the predicted value. This was done by measuring the distance our plane traveled along the straightaway, divided by the time needed to travel.

Ground handling of the plane performed sufficiently well. Braking and steering were non-issues as we were able to control the plane with ease. During flight tests in heavy crosswinds, the plane showed sufficient control authority as it was able to correct and compensate for the crosswind.

Pitch and lateral stability of the plane performed adequately during the test flights. However, the pilot required new trim inputs when flying laps with payload due to the aft CG shift. Power On/Off stalls were also conducted and the aircraft did not diverge from pilot control; the pilot had sufficient recovery time to correct for stall. A speed brake was tested by fully deflecting the flaperons on landing approach. The aircraft approach speed decreased substantially as a result and decreased landing overshoot.

5.5 Weight, Balance and Rated Aircraft Cost Worksheets

Weight Budget: The weight budget is summarized in Table 5.3, showing each subsystem and the individual components it contains. Different weighting was provided with the K_{fudge} factor among the subsystems. This parameter was an estimate used to provide weight estimates for subsystems that were historically overweight or underweight in USC's DBF competition aircraft. The relative weight of each component with respect to the total heavy gross weight was also shown. The dominating components included the motor, batteries, and the fuselage.

Balance Distribution: Table 5.4 lists the relative longitudinal separation from a reference location behind the motor and battery compartment. This origin was used to determine the aircraft CG with respect to the wing MAC, as well as the differential loading between the main gear and tail wheel. The wing leading edge position was found with respect to the origin in the XLE_{MAC} parameter and both the empty CG and heavy CG locations were also shown. The payload moved the CG aft about 22%, which was acceptable since the pitch stability static margin was on the order of 35%.

Rated Aircraft Cost: The final cost breakdown was summarized in Table 5.5. Cost was generally attributed to the propulsion system, which contained a multiplier that was 15 times larger than any other cost multiple. Thus the single motor and 30 cell battery pack were the most influential aircraft components. As seen in the Conceptual and Preliminary Design Phases, the wing and fuselage geometry were the second most influential parameters in the cost determination. The final rated aircraft cost was calculated to be 12.26.

Table 5.3. Weight Budget Worksheet

System	KFudge	Sub-Component	Weight Breakdown	% of Heavy Weight
PROPULSION	1.0	Sub-Total	**7.186**	**25.9%**
		1 Motor	1.563	5.63%
		1 Motor Mount / Heatsink	0.115	
		Battery wt incl. solder & jack	4.156	14.97%
		All Wiring	0.100	0.36%
		1 Speed Controller	0.150	0.54%
		1 Propeller	0.403	1.45%
		1 Spinner & Prop Nut	0.230	0.83%
		1 Motor Mount	0.46875	1.69%
WING	1.0	Sub-Total	**1.984**	**7.1%**
		Wing Spar	0.453	1.63%
		Wing Core	0.564	2.03%
		Wing Skin	0.967	3.48%
TAIL & Winglets	1.5	Sub-Total	**0.626**	**2.3%**
		HTail Skin	0.277	1.00%
		HTail Core	0.075	0.27%
		VTail Skin	0.201	0.72%
		VTail Core	0.072	0.26%
		Winglets	0.000	0.00%
RADIO	1.0	Sub-Total	**1.563**	**5.6%**
		Receiver	0.125	0.45%
		Servos	0.938	3.38%
		Battery Pack	0.500	1.80%
LANDING GEAR	1.0	Sub-Total	**2.229**	**8.0%**
		Main Gear Struts & Bolts	1.408	5.07%
		Main Wheels	0.541	1.95%
		MG Axle Hardware	0.100	0.36%
		Nose Wheel or Tail Wheel	0.030	0.11%
		Nose Gear Strut & Mount	0.000	0.00%
		Brakes, Tubing, Air Tank	0.149	0.54%
FUSELAGE	0.85	Sub-Total	**4.244**	**15.3%**
		Fuselage Skin	1.747	6.29%
		Bulkheads	2.496	8.99%

Airframe Weight =	**8.93**
Payload Weight =	**9.94**
Heavy Gross Weight =	**27.77**
Light Gross Weight =	**17.83**

Table 5.4. Balance Distribution Worksheet

Parts	C.G (midpoint) distance from Motor Blkhd (in)	Weight (lb)	Moment (in-lb)
Propeller	**-7.92**	0.40	-3.19
Servo for Nose Gear	60.72	0.00	0.00
Nose Wheel	60.72	0.03	1.85
Nosegear	60.72	0.00	0.00
Main Wheels	5.50	0.54	2.98
Horseshoe Strut (maingear)	5.50	1.41	7.74
Axle Hardware	5.50	0.10	0.55
Battery Pack	**1.08**	4.16	4.49
Radio Receiver	**38.12**	0.13	4.77
Receiver Battery	38.12	0.50	19.06
Motor + Mount	**-4.32**	2.03	-8.78
Brakes, Tubing, Bottle+Servo	**1.08**	0.34	0.36
Fuselage (40% length)	28.07	4.24	119.13
Speed Controller (Batt Pack +2"))	1.25	0.15	0.19
Wiring (@ controller)	38.12	0.10	3.81
Spinner & Prop Nut	-7.92	0.23	-1.82
Horizontal Tail+Servo	65.05	0.54	35.12
Vertical Tail +Servo	56.85	0.46	26.21
Wing (cg@mac/4)	16.05	1.98	31.85
2 Wing Servos (cg@mac/2)	18.35	0.38	6.88
Heavy Payload (softballs)	**19.92**	9.94	197.93

Total Weight (lbs) =	27.65
Total Moment (in-lbs) =	449.12
Actual X C.G. (total) =	**16.24**

Empty Weight (lbs) =	17.72
Payload MAX Weight (lbs)=	9.94
Gross Weight (no tail pad (lbs)) =	27.65

MAC (in) from Stable Sheet =	9.18
Target C.G.(%mac) from Stable Sheet =	27.00%
% Weight on Nose or Tail wheel =	19.5%
% Weight on Mainwheels =	80.5%
Required XLEmac (in) for desired balance =	**13.76**

Payload Length (in) =	32.4
Heavy Pitch Inertia (slug ft2) =	1.489

Empty C.G. (no payload) =	**14.18**

Table 5.5. Rated Aircraft Cost Worksheet

Cost Table						Total Cost	Rated Cost
Rated Aircraft Cost		Dims	Manuf. Hrs	Hrs Sub-Total	Cost Sub-Total	$12,261	12.26
MEW (Manufacturers Empty Weight) (lb.)				17.68	1767.65		14.4%
REP (Rated Engine Power)	= (1+.25*(#Motors-1))*BattWt			4.16	6234.3		50.8%
	# of Engines	1					
	Total Battery Weight (lbs)	4.16					
MFHR (Manufacturing Man Hours)				212.94	4258.8		34.7%
WBS1.0 (8hr/ftSpan + 8hr/ftMaxChord + 3 hr/control surface)	# of wings	1	84.3			13.8%	
	Wing Span	9.00					
	Max Wing Chord	0.79					
	# of control surfaces	2					
WBS2.0 (10hr/ft of length)	Fuselage Length (ft)	6.86	68.6			11.2%	
WBS3.0 (10hr/VertWithRudder + 10hr/horizWithElev)	Number of Vertical Surfaces	0	0.0			3.3%	
	Number of Vertical Tails	1	10.0				
	# of Horrizontal Tails	1	10.0				
WBS4.0 (5hr/srevo or controller)	# of Servos and Motor Contollers	6	30.0			4.9%	
WBS5.0 (5hr/Motor+5hr/Prop)	# of Motors	1	10.0			1.6%	

Fixed Parameters	
A (Manuafcturers Empty Weight Mulitiplier) ($/lb.)	100
B (Rated Engine Power Mulitiplier) ($/Watt)	1500
C (Manufacturing Cost Mulitiplier) ($/hour)	20

5.6 Detailed Drawing Package

The following are the summaries of the drawing packages.

- 3 view of airplane
- Isometric view of airplane, with labeled subsystems
- Top view of fuselage, showing all major structural components and attachment locations
- Side view of vertical stabilizer, with detailed specifications on the tail wheel assembly
- Isometric close up view of cooling system in the forward fuselage

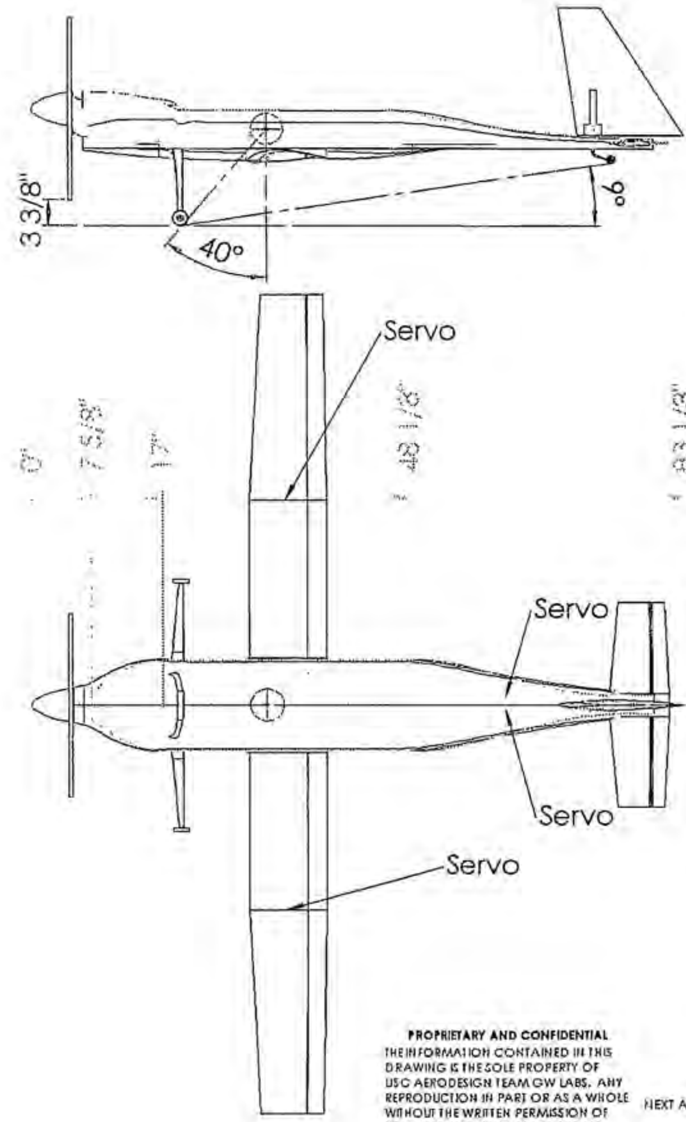

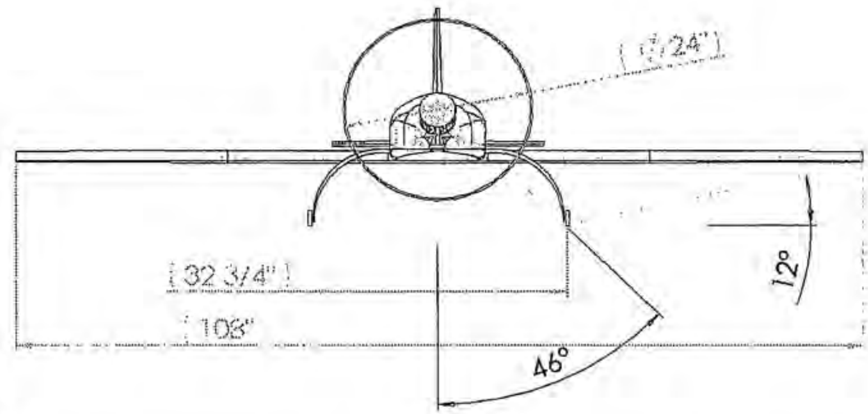

Calculated Geometry		Wing	H.Tail	V.Tail	Ventral
Total Area Sw, SH, Sv	ft2	6.85	1.18	1.13	0.00
MAC	ft	0.76	0.51	0.84	0.84
Y MAC	ft	2.17	0.55	0.61	0.00
Span	ft	9.00	2.30	1.42	0.00
Root Chord	ft	0.80	0.57	1.13	1.13
Tip Chord	ft	0.64	0.45	0.45	0.45
Root Incidence	deg	-1.40	-1.00	-	-
Tip Incidence	deg	-2.60	-1.00	-	-
Fuselage Height, Width, Length(incl spinner)	ft	0.65	1.08	6.92	

NEXT ASSY USED ON
APPLICATION

DIMENSIONS ARE IN INCHES
TOLERANCES:
FRACTIONAL ±
ANGULAR: MACH ± BEND ±
TWO PLACE DECIMAL ±
THREE PLACE DECIMAL ±

MATERIAL —

FINISH —

DO NOT SCALE DRAWING

	NAME	DATE
DRAWN	PMK	
CHECKED	SG	
ENG APPR.		
MFG APPR.		
Q.A.		
COMMENTS:		

USC AERODESIGN

SCrewball 01-02

SIZE A DWG. NO. REV.

SCALE:1:20 WEIGHT: SHEET 1 OF 1

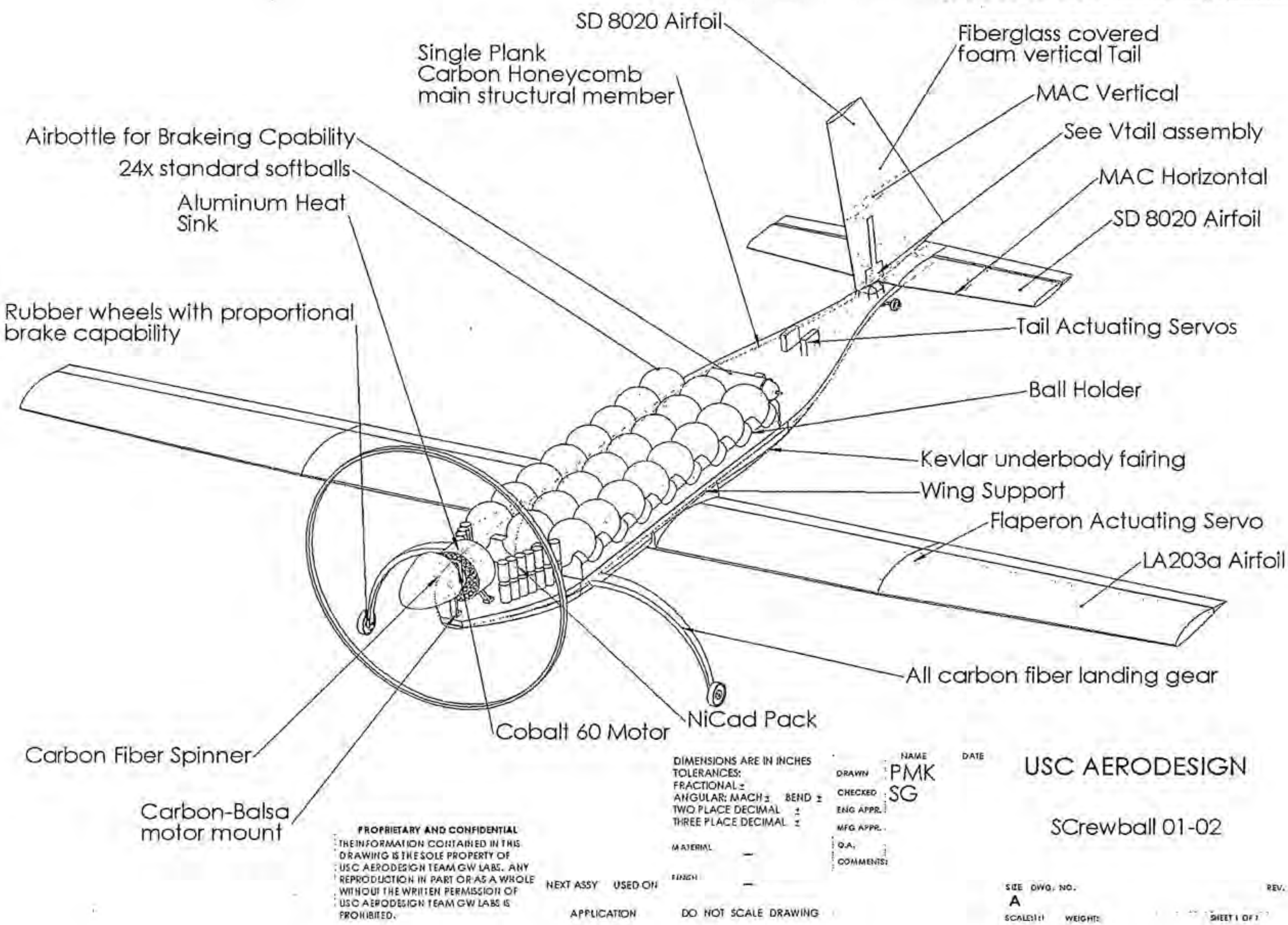
SD 8020 Airfoil
Single Plank
Carbon Honeycomb
main structural member
Fiberglass covered
foam vertical Tail
MAC Vertical
See Vtail assembly
MAC Horizontal
SD 8020 Airfoil
Airbottle for Brakeing Cpability
24x standard softballs
Aluminum Heat
Sink
Rubber wheels with proportional
brake capability
Tail Actuating Servos
Ball Holder
Kevlar underbody fairing
Wing Support
Flaperon Actuating Servo
LA203a Airfoil
All carbon fiber landing gear
NiCad Pack
Cobalt 60 Motor
Carbon Fiber Spinner
Carbon-Balsa
motor mount
PROPRIETARY AND CONFIDENTIAL
THE INFORMATION CONTAINED IN THIS DRAWING IS THE SOLE PROPERTY OF USC AERODESIGN TEAM GW LABS. ANY REPRODUCTION IN PART OR AS A WHOLE WITHOUT THE WRITTEN PERMISSION OF USC AERODESIGN TEAM GW LABS IS PROHIBITED.
NEXT ASSY
USED ON
APPLICATION
DIMENSIONS ARE IN INCHES
TOLERANCES:
FRACTIONAL ±
ANGULAR: MACH ± BEND ±
TWO PLACE DECIMAL ±
THREE PLACE DECIMAL ±
MATERIAL
FINISH
DO NOT SCALE DRAWING
NAME
DATE
DRAWN PMK
CHECKED SG
ENG APPR.
MFG APPR.
Q.A.
COMMENTS:
USC AERODESIGN
SCrewball 01-02
SIZE
DWG. NO.
REV.
A
WEIGHT:
SHEET 1 OF 1

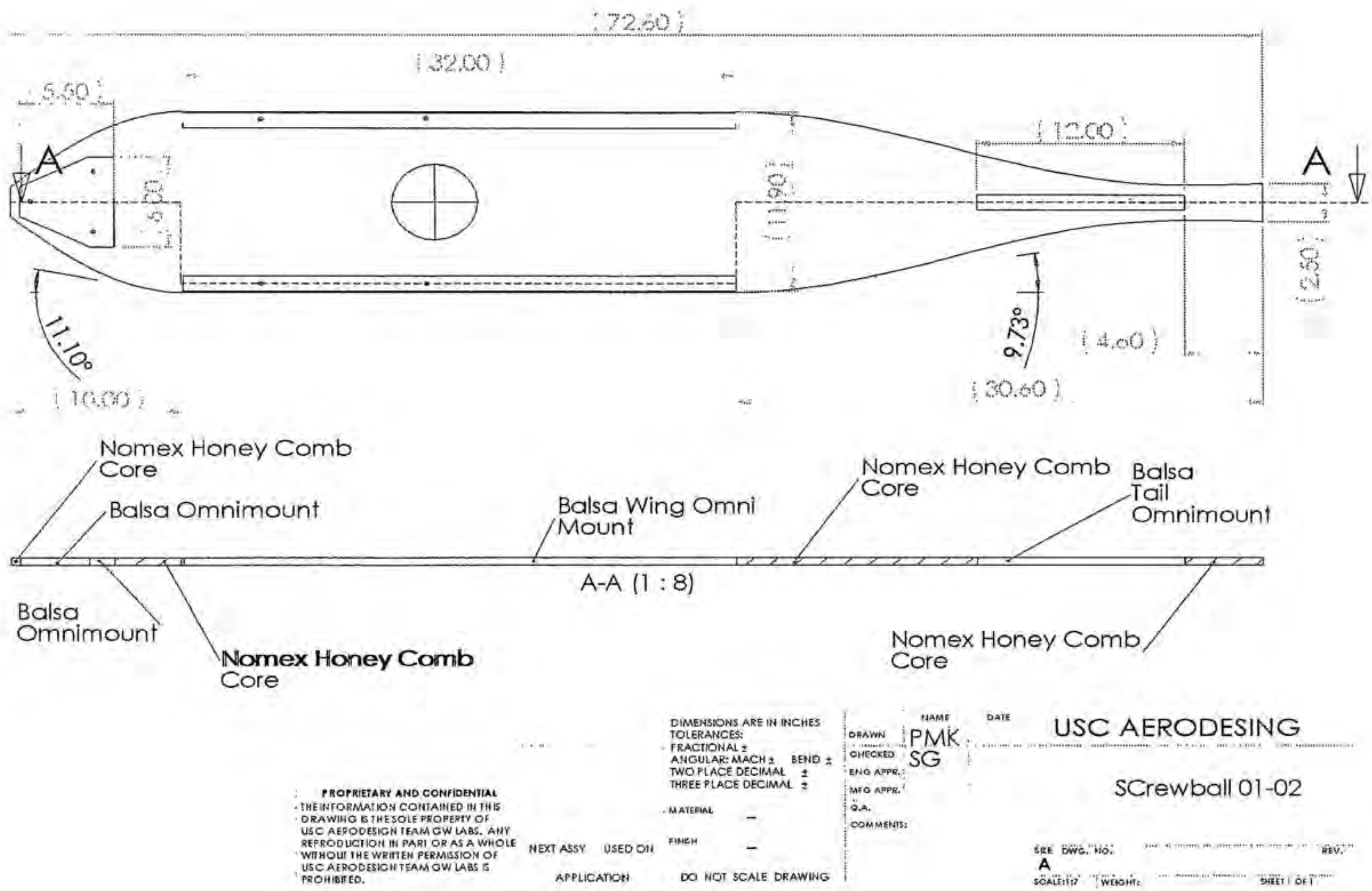
72.60
32.00
5.50
5.00
11.90
12.00
2.50
4.00
30.60
10.00
11.10°
9.73°
A
A
Nomex Honey Comb Core
Balsa Omnimount
Balsa Wing Omni Mount
Nomex Honey Comb Core
Balsa Tail Omnimount
A-A (1 : 8)
Balsa Omnimount
Nomex Honey Comb Core
Nomex Honey Comb Core
PROPRIETARY AND CONFIDENTIAL
THE INFORMATION CONTAINED IN THIS DRAWING IS THE SOLE PROPERTY OF USC AERODESIGN TEAM GW LABS. ANY REPRODUCTION IN PART OR AS A WHOLE WITHOUT THE WRITTEN PERMISSION OF USC AERODESIGN TEAM GW LABS IS PROHIBITED.
NEXT ASSY
USED ON
APPLICATION
DIMENSIONS ARE IN INCHES
TOLERANCES:
FRACTIONAL ±
ANGULAR: MACH ± BEND ±
TWO PLACE DECIMAL ±
THREE PLACE DECIMAL ±
MATERIAL
FINISH
DO NOT SCALE DRAWING
NAME
DATE
DRAWN PMK
CHECKED SG
ENG APPR.
MFG APPR.
Q.A.
COMMENTS:
USC AERODESING
SCrewball 01-02
SIZE DWG. NO.
A
REV.
SCALE:1:12
WEIGHT:
SHEET 1 OF 1

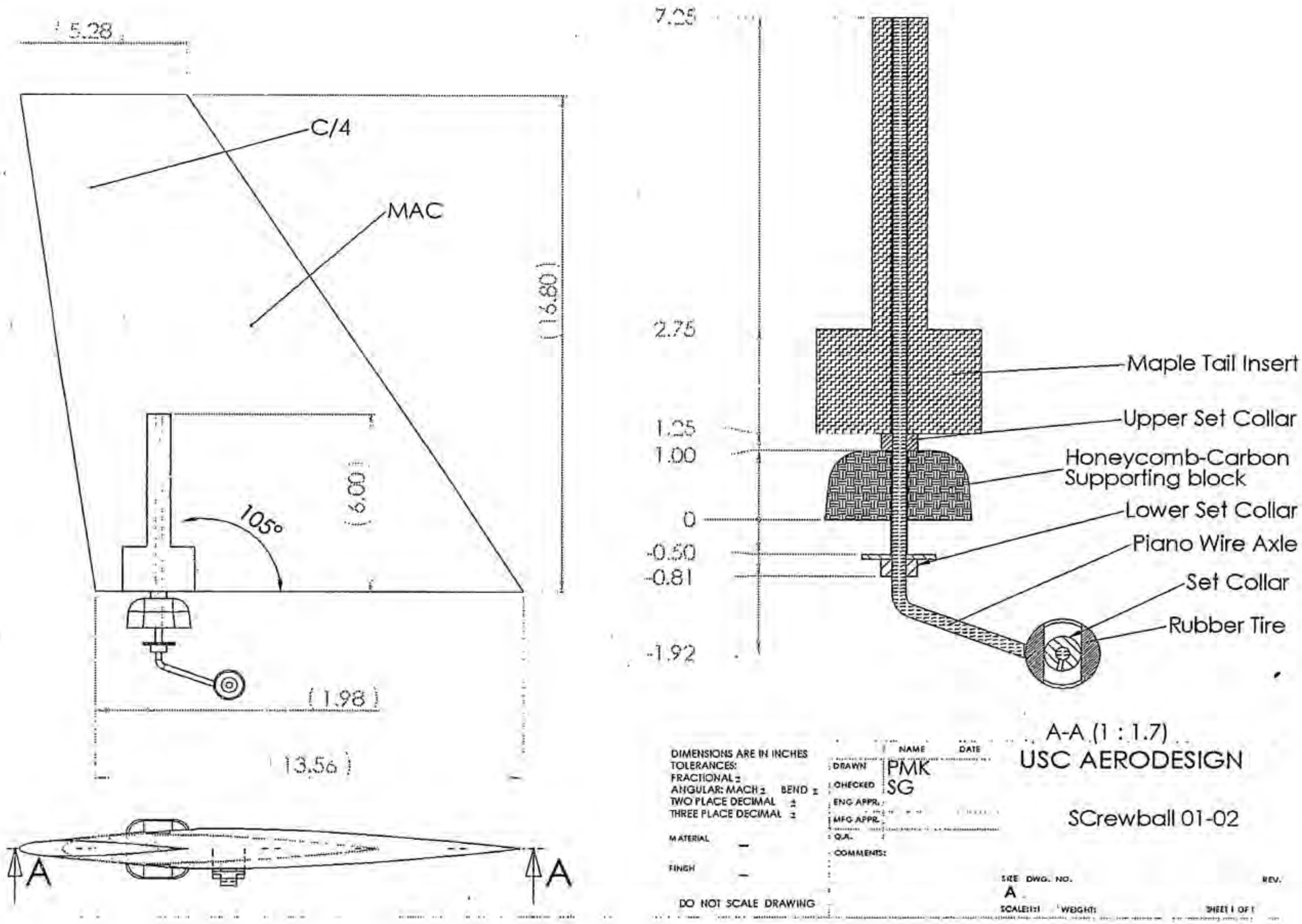
5.28
C/4
MAC
(16.80)
(6.00)
105°
(1.98)
13.56
A
A
7.25
2.75
1.25
1.00
0
-0.50
-0.81
-1.92
Maple Tail Insert
Upper Set Collar
Honeycomb-Carbon Supporting block
Lower Set Collar
Piano Wire Axle
Set Collar
Rubber Tire
A-A (1 : 1.7)
USC AERODESIGN
SCrewball 01-02
DIMENSIONS ARE IN INCHES
TOLERANCES:
FRACTIONAL ±
ANGULAR: MACH ± BEND ±
TWO PLACE DECIMAL ±
THREE PLACE DECIMAL ±
MATERIAL
FINISH
DO NOT SCALE DRAWING
NAME
DATE
DRAWN PMK
CHECKED SG
ENG APPR.
MFG APPR.
Q.A.
COMMENTS:
SIZE DWG. NO.
A
REV.
SCALE:1:1
WEIGHT:
SHEET 1 OF 1

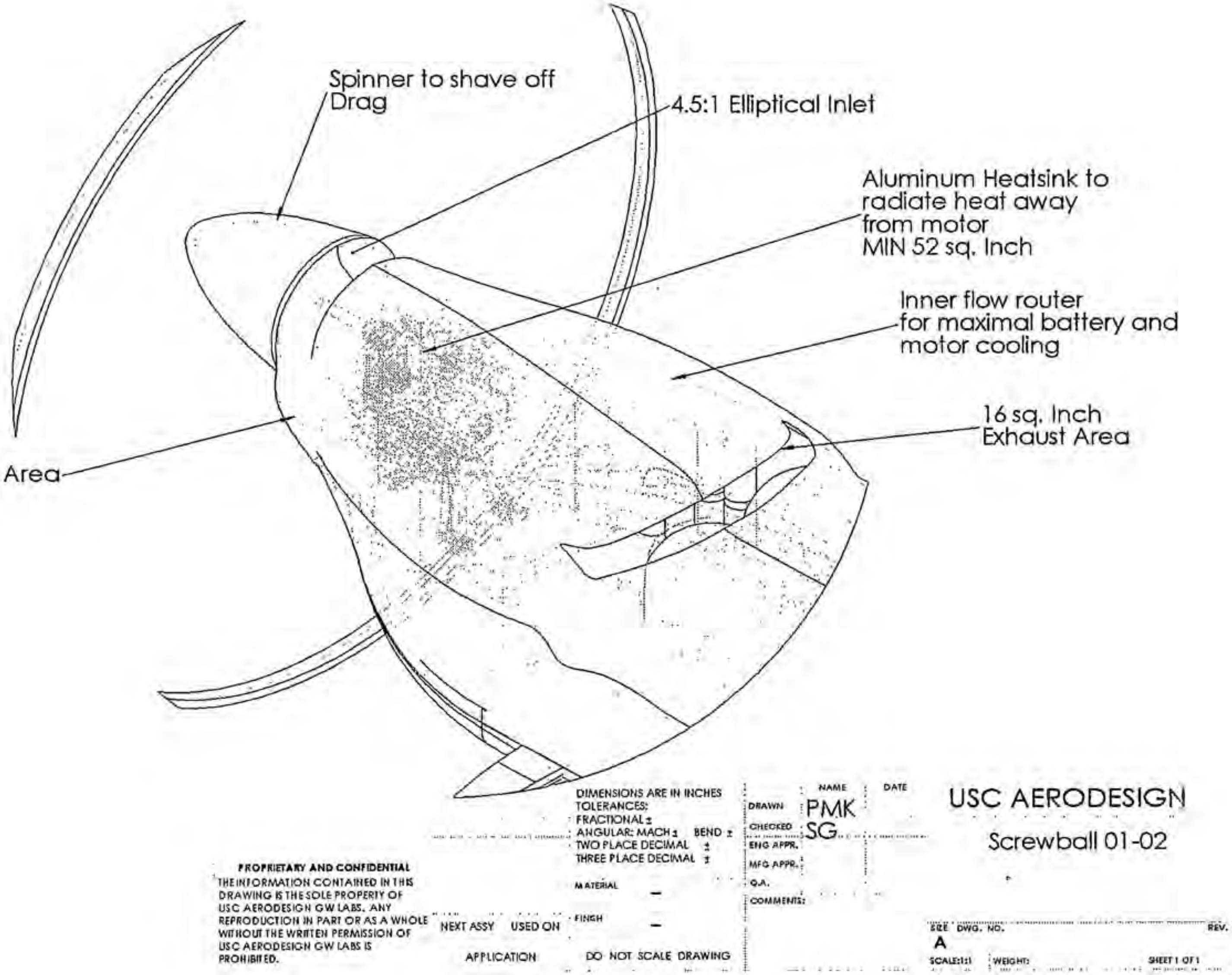

Spinner to shave off Drag
4.5:1 Elliptical Inlet
Aluminum Heatsink to radiate heat away from motor MIN 52 sq. Inch
Inner flow router for maximal battery and motor cooling
16 sq. Inch Exhaust Area
9 Sq. Inch Inlet Area
PROPRIETARY AND CONFIDENTIAL
THE INFORMATION CONTAINED IN THIS DRAWING IS THE SOLE PROPERTY OF USC AERODESIGN GW LABS. ANY REPRODUCTION IN PART OR AS A WHOLE WITHOUT THE WRITTEN PERMISSION OF USC AERODESIGN GW LABS IS PROHIBITED.
NEXT ASSY
USED ON
APPLICATION
DIMENSIONS ARE IN INCHES
TOLERANCES:
FRACTIONAL ±
ANGULAR: MACH ± BEND ±
TWO PLACE DECIMAL ±
THREE PLACE DECIMAL ±
MATERIAL
FINISH
DO NOT SCALE DRAWING
NAME
DATE
DRAWN PMK
CHECKED SG
ENG APPR.
MFG APPR.
Q.A.
COMMENTS:
USC AERODESIGN
Screwball 01-02
SIZE DWG. NO.
A
REV.
SCALE:1:1
WEIGHT:
SHEET 1 OF 1

6. Manufacturing Plan

6.1 Figures of Merit

FOM's were developed to help the team select manufacturing processes.

1. *Material Cost and Availability:* Materials that are difficult to obtain could increases construction time. Consideration was given more to materials that were readily available for purchase and relatively inexpensive.
2. *Required Level of Workmanship*: Many methods can be used to create the same component for the aircraft. Some methods, although better, require a high level of experience. Table 6.1 lists the team's skill with certain materials and methods. Although the team opted to use more common methods of construction, the option of using advanced manufacturing methods was frequently discussed. If use of an advanced method for a part was considered necessary, the more experienced members carried out the task.
3. *Repeatability and Crash-worthiness*: The idea of being able to create a part easily and quickly became an important factor for the manufacturing plan. Should a part fail during flight testing due to a crash or other reasons, the ability to make a new one or repair the damaged component was an essential element in choosing a manufacturing process. For this FOM, the key factor was to reduce the amount of downtime between flight tests.

6.2 Analytic Methods Used to Select Final Set of Manufacturing Processes

The amount of time needed to build the part was deemed crucial by the team. New processes cause longer build times, and there was often no guarantee that the part would come out right the first time. Thus, the team decided to use familiar methods of construction for complicated components such as the wing and fuselage. Cutting the amount of time required for building parts also allowed more time for flight testing. Instead of directly estimating build-time, those processes with the least manufacturing steps were favored. This is closely relates to part count as well. If a match existed in the skills matrix for the simplest process, it was selected. If not, the second preferred process was chosen.

6.3 Processes Selected for Major Component Manufacture

For the following components, a summary of the manufacturing processes used for construction, as well as any alternatives investigated, is included.

1. *Motor Mount*: Unidirectional carbon tape wrapped around the balsa/hardwood armature, formed the motor mount. The team also discussed using aluminum exclusively; this method would require a high level of workmanship, and was therefore not used for this sub component.
2. *Fuselage Plank*: The plank, located on the bottom of the fuselage, was constructed from carbon skins over a half inch Nomex honeycomb core. This part is featureless flat-stock except for simple balsa "rails" used for crush strength at hardpoints. The alternative would have been a

molded structural shell with structural bulkheads. The plank obviated the need for structural bulkheads and therefore simplified the build process.

3. *Fuselage Shell & Hatch*: The shell was shaped by hand from blue foam with templates for guidance. The foam was covered in MonoKote so a female mold could be laid up in fiberglass. A 2-ply carbon skin was laid-up in the mold. All details would be cut into the shell after it was fabbed. The hatch features 3 small hinges and a latch on the side for easy access to the payload. One alternative was considered. The blue foam master could have been used as a male mold, eliminating a step. However, this process was used last year, and the surface quality proved very poor.
4. *Wing and Empennage*: The wing was constructed by hot-wiring foam core sections using templates, then covering the foam with a layer of fiberglass. Carbon caps were added to carry bending loads. Separate structural tests on two-foot wing samples indicated that the caps alone would carry the bending loads and hence no "hard" spar webs were used. This eliminated a cutting step, web fab, and web installation. Instead, extra material was added to the leading edge section to provide shear continuity cap-to-cap. The foam provided core crush resistance. The pieces of foam and the spar caps where then put together, and vacuum bagged to finalize the wing. The empennage followed a similar construction to the wing. A dedicated spar web was a serious alternative since it was the lightest approach. However, reduced complexity and better surface finish argued for a spar-less wing. A Balsa built-up wing was eliminated by virtue of complexity.

6.4 Manufacturing Schedule

Figure 6.1 shows the manufacturing schedule, which details the build times for each component of the aircraft.

Table 6.1. Skill Matrix for ADT Workmanship rated on a scale from 1-5, with 5 defining a very high level of workmanship.

Member Name	Team Experience (Yrs)	Composite Workmanship	Machining Workmanship	Wood Workmanship
George Sechrist	5	5	5	5
Jerry Chen	4	5	5	5
Phillippe Kassouf	4	4	5	5
David Lazzara	4	3	5	5
Jacob Evert	5	5	5	5
Tim Bentley	3	3	5	5
Charles Heintz	4	4	5	5
George Cano	2	2	4	4
Stephane Gallet	2	3	4	4
Tyler Golightly	2	3	4	4
Jonathan Hartley	2	4	3	4
Tai Merzel	2	2	3	3
Brian Wetzel	2	1	3	3
Andres Figureroa	1	1	3	3
Billy Kaplan	1	1	3	3
Michael Mace	1	1	3	3
Cristina Nichitean	1	1	2	2
Doris Pease	1	1	2	2
Tim Schoen	1	1	3	3
Lester Kang	1	1	1	1

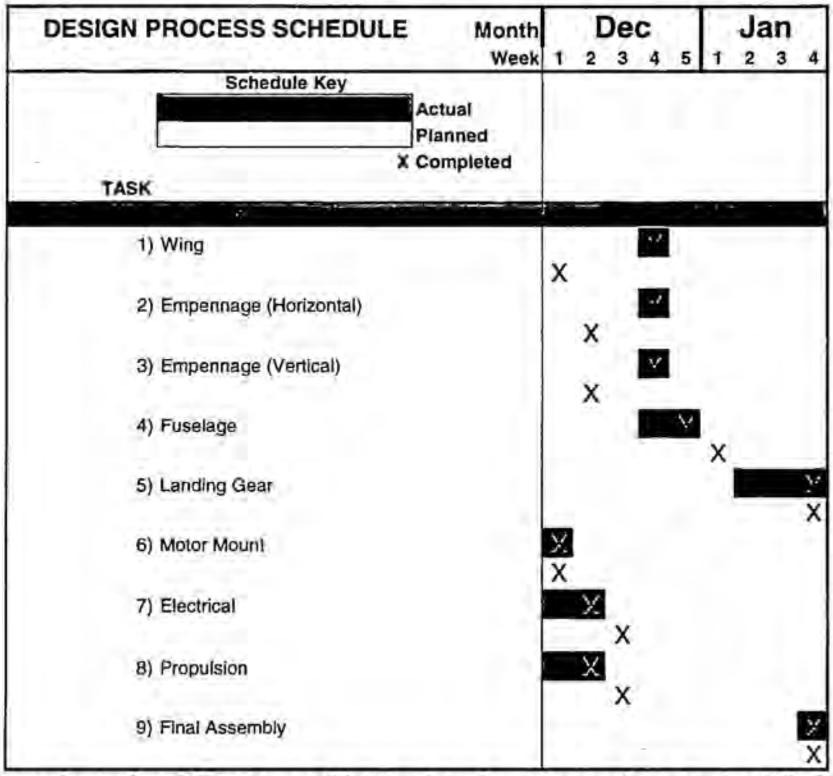

Figure 6.1. The Manufacturing Milestones Chart, showing planned and actual timing of construction events.

ρhastball

WEST VIRGINIA UNIVERSITY

April 26th – 28th, 2002

AIAA Cessna ONR – Student Design/Build/Fly Competition

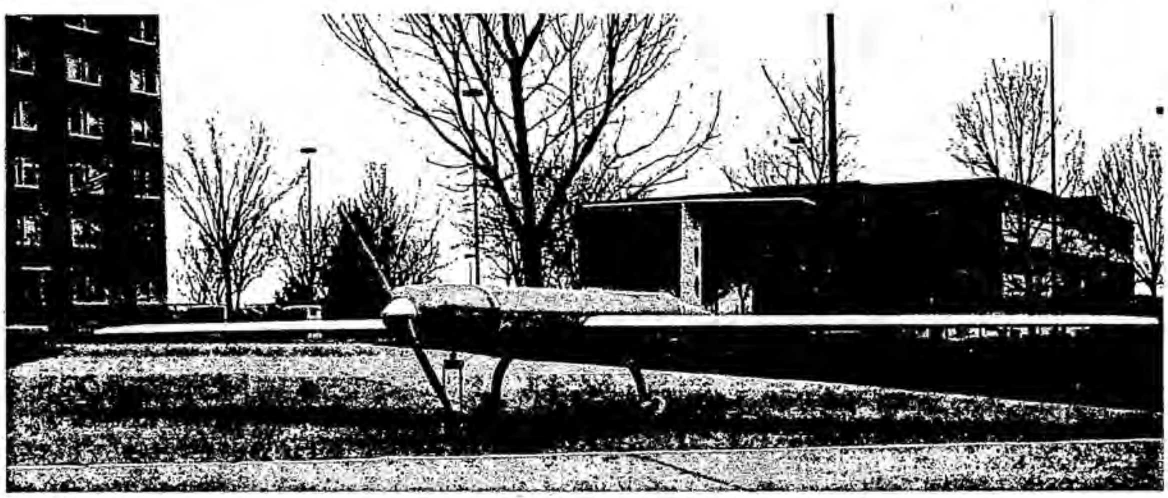

DEPARTMENT OF MECHANICAL AND AEROSPACE ENGINEERING

WEST VIRGINIA UNIVERSITY

MORGANTOWN, WV 26506

Table of Contents

1.0 Executive Summary

From the beginning of the design process, phastball was to be one of the most competitive planes that West Virginia University has ever built. Utilizing a combination of composite and traditional materials along with a focus on weight and flight performance, the plane is a razors edge balance of weight, strength, and performance. Newfound levels of construction detail have been incorporated into this year's entry, which is apparent when one notices the immaculate internal detail as well as the clean aerodynamic design and shape. From tip to tail, phastball promises to outperform the competition in all respects.

Upon consideration of this year's requirements, a streamlined design with low drag was going to be one of our greatest concerns in order to remain competitive. The balance of composite and traditional materials was considered carefully with respect to strength in target areas, weight in non-load bearing sections, and speed and ease of construction.

Based on the team members' previous knowledge of composite materials, the fuselage was constructed with composite materials, with structural reinforcement using traditional materials such as balsa wood and plywood. The wings are of a less exotic build, balsawood-sheeted foam, due to the inherent complexity that arises from attempting to produce exacting, complex wing geometries. With proper reinforcement, there is very little structural performance difference between the composite wings and the foam and balsawood wings. The fact that the wings do not require the time intensive process of making a mold means that they can be constructed in about one week.

The next consideration was the speed and flight performance of the aircraft. In order to reduce drag, the smallest possible fuselage cross-section was designed. There were as few sharp transitions in geometry as possible with the best utilization of internal space. All external surfaces were blended, with the purpose of reducing drag as much as possible.

The wing geometry is another facet of the design that greatly influences the performance. A triple break planform with slight dihedral and twist allows for an amazing combination of near elliptical lift distribution, high lift to drag ratio, and increased maneuverability.

Several tail geometries were considered, T-tail, V configuration and conventional tail. The decision to use the T-tail seemed natural due to the fact that it nearly eliminates the effects of downwash on the tail section.

Propulsion was debated down to two considerations. The first was a single motor, tractor configuration. The second was two motors mounted in the wing. Endurance, efficiency and low drag were the real deciding factors along with the added weight and point penalties for the extra motor. It was calculated that the single motor with proper prop choice could provide the needed thrust. This could be done without the added weight and loss of flight time due to the additional weight and battery drain created by the second motor. In addition, wing mounted motor nacelles add unwanted complexity and flow disturbance to the wing.

Another addition to the design was the use of flow-through air-cooling of internal components. Utilizing strategically placed air intakes, the motor and battery packs are cooled using forced air convection. Efficiency of both the batteries and motor are enhanced by lowering the temperature, which minimizes losses. Granted, there are some losses in the area of drag produced, but it is felt that the cooling effect outweighs the small drag increase.

To achieve this design several software packages were used in the design analysis. Programs were written in MATLAB and Maple to analyze to simulate the aircraft flight simulation. Additional programs such as Microsoft Excel, AutoCAD, ElectricCalc and MotoCalc were also used in the design phase of the project.

2.0 Management Summary

2.1 Architecture of the Design Team

Team phastball was comprised of three graduate students Kevin Ford, Michael Julius, and Edward Wen, two upperclassmen Jesse Ashby, Jason Gill and three underclassmen Jonathan Breckenridge, Peter Cooke, and Kuntal Vora. Peter Cooke, Edward Wen, and Kevin Ford have competed in the Design/Build/Fly competition in previous years. The three of them were in charge of organizing the team and organizing the different aspects of the design and construction process. The team met once a week to discuss the different aspects of the project and assigned individual work accordingly. For example, if the team were working on the wing, the work would be divided among those who were present. Some members would rough cut blocks of foam, others would cut templates, while others made skins to sheet the wings. This approach to the team architecture allowed everyone to work at their leisure depending on their individual schedules. Our goal with this approach was to have as many team members able to share any ideas they might have, fabricate any part, as it was needed, and to bring everyone's experience to the same level.

2.2 Assignment Areas and Management Summary

As described above, each team member was able to participate in every phase of the design and construction of the aircraft. There were however, three areas were experienced team members needed to take charge. Peter Cooke was the chief construction engineer, having over fourteen years of experience in constructing and flying RC aircraft. Kevin Ford was in charge of making purchases and getting materials and money donated to the team. Edward Wen was in charge of the design of the aerodynamics and the stability and control of the aircraft. Everyone on the team either had classes with each other or saw each other on a daily basis this kept the team members in close contact so ideas could be shared. Weekends proved to be the best time for everyone to meet to work for long periods of time. However, a lot of the work was done whenever the team members had free time. When team members had free time, they would get in contact with one another to work on the aircraft. Using this approach maximized the amount that was done by everyone. No one would be required to be at any certain place or time, which kept the project fresh for everyone. Table 2.1 is a summary of the project milestones' planned and actual start and finish dates. These dates were set so that each phase of the project (report and fly-off) would be finished by the dates set forth in the competition rules.

2.3 Personnel Goals and Accomplishments

Even though the majority of the work done on the aircraft was preformed by who was there at the time the team would like to acknowledge the members who went above and beyond on certain phases of the aircraft.

- Construction of the plug, mold, and fuselage – Pete and Kevin
- Landing gear and wheel pants - Jason and Jesse
- Booking reservations – Kuntal
- Design of the wing and stability and control analysis – Ed
- Fund raising – Jonathan and Mike

Table 2.1 Project Milestone Summary

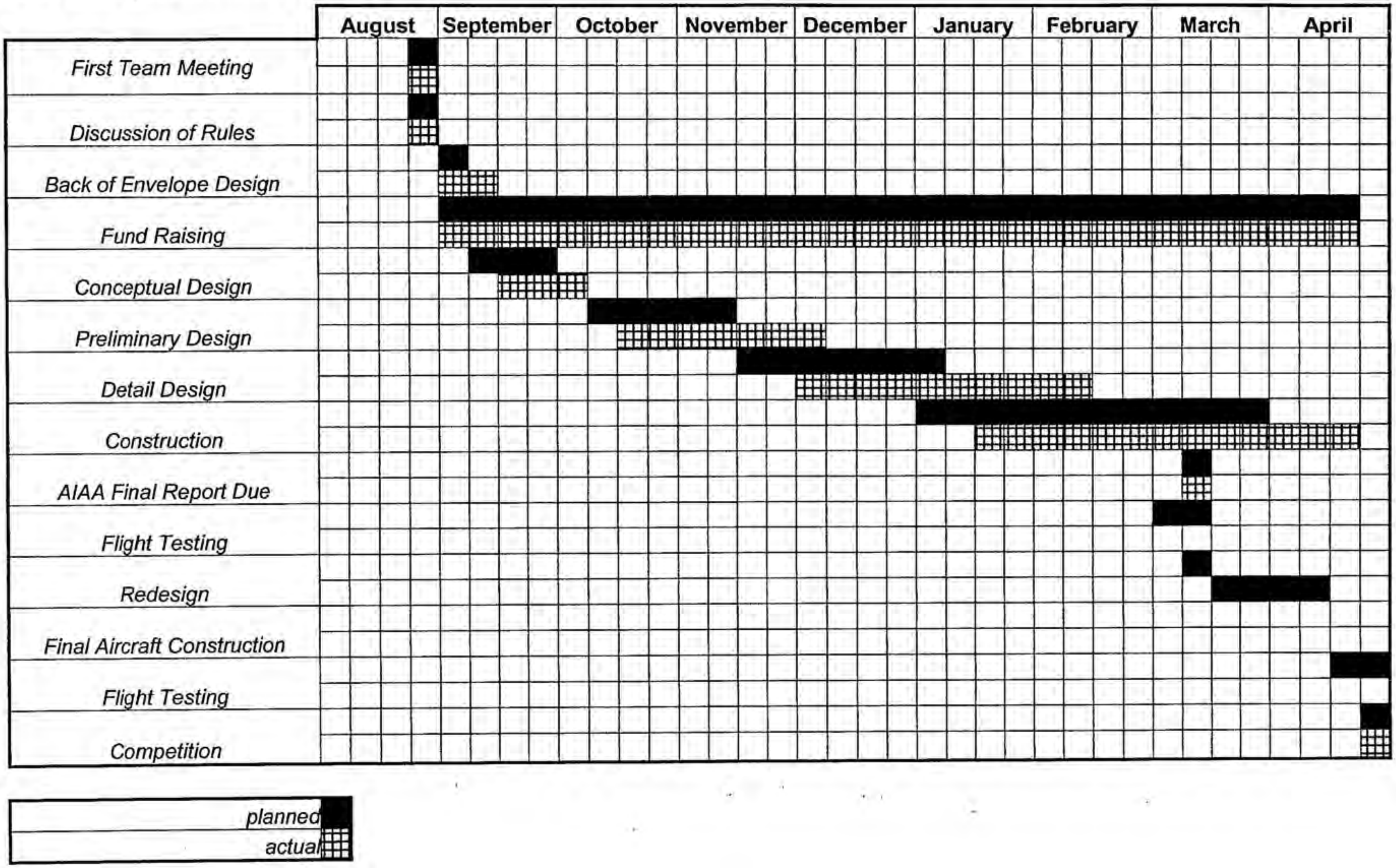

3.0 Conceptual Design

3.1 Discussion of Rules and Strategy

The mission profile of this year's competition was to design and construct an aircraft that can carry ten to twenty four softballs that can be easily removed and is able to fly without payload. The softballs must be a minimum of two directly abreast, having no staggered rows, and single height. Three different missions must be flown during the competition. During the first mission, "Position", the aircraft must fly two unloaded laps, complete a 360° turn in the direction opposite of the base, and final turns on the downwind leg of each lap. During the second mission, "Passenger Delivery", the aircraft must land and the ground grew must load the payload, take-off and fly two laps, completing the 360° turn as described above. During the third mission, "Return", the aircraft must land and the payload must be unloaded, the aircraft is then to fly two full laps of the course. For each mission the aircraft is required to take-off within 200ft. Figure 3.1 is a graphical representation of the mission profile. The following list highlights the competition rules:

- No payload may be carried internal to the wing proper
- Must be propeller driven and electric powered with an unmodified, over the counter model electric motor
- All motors must be from the Graupner or AstroFlight families of brushed electric motors
- Motors and batteries will be limited to a maximum of 40 Amp current draw
- Must use over the counter NiCad batteries
- Maximum battery pack weight is 5.0 lb
- Take-off gross weight with payload must be less than 55 lb

Based on the flight performance of the aircraft the single flight score is calculated using the following formula:

$$Single\ \ Flight\ \ Score = \frac{total\,\#\,laps\ \ flown\ +\ \#\,balls\ \ carried}{total\ \ mission\ \ time} \qquad (3.1)$$

The best three of five flights are then added together to achieve the total flight score. This is then entered into the following equation to determine the team score:

$$SCORE = \frac{written\ \ report\ \ score\ *\ total\ \ flight\ \ score}{rated\ \ aircraft\ \ \cos t} \qquad (3.2)$$

The rated aircraft cost, RAC, is penalty imposed on each team based on the simplicity of the aircraft. The RAC takes into account the number and size of the wings, tail, motors, batteries, servos, weight of the aircraft. Initial optimization of the aircraft was based on these rules and scoring methods.

3.2 Design Parameters Investigated

The team began the design of the 2002 entry by examining what worked for past WVU teams, other schools, as well as some new ideas, which were proposed by current members. Since several team members have been involved with this project for a long time and others have a great interest in RC aircraft a lot of time was saved on the simple principle that we have seen it work or we have seen it fail.

During the "back of the envelope" design phase, team members discussed the rules and everyone suggested their initial ideas to each other. From these discussions, three prominent aircraft configurations emerged. These ideas were further discussed and a consensus was formed that the following parameters were most import in the design of the aircraft: wing planform, tail configuration, payload and fuselage configuration, power plant, and landing gear. These parameters were then looked at based on their Figure of Merit, FOM. Using this approach early in the design stage allowed the team to quickly dismiss ideas that were either to difficult to construct or that the team felt would just not work. Table 3.1 Is the FOM breakdown of the individual design parameters.

3.3 Figures of Merit Breakdown

In the conceptual design stage, several generic baseline aircraft configurations were considered for further development. These configurations consisted of different wing planforms, tail configurations, payload size, and landing gear configurations. The number of each particular component was then evaluated based upon a set of Figures of Merit determined by the team, according to how the different numbers of each component would affect various aspects of the aircraft performance and RAC. If the number of components was favorable to a particular design variable, a value of 3 was assigned to that number of components. If the number of components was unfavorable, a value of 1 was assigned. If the number of components had a negligible effect on the design parameter, a 2 was assigned, the number 0 was assigned if it did not pertain to the parameter. The number of motors, wings, etc. with the highest FOM sum was selected for further evaluation.

Ease of construction

The competition requires each team to design, construct, and fly their aircraft. Approximately one school year was allotted for the team to complete everything. A weight multiplier of 3 was given to the construction of each component. The quicker the team could manufacture each component the more time could be spent optimizing and testing it.

Strength to Weight Ratio

Lowering the weight of the aircraft allows it to fly faster, carry more payload, and have a lower RAC. Each component of the aircraft must be built as light as possible yet withstand the loads that occur during the flight missions. Therefore, a weight multiplier of 2 was given to this category.

Handling

Due to the nature of the mission profile flight and ground handling qualities of the aircraft were discussed. During the "Position" and "Passenger Delivery" missions the aircraft must complete a 360o turn on each leg of the flight. Ground handling qualities of arise when the aircraft must taxi back to the starting line to begin the next mission.

Ease of Changing Payload

The total mission time is comprised of the time it takes the aircraft to navigate the course and the time it takes the ground crew to load and unload the payload. Different configurations of wing vertical placement, motor location, and tail type can affect the amount of time that is spent on the ground.

Rated Aircraft Cost

Different configurations and sizes of the aircraft components not only affect the flight characteristics of the aircraft the also affect the rated aircraft cost, RAC. Here the team examined how each component's parameters affected the RAC. The RAC is further discussed in section 3.6.

Cost

The cost of batteries, motors, servos, and other materials was a big concern for the team. Materials such as composites and epoxies were able to be purchased at a discount our received through donation. Other components such as batteries and motor needed to be purchased. Here the team looked at the components from previous year's aircraft that could be used over again and tried to minimize the amount of new components needed to be purchased

3.4 Figure of Merit Selection Process

3.4.1 Wing Planform

Elliptical (rejected)

Construction of an elliptical wing is too difficult. Cutting a foam core to shape could not be done. It therefore would have been shaped by hand and was deemed to difficult to construct.

Tapered (adopted)

A tapered wing is fairly easy to construct and has produced good results on past aircraft. It was therefore kept for further analysis.

Multi-break (adopted)

Multi-break planforms give similar characteristics to elliptical wings but are much easier to construct. The construction method is very similar to that of a tapered wing.

3.4.2 Wing Location

High (rejected)

The main benefit of a high wing is that it allows the fuselage to be placed lower to the ground and it has the lowest drag interference. After observing last year's competition, it was decided that the easiest access to the payload would be to load and unload from the top of the fuselage. A high wing was rejected since it would hinder the removable of the top half of the fuselage.

Mid (adopted)

Using a mid wing would give the advantage of tying the carry through spar structure in with the landing gear support and would also act as bulkhead in the fuselage. The team highly favored this approach due to its success on the 1997-1998 WVU entry.

Low (adopted)

Blending a low wing with the fuselage seemed like it would add to construction and frontal area. However, the low wing was kept since the final payload loading and unloading process was not yet decided.

Biplane (rejected)

Using a biplane would drastically raise the RAC and aircraft drag. Since there was no constraint on wingspan it was quickly rejected by the team.

3.4.3 Tail Configuration

Conventional (adopted)

The conventional tail is probably the simplest to construct and attach pushrods to servos. It is lighter than a T-tail since the vertical tail does not need to support the horizontal tail. However, the horizontal tail is in the wing wake and prop wash. Steering can be controlled with the same servo as the rudder and the elevator servo can be used to control the brakes.

V-tail (rejected)

The advantage of using a V-tail is reduced interference drag. The disadvantage is that the desirable handling qualities are not as stable as a T-tail or conventional tail. Using a V-tail would also raise the RAC by requiring another servo to control steering.

T-Tail (adopted)

The advantages of a T-tail are that the horizontal tail is lifted out of the wing wake and prop wash and that the vertical tail can be smaller due to end-plate effects. As with the conventional tail steering can be controlled with the same servo as the rudder and the elevator servo can be used to control the brakes.

Canard (rejected)

Canards are difficult to design so that they provide sufficient stability. More servos would have been required to control the aircraft raising the RAC. The team also felt that constructing a canard would add to the complexity of the aircraft and to the time spent constructing it.

3.4.5 Landing Gear

Tricycle (adopted) vs. Tail Dragger (rejected)

The payload can only be changed once the aircraft is at the starting line. Thus stable ground handling was important when selecting the landing gear. Since the location of the c.g. is behind the main gear an aircraft with a tail dragger configuration will tighten in a ground loop, resulting in poor ground handling qualities. Due to instability the tail dragger landing gear was rejected, tricycle landing gear does not have this problem. Stopping the aircraft once it reaches the starting line is also crucial. On a tail dragger, the brakes on the main gear would cause the aircraft to tip forward hitting the prop on the ground. With tricycle, gear the nose wheel prevents the aircraft from tipping forward.

3.4.6 Motors

One Motor (adopted) vs. Two Motors (rejected)

Several things factored into the selection of using only one motor. It was felt that AstroFlight had single motors capable of producing the required power. Second, the RAC with a second motor is much greater than that of just one motor.

3.5 Material Selection and Construction Techniques

The main goal in constructing any aircraft is to make each component as strong as needed and light as possible. Additionally, the team members had to take into account the required skill, cost, and time to construct the aircraft using different construction techniques. This posed several problems. The team member's experience was varied. Because of this limitation, special "classes" were set up by the senior team members to increase everyone's knowledge in different construction techniques. Time was also a limitation. Each member was taking a full course load, so construction time was limited. The team discussed typical UAV construction techniques in an attempt to determine the appropriate method needed to construct each component. Balsa wood, foam build-up, and composite material construction were investigated for each component.

3.5.1 Balsa Wood

One of the cheaper methods investigated, balsa wood construction is typically used to fabricate kit radio-controlled aircraft. This method consists of cutting ribs, spars, and stringers individually, and then assembling them to construct the wing, tail, or fuselage. However, as was learned with previous entries, this method is tedious and time consuming. However, this method was not completely ruled out since some components require minimal strength. Several members had previous experience working on a previous entry that used a balsa wing and ruled out the use of that type of wing due to the difficulties mentioned above.

3.5.2 Foam Build-up

The cheapest and easiest construction method is foam build-up method. This method has typically been used to construct UAV aircraft wings and consists of making templates of the desired airfoil shape and then using a hot-wire to cut the component out of a block of foam. A surface such as a thin layer of balsa wood or fiberglass is then applied. Previous WVU entries successfully used this method to build the wings. Balsa wood or spruce spars can easily be added to increase the strength of this type of wing. Foam build-up was also discussed for construction of the tail.

3.5.3 Composite Materials

Last year's team used composite materials for the construction of the wing. This was a laborious process that had several drawbacks. First, the time spent during construction was for one wing. If the team discovered a flaw in the wing design the time spent constructing the plug and mold would have been wasted. Second, the weight of last year's wings was much greater than predicted. Lightweight composite materials such as 1k carbon fiber are expensive. Due to these reasons the team felt that constructing the wing out of composites was not the way to go. Since the fuselage needs to basically be a hollow shell to house the payload, propulsion system, and avionics composite materials were highly discussed as a method to construct the fuselage. Repeatability is another advantage of composites. Once the required mold has been constructed, it can be used several times to produce identical parts. Previous WVU entries have also utilized composite materials for the construction of the landing gear. The 1997-1998 entry used a simple mold for the hand lay-up and vacuum bagging process. This proved to be a quick method to construct the landing gear.

3.6 Discussion of Rated Aircraft Cost

The rated aircraft cost can basically be described as the simplicity of the aircraft. It is a way for the competition to reward a team who can design an aircraft to perform the same goal with either a smaller or lighter aircraft, an aircraft with less batteries, an aircraft with a smaller wing area, etc.

3.6.1 Breakdown of the Rated Aircraft Cost

The overall rated aircraft cost (RAC) is calculated by the equation:

$$RAC,(\$thousands) = \frac{A \cdot MEW + B \cdot REP + C \cdot MFHR}{1000} \quad (3.3)$$

In the above equation, A, B, and C represent values of multipliers used to convert aircraft characteristics into manufacturing hours. The Manufacturer's Empty Weight Multiplier (MEW), Rated Engine Power (REP), and the Manufacturing Man Hours (MFHR) are a breakdown of the different aircraft components to be converted to man-hours. A more detailed explanation of these parameters is described below.

3.6.2 Manufacturer's Empty Weight Multiplier

The manufacturer's empty weight multiplier, MEW, is comprised of the weight of the aircraft without payload. In equation 3.3 A represents the manufacturer's empty weight multiplier and was given a value of $100/lb.

3.6.3 Rated Engine Power

The rated engine power, REP, was calculated using the following equation:

$$REP = battery \quad weight(1 + 0.25 * \#motors) \quad (3.4)$$

In equation 3.3 B represents the rated engine power multiplier and was given a value of $1500.

3.6.4 Manufacturing Man Hours

The manufacturing man hours, MFHR, further breaks down the components of the aircraft into the work breakdown structure, (WBS), and takes into account the number of wings and their size, the number of fuselages/pods, and their size, the number of horizontal and vertical surfaces, the number of servos used, and the number of motors and propellers used. In equation, 3.3 C represents the manufacturing cost multiplier and was assigned a value of $20/hr.

3.6.5 WBS 1.0 Wing

The rules state that 8hrs/ft of wing span, 8hrs/ft of max exposed wing chord, and 3hrs per control surface are to be used in the calculation of WBS 1.0.

3.6.6 WBS 2.0 Fuselage

WBS 2.0 consists of the length of the fuselage. 10hr/ft are used to calculate WBS 2.0.

3.6.7 WBS 3.0 Empenage

WBS 3.0 is the number of vertical and horizontal surfaces. For any vertical surface (winglets, struts, end plates, etc.) a penalty of 5hr per surface is to be assessed. For any vertical surface with an active control 10hr per surface is assessed. Any horizontal surface that is less than 25% of the span of the greatest span is assessed 10hr per surface.

3.6.8 WBS 4.0 Flight System

WBS 4.0 is the number of servos and controllers used on the aircraft. 5hrs was assigned per servo or controller.

3.6.9 WBS 5.0 Propulsion System

WBS 5.0 is the number of motors and propellers or fans used on the aircraft. 5hrs per motor, propeller, and fan was assigned.

3.7 Features that Produced the Final Configuration

Several questions had to be answered before the final configuration of the aircraft was decided upon. First, do we think this will work and can we construct it? Answers to this question were very valuable since several of the team members are RC aircraft builders and pilots. How does this affect the RAC was also asked. As described above adding another servo or changing the aspect ratio of the wing greatly affects the RAC. Lastly, the key design parameters described in section 3.2 and the FOMs described in section 3.3 produced the final configuration. Below is an outline of the final configuration:

- Mono wing either tapered or multi-break planform
- Single fuselage
- Single motor
- Conventional or T-tail depending on wing location
- Tricycle landing gear with breaks
- Mid or low wing depending on how payload is loaded - unloaded

Table 3.1 Figure of Merit breakdown of design parameters

level of importance: 3 favorable, 2 neutral, 1 unfavorable, 0 does not pertain		Ease of construction (x3)	Strength to Weight Ratio (x2)	Flight and Ground Handling (x1)	Ease of Changing Payload (1x)	RAC (x2)	Cost (x1)	Total FOM	Adopt (A) or Reject (R)
Wing Planform	Elliptical	1	2	3	2	3	3	21	R
	Tapered	*3*	*2*	*3*	*2*	*3*	*3*	27	*A*
	Multi-break	*3*	*2*	*3*	*2*	*3*	*3*	27	*A*
Wing Location in Fuselage	High	1	3	2	1	2	2	18	R
	Mid	*3*	*2*	*2*	*3*	*2*	*2*	24	*A*
	Low	*1*	*3*	*2*	*3*	*2*	*2*	20	*A*
	Bi-plane	0	1	3	1	1	1	9	R
Tail Configuration	*Conventional*	*3*	*2*	*3*	*0*	*3*	*0*	22	*A*
	V-Tail	2	2	3	0	1	0	15	R
	T-Tail	*3*	*1*	*3*	*0*	*3*	*0*	20	*A*
	Canard	1	2	1	0	1	0	10	R
Landing Gear	*Tricycle*	*3*	*2*	*3*	*0*	*0*	*0*	*16*	*A*
	Tail Dragger	3	2	1	0	0	0	14	R
Motors	*One motor*	*3*	*0*	*2*	*2*	*3*	*3*	22	*A*
	Two motors	2	0	2	1	1	1	12	R

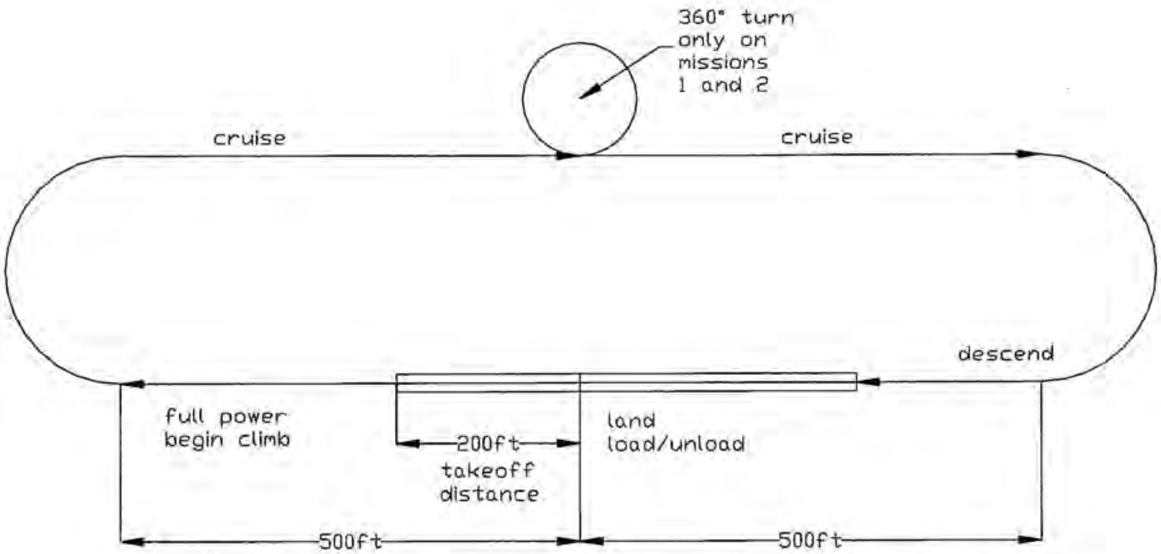

Figure 3.1 Mission Profile

4.0 Preliminary Design

4.1 Figures of Merit (FOM)

The "First Order FOM" that had the greatest impact on the overall score was identified by varying the parameters within the scoring formulas. They were as follows:

- Payload Capability
- Motor Power
- Battery Endurance
- Top Speed
- Battery Weight

The "Second Order FOM" which made a lesser impact to the overall score but were also viewed as important were the following:

- Fuselage cross-section and length
- Wingspan and maximum chord
- Empty weight

4.2 Baseline Configuration

The most important design parameter of the aircraft was payload. The number of balls was the starting point that allowed optimization of the other variables. To capture the effect of payload variation from 10 to 24 balls, three aircraft were examined and optimized to determine what area of payload range maximized the total score. These aircraft were 10, 18 and 24 balls with the 24 ball aircraft used as the baseline.

4.3 Assumptions

Based on the team's experience and judgment, a low drag baseline aircraft was chosen such that design trade studies could be performed. A high aspect ratio (10 or greater), mid-fuselage wing to provide a combination of low parasite drag at high speeds, low induced drag in the high G turns and easy access to the payload. Using 24 balls and a 5-lb. battery pack, the maximum gross weight (MGW) was estimated to be 24-lbs. and maximum empty weight (MEW) at 14 lbs. The entire mission was estimated to be completed in 5-5.5 minutes with motor run time of 4-4.5 minutes.

4.4 Simulation Program

To quantify the FOM #1, a simulation program was written in MATLAB to analyze the overall effects of the design parameters on the flight times and final scores. This program stepped the aircraft through a time increment till the mission phase was completed. The results were checked with the exact solution of the distance-time-velocity integral using the symbolic manipulator MAPLE. The results from MAPLE showed that 0.1-sec increment was reasonably accurate.

4.5 Propulsion System

Because of other projects in the WVU wind tunnel, testing of motor/battery/thrust combinations was not possible. In addition, thrust data from the 97/98 competition used brushless motors and so the team relied on ElectricCalc and MotoCalc as a virtual engine test stand. Previous competition results showed that these programs were usually optimistic in their prediction of thrust and battery duration and so a knock down factor of 0.90 was used to determine thrust as a function of velocity.

4.5.1 Motor Selection

Using data from previous competition's winning aircraft, power loading of 50 watts/lb. was used to determine the approximate motor size. The estimated weight of the aircraft was 24 lbs., which showed the AstroFlight 661 and 691 fitting the requirements. Both of these motors had a maximum continuous current capability of 35 amps and maximum voltage equivalent to 40 cells. Graupner motors were not considered because the larger size motors were only available through overseas purchase and the team already possessed AstroFlight speed controllers.

4.5.2 Battery Selection

For the past few years of this competition, the 2400-mah cells have been most popular because of their high capacity density (Table 4.1) and low internal resistances. Some 1400 and 1700 mah cells also have high energy density (mah/oz) but also higher internal resistance. In the event that the maximum weight of batteries would not be needed for the mission, alternative cell/pack combinations were examined to see if they could provide sufficient power by increasing voltage and decreasing capacity as shown in Table 4.1.

Cell zapping is used for high current (60A) electric RC competitions like the F5B. At the current levels in this competition (max 40A), the manufacturer showed 8% increase in voltage over unzapped cells. Zapped cells would be preferred but would depend on the team's ability to raise funds.

4.5.3 Propeller Selection

To provide the highest thrust at high speed and efficiency, the natural choice is for the pitch to diameter ratio (P/D) to be 1.0. P/D values higher or lower than 1.0 show a drop in efficiency as confirmed by several iterations performed with ElectricCalc and MotoCalc. For brevity, only P/D of 1.0 results are shown here.

4.5.4 Motor/Prop Combinations

Figure 4.1 shows some of the best motor/prop combinations using 36 x RC-2400 cells running approximately 4.5 minutes. The 691 and 661 motors were available in direct drive (DD) or geared (G) configuration. Currently, only the 2.75:1 gearbox is available commercially and no custom gearboxes or ratios for older gearboxes were considered in this trade study. The 641 motor was examined but could not produce sufficient power without increasing the number of motors and propulsion RAC.

Surprisingly, direct drive combinations would not produce more thrust than the best geared combinations unless the velocity was higher than ~120 ft/sec. However, the highest aircraft speed was estimated to be no more than ~120 ft/sec. Furthermore, both direct drive combinations were operating at the continuous current limit of 35A. At this amperage, serious heating problems could occur. Although the 691G (22 x 22) had the largest torque output available in the AstroFlight family of motors, the 661G with the correct propeller (18 x 18) could provide slightly more power to the propeller for the 4.5 run time. For speeds higher than ~85 ft/sec, the 661G combination provided more thrust than the 691G. The weight and integration of the large propellers into the airplane also favored the 661G. These factors are shown in Table 4.2 and led to the final decision to use the 661G with 18 x 18 prop.

4.6 Fuselage

4.6.1 Fuselage Shape

The fuselage had the competing requirements of short length, low drag and high payload capability. Three fuselage shapes were considered based on three different softball-packing configurations in Figure 4.2. Using the drag estimation techniques from [Anderson, Hoerner] the drag was estimated. In Table 4.3, the ranking shows that 2x12 is the best overall design. Length was not included as a FOM because tail moment arm drives the fuselage length requirements.

4.6.2 Fuselage Cross Section

A full-length fairing was incorporated into the fuselage cross-section to house the batteries. These batteries could be moved forward or aft as necessary to adjust CG position. (See Figure 4.3)

4.7 Wing

4.7.1 Airfoil

In the 97/98 competition, some notable aircraft reached speeds of 70 to 80 mph (100-117 ft/sec). With the motor and payload restrictions this year, it appeared reasonable to set 70 mph as an attainable top speed in the Position and Return mission segments. The heavy emphasis on speed drove the team to consider low to moderately cambered airfoils providing low drag at the predicted lift coefficient of 0.15-0.25 yet reasonably high Clmax of 1.1 or greater. The only airfoils considered were from the UIUC wind tunnel database and the top picks were the MH32, S7012, SD7003, RG-15, and E387. In general the drag polar (Figure 4.4) shows that these airfoils were optimized to perform at different lift coefficients. The lift polar shows that all the selected airfoils provide at least 1.1 Clmax. Although the SD7003 had the lowest drag in the target Cl, the stall behavior appeared very sharp in comparison to the other airfoils. The next lowest drag nearest the target Cl was S7012. Since it had a wider drag bucket and gentler stall characteristics, the S7012 was chosen as the baseline airfoil.

4.7.2 Aspect Ratio and Wingspan

High aspect ratio wings (10 or higher) provide lower induced drag but many issues pointed to the benefits of reducing aspect ratio. First, the RAC penalizes longer vs. shorter wingspans. Next, with very high aspect ratios, wing chords become smaller, reducing Reynolds number and increasing parasite drag. Finally, a thinner narrower wing is structurally less efficient. To help find the optimum wing configuration, the aspect ratio was varied in the simulation program. Figure 4.5 shows that the mission time did not vary strongly with aspect ratio despite the large increase of drag in the turns as a percent of the total drag (Figure 4.6, 4.7). The main driver on wingspan was sizing the tail span since it could only be 25% of the wingspan (see tail section). An aspect ratio of 8 was chosen to allow for reasonable tail span and the literature shows ARs 7 to 9 to be the best compromise.

4.7.3 Wing Area

Historical data showed that a wing loading limit of 50 oz/ft^2 could be used with a high lift device to allow slower landing speeds. Based on the initial weight estimate with payload of 24 lbs., a wing area of 8 ft^2 was used which resulted in a span of 8 ft using an AR = 8. This wing area allows the aircraft to just meet the takeoff field length limit with 196 ft in the Passenger configuration and 59 ft in the Position configuration with no headwind. Since strong headwinds are likely at the competition, it is probable that the takeoff field length, TOFL, requirement will be met.

4.8 Empennage

4.8.1 Horizontal Tail

From [Raymer] horizontal tail volume coefficients in the range of 0.5 to 0.8 and AR of 3 to 5 were desirable for this similar type aircraft. The long fuselage puts payload far from the CG so initially a volume of 0.80 was considered appropriate. The tail span had to be 25% or less of wingspan or else it would be considered a wing under the RAC. The impact on the RAC to add a second wing was very high and therefore a lower aspect tail or lower tail volume was considered. An AR of 2 tail was deemed as to provide too much drag and too difficult to integrate into the vertical tail, therefore the tail volume and AR were reduced to the low range of 0.5 and 3.

4.8.2 Vertical Tail

Typical values for vertical tail volume are between 0.03 and 0.08. Since the T-tail adds an endplate effect to the vertical, extra margin was believed to be available in this configuration. Integration of the vertical to the horizontal tail set the chord and taper ratio requirements. A tail volume of 0.04 was used.

4.9 Flight Profile

The planned course for the pilot to fly was designed to keep total time down and to be at a safe altitude of 30 feet in the event of an emergency maneuver. After takeoff, a pilot flies a slow climb out to 30 feet by the time the plane reaches the first turn. All turns are executed at the same bank angle for simplicity of simulation. When the plane is directly across the field from the pilot, the 360° turn is initiated. To slow the plane down for landing, the engine is shutoff at the end of the downwind leg to bleed off speed in the base turn and final approach. Moving the 360° turn to the end of the straightaway is one possibility to reduce speed even more but was not used in the Preliminary Design.

4.10 Turn Optimization

The simulation program showed that the tighter the turns, the lower the flying time. The limitation on turns then became Clmax and structural capability. Using the characteristics of the aircraft in the Position configuration and allowing 90% of CLmax, the maximum turn G was approximately 6Gs (80°-bank angle). For the Passenger Delivery configuration, the maximum turn G is approximately 3Gs (70°-bank angle) (Figure 4.8). If the G limits were exceeded, a stall would occur in the first turn when speed has not been built up and the CL requirement is high for both Passenger and Position mission segments. Lowering the flaps was a possibility in the turns but not evaluated in the preliminary design. Considering the maximum structural bending stress capability of the wings, the planned maximum G capability of the aircraft was set at 4Gs in the full payload configuration to provide a safety margin of 1.33.

4.11 Results of Aircraft Optimization

After several iterations with the simulation program, the second most important variable next to the number of balls was the weight of the battery pack. Figure 4.9 shows pack combinations that result in run time from 2.5 to 4.5 minutes and weights from 2.4 to 5 lbs. Using the individual trade study results for motor/prop, wing, fuselage, and battery cell type, ten study aircraft were put into the simulation program to evaluate Overall Score performance. (Figure 4.10) The Total Mission Time only varied from 4.3 to 4.9 minutes for all the aircraft studied and was not a strong driver for the Overall Score. In other words, extra speed from being smaller and lighter (10 balls) was good, but not good enough to overcome the fewer balls carried, even if the battery was very small.

An intermediate sized plane (18 balls) could be competitive but it would have to be very, very stingy on energy usage. The score of 153 (shown in dashed lines) with the 40 cell 1100-mah pack is pushing the pack to 100% usage and risking the 3-minute penalty for incomplete laps. In no case could it be shown to be advantageous to receive this penalty. The next best 18-ball configuration had a score of 143.

The aircraft with 24 balls provided much more flexibility. Configured with 40-cell 1400-mah pack, it would receive the highest score and also be pushing the pack limits, but this time only to 90% of capacity. A more conservative approach would be to use the 40 cell 1700 mah pack which would receive the same score as the best 18 ball aircraft while still having the option to improve upon that score.

4.12 Preliminary Design Summary

After trade studies on the motor/prop, cell type/pack size, wing/fuselage characteristics, flight profile, the major features of the aircraft based on the "First Order Drivers" were the following:

- Maximum payload for best scoring and propulsion flexibility (24 balls)
- Highest Thrust on expected speed range (661G motor, 18 x 18 prop)
- Maximum cell count available for motor for maximum power (40 cells)
- Cell capacity adjusted for mission duration and to reduce battery pack wt. (approx. 1700 mah)

The "Second Order Drivers", which affected the FOM but to a lesser extent, were:

- 2 x 12-ball fuselage for reduced drag, adequate tail arms.
- High G capable wing to reduce overall course length (approx. 4G)
- Sufficient wingspan to allow H-tail sizing (AR=8)

Table 4.1 Cell and Pack Characteristics for candidate battery cells

	Cell Characteristics					Pack Characteristics		
Cell Name	Capacity [Mah]	Wt/Cell [oz]	Int. Res. [Mohm]	Mah/oz	Mah/oz /Mohm	Max # Cell by Wt or Volt.	Pack Wt [oz]	Pack Energy [ft-lbs]
KR-1100AEL	1100	0.95	10.5	1,158	110	40	38.0	142,560
KR-1400AE	1400	1.05	11.5	1,333	116	40	42.0	181,440
CP-1700	1700	1.62	5.5	1,049	191	40	64.8	220,320
KR-1700AE	1700	1.48	8.5	1,149	135	40	59.2	220,320
RC-2000	2000	1.98	7	1,010	144	39	78.0	255,273
RC-2400	2355	2.15	4.9	1,095	224	36	78.0	276,817
CP-2400	2355	2.15	4.5	1,095	243	36	78.0	276,817

Table 4.2 FOM for motor/prop selection

Motor	Prop	Thrust	Heating	Prop Integration	Weight	Total
691G	22 x 22	3	3	1	1	8
661G	*18 x 18*	*3*	*3*	*2*	*2*	*10*
691DD	14 x 14	1	1	3	2	7
661G	12 x 12	1	1	3	3	8

Table 4.3 FOM for selection of payload configuration

Balls	Drag	Ease of Construction	Flexibility to Change	Total
2 x 12	2	3	3	8
3 x 8	1	3	3	7
2 x 12, 60% laminar	3	1	1	5

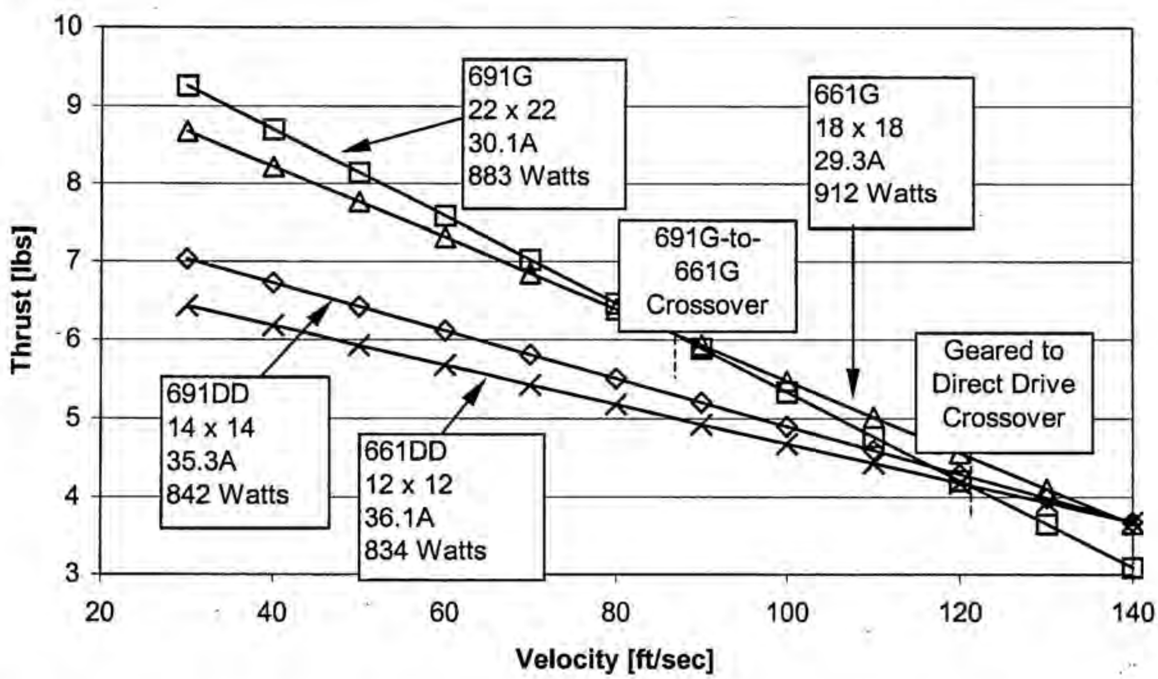

Figure 4.1 Best Motor/Prop combinations on 36 x RC-2400 with 4.5 minute duration

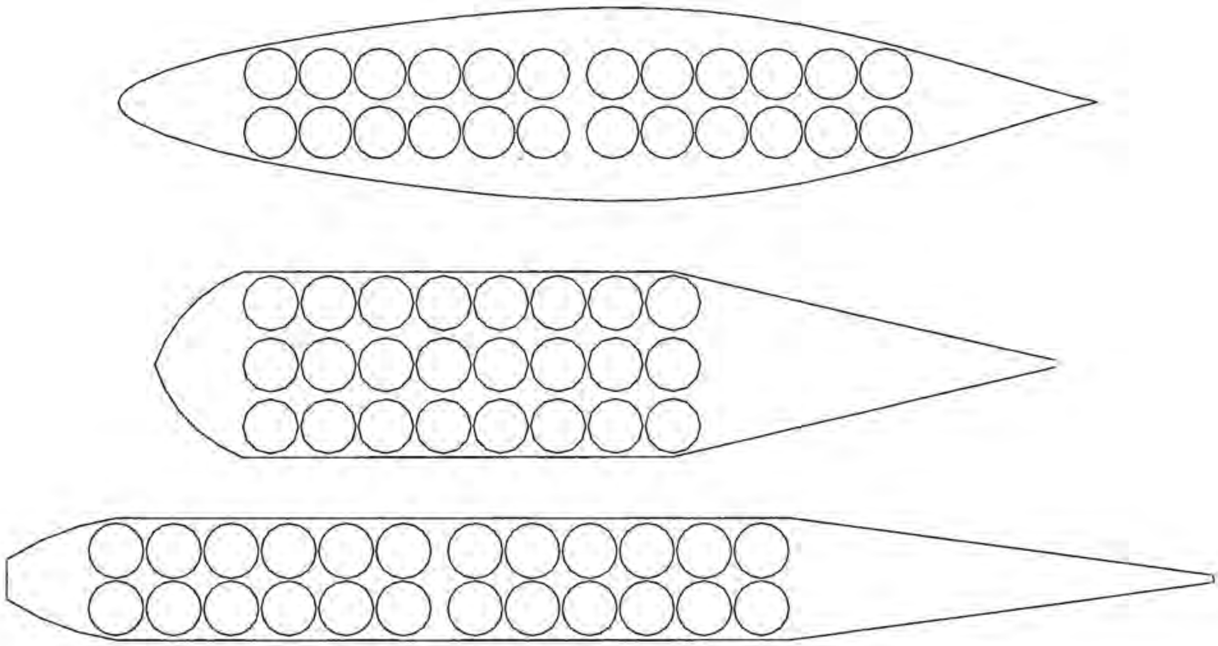

Figure 4.2 Fuselage payload configurations, 2 x 12 60% laminar, 3 x 8, and 2 x 12

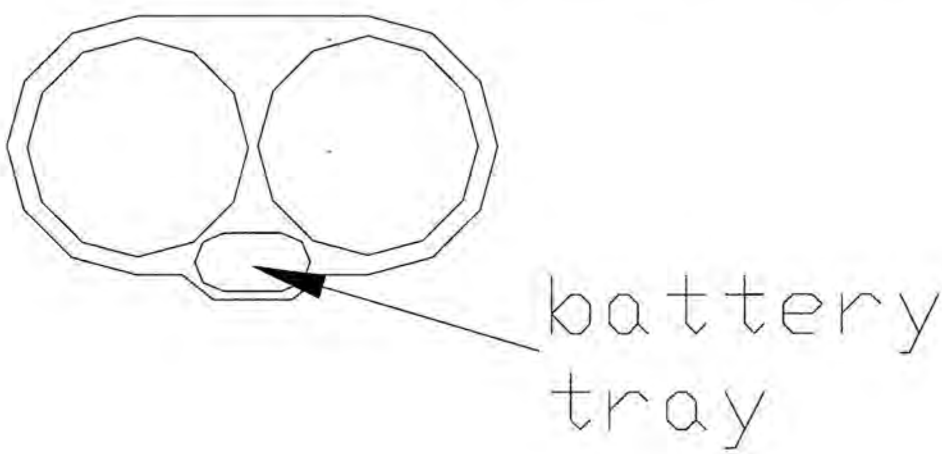

Figure 4.3 Fuselage cross-section showing adjustment of CG by moving battery pack

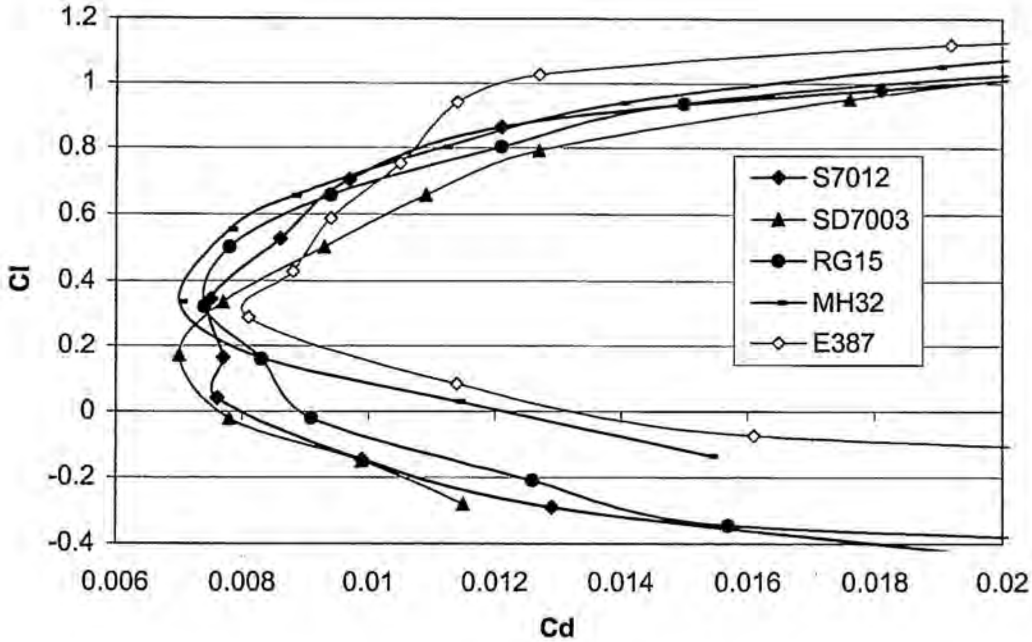

Figure 4.4 Airfoil comparison at Re = 300K

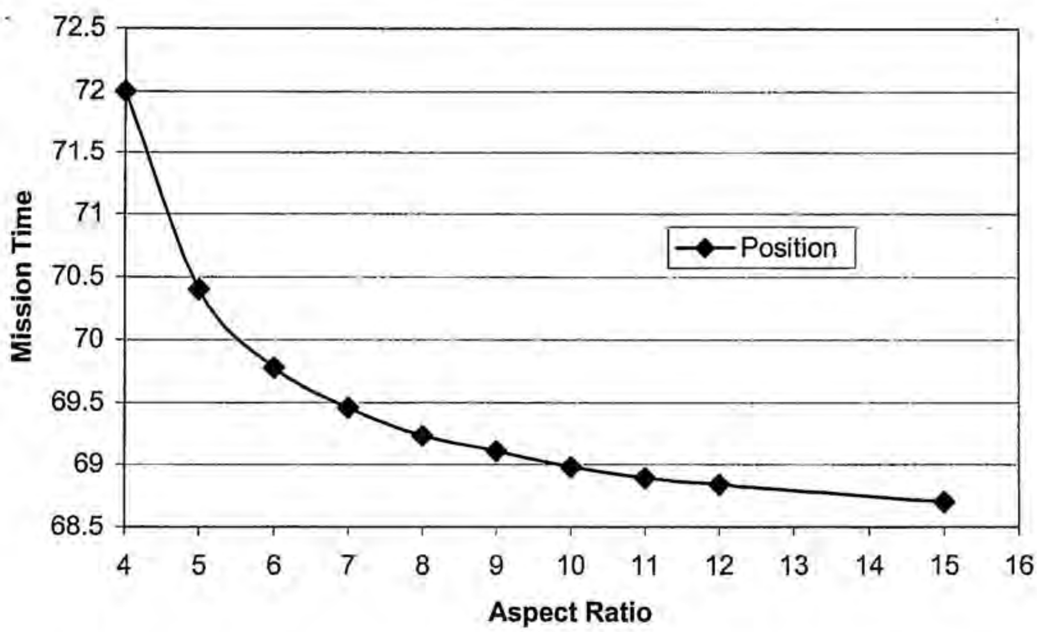

Figure 4.5 Reduction in Position Mission time with increasing AR

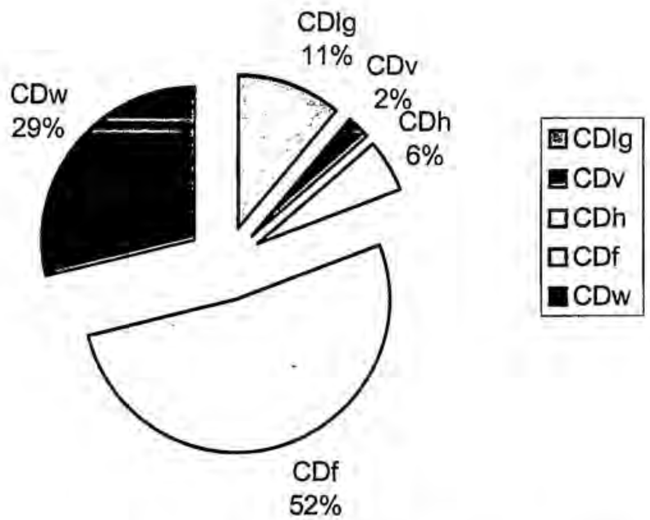

Figure 4.6 Drag breakdown at end of 1000 ft straightaway for passenger delivery

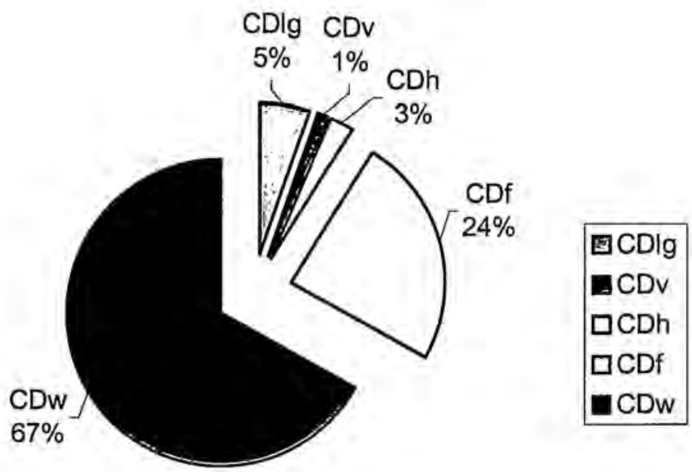

Figure 4.7 Drag breakdown at end of 3rd 180 deg for passenger delivery

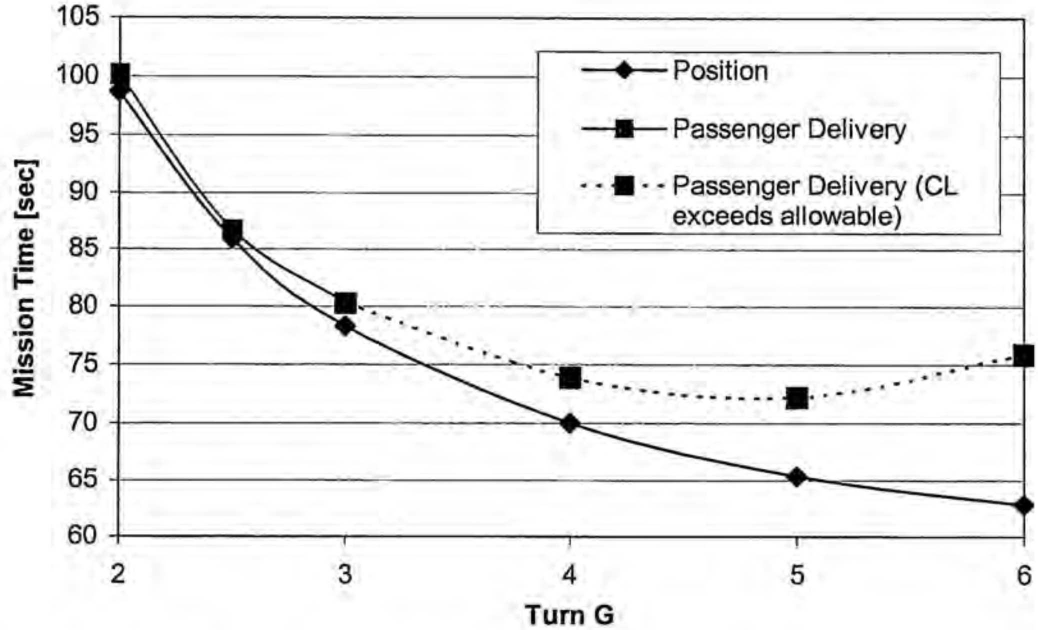

Figure 4.8 Limits on Turn G to reduce Mission Time

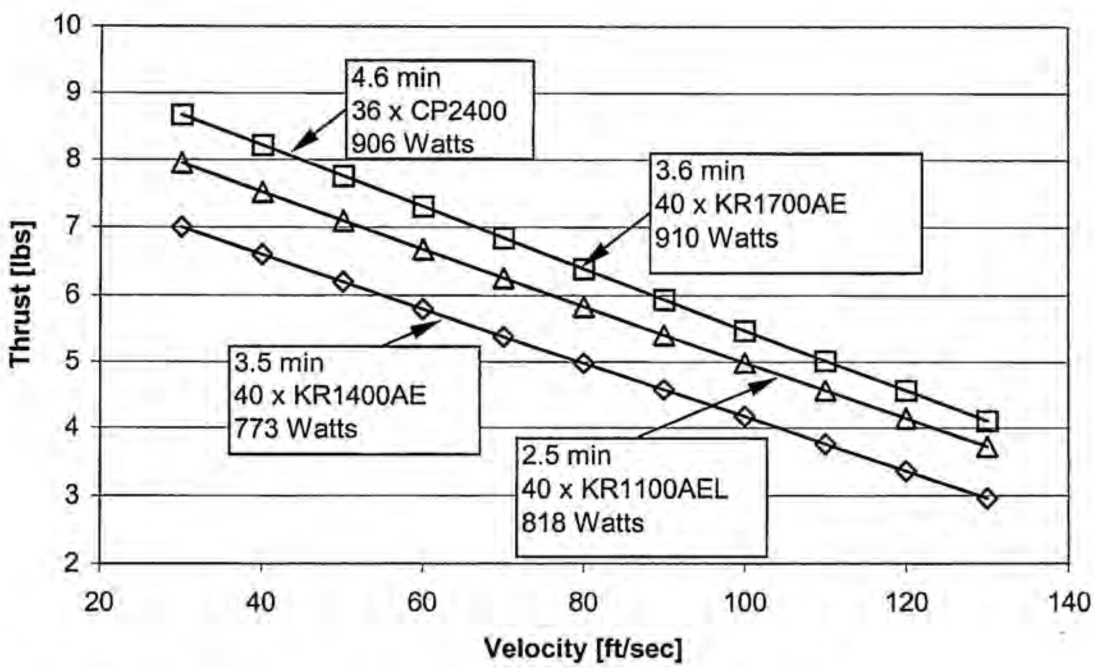

Figure 4.9 Battery pack combinations for a range of mission times

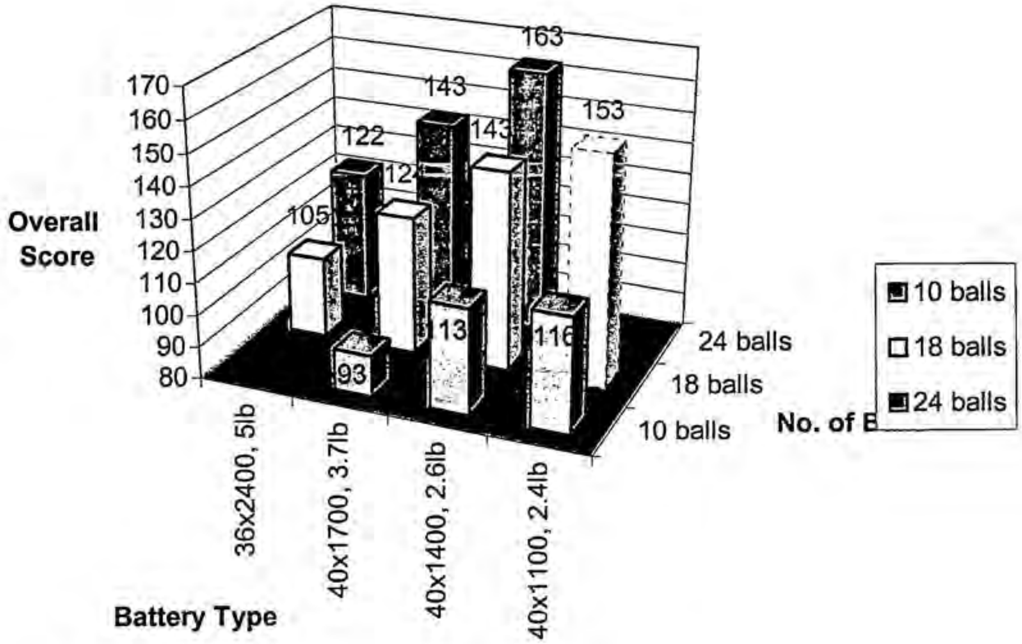

Figure 4.10 Overall Score for 10, 18, 24 ball airplane optimization

5.0 Detail Design

5.1 Weight Increase Items

A detailed look at the estimated weight showed that it required an increase of 2 to 3 pounds over the Preliminary Design weight estimate. This was mainly caused by the following:

- Decision to construct the wing in two halves required weight for the connection tube
- Structural reinforcement of fuselage for ground crew handling
- Actual weight of braking system higher than estimated weight
- T-tail stiffening required to reduce deflections
- Wing strengthening for 4G load with payload

Because these items would have increased the weight of the 10 and 18 ball aircraft, this change did not affect the relative strength of the 24 ball aircraft over the two study options, and therefore the payload configuration remained the same.

5.2 Wing Refinements

5.2.1 Wing Area

Because of the increase in weight, an 8.5% increase in wing area was made to keep wing loading to slightly below 50 oz/ft^2 and keep the TOFL within 200 ft. Keeping the same Aspect Ratio, the simulation program showed the wing area increase to have a minor effect on flight time. The RAC did increase slightly because of the increase in wingspan and max chord, but these changes were also very small.

5.2.2 Wing Planform

In the 97/98 DBF competition, the WVU entrant "Raptor" suffered from tip stall during high-G turns. The team used an untwisted RG15 airfoil with single taper planform at taper ratio 0.4 to reduce induced drag. This taper ratio was based on [Anderson], which showed the minimum induced drag occurs roughly at 0.3 for aspect ratios 4 to 10.

This year, the team wanted to design a plane with much better handling qualities in the turn, yet low overall induced drag. Based on information from the literature, many successful RC sailplane planforms used a constant local Cl from the root to 80% of semi-span and then dropped Cl off rapidly to the tip. In addition, these planforms used a combination of geometric and aerodynamic twist to provide protection against tip stall and insured that the entire wing passed through the zero lift line at the same angle of attack as the fuselage.

A program using the vortex lattice method outlined in [Anderson] was used to create and evaluate candidate planforms with the above guidelines in mind, as well as contribution to RAC. All planforms used an AR of 8 as determined from the previous study. To make a very flat Cl distribution from the root to 80% of semi-span, a large Cr was required, similar to an elliptical planform. Because of the penalty to the RAC for large Cr and span, a compromise position was taken with reduced Cr and almost constant Cl to 70% of semi-span. (Figure 5.1)

5.2.3 Final Airfoil Selection

As further protection against stall and for structural efficiency, a slightly thicker and cambered airfoil than the root S7012 was used on the tip. The S7032, SA7036, and SD7037 were evaluated using [UIUC wind tunnel] data (Figure 5.2). The SA7036 (9.2% t/c, 2.79% camber) was chosen because it provided lower drag compared to the other airfoils at low Cls, and provided 10% higher Clmax than the root S7012 over an alpha range of 11 to 15 degrees. In the planform, the S7012 went from root to 60% of semi-span and then transitioned to SA7036 at 92% of semi-span. In this section the wing is twisted nose down by the difference in the zero lift angles, or 1.9 degrees.

5.3 Handling Qualities

5.3.1 Horizontal-Tail

The low value for horizontal tail volume of 0.5 was kept in the detail design. The team had difficulty finding good data to approximate the static margin. Values for X_{AC} and CL_α on the wing-body were estimated from historical data but were very rough at best. The final value of the static margin was –0.18. The target value the team had expected was between -.20 and -.25 for reasonable handling qualities. The flight-testing program will be very conservative to determine if design changes are necessary.

Historical data shows elevator areas are typically 30 to 40% of total horizontal tail area. A value of 33% was chosen since it was felt that in a T-tail configuration, the tail is out of the downwash of the wing and its effectiveness is improved.

5.3.2 Vertical-Tail

To integrate well with the elevator, the rudder chord was made equal to the elevator. This corresponded to a rudder at 28% of total vertical tail area. This percentage is also typical for vertical tails.

5.3.3 Wing Control Surfaces

Because of the varied lift requirements of this competition, flaperons were deemed essential. The most obvious reasons for flaperons are to slow landing speeds and shorten TOFL during the heavy "Passenger Delivery" mission segment. Flaperons could also be mixed with elevator input to augment pitch up authority. Lastly, flaperons could be spoilerons and dump lift or slow the aircraft after touch down.

From historical data, flaps are typically sized at 20% of the chord and extend less than 50% of semi-span. In this design, flaperons were set at 20% chord and 60% of semi-span. The flaperons were purposely extended into the twisted region of the wing to assist in roll control in the event of stall caused by flaperon deflection.

5.4 Structural Design

5.4.1 V-n Diagram

The minimum and maximum load factors, n_{neg} and n_{pos}, express the maneuvering ability of an aircraft as a multiple of the acceleration due to gravity. Based on the limit load factors of the aircraft while turning, the limit load factors were determined to be n_{pos} = 4.0 and n_{neg} = -1.0. The V-n diagram (Figure

5.3) depicts the limit load factors as a function of airspeed. The positive and negative lift limit curves were calculated using the following equation:

$$n = \frac{0.5\rho_{air}V^2 S_W C_{L_{max}}}{W_{TO}} \tag{5.1}$$

5.4.2 Wing G Capability

The maximum 4G lift along the span was calculated using an elliptical lift approximation. This was possible since the wing was tapered and twisted to achieve a nearly elliptical lift distribution. Next, the distributed load of the wing was calculated along the span, refer to Figure 5.4. Using a trapezoidal approximation to calculate the area under the curve, the shear diagrams and moment diagrams were as in Figure 5.5 and Figure 5.6.

To handle the bending loads a carbon fiber wing spar tube extended from the root rib to 60% of semi-span. At the joint location in the fuselage, the same size carbon tube was used. A 6061-T6 .030" wall tube fit into the wing spar and fuselage carbon tubes and carried the bending loads between the three components. To carry bending loads past 60% of semi-span, two full span spruce spars ran from 30% of root chord to 30% of tip chord. The upper spruce spar was 3/8"x3/16" and the lower spruce spar 3/16"x3/16".

The wing G capability was then analyzed at two critical locations. The first location was at the wing root where there was the highest moment. The compressive stress was 17,500 psi, which provided a 1.9 safety factor from compressive yield at 34,000 psi. The second location was at 60% semi-span, where the carbon tube stopped and the spruce spars carried the bending. Using typical values of compression strength for spruce (3500 psi), the spruce/balsa section showed the spruce at 1150 psi, or a safety factor of 3.0 from yield.

5.5 Systems Architecture

The layout of motor, battery, receiver, control rods, servos, brakes, and payload in the aircraft are shown in the drawing package.

5.5.1 Servos

The minimum number of servos, including electronic speed controller, ESC, to have a functional aircraft was four - 2 aileron, 1 elevator, 1 rudder, and 1 ESC. Two functions which where deemed necessary were wheel braking and flaperons for camber changing. The elevator servo was used to make contact with the brake valve eliminating the need for an extra servo. Hitec HS-225 servos were chosen because of their high torque (56.3 oz-in), low weight (1.13 oz) and slim profile compared to standard servos.

5.5.2 Brakes

Over the counter pneumatic brakes were purchased from BVM. These brakes are typically used on RC jet aircraft and were placed only on the main gear to permit responsive nose gear steering while braking. The tank is pressurized to 100 psi before flight.

5.5.3 Motor/Battery Cooling

Motor and battery cooling is absolutely necessary at 30A continuous. Inlet cooling holes were incorporated in the front of the fuselage and an air path from the nose to the tail provides cooling for motor and batteries.

5.6 Performance

5.6.1 Takeoff

To check the worst case, the simulation program uses 1.1 V_{stall} with no flaperon deflection and no headwind to calculate a wheels up takeoff field length. For the 24-ball payload case, the TOFL is 194 ft and for the no payload case, the TOFL is 68 ft.

5.6.2 Climb Capability

The simulation program showed the maximum climb rate in the Passenger Delivery configuration was 9.64 ft/sec. (Figure 5.7) The minimum climb rate deemed acceptable was 5 ft/sec.

5.6.3 Mission Performance

The effect of a 20 mph headwind is included in the calculation by extending the actual length of the course by the relationship shown below. This method was used successfully by the 2000/2001 team and adds approximately 12% to the course length.

$$dist_{eff} = dist\left(\frac{1}{1-\left(\frac{V_{wind}}{V_{flight}}\right)}-1\right) \qquad (5.2)$$

Refinements were made to the estimated thrust and the final mission performance is shown in Figures 5.7, 5.8 and Table 5.1. Figure 5.8 describes the points on the course for the Position mission segment.

5.7 Aircraft Weight and Balance

The weight and balance spreadsheet is shown in Table 5.2. The final aircraft weight was 25.9 lbs and the CG was located 33.3 inches aft of the motor bulkhead datum line. This position is 28% of MAC. The payload fraction was 37%.

5.8 Rated Aircraft Cost Worksheet

The rated aircraft cost was calculated using the parameters set forth in the competition rules. A breakdown of the RAC is shown in Table 5.3 And Figure 5.10. The RAC for phastball was calculated to be 11.56.

5.9 Final Configuration

The final aircraft configuration is listed below and is shown in detail in the drawing package.

Wing Airfoil Panel 1	*S7012*
Wing Airfoil Panel 2	*S7012 to SD7036*
Wing Airfoil Panel 3	*SD7036*
Wing Aspect Ratio	*8*
Panel 1 Span	*2.5 ft*
Panel 2 Span	*1.33 ft*
Panel 3 Span	*0.33 ft*
Root Chord	*1.24 ft*
Break 1 Chord	*1.07 ft*
Break 2 Chord	*0.77 ft*
Tip Chord	*0.60 ft*
Panel 1 Area	*2.89 ft^2*
Panel 2 Area	*1.23 ft^2*
Panel 3 Area	*0.23 ft^2*
Horizontal and Vertical Tail Airfoil	*NACA 0005*
Wing Span	*8.33 ft*
Wing Area	*8.68 ft^2*
Horizontal Tail Area	*1.48 ft^2*
Vertical Tail Area	*0.792 ft^2*
Aileron Area per Wing	*0.52 ft^2*
Wing Root Incidence	*1.9°*
Maximum Gross Weight	*25.9 lb*
Softball Capacity	*24*
Landing Gear Type	*tricycle*
Landing Gear Span	*1.33 ft*
Motor	*AstroFlight 661*
Gear Ratio	*2.75 to 1*
Propeller	*18 x 18*
Predicted RAC	*11.56*

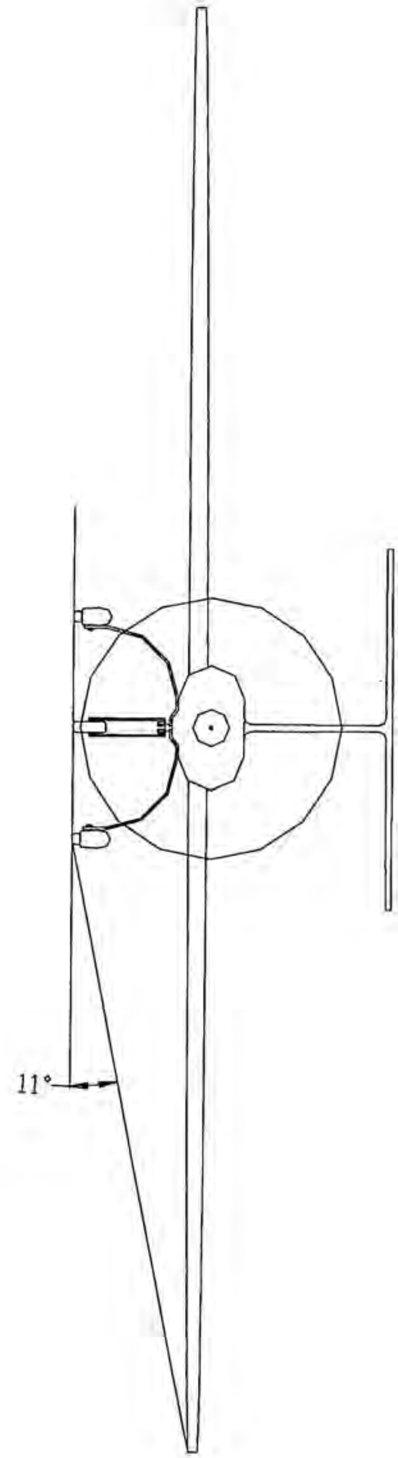
11°

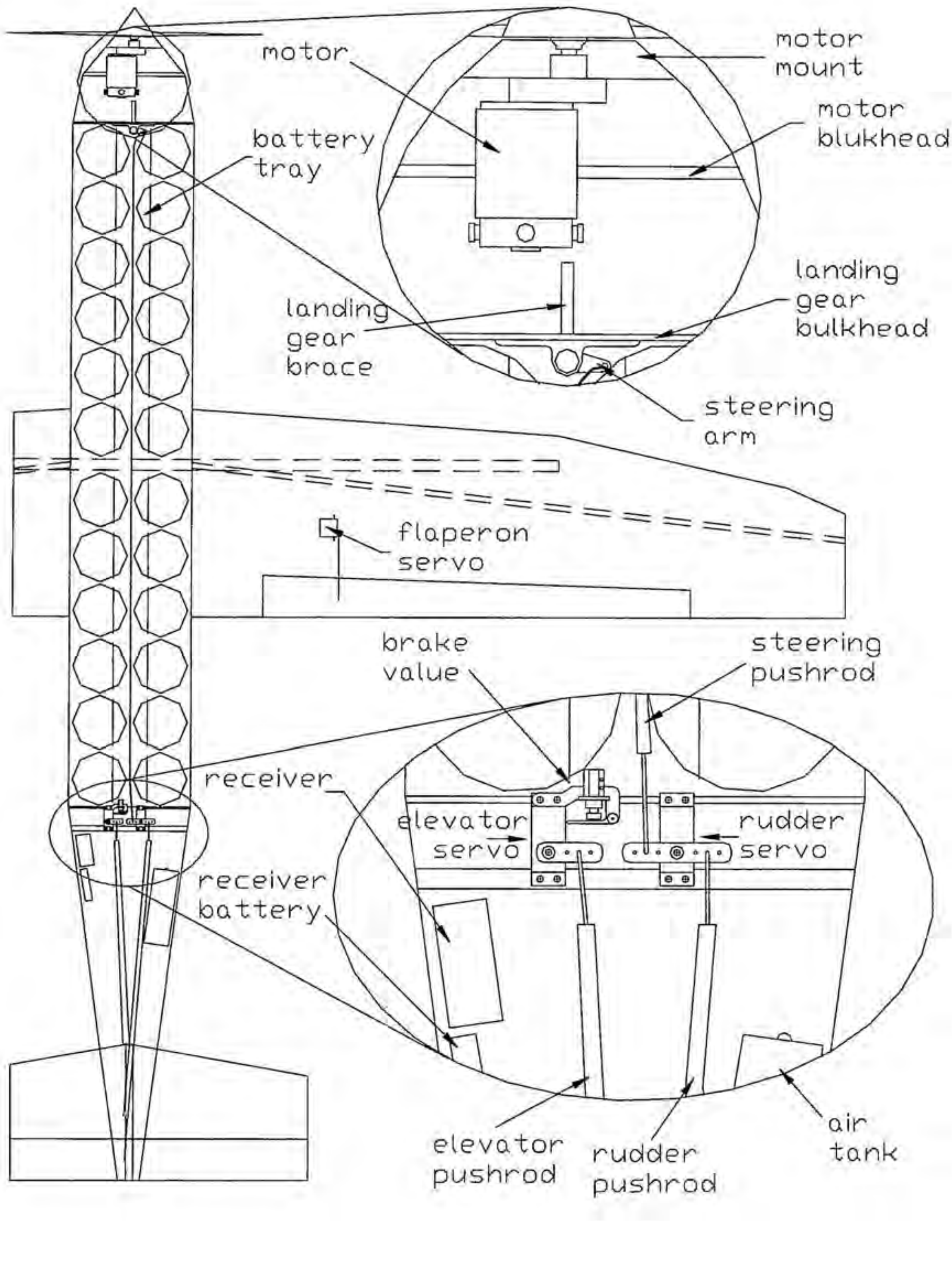
motor
motor mount
motor blukhead
battery tray
landing gear brace
landing gear bulkhead
steering arm
flaperon servo
brake value
steering pushrod
receiver
elevator servo
rudder servo
receiver battery
elevator pushrod
rudder pushrod
air tank

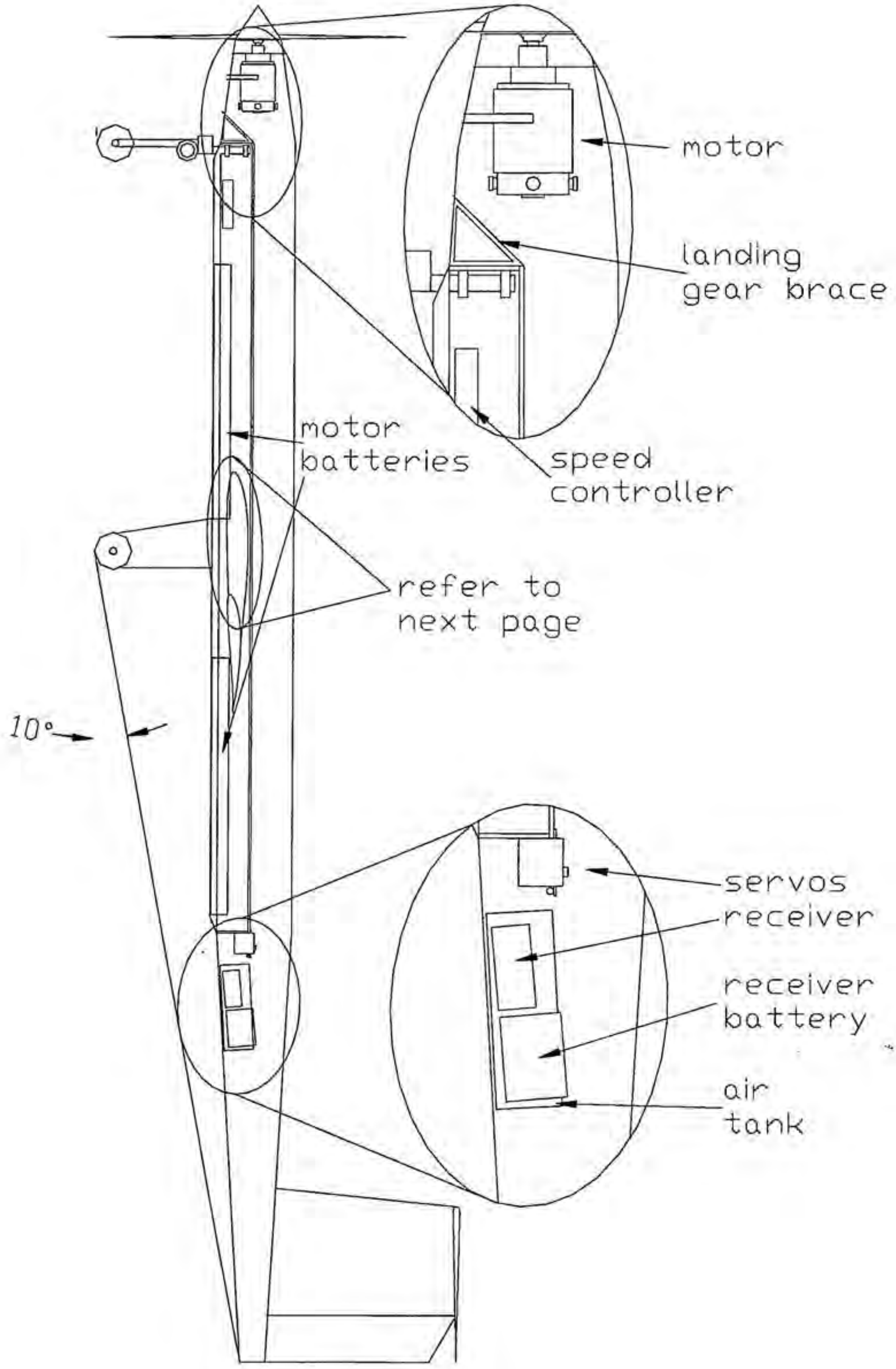
motor
landing
gear brace
motor
batteries
speed
controller
refer to
next page
10°
servos
receiver
receiver
battery
air
tank

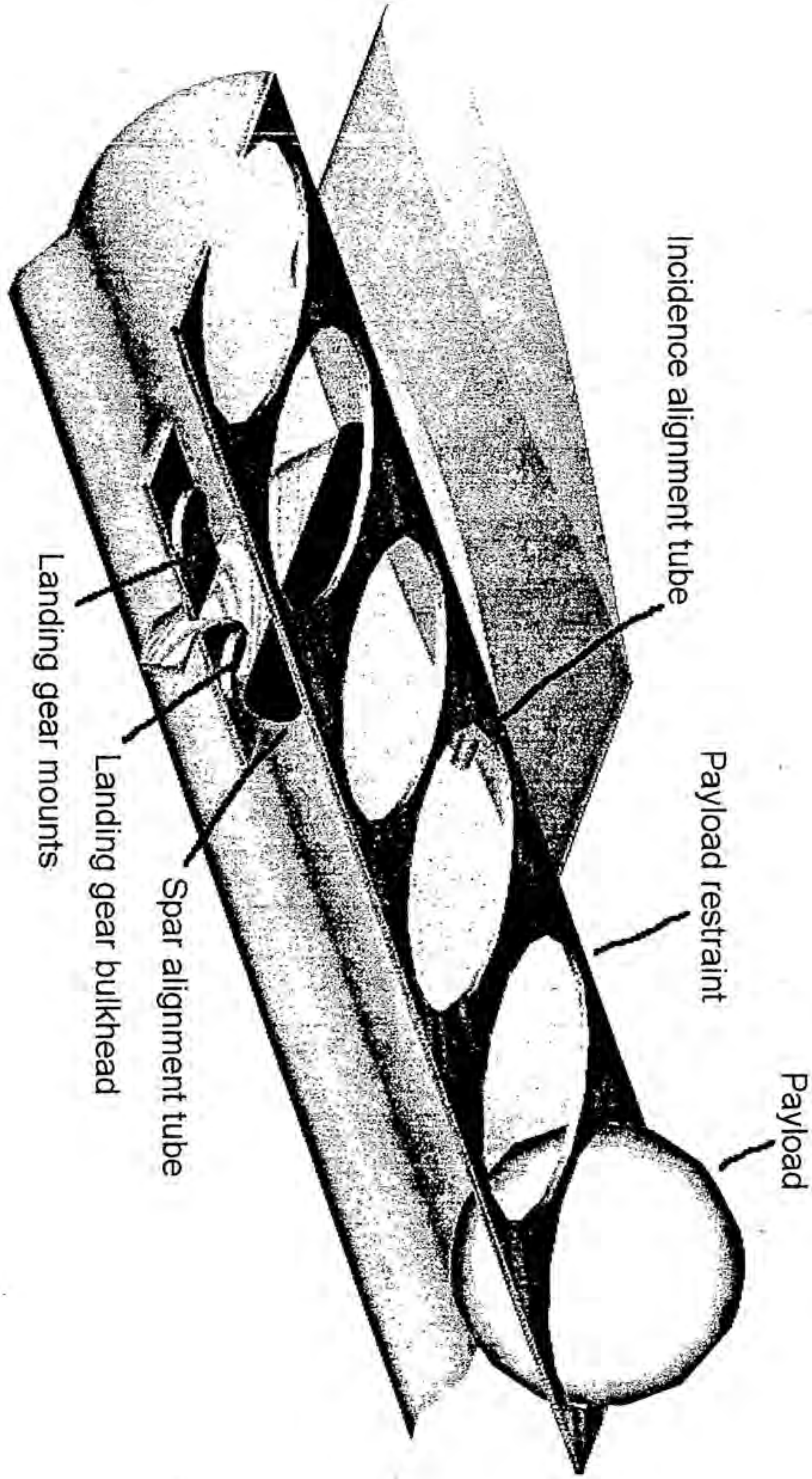
Incidence alignment tube
Payload restraint
Payload
Landing gear
Landing gear mounts
Landing gear bulkhead
Spar alignment tube

Table 5.1 Summary of Mission Performance

	Position	Passenger Delivery	Return
TOFL [ft]	68	194	68
Flight Time [sec]	73.9	89.1	62.9
Motor Run Time [sec]	60.8	74.6	49.8
Pit Time [sec]	40	40	0
Max Speed [ft/sec]	112	108	112
Max Turn Radius [ft]	101	152	101
Total Mission Time [sec]	266		
Total Mission Time [min]	4.4		

Table 5.2 Weight and Balance Spreadsheet

Component	Dist. [in]	Wt [oz.]	Wt [lbs]	% of MTOGW	Moment [oz-in]
Motor	3.0	26.8	1.7	6%	80
ESC	7.3	2.0	0.1	0.5%	14
Prop	-0.5	5.9	0.4	1%	-3
spinner	-0.5	2.9	0.2	1%	-1.5
nose gear	9.1	4.4	0.3	1%	40
main gear	34.5	13.1	0.8	3%	451
tail servos	57.8	3.0	0.2	1%	173
RX	61.0	1.2	0.1	0.3%	70
RX Battery	61.0	3.4	0.2	1%	206
air tank	61.4	1.2	0.1	0.3%	75
horizontal tail	77.5	4.2	0.3	1%	322
vertical tail	75.5	4.9	0.3	1%	372
wing	35.0	64.0	4.0	15%	2240
fuse	37.3	64.0	4.0	15%	2384
battery 1	41.0	30.0	1.9	7%	1230
battery 2	34.5	30.0	1.9	7%	1035
MEW	33.3	260.9	16.3	63%	8689
Payload	33.3	153.6	9.6	37%	5115
MTOGW	33.3	414.5	25.9	100%	13804

Table 5.3 RAC Worksheet

Description		Aircraft Parameter	Value ($ thousands)
MEW Manufacturers Empty Weight	aircraft empty weight	16.3lbs	
			1.63
REP Rated Engine Power	# of motors	1	
	total battery weight	3.86lbs	
			5.78
MFHR Manufacturing Man Hours	wing span	8.33ft	1.33
	max exposed wing chord	1.22ft	0.20
	# of control surfaces	2	0.12
	length of fuselage	7ft	1.40
	# of vertical surfaces	0	0.00
	# of vertical surfaces with control surfaces	1	0.20
	# of horizontal surfaces	1	0.20
	# of servos or motor controllers	5	0.50
	# of motors	1	0.10
	# of propellers of fans	1	0.10
		total RAC:	***11.56***

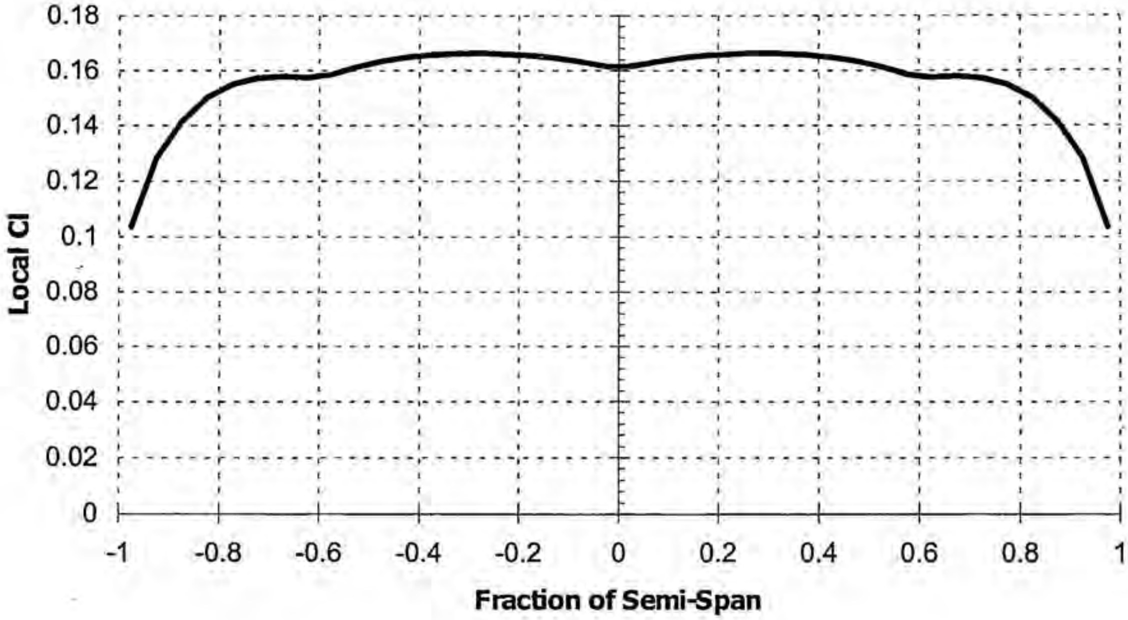

Figure 5.1 Span wise Cl distribution for final wing planform

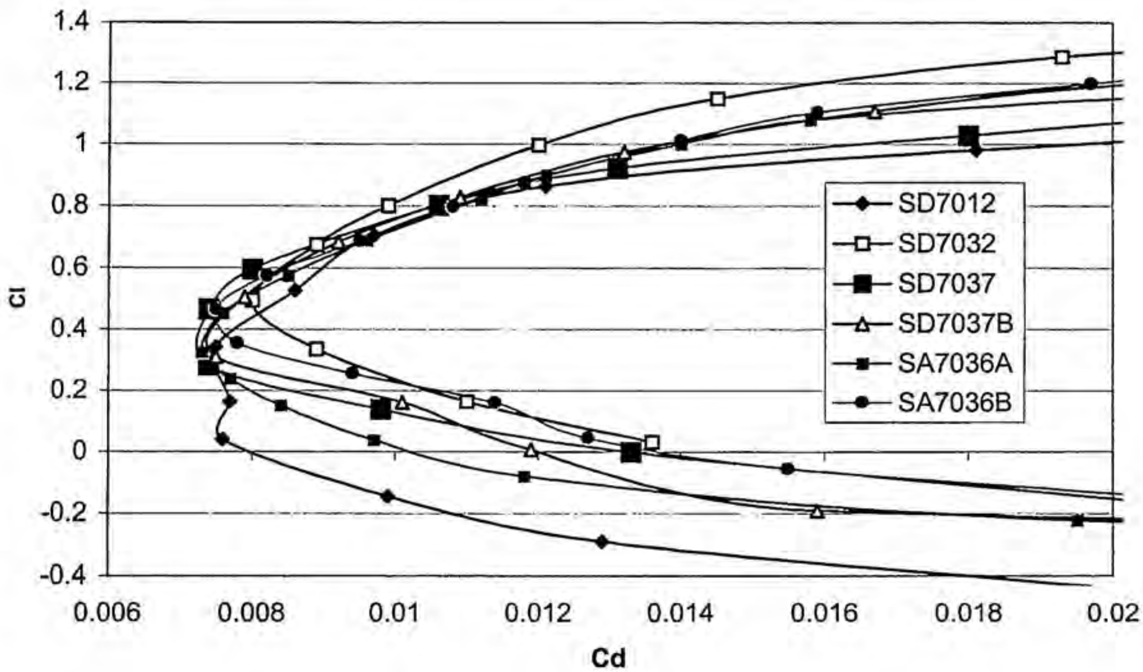

Figure 5.2 Airfoils evaluated for wing tip at Re=300K

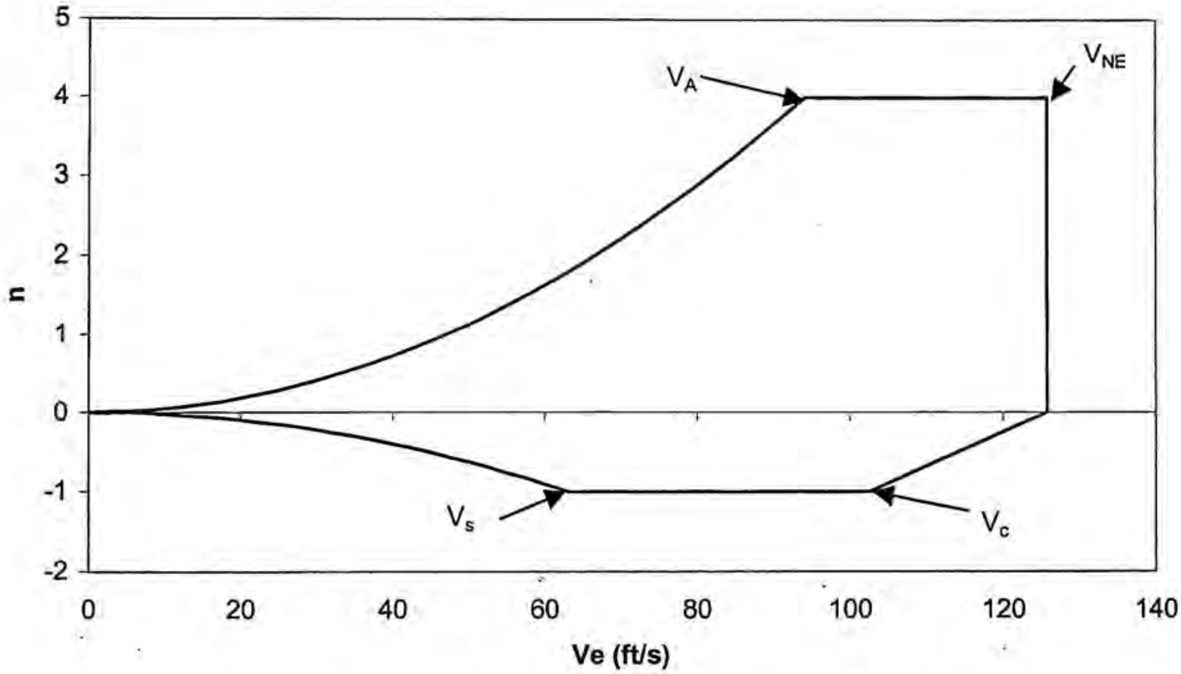

Figure 5.3 V-n diagram – Defines the flight speed envelope which must be adhered to for ensured structural integrity

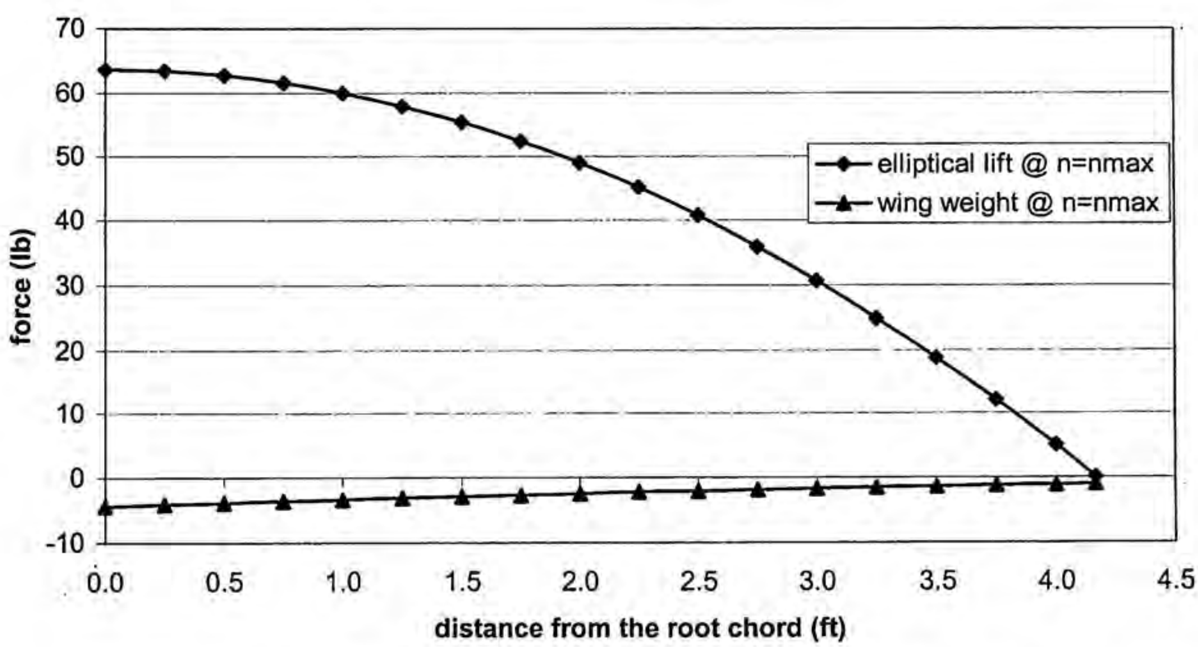

Figure 5.4 Flight load diagram due to lift and weight at load factor $n=n_{max}$

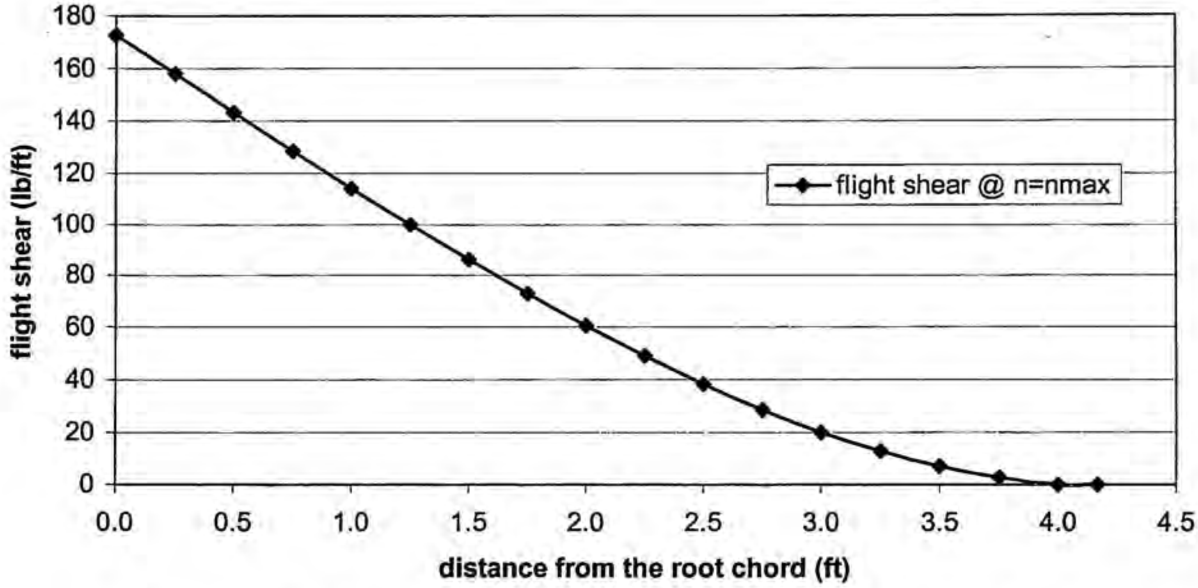

Figure 5.5 Flight shear diagram due to lift and weight at load factor $n=n_{max}$

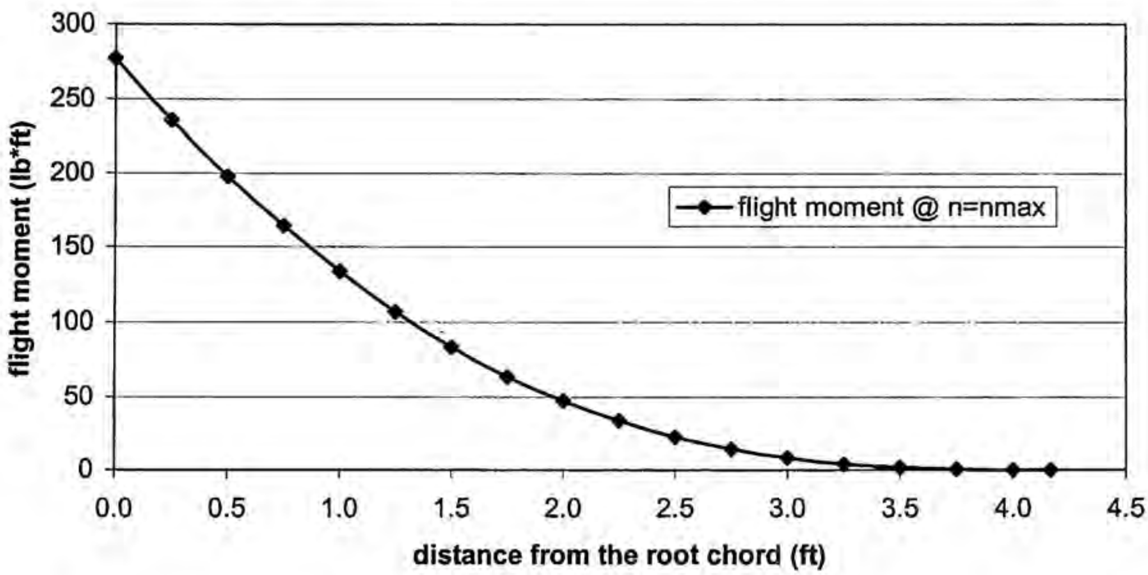

Figure 5.6 Flight bending moment diagram due to lift and weight at load factor $n=n_{max}$

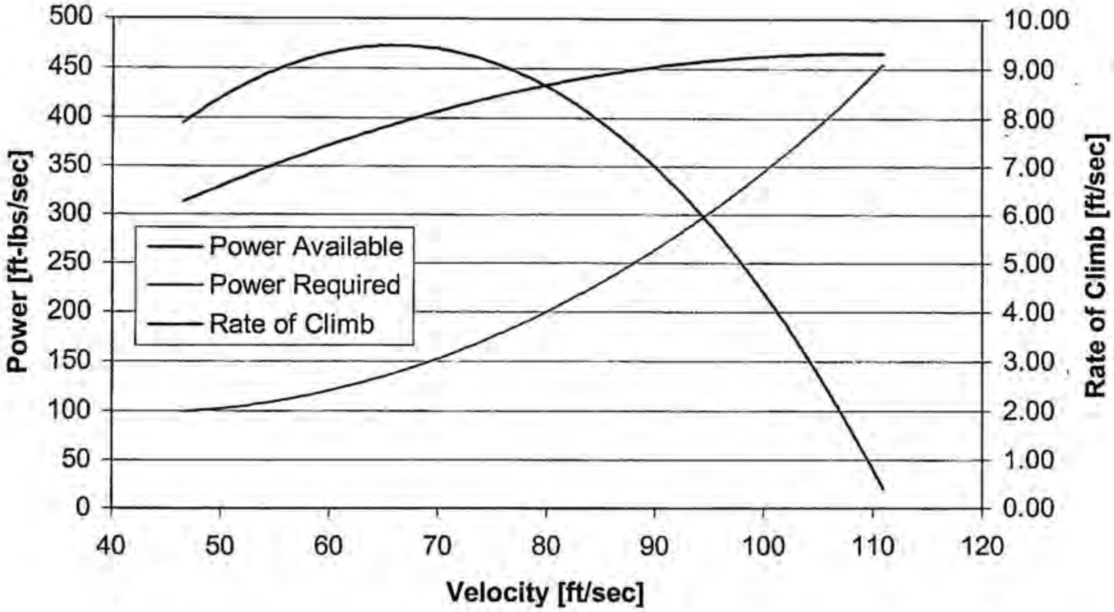

Figure 5.7 Power and Climb Performance in Passenger Delivery Configuration

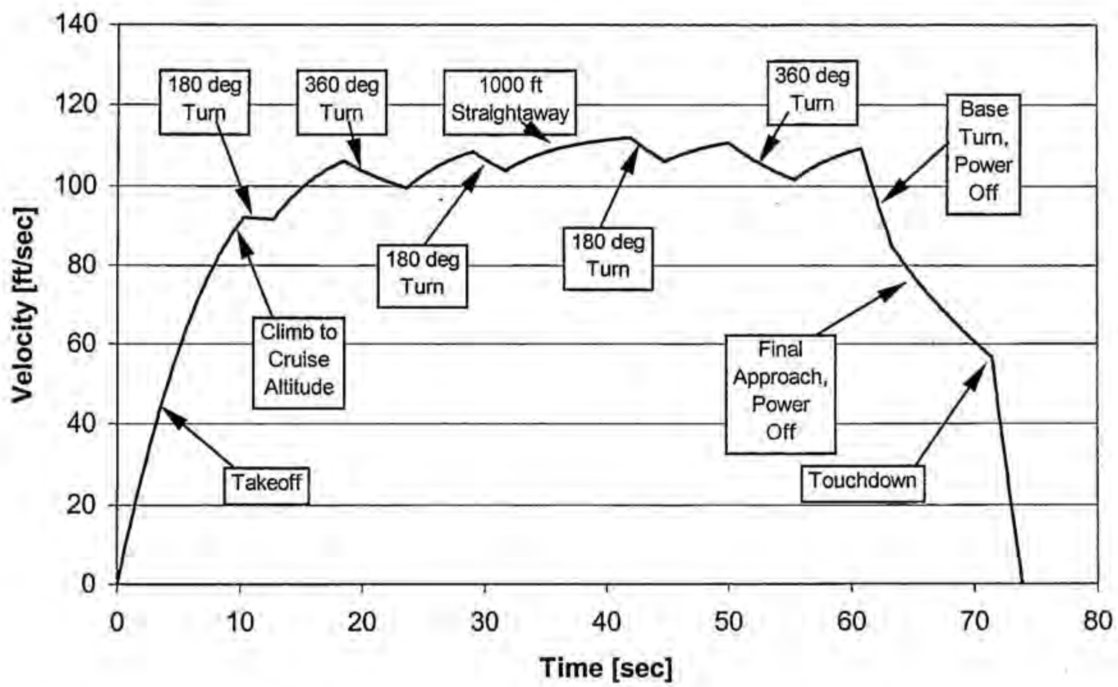

Figure 5.8 Velocity Profile during Position Mission Segment

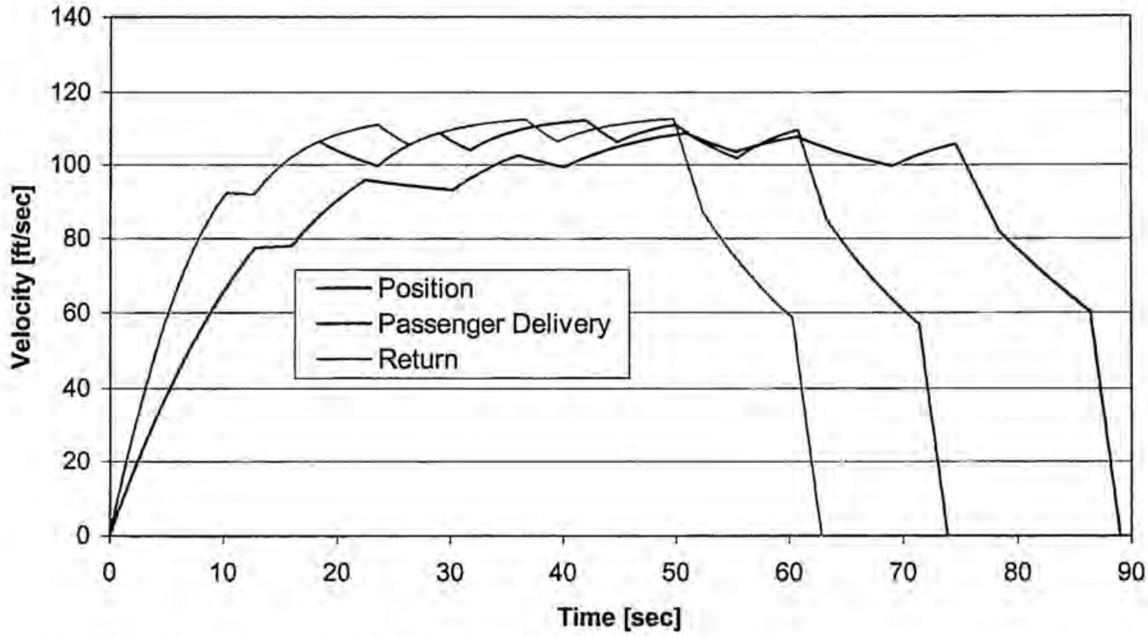

Figure 5.9 Velocity Profiles for all mission segments

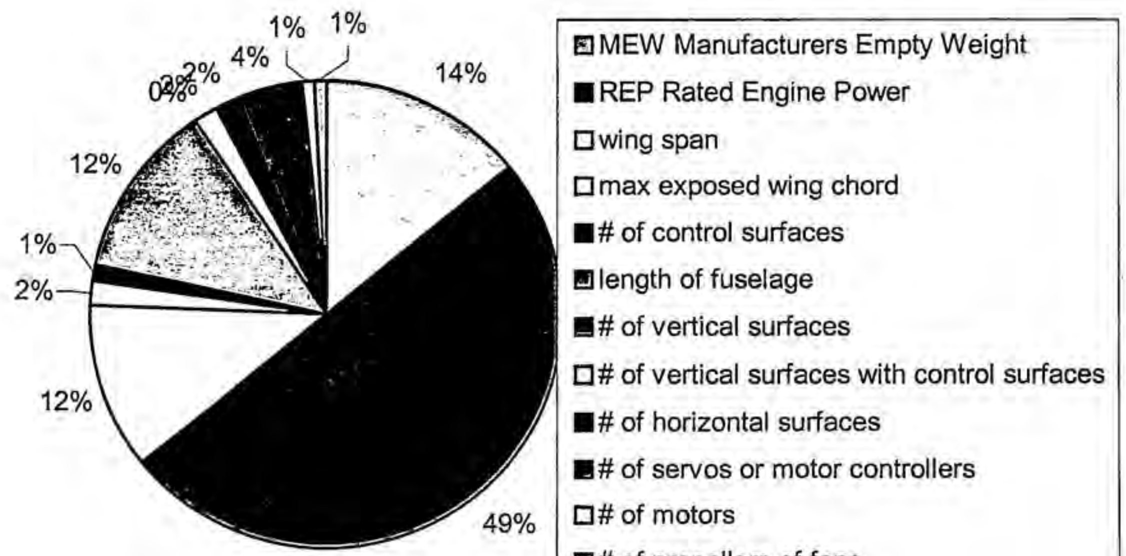

Figure 5.10 Breakdown of Rated Aircraft Cost

6.0 Manufacturing Plan

6.1 Manufacturing Processes Investigated

The fabrication and assembly of the aircraft components needed to be done quickly and within the limitations of the teams skill and available equipment at the University. During the construction of the aircraft, time was a nemesis to help keep the team on pace to finish the construction in time for the competition a manufacturing milestone schedule was created, refer to Table 6.1. To help manage the time requirements of the project while attaining the highest production and results, the manufacturing plan was evaluated using the following FOM shown in Table 6.1.

6.2 Figures of Merit Breakdown

The purpose of the figures of merit is essentially to help determine the pros and cons of each construction phase of the project. Using this process to guide the team in construction alternatives helped maximize production and efficiency. The figures of merit that were considered to be most influential in the final design were simplicity, time required, cost, strength to weight, and availability.

Simplicity

It was determined that there had to be some limitations as to the overall complexity of the aircraft to make it both producible and maintainable. If the construction of a single part was easily done, it was given a 5. If it was tedious or took skills not available by team members, it was given a 1.

Time required

Time was a large contributing factor as to the feasibility of construction for the aircraft. In order to complete construction on all the components of the aircraft, the team had little forgiveness in missed deadlines. For each process, the time required to produce the part was compared to the overall advantage of making the part. If a part was time consuming, it was given a 1, if it could be completed quickly, it was given a 5.

Cost

The cost of the project was a very significant parameter that was non-negotiable. An estimation of materials needed and salvageable materials from past projects was done from conception to minimize new purchases and thus overall aircraft cost. With a limited budget, the selected parts and materials were first compared on a pro-con basis for optimal results. Parts and materials with a low cost or donations were given a 5, high cost parts and materials were given a 1.

Weight

As in all aircraft, weight is a critical factor. It was the intention of this year's team to build a lightweight aircraft with a low profile. The weight consideration of this year's plane was one of the most critical aspects and most all decisions were based from it. Bulky and heavy parts and materials were given a 1, whereas light and slim parts and materials were given a 5.

Availability

The availability of materials needed to complete the manufacturing process was an important concern. If the material was donated or easily obtained, it was given a 1. If the material was expensive or needed special ordering and obtaining procedures, it was given a 5.

6.3 Process Selected for Major Component Manufacture

6.3.1 Fuselage

Hand lay-up of composite materials was used to construct the fuselage. The construction of the fuselage began by first producing a male plug that was identical to the final fuselage shape. The plug was constructed out of foam that was cut to shape using a hot wire. Once the foam was cut it was then covered with three layers of fiberglass. The fiberglass gave strength to the plug and was able to be sanded to a smooth finish. Several coats of body filler and light sanding were applied to achieve the desired finish. Next, a female mold was produced from the plug. The mold was made in two halves. Construction of the mold was done by first building a dam around the perimeter of the plug, then applying a release agent to the parts. Next, a 1/8" coating of surface coat was applied to the plug half and surrounding dam. Twenty layers of 6oz fiberglass were then applied to strengthen the mold.

Once the mold was constructed, the fuselage shells were constructed. A release agent was applied to each mold half before the lay-up process began. Several composite shells were manufactured to determine the final laminate to be used. These shells were comprised of combinations of fiberglass, Kevlar, and carbon fiber. Using this approach allowed the team members to develop the proper techniques for manufacturing composite components and produced spare fuselages. The laminate decided upon for the final fuselage was one layer of 3k x 1k carbon fiber for the lower half and two layers of 1.9oz Kevlar for the upper shell. Additional layers of material were added in strategic areas such as around the motor mount and landing gear mount. Plywood bulkheads were then added in areas of importance as well. The payload holder was fabricated out of 1/8" plywood. 3.75" holes were drilled so that the softballs could sit in the fuselage. Figure 6.1 is a picture of the construction of the fuselage.

6.3.2 Wing and Tail

The wing and tail were constructed out of 1lb density Styrofoam that was then sheeted with 1/16" balsa wood. First, blocks of Styrofoam were cut to the wing planform. Next, the spar and tube holes were cut into the entire wing. The wing was then cut into sections corresponding to the breaks in the wing planform. Next, templates were made for each section. The airfoil shape was then cut of each section using a hot wire. Each section was then glued together with epoxy and the entire wing was sanded smooth. Next, the spars and alignment tubes were glued into place. Then 4" x 48" x 1/16" sheets of balsa wood were then glued together with CA glue to form large panels. These panels were then adhered to the foam core using Elmer's Pro Bond Polyurethane Adhesive. The wings panels were then trimmed to match that of the foam core and leading edge stock was applied. Next the wings were sanded smooth. Flaperons were then cut out of the wing and the hinges were installed and the flaperons were reattached. The wings were then covered in monocote. Figure 6.2 is a picture of one of the wing panels before it was covered with monocote. Horizontal and vertical tail surfaces followed the same procedure.

6.3.3 Landing Gear

The landing gear was constructed out of carbon fiber. Previous year's entries were used as a starting point to determine the laminate needed to withstand landing. Several of the past WVU entries used a carbon landing gear. Their weights and number of layers were examined and scaled accordingly to this year's aircraft. Using this approach allowed the team to spend more time on the construction phase of the landing gear rather than attempting to design the landing gear using FEM. The landing gear was constructed using the following laminate $[\pm 45/0_2/\pm 45/0_4/\pm 45]_s$. The mold for the landing gear was constructed by cutting the shape out of foam, which was then laminated with a thin layer of Mylar. Hand lay-up and vacuum bagging techniques were then used to produce the final part.

6.3.4 Payload Restraint

Payload is restrained vertically when the fuse hatch is installed on the aircraft. Balls are restrained laterally and longitudinally with plywood structure built into the lower fuse half with hole diameters equal to the ball diameter. Refer to drawing package.

6.3.5 Other Components

Other aircraft components such as bulkheads, servo mounts, landing gear mounts, etc. were constructed out of plywood. Figure 6.4 is a picture of the servos used to control the rudder, elevator, steering, and brakes.

Table 6.1 Manufacturing milestones

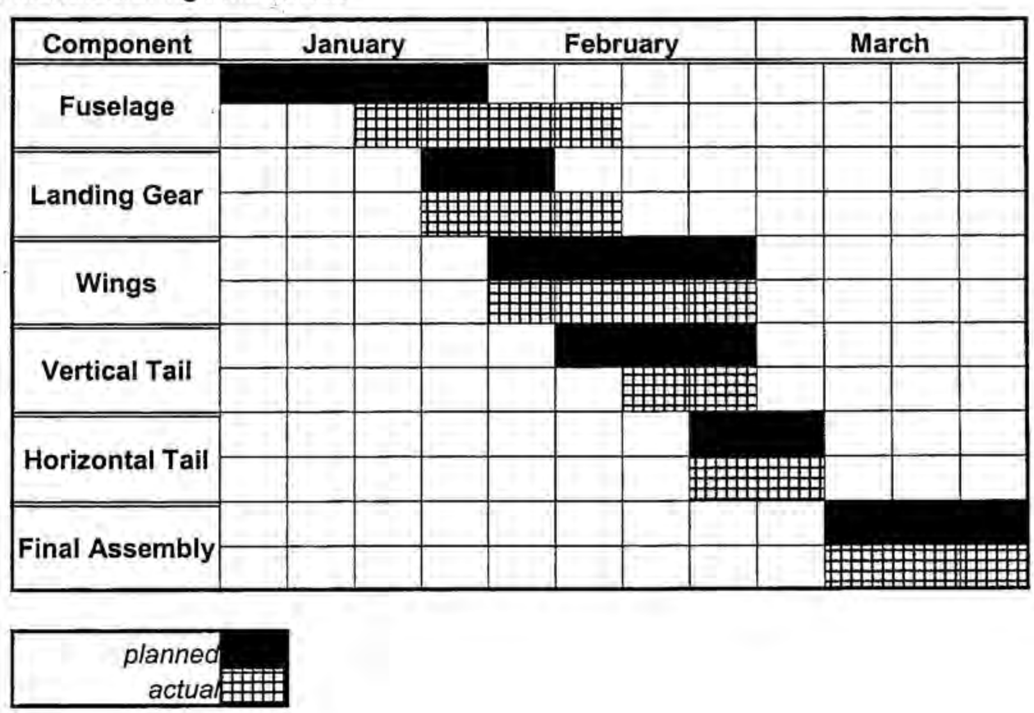

Table 6.2 Figure of Merit breakdown of manufacturing processes

		Simplicity (x5)	Cost (x1)	Strength to Weight (x6)	Time Required (x1)	Availability (x5)	Results
Wings and Empenage	Build up (balsa wood ribs, hardwood spars)	3	4	3	2	4	59
	Foam core with balsa wood sheeting	4	4	4	5	4	73
	All Composite	2	1	5	2	2	53
Tail	Build up (balsa wood ribs, hardwood spars)	3	5	4	3	4	67
	Foam core with balsa wood sheeting	4	4	4	5	4	73
	All Composite	2	1	5	2	2	53
Fuselage	Build up (balsa ribs, hardwood stringers)	3	3	3	3	4	59
	All Composite	2	1	6	2	4	69
Landing Gear	Purchase	5	5	3	5	2	63
	Aluminum	3	3	3	3	4	59
	All Composite	4	3	5	3	4	76

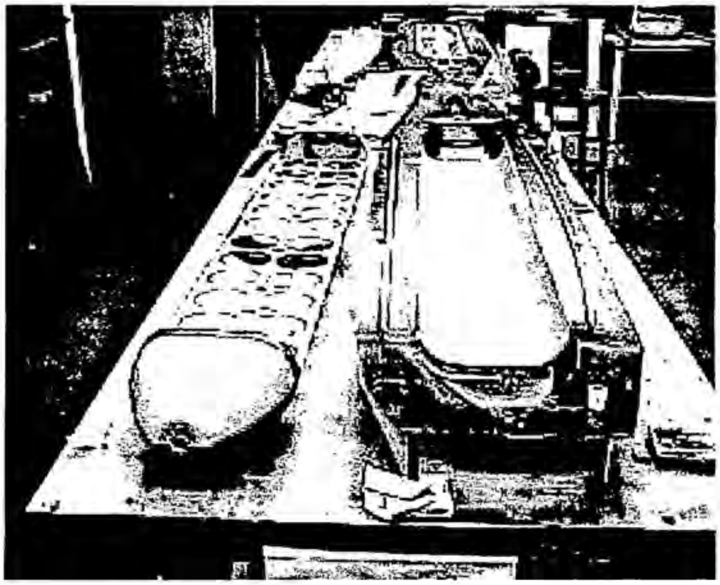

Figure 6.1 Picture of the construction of the fuselage

Figure 6.2 Foam wing sheeted with balsa

Figure 6.3 Carbon fiber landing gear with brake, wheel, and wheel pant

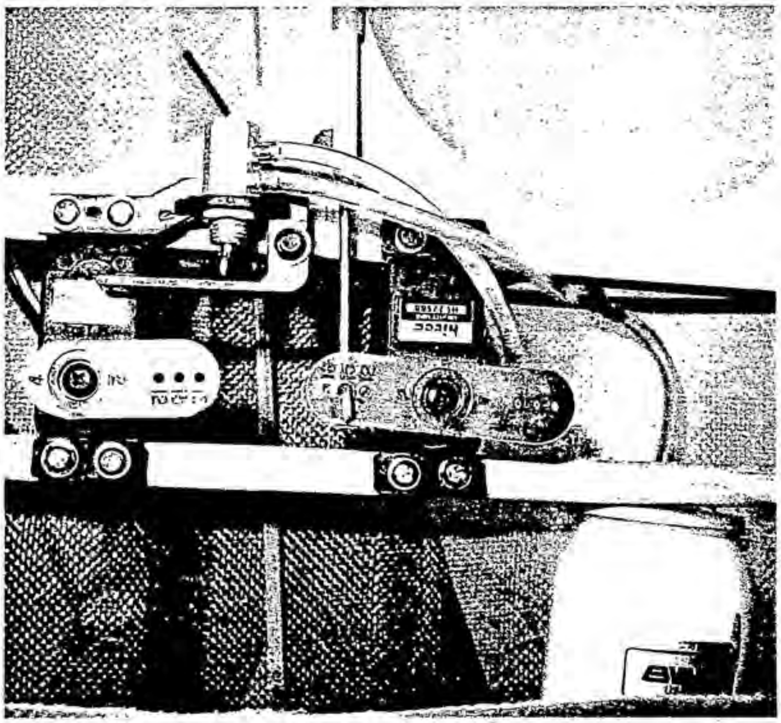

Figure 6.4 Rudder, elevator, steering, and brake servos

7.0 References

[1] Raymer, Daniel P., "Aircraft Design: A Conceptual Approach Third Edition," American Institute of Aeronautics and Astronautics, Inc., Reston, VA 20191

[2] Barbero, Ever J., "Introduction to Composite Materials Design," Taylor and Francis, Inc., Philadelphia, PA 19106

[3] Tomblin, John; Chaffin, Michael; Rexrode, Timothy; Ringler, Todd, "Detailed Structural Design of the F-120 Fuselage MAE 162," Presented to Dr. Nithiam Sivaneri August 11, 1989, Morgantown, WV 26505

[4] Sivaneri, N. "MAE 160 Design Project," West Virginia University, Morgantown, WV, 1999

[5] Anderson, John D. Jr., "Fundamentals of Aerodynamics," McGraw-Hill, Inc.

[6] Sun, C. T., "Mechanics of Aircraft Structures," John Wiley and Sons, Inc.

[7] Ford, Kevin J., "UAV Truss-Core Sandwich Composite Wing," Mechanical and Aerospace Engineering Department, West Virginia University, Morgantown, WV 26505

[8] Scarberry, Thomas T., "Electric Model Aircraft Propeller Analysis," Mechanical and Aerospace Engineering Department, West Virginia University, Morgantown, WV 26505

[9] http://cms.access.wvu.edu:8900/, accessed online February 2001, Loth, John L.

[10] Anderson, John D., "Introduction to Flight, 3rd Edition," McGraw Hill, 1989.